BIOACTIVE CONSTITUENTS FROM SOME *ZIZIPHUS* PLANTS AND STRUCTURAL MODIFICATION OF SOME NATURALLY DERIVED COMPOUNDS

A THESIS

BY

NATTHAKALN LOMCHOEY

Presented in Partial Fulfillment of the Requirements for The

Doctor of Philosophy Degree in Applied Chemistry

at Srinakharinwirot University

February 2016

BIOACTIVE CONSTITUENTS FROM SOME *ZIZIPHUS* PLANTS AND STRUCTURAL MODIFICATION OF SOME NATURALLY DERIVED COMPOUNDS

A THESIS

BY

NATTHAKALN LOMCHOEY

Presented in Partial Fulfillment of the Requirements for the

Doctor of Philosophy Degree in Applied Chemistry

at Srinakharinwirot University

February 2016

BIOACTIVE CONSTITUENTS FROM SOME *ZIZIPHUS* PLANTS AND STRUCTURAL MODIFICATION OF SOME NATURALLY DERIVED COMPOUNDS

AN ABSTRACT

BY

NATTHAKALN LOMCHOEY

Presented in Partial Fulfillment of the Requirements for the

Doctor of Philosophy Degree in Applied Chemistry

at Srinakharinwirot University

February 2016

Natthakaln Lomchoey. (2016). *Bioactive constituents from some Ziziphus plants and structural modification of some naturally derived compounds*. Thesis, Ph.D. (Applied Chemistry). Bangkok: Graduate School, Srinakharinwirot University. Advisor Committee: Assoc. Prof. Dr. Sunit Suksamrarn, Dr. Prasert Pattanaprateeb, Professor Dr. Alexei V. Demchenko.

Seven new 14–membered cyclopeptide alkaloids named cambodines A–G (**278**–**284**) together with two known compounds were isolated from *Ziziphus cambodiana* native to Thailand. Their structures were identified based on a combination of spectroscopic data, and five of the new compounds were found to contain a methylimidazolidinone ring. The first X–ray crystal structure of cambodine E (**282**) with 1–methylimidazolidin–4–one was reported herein. The stereochemistry of the new compounds was determined on the basis of circular dichroism and comparison of NMR data with reported compounds. All isolated cyclopeptides were evaluated for their antiplasmodial and antimycobacterial activities against *Plasmodium falciparum* and *Mycobacterial tuberculosis*, respectively. Compound **283** containing anomalous 1,2–dimethylimidazolidin–4–one exhibited antiplasmodial activity with IC_{50} value of 4.3 μg/mL (6.1 μM).

This work was also dedicated to *O*–glycosylation of two poorly soluble natural compounds to enhance their hydrophilicity and pharmacological activity. Each of the natural products, betulinic acid (**1**) and α–mangostin (**234**), has been derivatized as glycosides of the *D*–gluco, *D*–galacto and *D*–manno series using new methods for chemical glycosylation. Glycosyl acceptor **1** was *O*–glycosylated at C–3 using novel OFox donors to afford α–linked gluco– and galactoside, as well β–mannoside saponins (**291**, **297** and **304**, respectively). Glycosyl acceptor **234** was mono– or di–*O*–glycosylated at C–3 and/or C–6 positions to yield nine analogues (**272**–**274**, **314**–**315**, **319**–**320** and **324**–**325**). All synthetic glycosides will be tested *in vitro* and/or *in vivo* as prodrug candidates with improved hydrophilic properties. All synthetic glycosides were calculated for their Clog*P* by ACD/ChemSketch. The results showed all glycosides enhance hydrophilicity of their aglycone.

สารออกฤทธิ์ทางชีวภาพจากพืช *ZIZIPHUS* บางชนิด และการปรับเปลี่ยนโครงสร้างสารผลิตภัณฑ์ธรรมชาติบางชนิด

บทคัดย่อ

ของ

ณัฏฐกัลย์ ลมเชย

เสนอต่อบัณฑิตวิทยาลัย มหาวิทยาลัยศรีนครินทรวิโรฒ เพื่อเป็นส่วนหนึ่งของการศึกษา
ตามหลักสูตรปริญญาปรัชญาดุษฎีบัณฑิต สาขาวิชาเคมีประยุกต์
กุมภาพันธ์ 2559

ณัฏฐกัลย์ ลมเชย. (2559). *สารออกฤทธิ์ทางชีวภาพจากพืช ZIZIPHUS บางชนิดและการปรับเปลี่ยนโครงสร้างสารผลิตภัณฑ์ธรรมชาติบางชนิด*. ปริญญานิพนธ์ ปร.ด. (เคมีประยุกต์). กรุงเทพฯ: บัณฑิตวิทยาลัย มหาวิทยาลัยศรีนครินทรวิโรฒ. คณะกรรมการควบคุม: รองศาสตราจารย์ ดร.สุนิตย์ สุขสำราญ, ดร. ประเสริฐ พัฒนาประทีป, Professor Dr. Alexei V. Demchenko.

งานวิจัยนี้ได้แยกสารจากพืชตะครอง (*Ziziphus cambodiana*) ซึ่งค้นพบสารชนิดใหม่ 7 สาร คือ cambodines A–G (**278**–**284**) จัดเป็นสารสารไซโคลเปปไทด์อัลคาลอยด์ชนิด 14–เหลี่ยม และสารไซโคลเปปไทด์ 14–เหลี่ยม ที่มีผู้รายงานแล้ว 2 สาร การพิสูจน์โครงสร้างของสารที่แยกได้ทำได้โดยใช้เทคนิคทางสเปคโตรสโกปีต่างๆ พบว่าสารใหม่จำนวน 5 สาร มีหมู่ 1–methylimidazolidin–4–one จากโครงสร้างเอกซ์เรย์ของสาร cambodine E (**282**) ที่มีหมู่ 1–methylimidazolidin–4–one ซึ่งได้รายงานเป็นครั้งแรก ประกอบกับข้อมูล circular dichroism รวมทั้งการเปรียบเทียบข้อมูล NMR กับสารที่รายงานไว้แล้ว ทำให้ทราบสเตอริโอเคมีของสารที่แยกได้ จากการทดสอบฤทธิ์ต้านมาลาเรีย (*Plasmodium falciparum*) และวัณโรค (*Mycobacterial tuberculosis*) ของสารที่แยกได้ พบว่าสาร cambodine F (**283**) ซึ่งมีหมู่ 1,2–dimethylimidazolidin–4–one แสดงฤทธิ์ต้านมาลาเรียดีที่สุด ที่ IC_{50} 4.3 μg/mL (6.1 μM).

นอกจากนี้ ยังรายงานการสังเคราะห์สารอนุพันธ์ *O*–glycoside ต่างๆ ของสารผลิตภัณฑ์ธรรมชาติที่ละลายน้ำได้น้อย จำนวน 2 สาร คือ betulinic acid (**1**) และ α–mangostin (**234**) เพื่อเพิ่มความคุณสมบัติการละลายน้ำและฤทธิ์ทางชีวภาพ สาร *O*–glycoside ที่สังเคราะห์ขึ้นเป็นสารอนุพันธ์ในกลุ่ม D–gluco D–galacto และ D–manno โดยในการสังเคราะห์ทางเคมีนี้ สาร **1** จะเกิดปฏิกิริยา *O*–glycosylation ที่ตำแหน่ง C–3 โดยใช้ –OFox donors ได้สารอนุพันธ์ จำนวน 3 สาร ได้แก่ ชนิด α–linkage คืออนุพันธ์ glucoside (**291**) และ galactoside (**297**) ส่วน mannoside (**304**) จะเป็นชนิด β–linkage ในการสังเคราะห์สารอนุพันธ์ของ **234** ได้สารอนุพันธ์ *O*–glycoside ในกลุ่ม mono– หรือ di–O–ที่ตำแหน่ง C–3 และ/หรือ C–6 จำนวน 9 สาร (**272**–**274**, **314**–**315**, **319**–**320** และ **324**–**325**) จากการคำนวณค่า Clog*P* โดยใช้โปรแกรม ACD/ChemSketch พบว่าสารอนุพันธ์ที่สังเคราะห์ได้ทั้ง 12 สาร มีคุณสมบัติละลายน้ำได้ดีกว่าสารตั้งต้นแต่ละชนิด ซึ่งจะดำเนินการทดสอบฤทธิ์ทางชีวภาพต่อไป

The thesis title

"Bioactive constituents from some *ziziphus* plants and structural modification of some naturally derived compounds"

By

Natthakaln Lomchoey

has been approved by the Graduate School as partial fulfillment of the requirements for the Doctor of Philosophy Degree in Applied Chemistry of Srinakharinwirot University.

..... Acting Dean of Graduate School

(Assoc. Prof. Dr. Dusadee Yoelao)

February , 2016

Thesis Committee

..... Major advisor

(Assoc. Prof. Dr. Sunit Suksamrarn)

..... Co–advisor

(Dr. Prasert Pattanaprateeb)

..... Co–advisor

(Prof. Dr. Alexei V. Demchenko)

Oral Defense Committee

..... Chair

(Prof. Dr. Apichart Suksamrarn)

..... Committee

(Assoc. Prof. Dr. Sunit Suksamrarn)

..... Committee

(Dr. Prasert Pattanaprateeb)

..... Committee

(Prof. Dr. Alexei V. Demchenko)

..... Committee

(Assoc. Prof. Dr. Siritron Samosorn)

Acknowledgements

The first and foremost, I gratefully acknowledge grants from my supervisor Assoc. Prof. Dr. Sunit Suksamrarn, for her invaluable hospitality, helpful supervision, hearty encouragement and research assistantship support throughout this work.

This work was financially supported by The Thailand Research Fund, supports from The Royal Golden Jubilee Ph.D. (RGJ) Program.

I would like to express my sincere thanks to my co–advisors and committee members, Prof. Dr. Apichart Suksamrarn, Dr. Prasert Pattanaprateeb, Prof. Dr. Alexei V. Demchenko, Assoc. Prof. Dr. Siritron Samosorn, for reading and editing the thesis for common English language and grammar mistakes.

I would like to express my sincere gratitude to my co–advisor Prof. Dr. Alexei V. Demchenko, Department of Chemistry and Biochemistry, University of Missouri–St. Louis (UMSL), for his hospitality collaboration' support on glycosylation research and warmest welcome to Glycoworld for nine months at UMSL. I would like to acknowledge my dear sister, Dr. Jagodige P. Yasomanee for her encouragement and helpful supervision in regards to glycosylation of natural products. In addition, I would like to thank my "Glycoworld" friends (Satsawat Visansirikul, Salvatore Pistorio, Xiao Jia, Mithila Bandara, Tinghua Wang, Matteo Panza and Michael Mannino) for their friendship and enjoyable experience.

I am grateful to Dr. Panomwan Panseeta, Department of Chemistry, Chulachomklao Royal Military Academy, for our collaboration work on *Ziziphus* plants, and also thank her for her guidance and supervision in regards to the structure elucidation of cyclopeptide alkaloids. I am also indebted to Audchara Seankham for her help in isolation of some *Ziziphus* plants.

This work was supported by the Center of Excellence for Innovation in Chemistry (PERCH–CIC). I am indebted to Mr. Wicharn Wisetsri and Mr. Jessada Netsawangwicha for providing us with the plant materials.

I am grateful to Assist. Dr. Pichit Sudta and Mr. Payung Jiarawapi for recording some of the nuclear magnetic resonance spectra, Mr. Nitirat Chimnoi, Chulabhorn Research Institute for recording the HRMS, Mr. Samran Prabpai and Assoc. Prof. Dr. Palangpon Kongsaeree, Department of Chemistry, Faculty of Science, Mahidol University for X–ray diffraction data, and, to Prof. Dr. Apichart Suksamrarn and Ms. Kanyarat Chanchang, Department of Chemistry, Faculty of Science, Ramkhamhaeng University for recording the ESIMS and optical rotations.

I would also wish to thank other Assoc. Prof. Dr. Sunit's students for their assistance in the laboratory and my special thanks also go to my teachers, friends, colleagues and staff of the Department of Chemistry, Faculty of Science, Srinakharinwirot University. I am truly appreciative of their friendship and kind support.

My gratitude goes out to myself for the most powerful patience for many years throughout this study.

Last, but most importantly, I wish to express my profound gratitude to my family: parents, grandparents and sisters for their unconditional love and support throughout my whole life. This work would not have been successful without their forceful encouragement.

Natthakaln Lomchoey

TABLE OF CONTENTS

Chapter	Page
1 INTRODUCTION	
Background	1
Ethnopharmacological uses	1
Structural modification of some naturally derived compounds	3
Objectives of the study	4
2 REVIEW OF LITERATURES	
Chemical constituents of *Ziziphus* plants	5
Cyclopeptide alkaloids	5
Classifications and nomenclature of cyclopeptide alkaloids	5
Structural elucidation of cyclopeptide alkaloids	11
Stereochemistry of cyclopeptide alkaloids	11
Stereochemistry of β–hydroxy amino acid	11
Macrocyclic ring (β–hydroxy– and ring–bound amino acids)	12
Stereochemistry determination by hydrolysis	13
Stereochemistry determination by using synthetic dipeptides	15
Stereochemistry determination by total synthesis of cyclopeptide alkaloids	16
Stereochemistry determination by X–ray diffraction	19
Recent reports on new cyclopeptide alkaloids obtained from *Ziziphus* plants	22
Bioactivities of cyclopeptide alkaloids	31
Antiplasmodial and antimycobacterial activities	31

TABLE OF CONTENTS (continued)

Chapter	Page
2 (continued)	
Antibacterial activities	31
α–Glucosidase inhibitory activity	32
Urease inhibitory activity	32
Antinociceptive effects	33
11β–hydroxysteroid dehydrogenase (11β–HSD) inhibition	33
Pentacyclic triterpenes and saponins	34
Lupane–type triterpene	34
Ceanothane–type triterpene	37
Ursane–type triterpene	39
Oleanane–type triterpene	40
Dammarane–type saponin	41
Jujubogenin saponin	41
Pseudojujubogenin saponin	45
Protojujubogenin saponin	46
Lotugenin saponin	47
Joazeirogenin saponin	49
Other triterpenes	49
Bioactivities of triterpenes and saponins	50
Flavonoids and their glycosides	52
Flavonoids and phenolic compounds	52
Flavonoid *O*–glycosides	54
Flavonoid *C*–glycosides	54
Recent bioactivities of flavonoid and glycosides	54

TABLE OF CONTENTS (continued)

Chapter **Page**

2 (continued)

Simultaneous analysis of bioactive constituents from *Ziziphus* plants..... 55

Structural modification of some naturally derived compounds..... 57

Glycosylation of betulinic acid..... 57

Glycosylation of α–mangostin..... 67

3 EXPERIMENTAL

Plant materials..... 71

General experimental procedures..... 71

Extraction and isolation procedures..... 72

Extraction of the dried root bark of *Z. cambodiana*..... 72

The EtOAc extract..... 72

The MeOH extract..... 73

Extraction of the root of *Z. oenoplia* Mill. var. *brunoniana*..... 80

Extraction of the root of *Z. oenoplia* Mill. var. *oenoplia*..... 81

Bioassay procedure..... 82

Structural modification of some naturally derived compounds..... 82

Glycosylation of betulinic acid..... 82

Glycosylation of α–mangostin..... 93

4 RESULT AND DISCUSSION

Cyclopeptide alkaloids from *Ziziphus* plants..... 105

The MeOH extract of *Z. cambodiana* root bark..... 105

Compounds belong to 4(14)–integerrine–type cyclopeptide alkaloid… 107

TABLE OF CONTENTS (continued)

Chapter	Page
4 (continued)	
Compounds belong to 5(14)–scutianine A–type cyclopeptide alkaloid…	118
Neutral compound related to 14–membered ring cyclopeptide alkaloid.	129
Known alkaloids……..……...	132
The roots of *Z. oenoplia* (L.) Mill. var. *brunoniana*……..	141
The roots of *Z. oenoplia* Mill. var. *oenoplia*……...	141
Structural modification of some naturally derived compounds……...	141
Glycosylation of betulinic acid.....	141
Glycosylation of α–mangostin.....	147
5 CONCLUSION…….	156
BIBLIOGRAPHY……...	159
APPENDIX……	175
GLOSSARY……..……...	216
VITA……..……...	223

LIST OF TABLES

Table		Page
1	Basic subtypes of cyclopeptide alkaloids.....	7
2	NMR data assignments of the configurations of β–OH amino acid.....	12
3	IC_{50} values (μg/mL) for cytotoxicities on three cancer cell lines, antibacterial and antifungal activities.....	50
4	Inhibitory effects of jujubosides A (**153**), B (**154**), A_1 (**163**) and C (**165**), and acetyljujuboside B (**164**) on the histamine release.....	50
5	Inhibitory effects of jujubosides A (**153**), A_1 (**163**), C (**165**), D (**180**) and E (**181**) against lipoxygenase.....	51
6	Cytotoxicity of saponins **238**–**240** and **242**–**247**.....	61
7	Cytotoxicity of synthetic saponins **254**–**265**.....	64
8	Cytotoxicity of (IC_{50}) and haemolytic (HD_{50}) activities of triterpenenes **1**, **114**, **115** and chacotriosidesaponins **266**–**267**.....	67
9	Zone of inhibition measured in antibacterial activity assay of α–mangostin and glycoside derivatives by agar diffusion bioassay against Gram–positive bacteria.....	70
10	Isolated cyclopeptide alkaloids from *Z. cambodiana* plants.....	106
11	NMR spectral data for compounds belong to 4(14)–integerrine–type cyclopeptide alkaloid in $CDCl_3$.....	108
12	^1H–, ^{13}C– and 2D NMR data of compound **E** in $CDCl_3$.....	113
13	^1H–, ^{13}C– and 2D NMR data of compound **B** in $CDCl_3$.....	115
14	^1H–, ^{13}C– and 2D NMR data of compounds **D** in $CDCl_3$.....	118
15	NMR spectral data for compounds belong to 5(14)–scutianine A–type cyclopeptide alkaloid.....	119
16	NMR spectral data for compound A in $CDCl_3$ + methanol–d_4.....	121
17	^1H–, ^{13}C– and 2D NMR data of compound **C** in $CDCl_3$.....	125
18	^1H–, ^{13}C– and 2D NMR data of compound **F** in $CDCl_3$.....	128
19	^1H–, ^{13}C– and 2D NMR data of compound **G** in $CDCl_3$.....	130
20	Comparison of ^1H– and ^{13}C NMR data of compound **H** with frangufoline (**6**)..	133

LIST OF TABLES (continued)

Table		Page
21	^{1}H–, ^{13}C– and 2D NMR data of compound **I** in $CDCl_3$……	137
22	Comparison of ^{1}H– and ^{13}C NMR data of compound **I** with lotusanine (**24**)....	139
23	Bioactivities of cyclopeptide alkaloids (μg/mL)……	140
24	Calculated log*P* of betulinic acid saponins……..	145
25	Condition study for the synthesis of α–mangostin perbenzoylated glycosides……	148
26	Synthesis of α–mangostin perbenzoylated glycosides……	150
27	Debenzoylation of perbenzoylated analogues and calculated log*P* of glycopyranosyl α–mangostins…….……..	151
28	^{1}H– and ^{13}C NMR data of 3,6–di–*O*–glycosyl mangostin analogues……	153
29	^{1}H– and ^{13}C NMR data of 6–*O*–glycosyl mangostin analogues……	154
30	^{1}H– and ^{13}C NMR data of 3–*O*–glycosyl mangostin analogues……	155

LIST OF FIGURES

Figure		Page
1	Structure of betulinic acid (**1**).....	4
2	Structures of homocyclopeptide and heterocyclopeptide.....	6
3	Structures of the 13–, 14– or 15–membered ring cyclopeptide alkaloids.....	6
4	Generic structure for cyclopeptide alkaloids.....	6
5	Structures of paliurine B (**27**) and hemsine B (**28**).....	13
6	Structure of waltherine C (**31**).....	14
7	Stereoscopic view of the minimized mucronine J (**32**) as calculated by MM2 calculations.....	15
8	Structures of paliurine B (**27**) and *L*–Phe(OMe)–*L*–Ile(*N*Me$_2$) (**33**).....	15
9	Structures of mauritines A–F (**34**–**39**) and dipeptide precursor **40**.....	16
10	Structures of compounds **49**–**59**.....	18
11	X–ray crystallographic of franganine methiodide (**7′**).....	19
12	Structures of cyclopeptide alkaloids **60**–**62**.....	20
13	X–ray crystallographic of acetyl derivatives **61′**–**62′**.....	20
14	The X–ray crystal structure for nummularine B methiodide (**5′**).....	21
15	The X–ray crystal structure of amaiouine (**63**).....	21
16	Structures of sativanines **64**–**67**.....	22
17	Structures of compounds **68**–**73**.....	23
18	Structures of oxyphyllines A–D (**74**–**77**).....	24
19	Structures of xylopyrines A–H (**88**–**95**) and jubanine A (**96**).....	26
20	Structure of integerressine (**99**) and crenatine A (**100**).....	29
21	Structures of cyclopeptide alkaloids **101**–**106**.....	30
22	Structures of compounds **107**–**108** and 1–deoxynojirimycin.....	32
23	Structures of compounds **109**–**113**.....	33

LIST OF FIGURES (continued)

Figure		Page
24	Basic structure of lupane–type triterpene.....	34
25	Structures of structure of lupane–type triterpenes **1** and **114**–**125**.....	35
26	Basic structure of ceanothane–type triterpene.....	37
27	Structures of ceanothane–type triterpenes **126**–**135**.....	38
28	Basic structure of ursane–type triterpene.....	39
29	Structures of ursane–type triterpenes **136**–**141**.....	39
30	Basic backbones and structures of oleanane–type triterpenes **142**–**147**.....	40
31	Some basic structures of dammarane–type saponin.....	41
32	Structures of jujubogenin (**148**) dammarane saponins **153**–**165**.....	42
33	Structures of saponins **166**–**169**.....	43
34	Structures of saponins **170**–**181**.....	44
35	Structures of 3–*O*–β–*D*–glucopyranosyl pseudojujubogenin (**182**).....	45
36	Basic backbone and structures of protojujubogenin saponins **183**–**186**.....	46
37	Basic backbone and structures of lotugenin (**151**) and saponins **187**–**195**.....	48
38	Structures of joazeirogenin (**152**), joazeirosides A (**196**) and B (**197**).....	49
39	Structures of compounds **198**–**201**.....	49
40	Structures of flavonoids and phenolic compounds **202**–**214**.....	52
41	Structures of flavonoid *O*–glycosides **215**–**223**.....	53
42	Structures of flavonoid *C*–glycosides **224**–**228**.....	55
43	Structures of compounds **229**–**233**.....	56
44	Trichloroacetimidate (TCA) glycosyl donors **235**–**237**.....	59
45	Trichloroacetimidate (TCA) glycosyl donors **249**–**251**.....	62
46	Selected HMBC COSY and NOESY correlations for compound **E**.....	110

LIST OF FIGURES (continued)

Figure		Page
47	Comparison of ROESY correlations in apetaline B (**105**) and NOESY correlations in compound **E**…….……..	111
48	ORTEP plots of the X–ray crystal structure and Energy–minimized structure of compound **E** by MM2 calculation…….	112
49	Selected HMBC COSY and NOESY correlations of compound **B** ……	116
50	Selected HMBC COSY and NOESY correlations of compound **D** ……	117
51	Selected HMBC COSY and NOESY correlations of compound **A** ……	122
52	Selected HMBC COSY and NOESY correlations of compound **C** ……	124
53	Selected HMBC COSY and NOESY correlations of compound **F** ……	129
54	Selected HMBC COSY and NOESY correlations of compound **G** ……	131
55	Selected HMBC, COSY and NOESY correlations for compound **H** …….	134
56	Selected HMBC, COSY and NOESY correlations for compound **I** ……...	136
57	Structures of lotusanine B (**21**), amaiouine (**63**) and waltherine A (**332**)……..	138
58	Cyclopeptide alkaloids from selected Thai *Z. cambodiana* ……	157
59	Synthetic glycosides ……...	158
60	^{1}H– and ^{13}C NMR of compound **A** in $CDCl_3$ + few drops of CD_3OD (sss3096, cambodine A)…….	176
61	^{1}H– and ^{13}C NMR of compound **B** in $CDCl_3$ (sss3155, cambodine B)……...	177
62	^{1}H– and ^{13}C NMR of compound **C** in $CDCl_3$ (sss4402, cambodine C)…….	178
63	^{1}H– and ^{13}C NMR of compound **D** in $CDCl_3$ (sss4732, cambodine D)…….	179
64	1H– and ^{13}C NMR of compound **E** in CDCl3 (sss4759, cambodine E)……	180
65	1H– and ^{13}C NMR of compound **F** in CDCl3 (sss4759, cambodine F)…….	181
66	1H– and ^{13}C NMR of compound **G** in CDCl3 (sss4767, cambodine G)……	182
67	1H– and 13C NMR of compound H in CDCl3 (sss4449, frangufoline)…….	183

LIST OF FIGURES (continued)

Figure		Page
68	^{1}H– and ^{13}C NMR of compound **I** in $CDCl_3$ (sss4635, lotusanine B)……..	184
69	^{1}H– and ^{13}C NMR of 28–*p*–methoxy benzyl betulinic acid (**1′**) in $CDCl_3$……	185
70	^{1}H– and ^{13}C NMR of 3–*O*–(3,4,6–tri–*O*–acetyl–α–*D*–glucopyranosyl) 28–*p*–methoxy–benzyl betulinic acid (**290**) in $CDCl_3$……..	186
71	^{1}H– and ^{13}C NMR of 3–*O*–α–*D*–glucopyranosyl betulinic acid (**291**) in methanol–d_4……	187
72	^{1}H– and ^{13}C NMR of 3,3–difluoro–3*H*–indol–2–yl 2,3–di–*O*–benzyl–4,6–*O*–benzoyl–α–*D*–galactopyranoside (**292**) in $CDCl_3$……..	188
73	^{1}H– and ^{13}C NMR of 2,3–di–*O*–benzyl–4,6–di–*O*–benzoyl–α–*D*–galactopyranosyl 28–*p*–methoxy–benzyl betulinic acid (**295**)……	189
74	^{1}H– and ^{13}C NMR of 2,3–di–*O*–benzyl–α–*D*–galactopyranosyl 28–*p*–methoxy–benzyl betulinic acid (**296**) in $CDCl_3$……..	190
75	^{1}H– and ^{13}C NMR of 3–*O*–α–*D*–galactopyranosyl betulinic acid (**297**) in $CDCl_3$ + methanol–d_4……	191
76	^{1}H– and ^{13}C NMR of 3,3–difluoro–3*H*–indol–2–yl 2–*O*–benzyl–4,6–*O*–benzylidene–3–*O*–picoloyl–α–*D*–mannopyranoside (**298**) in $CDCl_3$……	192
77	^{1}H– and ^{13}C NMR of 3–*O*–(2–*O*–benzyl–4,6–*O*–benzylidene–3–*O*–picoloyl–β–*D*–mannopyranosyl) 28–*p*–methoxy–benzyl betulinic acid (**301**) in $CDCl_3$.	193
78	^{1}H– and ^{13}C NMR of 3–*O*–(2–*O*–benzyl–4,6–*O*–benzylidene–β–*D*–mannopyranosyl) 28–p–methoxy–benzyl betulinic acid (**302**) in $CDCl_3$ (NL299)……	194
79	^{1}H– and ^{13}C NMR of 3–*O*–(2–*O*–benzyl–β–*D*–mannopyranosyl) 28–*p*–methoxy–benzyl betulinic acid (**303**) in $CDCl_3$ (NL290)……..	195
80	^{1}H– and ^{13}C NMR of 3–*O*–β–*D*–mannopyranosyl betulinic acid (**304**) in methanol–d_4 pyridine–d_5 (NL304)……..	196
81	^{1}H– and ^{13}C NMR of 6–*O*–benzoyl mangostin (**234′**) in $CDCl_3$ (NL110)…….....	197

LIST OF FIGURES (continued)

Figure		Page
82	^{1}H– and ^{13}C NMR of 3,6–di–*O*–(2,3,4,6–tetra–*O*–benzoyl–*β*–*D*–glucopyranosyl)–6–*O*–benzoyl mangostin (**311**) in $CDCl_3$ (NL93, sss6433)…	198
83	^{1}H– and ^{13}C NMR of 3,6–di–*O*–(2,3,4,6–tetra–*O*–benzoyl–*β*–*D*–galactopyranosyl)–6–*O*–benzoyl mangostin (**312**) in $CDCl_3$ (NL59, NL96)…..	199
84	^{1}H– and ^{13}C NMR of 3,6–di–*O*–(2,3,4,6–tetra–*O*–benzoyl–*α*–*D*–mannopyranosyl)–6–*O*–benzoyl mangostin (**313**) in $CDCl_3$ (NL122(1), sss6431)…….	200
85	^{1}H– and ^{13}C NMR of 3,6–di–*O*–*β*–*D*–glucopyranosyl mangostin (**272**) in pyridine–d_5 (NL259, sss6450)……	201
86	^{1}H– and ^{13}C NMR of 3,6–di–*O*–*β*–*D*–galactopyranosyl mangostin (**314**) in pyridine–d_5 (NL247, sss6451)……	202
87	^{1}H– and ^{13}C NMR of 3,6–di–*O*–*α*–*D*–mannopyranosyl mangostin (**315**) in pyridine–d_5 (NL267, sss6452)……	203
88	^{1}H– and ^{13}C NMR of 6–*O*–(2,3,4,6–tetra–*O*–benzoyl–*β*–*D*–glucopyranosyl)–mangostin (**316**) in $CDCl_3$ (NL92)…….	204
89	^{1}H– and ^{13}C NMR of 6–*O*–(2,3,4,6–tetra–*O*–benzoyl–*β*–*D*–galactopyranosyl)–mangostin (**317**) in $CDCl_3$ (NL117, sss6436)…….	205
90	^{1}H– and ^{13}C NMR of 6–*O*–(2,3,4,6–tetra–*O*–benzoyl–*α*–*D*–mannopyranosyl)–mangostin (**318**) in $CDCl_3$ (NL98(1))……	206
91	^{1}H– and ^{13}C NMR of 6–*O*–*β*–*D*–glucopyranosyl mangostin (**273**) in $CDCl_3$ + 15 drops of methanol–d_4 (NL103)……..	207
92	^{1}H– and ^{13}C NMR of 6–*O*–*β*–*D*–galactopyranosyl mangostin (**319**) in $CDCl_3$ + 15 drops of pyridine–d_5 (NL114, sss6447)…….	208
93	^{1}H– and ^{13}C NMR of 6–*O*–*α*–*D*–mannopyranosyl mangostin (**320**) in $CDCl_3$ + 15 drops of methanol–d_4 (NL246, sss6441)……..	209
94	^{1}H– and ^{13}C NMR of 3–*O*–(2,3,4,6–tetra–*O*–benzoyl–*β*–*D*–glucopyranosyl)–6–*O*–benzoyl mangostin (**321**) in $CDCl_3$ (NL128(1), sss6428)……	210

LIST OF FIGURES (continued)

Figure		Page
95	^{1}H– and ^{13}C NMR of 3–*O*–(2,3,4,6–tetra–*O*–benzoyl–*β*–*D*–galactopyranosyl)–6–*O*–benzoyl mangostin (**322**) in $CDCl_3$ (NL238(1), sss6437)……	211
96	^{1}H– and ^{13}C NMR of 3–*O*–(2,3,4,6–tetra–*O*–benzoyl–*α*–*D*–mannopyranosyl)–6–*O*–benzoyl mangostin (**323**) in $CDCl_3$ (NL254, sss6426)……....	212
97	^{1}H– and ^{13}C NMR of 3–*O*–*β*–*D*–glucopyranosyl mangostin (**324**) in $CDCl_3$ + 10 drops of pyridine-d_5 (NL260, sss6444)……	213
98	^{1}H– and ^{13}C NMR of 3–*O*–*β*–*D*–galactopyranosyl mangostin (**325**) in $CDCl_3$ + 15 drops of pyridine-d_5 (NL261, sss6443)……	214
99	^{1}H– and ^{13}C NMR of 3–*O*–*α*–*D*–mannopyranosyl mangostin (**325**) in $CDCl_3$ + 15 drops of pyridine-d_5 (NL262, sss6445)……	215

LIST OF SCHEMES

Scheme		Page
1	Sanjoinine A or frangufoline (**29**) was transformed into its epimer, sanjoinine–Ah_1 (**30**), by heat treatment	14
2	Key macrocyclization steps by intramolecular amidation **41**–**44**	17
3	EIMS fragment patterns of oxyphylline A (**74**)	25
4	Partial hydrolysis procedure of xylopyrines A (**88**), B (**89**), D (**91**), E (**92**) and jubanine A (**96**)	28
5	Partial hydrolysis procedure of xylopyrine F (**93**)	28
6	Synthesis of betulinic acid glycosides **238**–**240**	59
7	Synthesis of lupeol glycosides **242**–**244**	60
8	Synthesis of betulin glycosides **245**–**247**	60
9	Synthesis of saponins **254**–**265**	63
10	Synthesis of saponins **266**–**267**	67
11	Synthesis of α–mangostin glycosyl analogues	68
12	Structures of α–mangostin glycosides obtained from enzymatic synthesis	69
13	Extraction procedure of *Z. cambodiana* root bark	74
14	Isolation of compounds from the EtOAc extract I of *Z. cambodiana* root bark	75
15	Isolation of compounds from the EtOAc extract II of *Z. cambodiana* root bark	76
16	Isolation of compounds from the MeOH of *Z. cambodiana* root bark	77
17	Extraction procedure of *Z. oenoplia* Mill. var. *brunoniana* root	80
18	Extraction procedure of *Z. oenoplia* Mill. var. *oenoplia* root	81
19	EI fragments of compound **E**	109

LIST OF SCHEMES (continued)

Scheme		Page
20	EI fragments of compound **A**.....	120
21	EI fragments of compound **F**.....	126
22	General mechanisms of glycosylation.....	142
23	3–*O*–Picoloyl–assisted β–*D*–mannosylation.....	143
24	Condition studies of the synthesis of betulinic acid saponins.....	144
25	Overall synthetic sequences of betulinic acid saponins.....	146
26	Synthesis of α–mangostin glycosides.....	149

CHAPTER 1
INTRODUCTION

Background

The genus *Ziziphus* is a group of spiny shrubs or thorny scandent and small trees that belongs to the buckthorn family Rhamnaceae (Smitinand, 2001). Their edible fruits such as *Z. jujube* (Jujube) and *Z. mauritiana* (Ber, Indian jujube or Phutsa in Thai) are important plants for the economy. Dried jujube fruits have been commonly utilized as food, food additive, and flavoring for thousands of years due to their high nutritional value (Li, J. et al., 2007). In addition, some *Ziziphus* plants offer a useful supply of the animal feedstock, nutrients, medicine, construction material and fuel (Goyal, Nagori and Sasmal, 2012). The *Ziziphus* plants are widespread in tropical and subtropical areas with a family of 58 genera and 900 species worldwide (Bhattacharyya and Johri, 1998), particularly in arid regions (Gardner, Sidisunthorn and Anusarnsunthorn, 2000) with 100 species distributed in the tropical America, Africa, the Mediteranean region, Indo–Malaysia, and Australia, and also the tropical parts of India, Nepal, Pakistan, Bangla Desh and Sri Lanka (Bhattacharyya and Johri, 1998) and Thailand (Smitinand, 2001).

There are only ten *Ziziphus* plants of nine species in Thailand that include *Z. angustifolia* (Miq.) Hatus Ex Steenis (Phutsa bai liam), *Z. attopoensis* Pierre (Kamlang suea khrong), *Z. brunoniana* Clarke ex Brand. or *Z. oenoplia* Mill. var. *brunoniana* (Nam lep maeo). *Z. oenoplia* Mill. var. *oenoplia* (Nam lep yiao), *Z. calophylla* Wall. (Chin chi), *Z. cambodiana* Pierre (Takhrong), *Z. incurva* Roxb. (Ta–chu–mae), *Z. jujuba* Mill. (Phutsa chin), *Z. mauritiana* Lam. or *Z. jujube* Lam. (Phutsa) and *Z. rugosa* Lam. (Ma khwat) (Smitinand, 2001).

Ethnopharmacological uses

Various medicinal properties are attributed to many species of the Rhamnaceous *Ziziphus* in the traditional medicine. They have been used in folk medicine to cure disorders in several countries, and below is a list of representative examples.

The *Z. apetala* fruits have been used as a Chinese folk herb to relieve symptoms of eczema and skin allergies (Han, J. et al., 2011).

The leaves and aerial parts of *Z. glabrata* (or *Z. trinervia*) are traditionally used in Indian folk medicine to treat inflammation, to relieve pain, convulsions and viral infections (Kirtikar, et al., 1975).

The stem bark aqueous extract of *Z. joazeiro* is acclaimed to be a powerful Brazilian medicine against fever, respiratory tract infections, chronic bronchitis, dental plaque and other ailments (Nunes et al., 1987).

Z. jujuba also known as Jujube has been used as a traditional Chinese medicine for the treatment of fatigue, anorexia and loose stools in deficiency syndromes of the spleen and of hysteria in women (Li, J. et al., 2007).

Z. lotus is used as a traditional herb in Libya for treatment of sore throats; alleviate stress and helps to relieve symptoms of the common cold (Naili et al., 2010).

Z. mucronata is employed by the natives in central and southern Africa for the treatment of diarrhea, dysentery, and skin infections (Joullie and Nutt, 1983).

Z. nummularia is a medically important herb in Pakistan. The leaves of *Z. nummularia* are commonly fed to goats and sheep besides grazing (Maharaj and Dwivedi, 2002). *Z. nummularia* is also used in the medicinal system of Indo–Pakistan; the bark is known to have antibacterial and analgesic activities (Shah et al., 1990).

Z. rugosa is used for the treatment of diarrhea, menorrhagia and infection of teeth in the Indian folk medicine (Kirtihar and Basu, 1975; Acharya et al., 1988).

Z. sativa bark is used in Pakistan to heal ulcers and wounds. The gum of this plant species is used to treat eye disease while the syrup of the dried fruit is used to treat bronchitis (Kirtikar and Basu, 1984).

Z. spina–christi has various medicinal properties such as ash of the wood mixed with vinegar is prescribed for local application in the treatment of serpent bites in Egypt. In addition, the Bedouins and Egyptians use the cataplasms of leaves for abscesses and furuncles and cataplasms of fresh green leaves are put on swollen eyes at night (Boulos, 1983).

The seed of *Z. vulgaris* var. *spinosus* is reported to be the most important herb for the treatment of insomnia, as sedatives, as nerve tonics (Huh, 1981), and to treat arrhythmias (Cho, Ro and Hong, 1976) in Chinese traditional medicine.

In Thailand, bark and leaf of *Z. mauritiana* are used as a treatment of diarrhea, vomiting and ulcers, fruit is used to treat diarrhea and fever (Bunyapraphatsara and Chokechaijaroenporn, 1999).

The stem of *Z. cambodiana* is used as an antiinfectious herb (Suksamrarn et al., 2006). Moreover, in Cambodia it is commonly used traditionally as a treatment of fever (Hout et al., 2006).

The root bark of *Z. oenoplia* has been used for treatment of ulcers, antiinfectious, antidiabetic and diuretic in Thai folk medicine (Bunyapraphatsara and Chokechaijaroenporn, 2000). It is one of the folk herbal plants, commonly used as hepaoprotective agents in India (Pundir et al., 2009).

Previous phytochemical studies have established the genus *Ziziphus* to be a rich source of cyclopeptides (Tschesche, Kaussmann and Manske, 1975), lupane and ceanothane triterpenes (Suksamrarn et al., 2006). Other types of compounds discovered include saponins (Renault et al., 1997), flavonoids (Maciuk et al., 2003), flavonoid glycosides (Li, X. et al., 2007), steroids (Chauhan and Srivastava, S. K., 1978), pectin, lipids (Goyal, Nagori and Sasmal, 2012) and aliphatic compounds (Srivastava, S. K. and Srivastava, S. D., 1979). Some *Ziziphus* saponins such as jujubosides were reported to be haemolytic, anxiolytic, sedative and sweetness inhibiting agent. Cyclopeptide alkaloids exhibited sedative, hypoglycemic, anti–infectious, antiplasmodial, antimicrobial, antidiabetic, diuretic, anti–inflammatory, analgesic and anticonvulsant activities (Goyal, Nagori and Sasmal, 2012).

From these interesting biological properties, some Thai *Ziziphus* plants (*Z. cambodiana, Z. oenoplia* Mill. var. *brunoniana* and *Z. oenoplia* Mill. var. *oenoplia*) are therefore selected for this study to search for bioactive compounds.

Structural modification of some naturally derived compounds

Several naturally occurring compounds exhibited less potent bioactivities because of their limited solubility in aqueous medium and/or stability. There are several routes that can be used to improve these issues, such as structural modification into water soluble salts, polyhydroxy groups or glycosides.

This study will be focused on the structural modification of some bioactive natural compounds available in our laboratory such as betulinic acid (**1**). Compound **1** is the major

widely distributed pentacyclic lupane–type triterpene in *Ziziphus* plants including in Thai *Z. oenoplia* (Aunchai, 2002), *Z. cambodiana* (Panseeta, 2004; Suksamrarn et al., 2006), *Z. rugosa* (Netsawangwicha, 2005), *Z. attopoensis* (Maneekaew, 2007) and *Z. mauritiana* (Panseeta, 2009). It has been reported as anti–HIV (Kashiwada et al., 2000), antiplasmodial (Ziegler et al., 2004; Suksamrarn et al., 2006), antituberculosis (Cantrell et al., 2001; Suksamrarn et al., 2006) and anticancer (You et al., 2003) agents. Zuco et al. (2012), have proved that betulinic acid is selective against cancer cells without affecting normal cells.

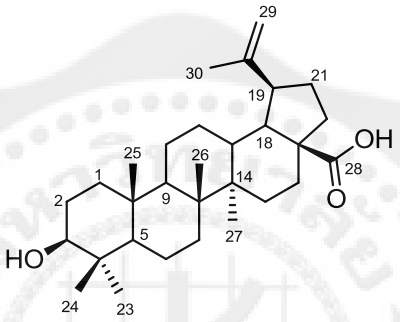

Figure 1 Structure of betulinic acid (**1**)

The pharmacological uses of **1** as therapeutic agents are limited however, because of their poor aqueous solubility and pharmacokinetic properties including absorption, distribution, metabolism and elimination (Udeani et al., 1999). In order to overcome these limitations, modification of betulinic acid into its aqueous soluble analogues would be of high interest.

Objectives of the study

1. To isolate and purify chemical constituents from Thai *Ziziphus* plants, *Z. cambodiana, Z. oenoplia* Mill. var. *brunoniana* and *Z. oenoplia* Mill. var. *oenoplia.*
2. To elucidate the chemical structures of the isolated compounds.
3. To modify the chemical structure of some naturally derived compounds.
4. To evaluate some biological activities of the obtained phytochemicals and/or the synthesized analogues.

CHAPTER 2
REVIEW OF LITERATURE

The aims of this study are to isolate, purify and elucidate the chemical constituents from Thai *Z. cambodiana*, *Z. oenoplia* Mill. var. *brunoniana* and *Z. oenoplia* Mill. var. *oenoplia*, as well as to perform the structural modification of natural compounds and evaluate their bioactivity. Therefore, this section presents a literature overview of the current state–of–the–art in these areas.

Chemical constituents of *Ziziphus* plants

Previous studies have revealed that the genus *Ziziphus* contains various constituents as follows:

1.1 Cyclopeptide alkaloids

1.1.1 Classification and nomenclature of cyclopeptide alkaloids

Cyclopeptide alkaloids are widely distributed among plants of the Rhamnaceae family and have also been found in several other families including Asteraceae, Celastraceae, Euphobiaceae, Menispermaceae, Pandaceae, Rubiaceae, Sterculiaceae and Urticaceae. These alkaloids can be found in almost every part: leaves, stem bark, root bark and seed. They often occur in minute amounts and as complex mixtures. The total yield from the dried plant material is ranging between 0.01–1 % (Gournelis, Laskaris and Verpoorte, 1998).

The plant cyclopeptides are divided into two classes according to systematic structural classification of the skeletons, whether formed with amino acid peptide bonds or not (Tan and Zhou, 2006). Many of these are homocyclopeptides, formed with amino acid peptide bonds, and heterocyclopeptides, comprising amino acid peptide bonds and styrylamine moiety (Figure 2).

Cyclopeptide alkaloids are found as characteristic components of the plant species that belong to the genus *Ziziphus*. These heterocyclopeptides are typically based on macrocyclic rings that embody a *p*– or *m*–ansa structures with one styrylamine moiety and contain three or four α–amino acid residues. Among these, in 10– or 12–membered rings the peptide type bridge spans the 1,3 or 1,4 positions of benzene ring. In 13– and 14–membered rings consist of a 10–membered bridge spans involving *p*– and *m*–ansa,

respectively, whereas the 15–membered compounds embody a *m*–ansa structure with a 12–membered ring bridge spans (Figure 3) (Gournelis, Laskaris and Verpoorte, 1998).

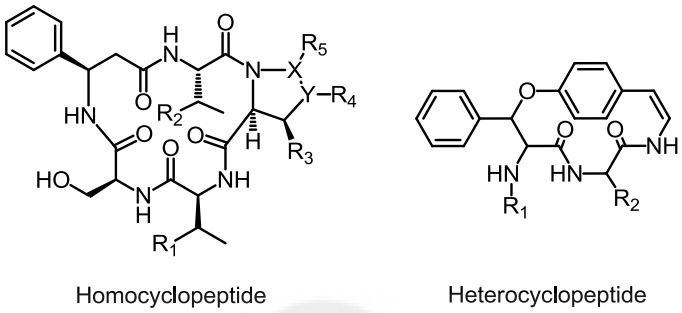

Figure 2 Structures of a homocyclopeptide and a heterocyclopeptide

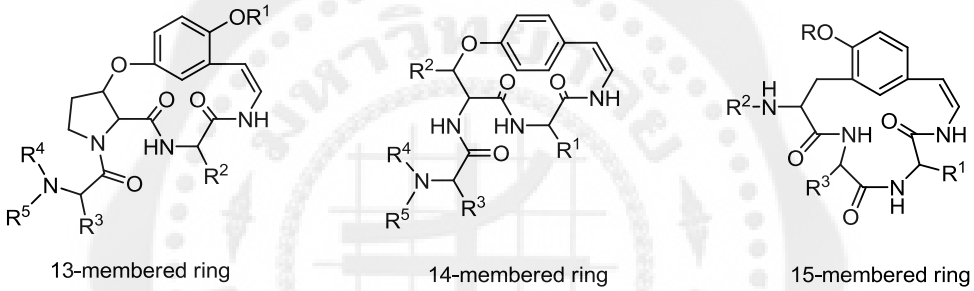

Figure 3 Structures of the 13–, 14– or 15–membered ring cyclopeptide alkaloids

The 13–, 14– or 15–membered ring cyclopeptide alkaloids are classified according to the number of 4– (bearing A, B, C and D) or 5– (with A, B, C, D and E) units in the structural skeletons (Figure 4). Consequently the cyclopeptide alkaloids are subdivided into groups with the following annotations: 4(13)–, 5(13)–, 4(14)–, 5(14)–, and 5(15)–. The 4(14)– and 5(14)–compounds are further subdivided according to the nature of the β–OH amino acid (unit B) (Gournelis, Laskaris and Verpoorte, 1998).

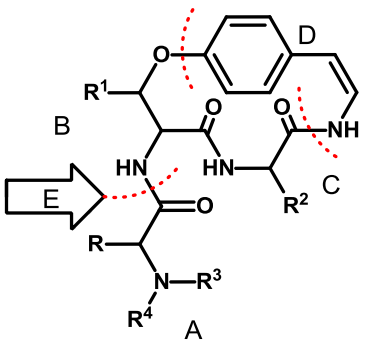

A = basic terminal (end) amino acid,

B = β–hydroxy–amino acid,

C = ring–bound amino acid,

D = styrylamine unit,

Sometimes between A and B unit an additional (intermediary) amino acid is interposed and designated as E.

Figure 4 A generic structure of cyclopeptide alkaloids

The subtypes of cyclopeptide alkaloids are classified according to the first compound found as shown in Table 1 (Gournelis, Laskaris and Verpoorte, 1998).

Table 1 Basic subtypes of cyclopeptide alkaloids

Macrocyclic rings	Number of units	Subtypes
13–membered	4	**4(13)–Nummularine C–type** The B and D units are *β*–hydroxyproline and an oxystyrylamine moiety, respectively, units A and C can be any amino acids. For example: 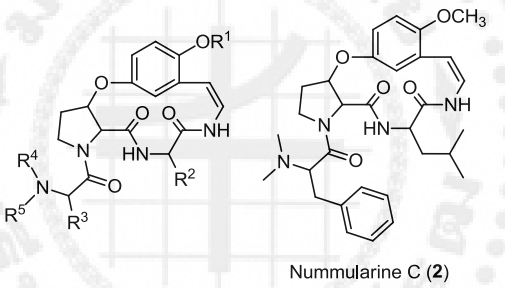 Nummularine C (**2**) 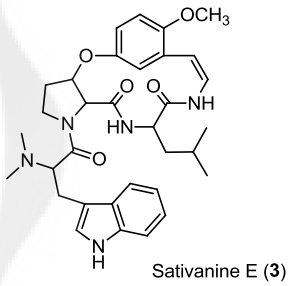 Sativanine E (**3**)
	5	**5(13)–Ziziphine A–type** The B and D units are *β*–hydroxyproline and an oxystyrylamine moiety, respectively, units A, C and E can be any amino acids. For example: 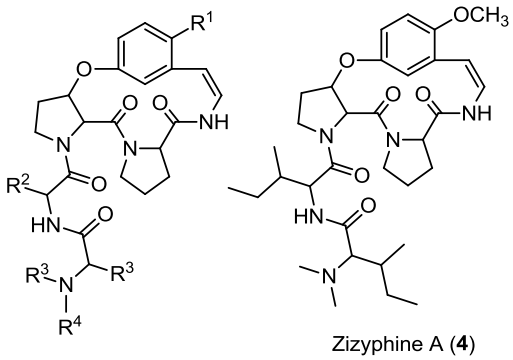 Zizyphine A (**4**) 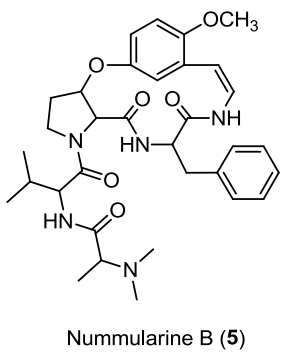 Nummularine B (**5**)

Table 1 (continued)

Macrocyclic rings	Number of units	Subtypes
14–membered	4	**4(14)–Frangulanine–type** The B and D units are *β*–hydroxyleucine and a styrylamine moiety, respectively, units A and C can be any amino acids. For example: 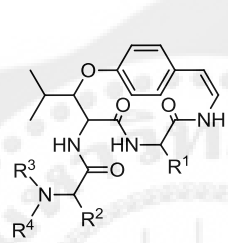 Frangulanine (**6**) or Ceanothamine A or Daechuine S2) 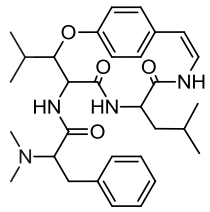 Franganine (**7**) **4(14)–Integerrine–type** The B and D units are *β*–hydroxyphenylalanine and a styrylamine, respectively, units A and C can be any amino acids. For example: 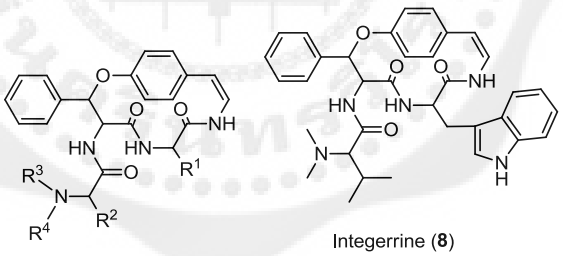 Integerrine (**8**) 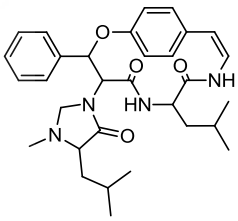 Nummularine G (**9**) **4(14)–Amphibine F–type** The B and D units are *β*–hydroxyproline and a styrylamine, respectively, units A and C can be any amino acids. For example: 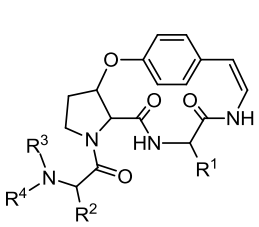 Amphibine F (**10**) 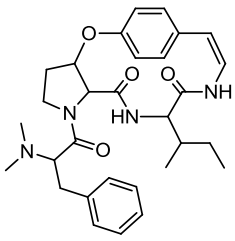 Lotusine A (**11**)

Table 1 (continued)

Macrocyclic rings	Number of units	Subtypes
14–membered	4	**4(14)–Pandamine–type** The B unit is *β*–hydroxyleucine. Unit D is a 2–alkoxy–2–(*p*–hydroxyphenyl)ethylamine, instead of a styrylamine moiety, units A and C can be any amino acids. For example: 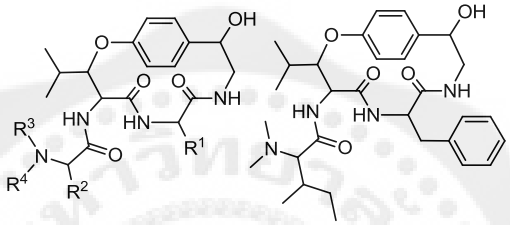 Pandamine (**12**) 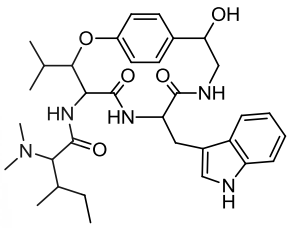 Discarine K (**13**)
	5	**5(14)–Scutianine A–type** The B unit is *β*–hydroxyproline or *β*–hydroxyphenylalanine. Unit D is a styrylamine moiety, units A, C and E can be any amino acids. For example: 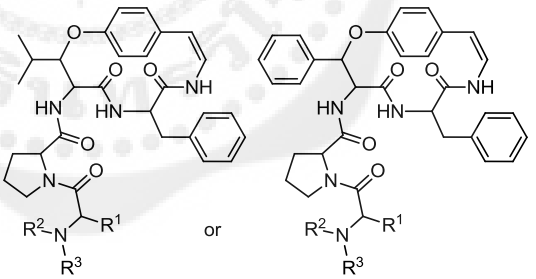 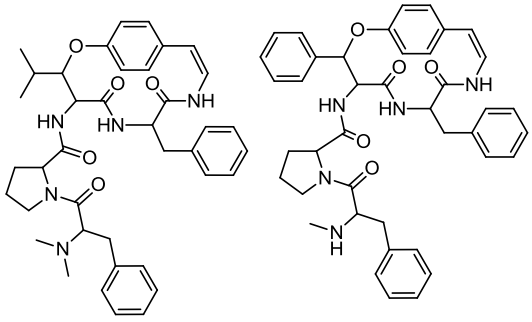 Scutianine A (**14**) Feretine (**15**) (or *N*-Desmethyladouetine Z)

Table 1 (continued)

Macrocyclic rings	Number of units	Subtypes
14–membered	5	**5(14)–Amphibine B–type** The B and D units are *β*–hydroxyproline and a styrylamine, respectively, units A and C can be any amino acids. For example: 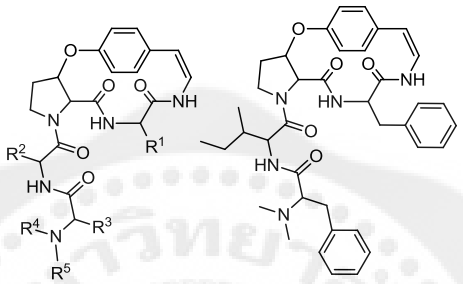 Amphibine B (**16**) 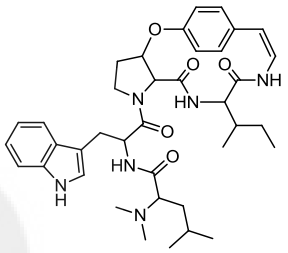 Amphibine E (**17**)
15–membered	4	**4(15)–Mucronine A–type** The cyclopeptide alkaloids of this type consist of 3 units of amino acid (A, B, and C) and include unit D that is an oxystyrylamine moiety. For example: 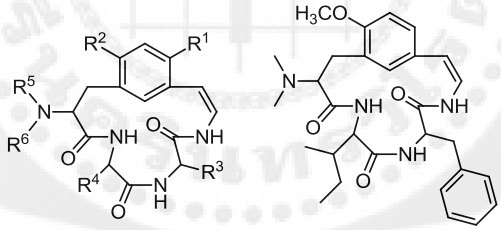 Mucronine A (**18**) 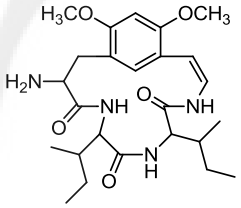 Mucronine G (**19**)
14–membered	4 or 5	**Neutral compounds related to 14–membered cyclopeptide alkaloids** The B unit is any *β*–hydroxyamino acids. Units C and D can be any amino acids and a styrylamine residue, respectively, as well as a neutral moiety as unit A, such as coumaroyl,. For example: 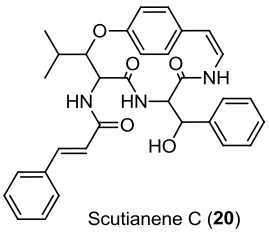 Scutianene C (**20**) 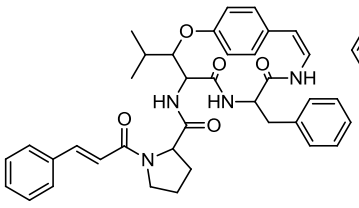 Lotusanine B (**21**) 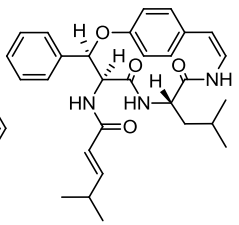 Discarene C (**22**)

1.1.2 Structural elucidation of cyclopeptide alkaloids

Mass spectrometry (MS) and NMR spectroscopy are significant tools in structural elucidation of cyclopeptide alkaloids. MS is extensively used for structural determination that allows to compare the new data with previous value reports for various groups of cyclopeptide alkaloids. Electron impact mass spectrometry (EIMS) is extensively used for structure elucidation of cyclopeptide alkaloids. EIMS helps to describe a constant basic pattern of fragments that are representative of the nature of the amino acid units present in each cyclopeptide alkaloid (*see section* 2.1.4, p.25) (Tschesche, Kaussmann and Manske 1975; Gournelis, Laskaris and Verpoorte, 1998).

The 13–membered ring cyclopeptides bearing the relieved conjugation of the styrylamine chromophore, displayed the intense UV absorption bands at around 270 and 320 nm. Conversely, the 14–membered cyclopeptide alkaloids lacked these absorption bands due to the ring strain of the macrocyclic system (Gournelis, Laskaris and Verpoorte, 1998). As an exception, 14–membered cyclopeptides containing the coumaroyl unit show absorption bands at around 240 and 280 nm (Abu–Zarga et al., 1995). The presence of a tryptophan moiety showed the absorption bands at around 220, 270 and 290 nm (Gournelis, Laskaris and Verpoorte, 1998). Their IR spectra also exhibited diagnostic peaks for the functional groups of amino and amido (3291–3393 cm^{-1}), amide (1679–1693 cm^{-1}) and aryl ether (1221–1237 cm^{-1}) (Panseeta et al., 2011).

Notably, some cyclopeptide alkaloids developed an intense blue coloration with anisaldehyde–H_2SO_4 reagent on TLC. However, for some cyclopeptide alkaloids comprising a tryptophan unit, a strong orange coloration was observed instead (Suksamrarn et al., 2005).

1.1.3 Stereochemical determination in cyclopeptide alkaloids

1.1.3.1 Stereochemistry of *β*–hydroxy amino acid

^{1}H NMR spectral analysis for the vicinal coupling constant of *β*–OH amino acid, H–8 and H–9 have proved useful for determining of the structure and relative configuration of cyclopeptide alkaloids. In particular, the coupling constant $^3J_{8,9}$ of the *erythro* vicinal protons in waltherine B (**23**) (Morel et al., 1999) and scutianine E (**24**) (Tschesche et al., 1974a) was found to be approximately 8 Hz**.** However, for the *threo* compounds, such as condaline A (**25**) (Morel et al., 2002) and discarene D (**26**) (Giacomelli

et al., 2001), $^{3}J_{8,9}$ *ca.* 0–2 Hz (Table 2). ^{13}C NMR spectroscopy is used for the elucidation of the absolute configuration of the β–OH amino acid. For example, in scutianine E (**24**), which was assigned the *D–erythro* configuration, C–9 and C–8 resonate at *ca.* 87 and 53 ppm, respectively. In case of the *D–erythro* form, the C–β or C–9 resonate at *ca*. 87 ppm while in *L–erythro* form those are at *ca.* 81 ppm. C–α or C–8 display peaks at *ca*. 53 ppm for the *D–erythro* form and at *ca*. 55 ppm for the *L–erythro* form (Table 2).

Table 2 NMR data assignment for different configurations of β–OH amino acid

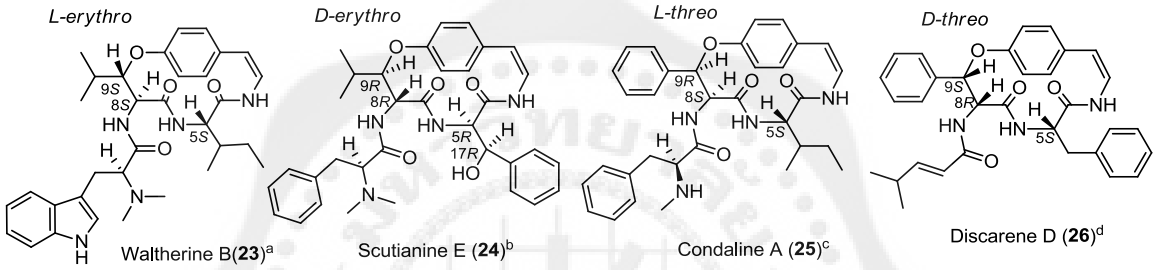

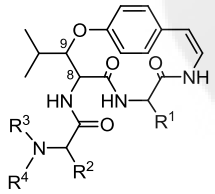

Configuration	*ca.* δ_C of C–8 (ppm)	*ca.* δ_C of C–9 (ppm)	*ca.* $J_{8,9}$ (Hz)
L–erythro[a]	55	81	8
D–erythro[b]	53	87	8
L–threo[c]	55	86	0–2
D–threo[d]	55	82	0–2

[a] Morel et al., 1999 ; [b] Tschesche et al., 1974a ; [c] Morel et al., 2002 ; [d] Giacomelli et al., 2001

1.1.3.2 Macrocyclic ring (β–hydroxy– and ring–bound amino acids)

Stereochemistry in the macrocyclic ring nucleus of 13–membered ring cyclopeptide alkaloids, such as zizyphine A–type paliurine B (**27**), were absolutely assigned by the CD spectral analysis, which exhibited three strong negative Cotton effects (CE) at 252, 267 and 314 nm (Lin et al., 2000), and small positive CEs at 229 and 356 nm. This spectra indicated the 5*S*,8*S*,9*S*–configuration (Schmidt et al., 1983), whereas, the spectra for 14–membered ring displayed intense negative CE at around 240 nm and a weak positive one at around 290 nm, also showing the same 5*S*,8*S*,9*S*–configuration as that of 13–membered cyclopeptides (Gournelis, Laskaris and Verpoorte, 1998). 5(14)–Amphibine

B–type hemsine A (**28**) showed a strong negative CE at 236 nm and a positive CE at 274 nm (Lin et al., 2003).

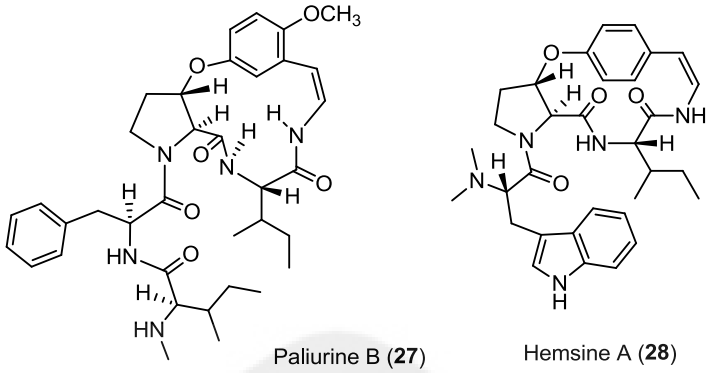

Figure 5 Structures of paliurine B (**27**) and hemsine B (**28**)

1.1.3.3 Stereochemistry determination by hydrolysis

The absolute configuration of the ring–bound amino acid and the terminal amino acid residues was successfully confirmed by the chiral assignment of hydrolisate amino acid after the chemical degradation.

The absolute stereochemistry of the C–5 ring–bound alanine and of the *N,N*–dimethyl tryptophan side chain in 4(14)–frangulanine–type waltherine C (**31**) was determined by total hydrolysis in acidic and basic conditions. Thus, the total hydrolysis of waltherine C (**31**) was performed in a sealed tube at 110 ^{o}C with 6 N HCl for 15 h, followed by the treatment with $Ba(OH)_2$–$8H_2O$ at 125 ^{o}C for 20 h. The hydrolysate was subsequently determined by chiral phase gas chromatography (CPGC). The results showed that both *N,N*–dimethyl tryptophan and alanine have an *L*–(*S*)–configuration. The β–hydroxyleucine of waltherine C (**31**) (Figure 6) was classified as *L*–*erythro*–(8*S*,9*S*)–configuration (Morel et al., 1999).

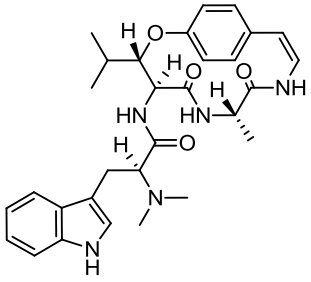

Figure 6 Structure of waltherine C (**31**)

Han et al. reported on the assignment of the absolute stereochemistry of sanjoinine A or frangufoline (**29**) and its epimer, sanjoinine Ah_1 (**30**) by heat treatment at 220 ^{o}C (Scheme 1). The configurations of the basic end *N,N*–dimethylphenylalanine and leucine of the ring–bound amino acid in sanjoinine A (**29**) and artifact sanjoinine Ah_1 (**30**) were determined by gas chromatography of diastereomeric derivatives of individual amino acid units in the hydrolysates. The absolute configurations of *N,N*–dimethylphenylalanine in sanjoinine A or frangufoline (**29**) and sanjoinine Ah_1 (**30**) were elucidated to be an (*S*)–*L*–form and (*R*)–*D*–form, respectively. The leucine moiety in both structures was proven to be an (*S*)–*L*–form (Han, B. H. et al., 1987).

Scheme 1 Sanjoinine A or frangufoline (**29**) was transformed into its epimer, sanjoinine–Ah_1 (**30**), by heat treatment

The absolute configuration of the ring bound amino acid, isoleucine and the basic end *N,N*–dimethyl leucine of 4(14)–amphibine B–type mucronine J (**32**) was determined as all–*S*–configuration bearing *L*–*erythro*–(8*S*,9*S*)–β–hydroxyleucine. For the purpose of this study, mucronine J (**32**) was treated with 8 N HCl in a sealed tube at 110 ^{o}C. The hydrolysates were subsequently derivatized for GC analysis by dissolving in CH_2CL_2, followed by the treatment with trifluoroacetic anhydride. Then, the mixture was successively analyzed on a chiral Chirasil–*L*–Val (*N*–propionyl–*L*–valine–*tert*butylamide polysiloxane) quartz capillary column. The structure of mucronine J (**32**) was calculated using molecular modeling with the MM2–derived force field to obtain the lowest energy conformation (Figure 7) (Auvin et al., 1996).

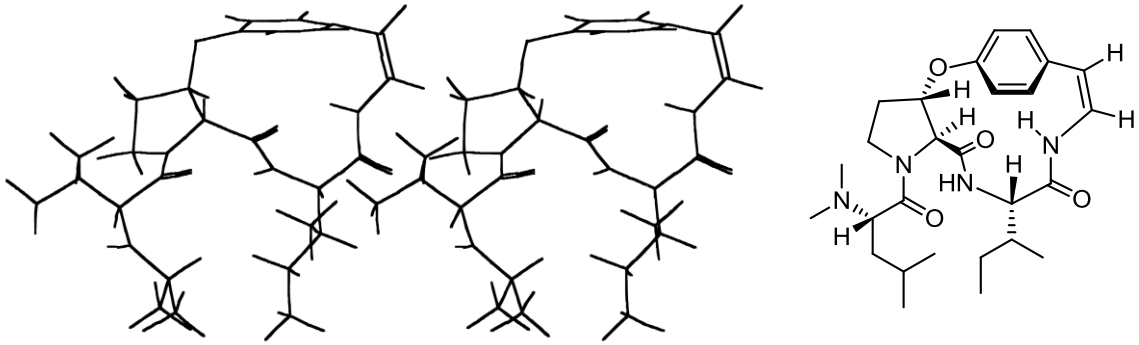

Figure 7 Stereoscopic view of the minimized mucronine J (**32**) as calculated by MM2 calculations

1.1.3.4 Stereochemical determination of the intermediate and basic end amino acid

The stereochemistry of the intermediate and basic end amino acids in the 5(13)–zizyphine A–type cyclopeptide alkaloid paliurine B (**27**) was assigned as the *L*–form (all–*S*–configuration) by analysis of its NMR spectra and confirmed by the NMR analysis of the related synthetic dipeptide *L*–Phe(OMe)–*L*–Ile(NMe_2) (**33**) (Figure 8) (Lin et al., 2000).

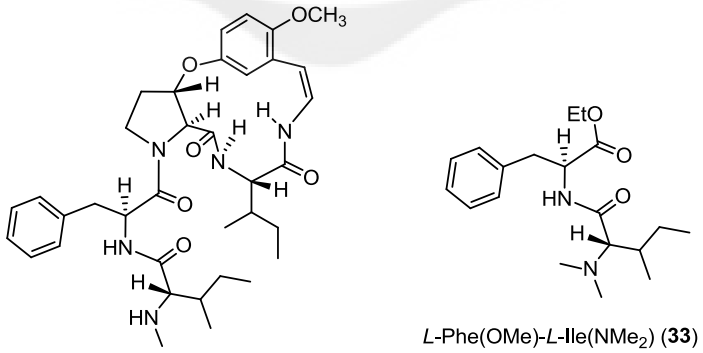

Paliurine B (**27**)

L-Phe(OMe)-*L*-Ile(NMe_2) (**33**)

Figure 8 Structures of paliurine B (**27**) and *L*–Phe(OMe)–*L*–Ile(NMe_2) (**33**)

1.1.3.5 Stereochemistry determination by total synthesis of cyclopeptide alkaloids

The absolute stereochemistry of some isolated cyclopeptide alkaloids were confirmed by comparison with NMR spectra of synthetic cyclopeptide alkaloids.

For example, mauritines A–F (**34**–**39**) cyclopeptide alkaloids of 5(14)–amphibine B–type (for **34**–**35** and **37**–**39**) and 4(14)–amphibine F–type (for **36**) (Figure 9) were synthesized to confirm their absolute stereochemistry as all *S*–configurations. This approach led to complete assignment of proton and carbon NMR spectroscopy signals for these natural products. The synthesis of mauritines A–F (**34**–**39**) was accomplished featuring a strategy involving the key cycloetherification reaction based on an intramolecular S_NAr reaction, starting from cyclization of dipeptide precursor **40** to give a macrocyclic ring (Laib et al., 2000; Cristau et al., 2005).

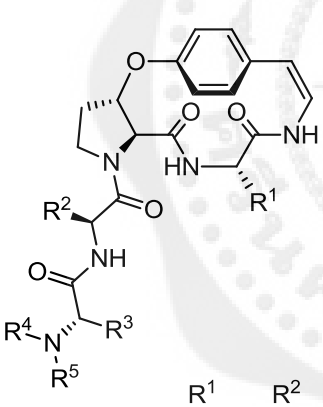

	R^1	R^2	R^3	R^4	R^5
Mauritine A (**34**) :	A	D	CH_3	CH_3	CH_3
Mauritine B (**35**) :	A	D	B	CH_3	CH_3
Mauritine D (**37**) :	B	E	B	CH_3	CH_3
Mauritine A (**38**) :	C	D	CH_3	CH_3	CH_3
Mauritine F (**39**) :	A	D	CH_3	CH_3	H

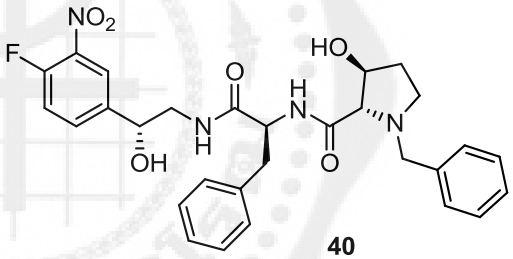

40

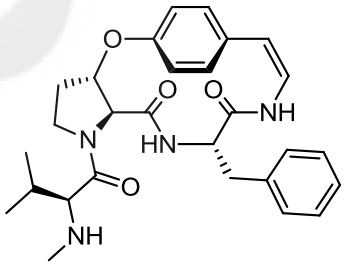

Mauritine C (**36**)

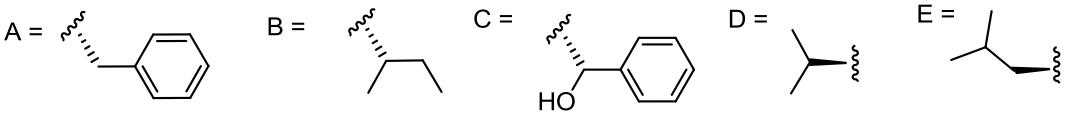

Figure 9 Structures of mauritines A–F (**34**–**39**) and dipeptide precursor **40**

The absolute configurations of 5(13)–zizyphine A–type cyclopeptide alkaloids paliurines E (**41**) and F (**42**), ziziphines N (**43**) and Q (**44**) (Scheme 2) were also confirmed by total syntheses of these cyclopeptide alkaloids. A key feature of the syntheses of macrocyclic rings **45** (for **41** and **42**) and **46** (for **43** and **44**) is an intramolecular amidation of vinyl iodide **47** (for **44**) and **48** (for **45**). This approach allowed to address two synthetic challenges associated with cyclopeptide alkaloids, the formation of the enamide and macrocyclization, concomitantly (Scheme 2). The absolute configuration of paliurines E (**41**) and F (**42**), ziziphines N (**43**) and Q (**44**) were elucidated as all–*S*–configuration (Toumi et al., 2009). Moreover, the comparison of spectroscopic data for the synthetic ziziphines N (**43**) and Q (**44**) (Toumi et al., 2009) showed the signals matching those of the naturally isolated compounds (Suksamrarn et al., 2005). Thus, the absolute configuration of natural ziziphines N (**43**) and Q (**44**) reported by the Suksamrarn group were additionally confirmed by this work.

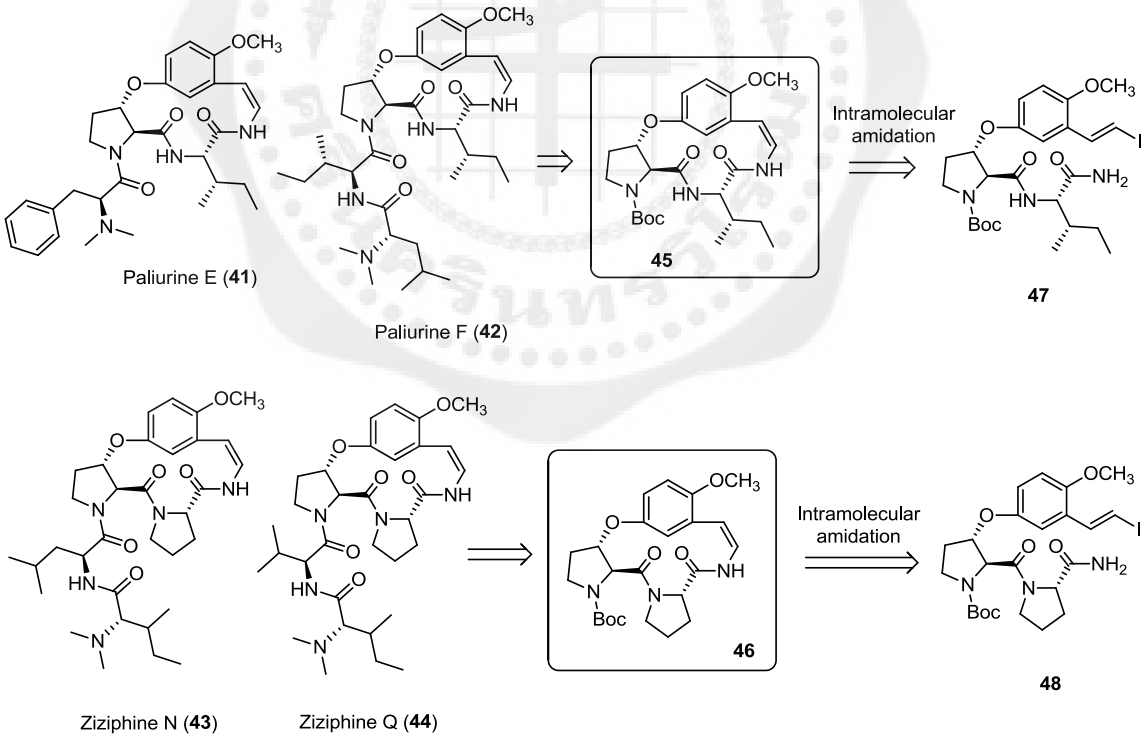

Scheme 2 Key steps for macrocyclization by intramolecular amidation

Mostardeiro et al., have determined the stereochemistry of three 4(14)–integerrine–type cyclopeptide alkaloid discarines C (**49**) and D (**50**), and myrianthine A (**51**) (Figure 10) isolated from *Discaria febrifuga*. This was accomplished by a combination of NMR spectral analysis, enantioselective gas chromatography, and comparison of NMR data with those of synthetic tripeptides, key precursors of the target compounds. The data for discarines C (**49**) and D (**50**), and myrianthine A (**51**) indicated the presence of the same *β*–hydroxyphenylalanine and the same basic end amino acid (*N,N*–dimethylleucine) residued. In addition, the data indicated the presence of a different unit for the ring–bound amino acid as leucine, phenylalanine, isoleucine for compounds **49–51**, respectively (Figure 10). The synthesis of peptides was started from dipetide *Z*–*L*–Leu–*D,L*–*threo*–Phe–(*β*–OH)–OH (**52**). The *L*– and *D*–*erythro* 3–phenylserine derivatives (**53**–**55**) were obtained by Mitsunobu reaction of the *threo*–tripeptides. Importantly, the byproducts (**56**–**58**) were also possible synthetic intermediates of rare cyclopeptide alkaloids comprising imidazolidin–4–one ring. Thus, this strategy also allowed to obtain the corresponding peptide with an imidazolidin–4–one ring, such as nummuraline G (**9**) and sativanine B (**59**) (Figure 10) (Mostardeiro et al., 2013).

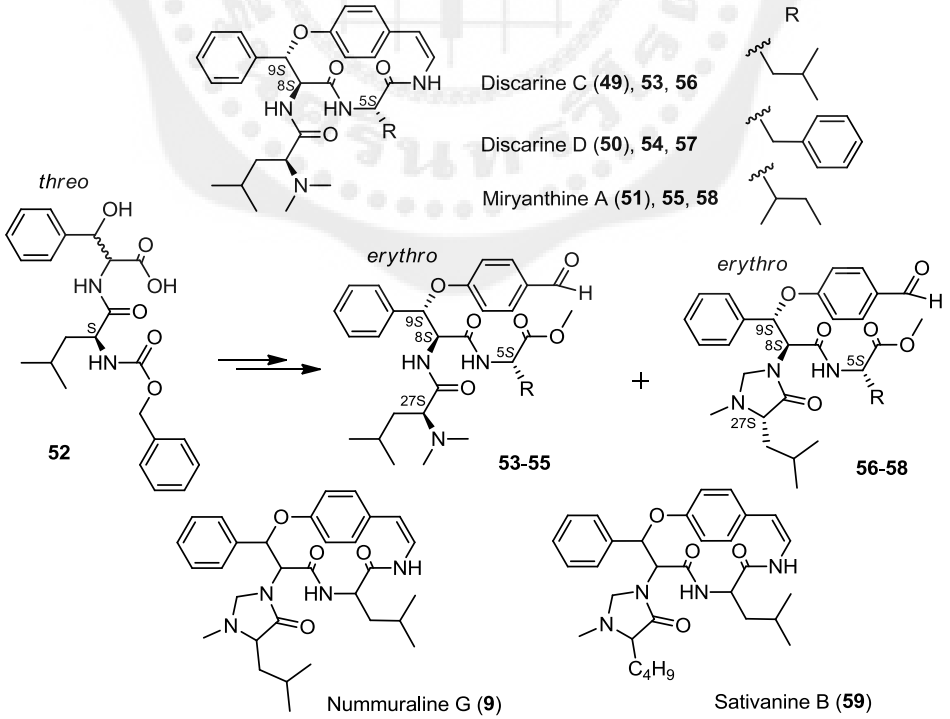

Figure 10 Structures of compounds **49**–**59**

1.1.3.6 Stereochemistry determination by X–ray diffraction

Spectroscopic and CD analysis are important tools for establishing the relative and absolute configuration of β–hydroxyamino acids. The absolute configuration of all α–amino acids can be accomplished by comparing the aforementioned methods with the data obtained by X–ray diffraction analysis. There are four X–ray structures of cyclopeptide alkaloids known to date.

The absolute configuration of 4(14)–frangulanine type franganine (**7**), a cyclopeptide alkaloid isolated from the methanol root bark extract of *Discaria americana*, was established on the basis of detailed NMR spectroscopic data and X–ray diffraction analysis of franganine methiodide salt (**7′**) (Caro et al., 2012). The configuration attributed to C–8 and C–9 via NMR data ($^3J_{8,9}$ values of 8.4, 7.2 and 8.0 Hz in methanol–d_4, $CDCl_3$ and DMSO–d_6, respectively) was consistent with the absolute configuration obtained by X–ray diffraction. Thus, franganine possesses all *S* absolute configurations at C–8, C–9 (*L–erythro*), C–5, and C–26 (Figure 10) and macrocyclic arrangement in its X–ray structure is closely related to the stereoscopic view of the minimized mucronine J (**32**) as suggested by MM2 calculations (Figure 11) (Auvin et al., 1996).

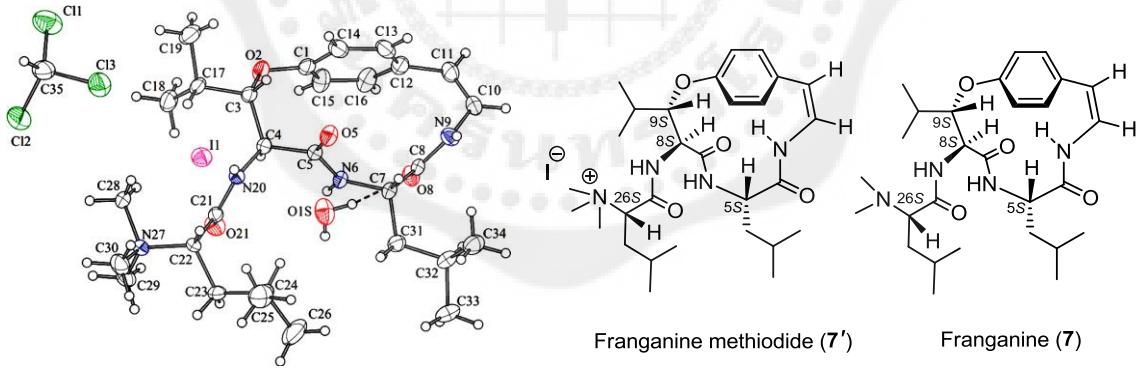

Figure 11 X–ray crystallographic structure of franganine methiodide (**7′**)

The structures of diastereoisomeric compounds of scutianene E (**60**), 8,9,17–*tris*–*epi*–scutiaene E (**61**), 17–*epi*–scutianene E (**62**) (Figure 12) from *Scutia buxifolia* Reiss, were elucidated by spectroscopic analysis. The stereochemical assignments for **61** and **62** were confirmed by X–ray diffraction analysis of their respective *O*–acetyl derivatives **61′**–**62′** (Figure 13) (Maldaner et al., 2011).

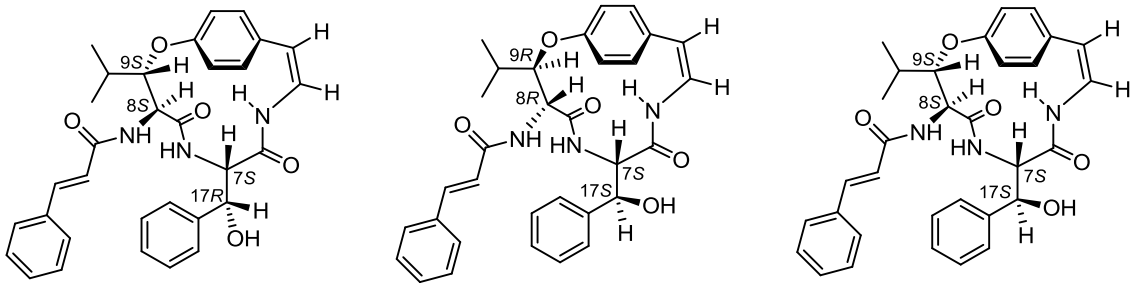

Scutianene E (**60**) 8,9,17-*tris*-*epi*-Scutiaene E (**61**) 17-*epi*-Scutianene E (**62**)

Figure 12 Structures of cyclopeptide alkaloids **60**–**62** from *Scutia buxifolia*

The X–ray analysis of *O*–acetyl derivatives **61′**–**62′** (Figure 13) possessed the absolute stereochemistry 8*R*,9*R* (*D*–*erythro*–*β*–hydroxyleucine), 5*S*,17*S* (*L*–*erythro*–*β*–hydroxyphenylalaine) for **61** and 8*S*,9*S* (*L*–*erythro*–*β*–hydroxyleucine), 5*S*,17*S* (*L*–*erythro*–*β*–hydroxyphenylalaine) for **62** (Maldaner et al., 2011).

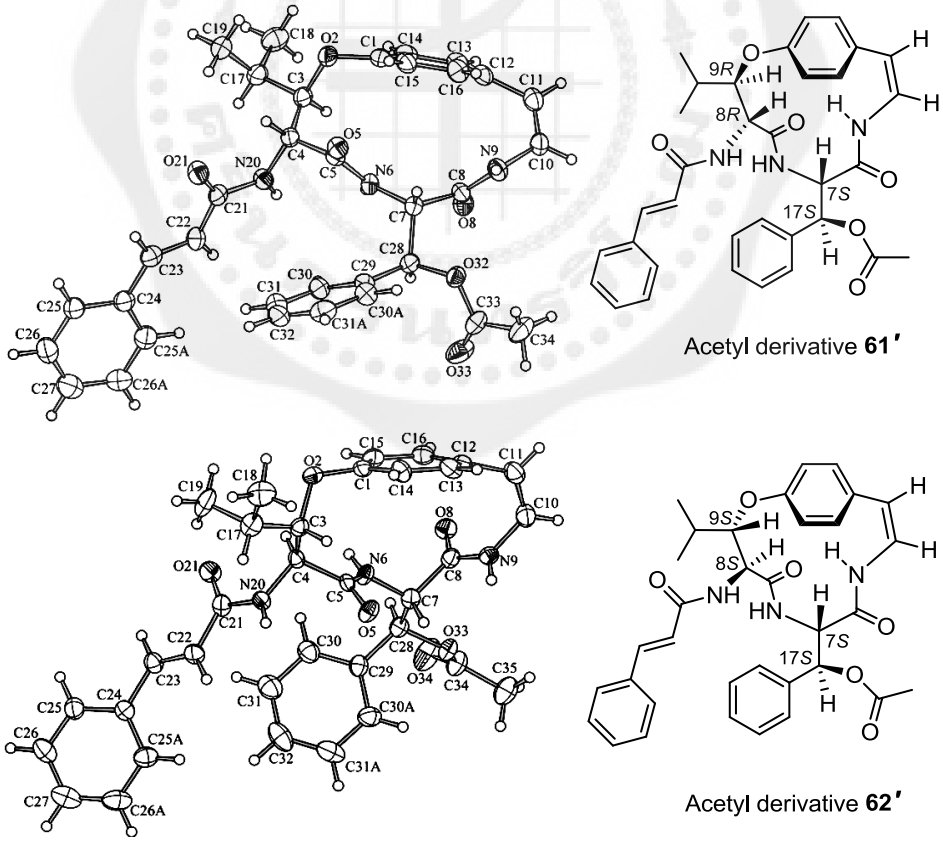

Acetyl derivative **61′**

Acetyl derivative **62′**

Figure 13 X–ray crystallographic structures of acetyl derivatives **61′**–**62′**

The absolute configuration of 5(13)–ziziphine A–type nummularine B (**5**) (Panseeta et al., 2011) was proved by X–ray diffraction analysis of its respective methiodide salt (**5′**) (Figure 14) (Panseeta et al., 2011). This was the first single crystal X–ray diffraction study of a 13–membered ring cyclopeptide, nummularine B methiodide (**5′**). This study along with the spectral analysis allowed to assign the absolute configuration as all *S* at the amino acid residues (Figure 14). The X–ray analysis of **5′** also provided the absolute configurations for related structures of 13–membered cyclopeptide alkaloids (*see also* section 2.1.4, p.23) by comparison of the spectroscopic data with those of nummularine B (**5**) and its methiodide salt (**5′**) (Panseeta et al., 2011).

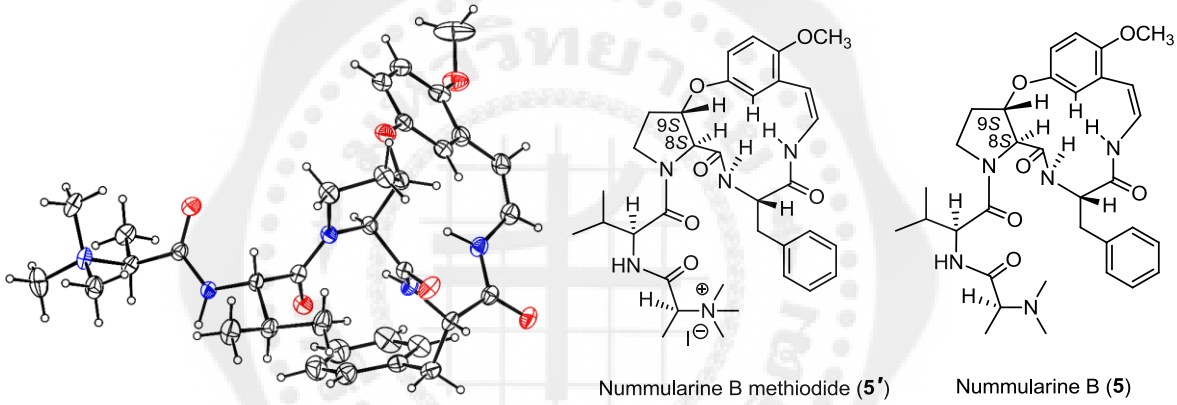

Figure 14 The X–ray crystal structure of nummularine B methiodide (**5′**)

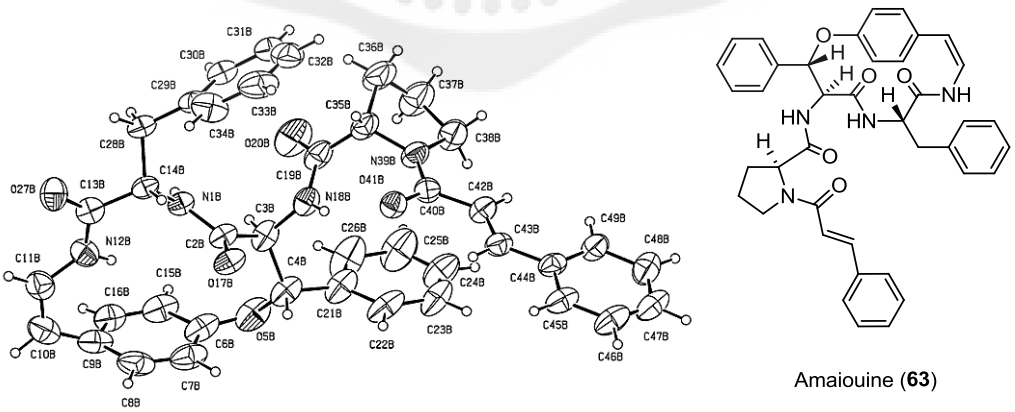

Figure 15 The X–ray crystal structure of amaiouine (**63**)

The structure of amaiouine (**63**), a neutral compound related to the 4(14)–cyclopeptide alkaloid family from the leaves of *Amaioua guianensis* was elucidated by NMR

spectroscopy and its relative all *S*–configurations were confirmed by X–ray crystallography (Figure 15) (de Oliveira et al., 2009).

1.1.4 Recent reports on new cyclopeptide alkaloids obtained from *Ziziphus* plants

Collection of plant cyclopeptide alkaloids up to 2005 have been extensively reviewed by Gournelis, Laskaris and Verpoorte (1998), Tan and Zhou (2006) and EL–Seedi et al., (2007). Recent studies on new *Ziziphus* cyclopeptide alkaloids are as follows.

Three cyclopeptide alkaloids, 5(13)–ziziphine A–type sativanine M (**64**) and 4(13)–nummularine C–type sativanines N–O (**65**–**67**) (Figure 16) were isolated from the stem bark of *Z. sativa*. Their structures have been established by spectral analysis. Stuctures of the ring–bound and terminal amino acid residues were proved by acid hydrolysis with 6 N HCl; and the hydrolysates were examined by paper chromatography (PC) using ninhydrin as spray reagent for visualization. The amino acids in the hydrolysates were identified by comparison with authentic samples (Singh S. et al., 2006; Pandey M. B. et al., 2008b). Sativanine M (**64**) was deformylated by the treatment with 0.5 N HCl followed by basified with NH_3 to give sativanine C (**67**) (Pandey M. B. et al., 2008b). However, the absolute configuration of **64** and **67** have not been described.

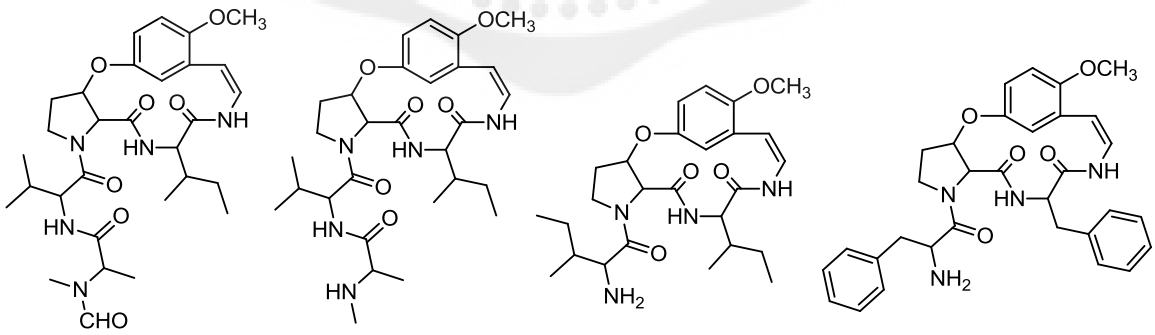

Sativanine M (**64**) Sativanine C (**67**) Sativanine N (**65**) Sativanine O (**66**)

Figure 16 Structures of sativanines **64**–**67**

Mauritine K (**68**) (Figure 16), a 5(14)–amphibine B–type cyclopeptide alkaloid isolated from the root bark of *Z. mauritiana,* was reported as a new antifungal agent (Singh A. K. et al., 2007).

Two cyclopeptide alkaloids from *Z. mauritiana* were reported by our group. The first 14–membered ring cyclopeptide isolated from this plant species, a 4(14)–integerrine–type, mauritine L (**69**) and the second one, a 5(13)–cyclopeptide alkaloid mauritine M (**70**), comprise tryptophan as an intermediate amino acid (Figure 17).

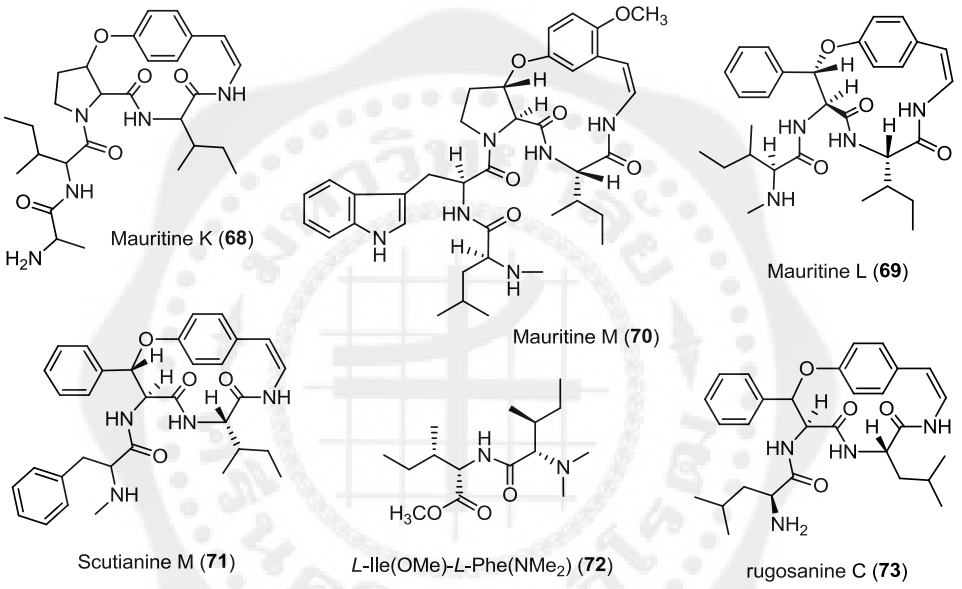

Figure 17 Structures of compounds **68**–**73**

The stereochemistry of mauritine L (**49**) was established as all *S*–configurations by the NMR spectroscopic data analysis of the macrocyclic part with those of the previously studied scutianine M (**71**). The latter is composed of the same macrocyclic ring, wherein the *L*–amino acid structures and location were determined by the analysis of hydrolysates and determining the values for *J* coupling constants (Morel et al., 2005). The configuration of terminal *N*–methylisoleucine was established by comparison of the ^{13}C NMR spectroscopic data with those of the synthesized dipeptide, *L*–Ile(OMe)–*L*–Ile(NMe_2) (**72**) (Lin H. Y. et al., 2000) and of the terminal *N*–methylisoleucine in paliurine B (**27**) (Lee S. S., Su and Liu, 2001). The spectral analysis of mauritine M (**70**) showed that its stereochemistry is comparable to that of nummularine B (**5**) (Figure 14). In addition, strong

NOE enhancements between NH–3/H–12 and between H–12/H–9 displayed in mauritine M (**70**) were consistent with the endocyclic arrangements among the three protons in the X–ray crystal structure for nummularine B methiodide (**5′**) (Figure 14). This evidence led to the conclusion that the mauritine M (**50**) shares the same stereochemistry, both at the ring nucleus and at the acyclic part, with **5′** (Panseeta et al., 2011).

Mauritine M (**70**) exhibited potent antiplasmodial activity against *Plasmodium falciparum* with the IC_{50} value of 3.7 μM and also showed weak activity (MIC 72.8 μM) against *Mycobacterium tuberculosis*. Conversely, Mauritine L (**69**) was inactive in the same tests (*see also* section 1.1.5.2, p.32) (Panseeta et al., 2011).

Rugosanine C (**73**), an 4(14)–integerrine–type cyclopeptide alkaloid comprising terminal amino acid with uncommon free terminal NH_2 function (Figure 17), was isolated from the root bark *Z. rugosa* (Singh J. P., Raghubanshi and Yadava, 2013).

Four cyclopeptide alkaloids oxyphyllines A–D (**74**–**77**) (Figure 18) were isolated from *Z. oxyphylla*. In 2007, one new cyclopeptide alkaloid of 5(14)–scutianine A–type, oxyphylline A (**74**) has been isolated from the stem bark of *Z. oxyphylla* (Inayat–ur–Rahman, 2007). Two 14–membered cyclopeptide alkaloids named oxyphyllines B (**75**) and C (**76**) (5(14)–scutianine A–type and 5(14)–amphibine B–type, respectively), were isolated from the stem and roots of *Z. oxyphylla* Edgew (Kaleem et al., 2012). 4(13)–Nummularine C–type oxyphylline D (**77**) was also obtained from the roots of the same plant species (Kaleem et al., 2013b).

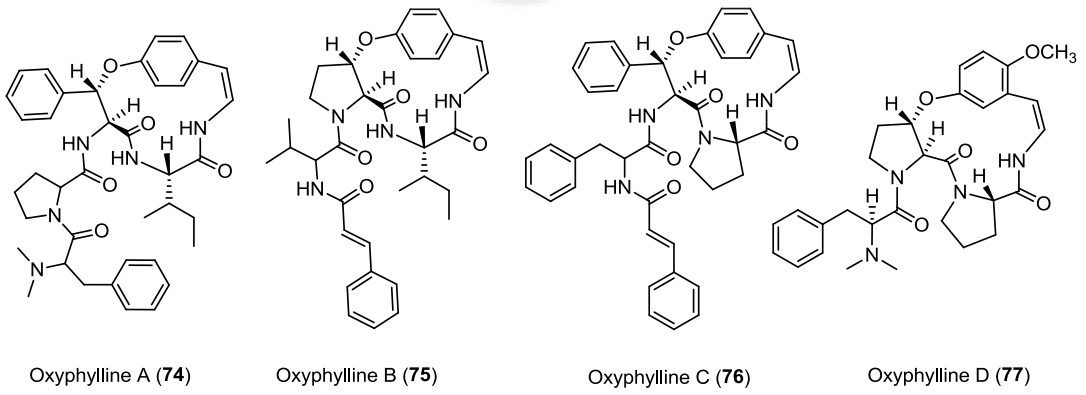

Figure 18 Structures of oxyphyllines A–D (**74**–**77**)

The structure of oxyphylline A (**74**) has been established on the basis of spectral studies, particularly 2D NMR as well as HRFABMS and ESIMS. Its EIMS spectra gave a fragmentation pattern (Scheme 3) with the characteristic base peak at *m/z* 148 (fragment **84**) indicating the presence of *N,N*–dimethylphenylalanine as the terminal amino acid. The basic structure of the compound was evident from the appearance of the ion peaks at *m/z* 624 and 91 for which the fragments **78** and **79** were proposed. The basic structure was also evident from the appearance of the ion fragments at *m/z* 608 and 107 for which the structures **82** and **85** were proposed. The appearance of ion **85** (*m/z* 107) and its further fragmentation to ion at *m/z* 105 (**86**) and then at *m/z* 77 (**87**) indicated that oxyphylline A (**74**) possesses benzyl alcohol moiety. The ion peak at *m/z* 365 (fragment **81**) corresponded to the macrocyclic ring of oxyphylline A (**74**). Other structures were further degraded to their related fragments, as shown in Scheme 3 (Inayat–ur–Rahman et al., 2007).

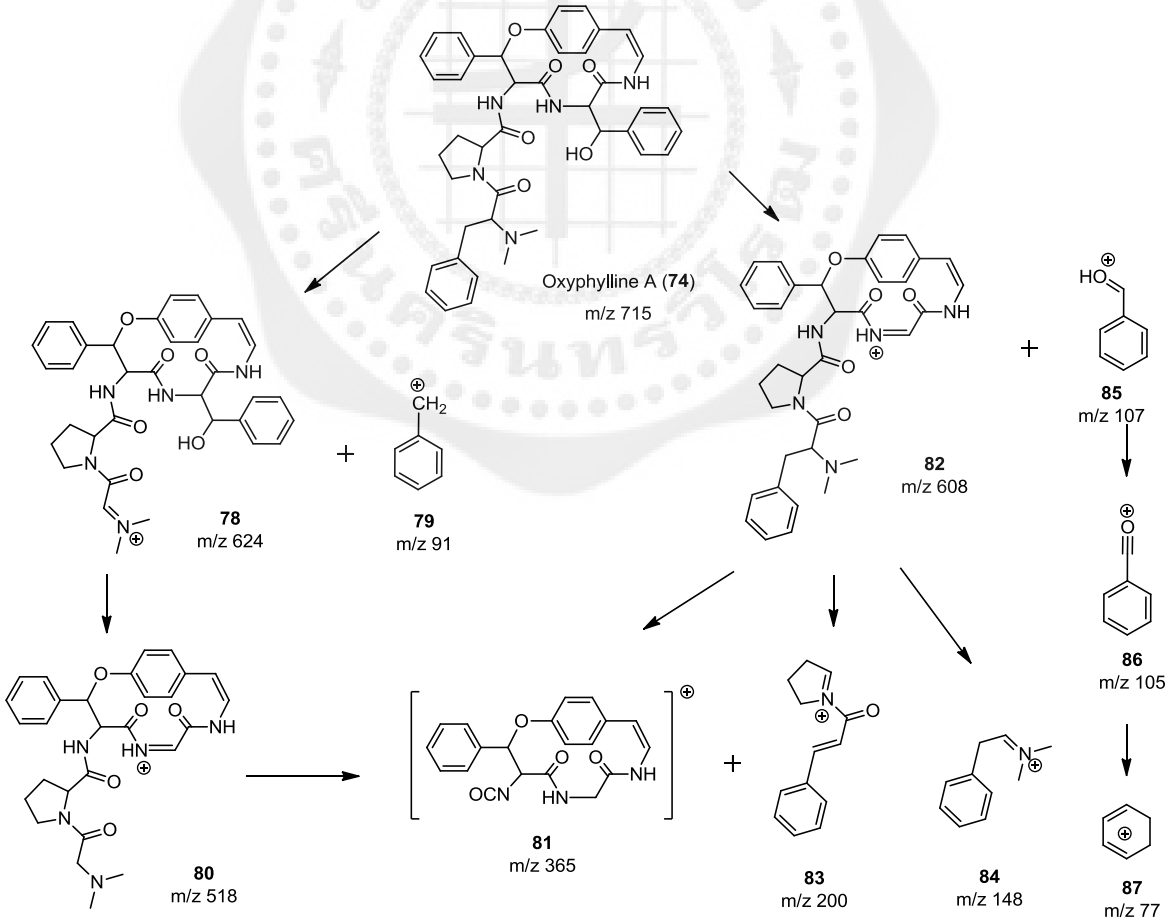

Scheme 3 EIMS fragment patterns of oxyphylline A (**55**)

Oxyphylline B (**75**) exhibited antibacterial activity against *Escherichia coli* (MIC 5 µg/mL). Oxyphylline C (**76**) showed weak antibacterial activities against *E. coli* (MIC 10 µg/mL) and *S. aureus* (MIC 10 µg/mL) (Kaleem et al., 2012).

Phytochemical investigations of *Z. xylopyra* have been established by Pandey et al: eight new cyclopeptide alkaloids xylopyrines A–H (**88**–**95**) (Figure 19) were reported and their basic structures have been elucidated by spectral studies with the aid of chemical conversion. However, the stereochemistry of the new cyclopeptides is yet unknown. New 4(13)–nummularine C–type xylopyrines A (**88**) and B (**89**) (Singh A. K. et al., 2007b), 4(14)–integerrine–type xylopyrines C (**90**) (Singh A. K. et al., 2008) and F (**93**) (Pandey M. B. et al., 2008c), have been isolated from the root bark. Two 4(13)–nummularine C–type, xylopyrines D (**91**), and E (**92**) were isolated from the bark (Pandey M. B. et al., 2008a). Two 4(14)–integerrine–type cyclopeptide alkaloids, xylopyrines G (**94**) and H (**95**), have been successively isolated from the aerial bark of this *Ziziphus* plant. Xylopyrine G (**94**) is a rare type cyclopeptide alkaloid comprising *N*–formyl of terminal amino acid (Pandey M. B. et al., 2012).

Pandey et al. also reported on the isolation of a new 4(13)–nummularine C–type cyclopeptide alkaloid jubanine E (**96**) from the bark of *Z. jujuba* (Pandey M. B. et al., 2008a).

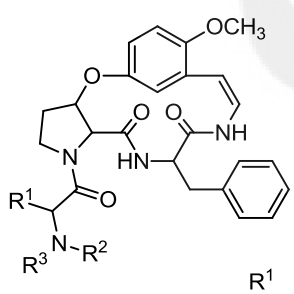

A = 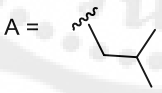

B = 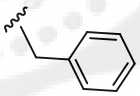

C = 

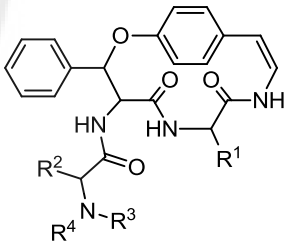

	R^1	R^2	R^3
Xylopyrine A (**88**) :	A	CH_3	CH_3
Xylopyrine B (**89**) :	B	CH_3	CH_3
Xylopyrine D (**91**) :	C	CH_3	CH_3
Xylopyrine E (**92**) :	C	H	H
Jubanine E (**96**) :	B	CH_3	H

	R^1	R^2	R^3	R^4
Xylopyrine C (**90**) :	B	B	CH_3	H
Xylopyrine F (**93**) :	A	A	H	H
Xylopyrine G (**94**) :	B	A	CH_3	CHO
Xylopyrine H (**95**) :	B	A	CH_3	H

Figure 19 Structures of xylopyrines A–H (**88**–**95**) and jubanine E (**96**)

The amino acid units in xylopyrines A–H (**88**–**95**) and jubanine E (**96**) were determined by the total and partial hydrolysis and the hydrolysates were examined by the comparison of the paper chromatography results with those of authentic samples as follows.

Total hydrolysis

Each cyclopeptide alkaloid was hydrolyzed with 6 N HCl by heating in a sealed tube on the oil bath at 120 ^{o}C for 24 h. This allowed to obtain each amino acid as individual structures. The hydrolysates were studied by paper chromatography eluting with *n*–BuOH–AcOH–H_2O (4:1:5) and the spots were visualized by spraying with ninhydrin. The individual aminoacids have been identified by comparison with authentic amino acid samples (Singh A. K. et al., 2007; Singh A. K. et al., 2008; Pandey M. B. et al., 2008a; Pandey, M. B.; 2008b; Pandey M. B. et al., 2012).

Partial hydrolysis

Each cyclopeptide alkaloid was heated on a water bath and then treated with a mixture of conc. HCl:AcOH:H_2O (1:1:1). A conventional work–up of all of cyclopeptide alkaloids furnished identical macrocyclic residues. Some macrocyclic residues were further hydrolyzed with 6 N HCl for full degradationto detect the ring–bound amino acid.

Xylopyrines A (**88**), **B** (**89**), **D** (**91**), **E** (**92**) **and jubanine A** (**96**)

These five cyclopeptide alkaloids share the same macrocyclic ring, which was demonstrated to be a styrylamine unit, β–hydroxyproline, and phenylalanine as the ring–bound amino acid. After each cyclopeptide alkaloid had reacted with conc. HCl:AcOH:H_2O (1:1:1) macrocyclic compound **97** was obtained (Scheme 4). Then, compound **97** was hydrolyzed with 6 N HCl in a sealed tube for 18–20 h at 120 ^{o}C on oil bath. This reaction gave the ring–bound amino acid phenylalanine, as determined by co–Paper, co–TLC chromatography and co–MS by comparison with the authentic sample, and superimposable IR (Singh A. K. et al., 2007; Pandey M. B. et al., 2008a; Pandey M. B. et al., 2008b).

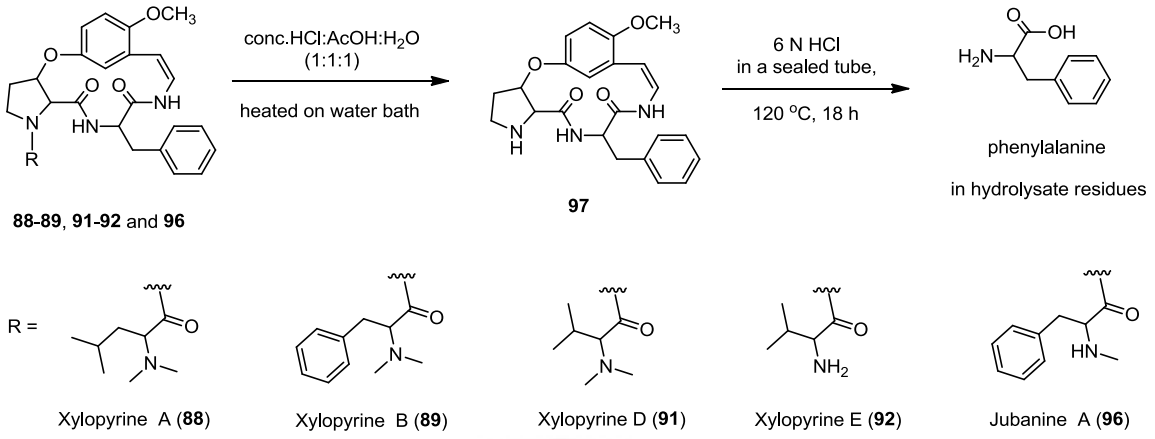

Scheme 4 Partial hydrolysis procedure for xylopyrines A (**88**), B (**89**), D (**91**), E (**92**) and jubanine A (**96**)

Xylopyrine F (**93**)

A hydrolysis of xylopyrine F (**93**) by a mixture of conc. HCl:AcOH:H_2O (1:1:1) furnished a macrocyclic compound **98** (Scheme 5), which was further hydrolyzed with 6 M HCl in a sealed tube for 18 h at 120 ^{o}C to produce leucine, observed by co–PC comparison with the authentic sample (Pandey M. B. et al., 2008c).

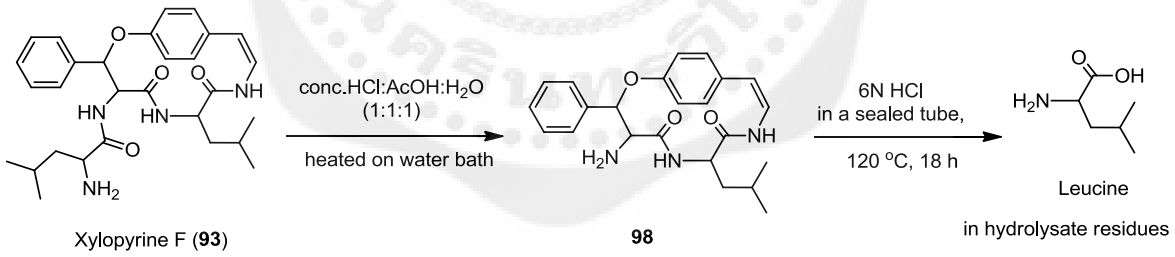

Scheme 5 Partial hydrolysis procedure of xylopyrine F (**93**)

Methylation

Each xylopyrines F (**95**) and H (**95**) were treated with HCHO and $NaBH_4$ to yield the corresponding *N*–methylated products (Pandey M. B. et al., 2008b; Pandey M. B. et al., 2012), which were established as discarine C (**49**) (Digel et al., 1983) and integerressine (**99**) (Lagarias et al., 1979) (Figure 19), respectively.

Deformylation of xylopyrine G (**94**)

Xylopyrine G (**94**) was deformylated by the treatment with 0.5 N HCl in MeOH at RT for 48 h, to yield a xylopyrine H (**95**), which was subsequently treated with HCHO and $NaBH_4$ (Pandey M. B. et al., 2012). The structure of *N*–methylated product **100** was elucidated as crenatine A (Figure 20) (Silva et al., 1974).

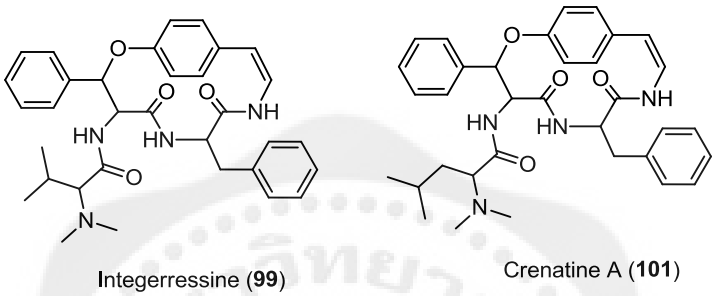

Figure 20 Structure of integerressine (**99**) and crenatine A (**100**)

Six new 5(14)–amphibine B–type cyclopeptide alkaloids have been isolated from stems of Chinese *Z. apetala*. Three of them, apetaline A (**101**), mauritine A *N*–oxide (**102**) and epimauritine A *N*–oxide (**103**), a derivative of epimauritine A (**104**), were reported as novel structures containing an oxime or *N*–oxide moiety. Apetaline B (**105**) and apetaline C (**106**) are uncommon type cyclopeptide alkaloids comprised of imidizolidin–4–one ring and *N*–formyl terminal amino acid, respectively (Figure 21). Their structures were determined by analysis of spectroscopic data together with chemical methods. Configurations of cyclopeptide alkaloids **101**–**106** were determined by acid hydrolysis over Marfey's method (Marfey and Ottesen, 1984). Each cyclopeptide alkaloid was dissolved in 6 N HCl in a sealed glass tube and incubated at 115 ^{o}C for 24 h. The hydrolysate was treated with $NaHCO_3$ followed by 1% N*α*–(2,4–dinitro–5–fluorophenyl)–*L*–alaninamide (*L*–FDAA, Marfey's reagent). The mixture was dissolved in 50% aqueous CH_3CN to yield respective FDDA derivatives. Chemical conversion of an amino acid with an FDAA derivative produces a diastereomer referred to as 2,4–dinitrophenyl–5–*L*–alaninamide amino acid or simply DNPA–amino acid. The standard amino acids (*D*–Phe, *L*–Phe, *D*–Val, *L*–Val, *D*–*N*–methylalanine, *L*–*N*–methylalanine, *D*–*N*,*N*–dimethylalanine, and *L*–*N*,*N*–dimethylalanine) were also treated with the above method. A small amount of the FDAA

derivative was then analyzed by HPLC with a RP–18 column. The absolute stereochemistry of a macrocyclic ring of all isolated cyclopeptide alkaloids was elucidated as all *S*–configurations (Figure 21) (Han J. et al., 2011).

Cyclopeptide alkaloids **101**–**106** were tested as antidepressants in mice, 11*β*–hydroxysteroid dehydrogenase (11*β*–HSD) inhibition *in vitro* and cytotoxic activity against immortal HeLa cell line and human gastric cancer BGC–823 cell lines, but none exhibited any activity (Han J. et al., 2011).

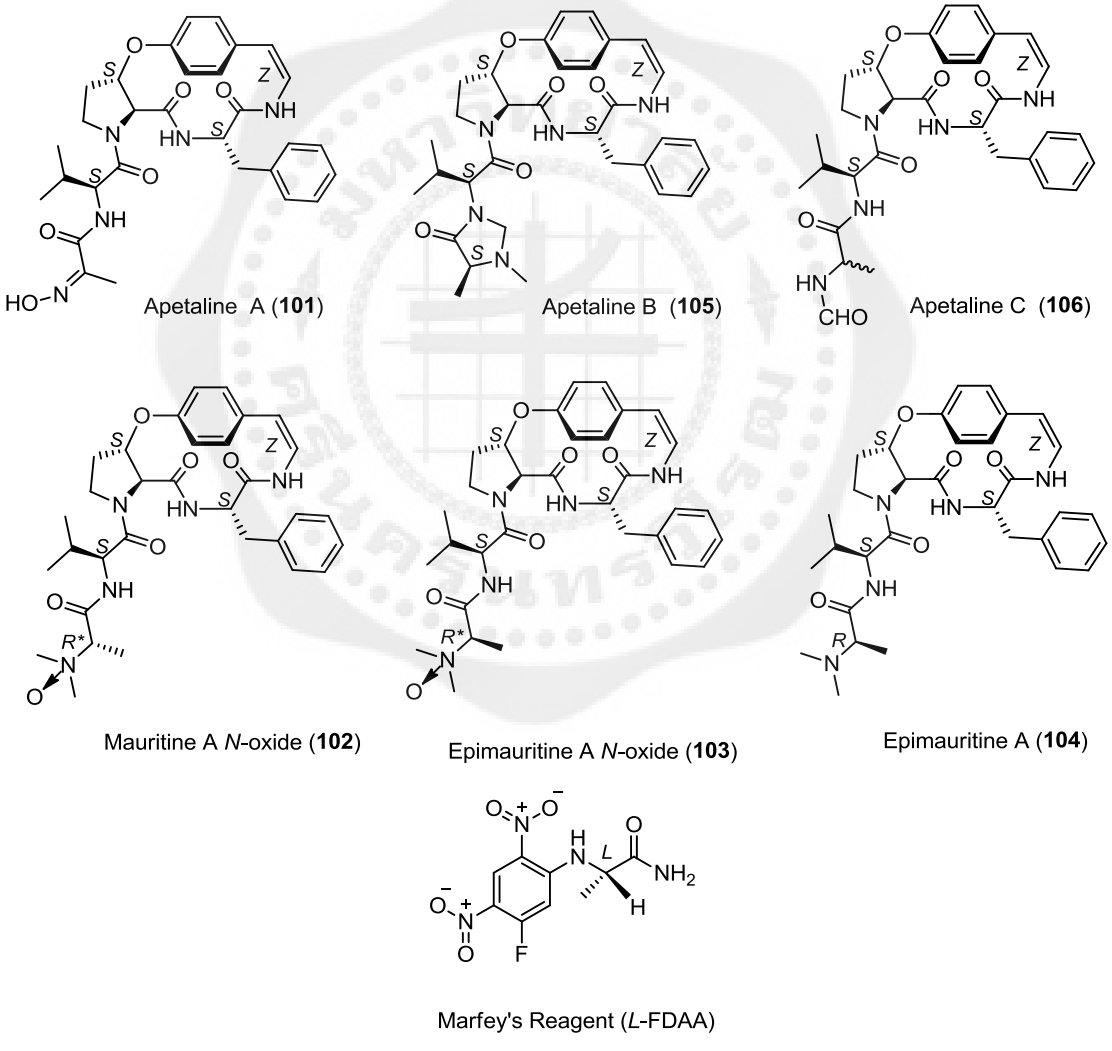

Figure 21 Structures of compounds **101**–**106**

1.1.5 Bioactivities of cyclopeptide alkaloids

Although antibacterial (Tschesche et al., 1974; Pandey V. B. and Devi, 1990), antifungal (Pandey V. B. and Devi, 1990; Giacomelli et al., 2004), antiplasmodial (Suksamran et al., 2005), antimycobacterial (Suksamran et al., 2005), sedative (Han B. H. and Park, 1987), and immunostimulant (Lin H. Y.; et al, 2000) activities have been reported for some cyclopeptide alkaloids, no cyclopeptide alkaloids have been used for new drug research and development due to their limited availability (Tan and Zhou, 2006). Reviewed herein are the developments in the field of cyclopeptide alkaloids that have emerged from 2006.

1.1.5.1 Antiplasmodial and antimycobacterial activities

The *in vitro* antiplasmodial and antimycobacterial effects of cyclopeptide alkaloids mauritine L (**69**), mauritine M (**70**), nummularine B (**5**), nummularine H (**107**) and hemsine A (**28**) (Figure 22), isolated from *Z. mouritiana*, and nummularine B methiodide (**5′**) were reported. Mauritine M (**50**), nummularine H (**92**) and hemsine A (**93**) exhibited potent antiplasmodial activity against *Plasmodium falciparum* with the IC_{50} values of 3.7, 4.2 and 7.3 μM, respectively. Nummularine B (**42**) was moderately active (IC_{50} 10.3 μM), whereas mauritine L (**69**) and nummularine B methiodide (**5′**) were inactive. The nummularine H (**107**) demonstrated interesting antituberculosis effect against *Mycobacterium tuberculosis* with the MIC value of 4.5 μM, and mauritine M (**70**) showed weak activity (MIC 72.8 μM). Mauritine L (**69**), nummularine B (**5**), nummularine B methiodide (**5′**) and hemsine A (**28**) were inactive to the same test. The structure–activity relationship established that a relatively high antiplasmodial activity of mauritine M (**70**), nummularine H (**107**) and hemsine A (**28**) could probably be due to the presence of the *β*–hydroxyproline unit and the terminal *N*–methylated or *N,N*–dimethylated amino acid residues (Panseeta et al., 2011).

1.1.5.2 Antibacterial activities

Two 14–membered ring cyclopeptide alkaloids, oxyphyllines B (**56**) and C (**57**), isolated from *Z. oxyphylla* were investigated. Oxyphylline B (**56**) exhibited antibacterial activities against *Escherichia coli* (MIC 5 μg/mL), higher than oxyphylline C (**57**), and also weak antimicrobial activities against *Staphylococcus aureus* (MIC 25 μg/mL),

Pseudomonas aeruginosa (MIC 50 μg/mL) and *Salmonella typhi* (MIC 50 μg/mL). Oxyphylline C (**57**) showed weak antibacterial activities against *E. coli* (MIC 10 μg/mL), *S. aureus* (MIC 10 μg/mL), *P. aeruginosa* (MIC 50 μg/mL) and *S. typhi* (MIC 50 μg/mL) (Kaleem et al., 2012).

1.1.5.3 α–Glucosidase inhibitory activity

Choudhary et al., presented the first report of the antidiabetic activities of cyclopeptide alkaloids as novel inhibitors for α–glucosidase enzyme and for protein glycation. Three known cyclopeptide alkaloids, hemsine A (**28**), nummularine C (**2**) and nummularine R (**108**) (Figure 22), isolated from traditionally used antidiabetic plant *Z. oxyphylla*, displayed a potent α–glucosidase inhibition and a moderate anti–glycation activity. Cyclopeptides **2**, **28** and **108** exhibited inhibition for α–glucosidase enzyme with IC_{50} values of 394.0, 212.1 and 215.1 μM, respectively, which are more potent than the standard, 1–deoxynojirimycin (IC_{50} 441.0 μM). Hemsine A (**28**) and nummularine R (**108**) also exhibited a moderate anti–glycation activity with IC_{50} values of 277.7, 720.2 μM, respectively. The results indicate that these compounds have a potential to control the postprandial hyperglycemia and associated diabetes complications due to glycation of proteins (Choudhary et al., 2011).

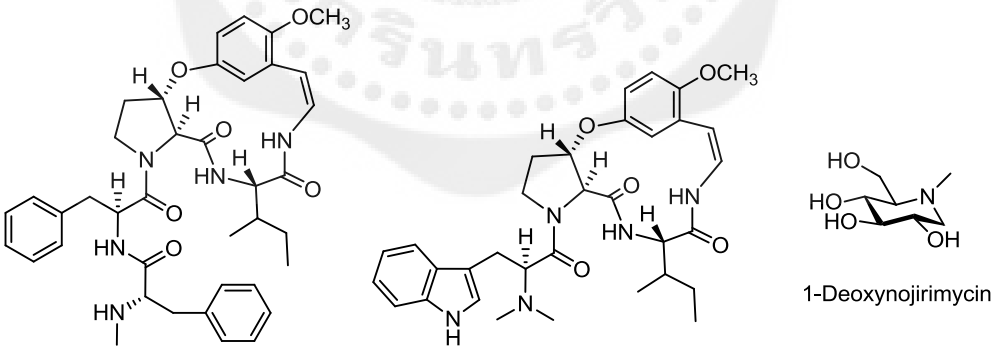

Figure 22 Structures of compounds **107**–**108** and 1–deoxynojirimycin

1.1.5.4 Urease inhibitory activity

Cyclopeptide alkaloids isolated from *Z. oxyphylla*, oxyphylline D (**77**), nummularine C (**2**) and nummularine R (**107**) were reported as urease inhibitors. However,

oxyphylline D (**77**), nummularine C (**2**) and nummularine R (**108**) exhibited weak activity with of 58.2%, 35.7%, 29.3% inhibition, respectively (Kaleem et al., 2013b).

1.1.5.5 Antinociceptive effects

Trevisan et al. investigated a potential antinociceptive effect of six 14–membered cyclopeptide alkaloids namely franganine (**7**), discarine B (**109**), scutianines B (**110**), C (**111**), and D (**112**) as well as adouetine X (**113**) (Figure 22) in mice. Their possible mechanism of action and ability to develop undesirable side effects have also been studied (Table 3). Among the compounds tested, only franganine (**7**) and adouetine X (**113**) produced antinociceptive effects in a mouse model of acute pain without inducing undesirable side effects (Trevisan et al., 2009).

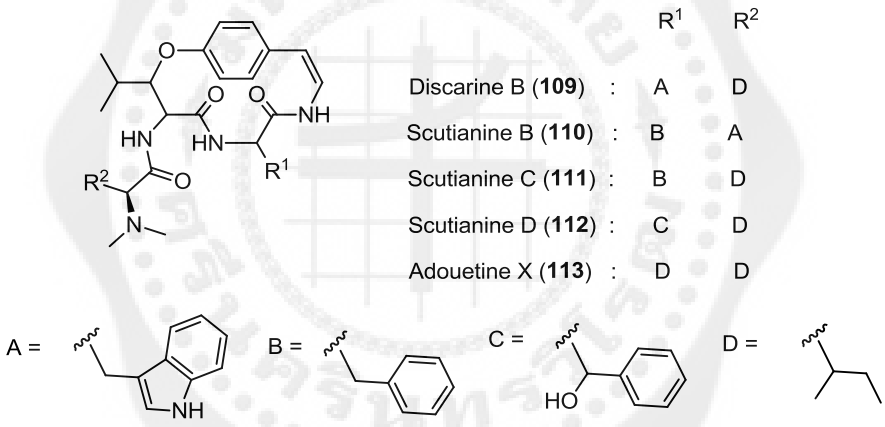

Figure 23 Structures of compounds **109**–**113**

1.1.5.6 11*β*–hydroxysteroid dehydrogenase (11*β*–HSD) inhibition

Mauritines A (**34**) and F (**39**) and cyclopeptide alkaloids **101**–**106** were tested for inhibition of human and murine 11*β*–HSD1 and 11*β*–HSD2 enzymes *in vitro*. Only mauritine A (**34**) showed inhibitory activity on 11*β*–HSD1, with IC_{50} values of 52.0 (human) and 31.2 μg/mL (mouse). Although a mixture of alkaloids from roots was evaluated for antidepressant activity on mice, no activity in forced swimming, tail suspension, or open–field tests was detected. All compounds were tested for their cytotoxic activity against HeLa and BGC–823 cancer cell lines, but none exhibited cytotoxicity (Han J. et al., 2011).

1.2 Pentacyclic triterpenes and saponins

Triterpenes are a large group of natural products derived from C30 isoprene precursors. Most triterpenoids are 6–6–6–5 tetracycles, 6–6–6–6–5 or 6–6–6–6–6 pentacycles (Xu R., Fazio and Matsud, 2004). Triterpenes can be found in both free form as sapogenins, and attached to glycosides as saponin glycosides. Saponin glycosides are naturally occurring compounds that are divided into two major classes depending on their aglycone (sapogenin), which can be either triterpenoid or steroid. Their structures are varied by the number of sugar units attached at different positions (Hostettmann and Marston, 1995). Usually, the sugar units are found at the C–3 and/or C–28 positions (Bruneton, 1999). Pentacyclic triterpenes are promising secondary metabolites in plants, which are assembled from six isoprene units through the cytosolic mevalonate pathway (Xu R., Fazio and Matsud, 2004). The pentacyclic triterpenes can be further classified into several subgroups depending on their particular structures such as lupane, ceanothane, oleanane, dammarane or ursane groups. Lupane– and ceanothane–type structures are notable pentacyclic triterpenes of genus *Ziziphus* (Suksamrarn et al., 2006).

1.2.1 Lupane–type triterpene

Lupane–type triterpene is a series of 6–6–6–6–5 pentacyclic triterpene molecules, which composed of an isopropenyl moiety at C–19 (Figure 24). Lupane triterpenes are commonly produced by several plants as along with many other triterpenes. The genus *Ziziphus* is well known for the high content of lupane triterpenes, especially betulinic acid (**1**) (Suksamrarn et al., 2006).

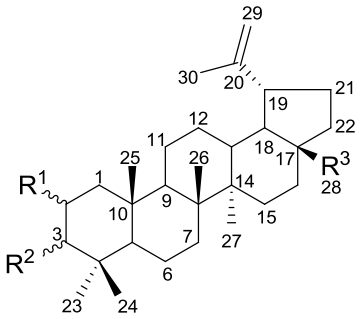

Figure 24 Basic structure of a lupane–type triterpene

The major triterpene, betulinic acid (**1**) or 3–hydroxy–lup–20(29)–en–28–oic acid, is a widely distributed pentacyclic lupane–type triterpene in *Ziziphus* plants. It was found in *Z. oenoplia* (Nahar et al., 1997; Aunchai, 2002), *Z. rugosa* (Tripathy et al., 1988; Kulshreshtha et al., 1972; Netsawangwicha. 2005), *Z. cambodiana* (Panseeta, 2004; Suksamrarn et al., 2006), *Z. attopoensis* (Maneekaew, 2007), *Z. jujube* (Lee S. S. et al., 1995; Yagi et al., 1978b; Lee S. M. et al., 2004) and *Z. mauritiana* (Panseeta, 2009; Jou et al., 2004).

Lupeol (**114**) was isolated from *Z. rugosa* (Nahar et al., 1997; Aunchai, 2002), *Z. cambodiana* (Panseeta, 2004; Suksamrarn et al., 2006), *Z. attopoensis* (Maneekaew, 2007) and *Z. mauritiana* (Chauhan et al., 1978).

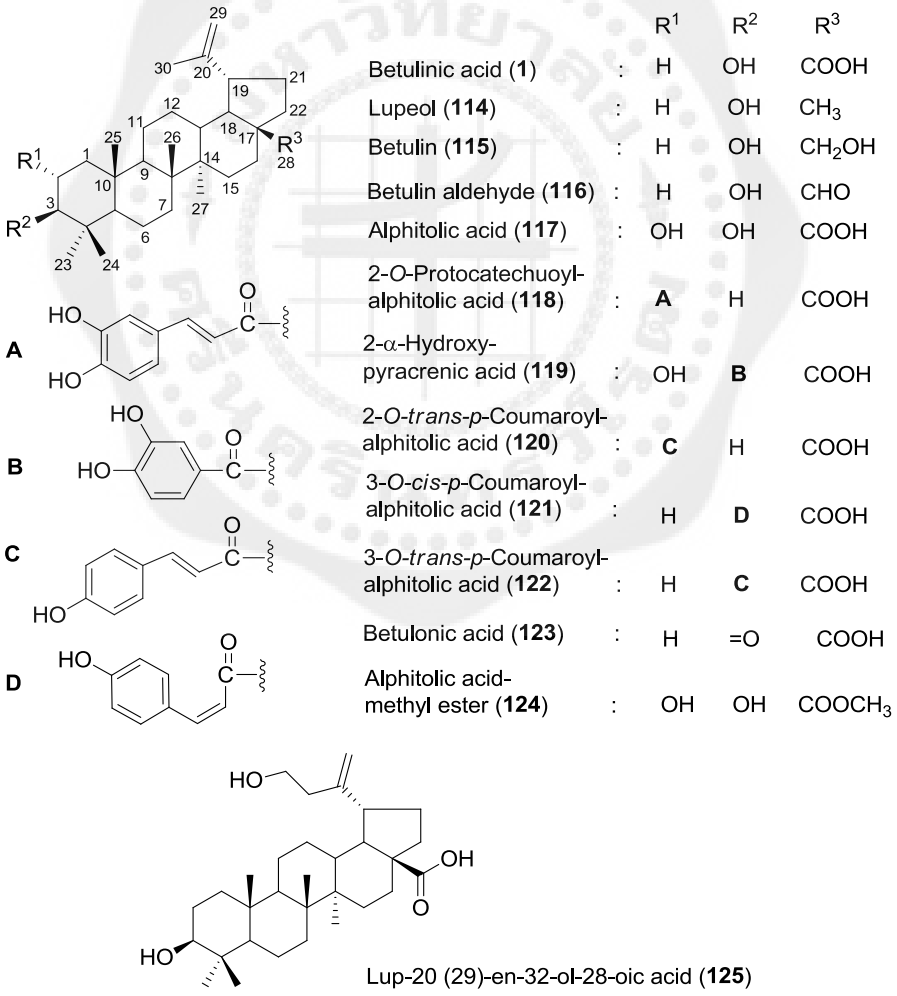

Figure 25 Structure of lupane–type triterpenes **1** and **114**–**125**

Betulin (**115**), a closely related compound to betulinic acid, was isolated from the root of *Z. jujuba* Mill var *spinosa* (Lee S. S. et al., 1995), the root bark of *Z. rugosa* (Nahar et al., 1997; Tripathy et al., 1988; Netsawangwicha. 2005) and the stem of *Z. mauritiana* (Chauhan et al., 1978).

Betulinaldehyde (**116**) was isolated from *Z. rugosa* (Nahar et al., 1997; Netsawangwicha. 2005), *Z. cambodiana* (Panseeta, 2004; Suksamrarn et al., 2006) and the twig of *Z. attopoensis* (Maneekaew, 2007).

Alphitolic acid (**117**) that displays the additional α–OH group at C–2 of betulinic acid (**1**), was found in *Z. rugosa* (Kulshreshtha et al., 1972; Netsawangwicha. 2005), *Z. cambodiana* (Panseeta, 2004; Suksamrarn et al., 2006), *Z. attopoensis* (Maneekaew, 2007), *Z. jujube* (Yagi et al., 1978a; Lee S. M. et al., 2003) and *Z. mauritiana* (Sharma et al., 1982).

2–*O*–Protocatechuoylalphitolic acid (**118**) and 2–α–hydroxypyracrenic acid (**119**) were isolated from the water–insoluble fraction of the ethanolic extract of *Z. jujuba* var. *spinosa* root (Lee S. S. et al., 1996).

p–Coumaroylate of alphitolic acid or 2–*O*–*trans*–*p*–coumaroyl alphitolic acid (**120**) was isolated from the fruit of *Z. jujube* (Yagi et al., 1978), the root bark of *Z. rugosa* (Netsawangwicha. 2005), and the root bark of *Z. cambodiana* (Panseeta, 2004; Suksamrarn et al., 2006).

3–*O*–*cis*–*p*–Coumaroyl alphitolic acid (**121**) and 3–*O*–*trans*–*p*–coumaroyl alphitolic acid (**122**) were isolated from the fruit of *Z. jujube* (Yagi et al., 1978b; Lee S. M. et al., 2003).

Betulonic acid (**123**) was isolated from the fruit of *Z. jujube* (Yagi et al., 1978b; Huang et al., 2001; Lee S. M. et al., 2003) and the stem of *Z. mauritiana* (Chauhan et al., 1978).

A lupane triterpene isolated from the seeds of *Z. jujuba* var. *spinosa* was named as alphitolic acid methyl ester (**124**) or identified as 2α,3β–dihydroxy–lup–20(29)–en–28–oic acid methyl ester (He, Pan and Min, 2006).

Lup–20 (29)–en–32–ol–28–oic acid (**125**), a novel lupenoic acid derivative with hydroxyl methylene group attached to C–30, was isolated from leaves of *Z. jujube* (Sahu et al., 2008).

1.2.2 Ceanothane–type triterpene

The ceanothane–type triterpene is a series of 5–6–6–6–5 pentacyclic triterpenes in which five–membered ring A replaces the six–membered ring found in the lupane–type triterpenes. Remarkably, since all of the reported ceanothane–type triterpenoids belong to the family Rhamnaceae, the ceanothane–type triterpenoids could be a chemical marker for the Rhamnaceous plants (Guo et al., 2011a).

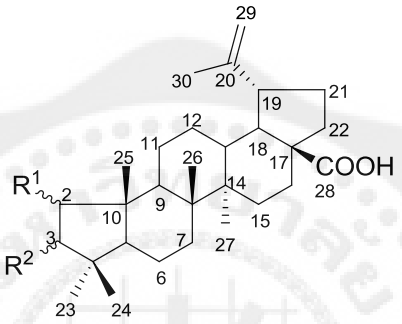

Figure 26 Basic structure of a ceanothane–type triterpene

Ceanothic acid (**126**) was isolated from the root of *Z. jujuba* Mill var. *spinosa* (Lee S. S., Lin and Chen, 1995; Lee S. M. et al., 2003), the root bark of *Z. cambodiana* (Suksamrarn et al., 2006), *Z. rugosa* root bark (Netsawangwicha. 2005), the leaves of *Z. glabrata* (Ganapaty et al., 2006) and the root *Z. mauritiana* (Panseeta, 2009; Jou et al., 2004).

A related structure of ceanothic acid named ceanothanolic acid (**127**) was isolated from *Z. rugosa* (Netsawangwicha, 2005) and it was also found in *Z. cambodiana* (Arai et al., 2008).

Two ceanothic acid derivertives, 3–*O*–protocatechuoyl ceanothic acid (**128**) was isolated from the root of *Z. jujuba* var. *spinosa* (Lee S. S., Lin and Chen, 1996) and 3–*O*–vanillyl ceanothic acid (**129**) was isolated from the root bark of *Z. cambodiana* (Suksamrarn et al., 2006).

Two ceanothane aldehydes, zizyberanalic acid (**130**) and zizyberenalic acid (**131**) were found in the fruit of *Z. jujuba* Mill (Lee S. M. et al., 2004) and the root bark of *Z. cambodiana* (Suksamrarn et al., 2006; Arai et al., 2008). A–norlupa–2,20–diene–

14,17–dicarboxylic acid or ceanothenic acid (**132**) was isolated from the roots of *Z. mauritiana* (Jou et al., 2004) and the leaf of *Z. jujube* (Monda and Kundu, 1998).

Epiceanothic acid (**133**) and 24–hydroxyceanothic acid (**134**) were also isolated from EtOAc extract of *Z. mauritiana* root (Panseeta, 2009). In addition, 24–hydroxyceanothic acid (**134**), also known as granulosic acid, was isolated from the leaves of *Z. glabrata* (Ganapaty et al., 2006).

A new ceanothane–type triterpene, 2α–aldehydo–A(1)–norlup–20(29)–en–27,28–dioic acid, named as zizyberanal acid (**135**), has been isolated from the fruits of *Z. jujube* (Guo et al., 2009b).

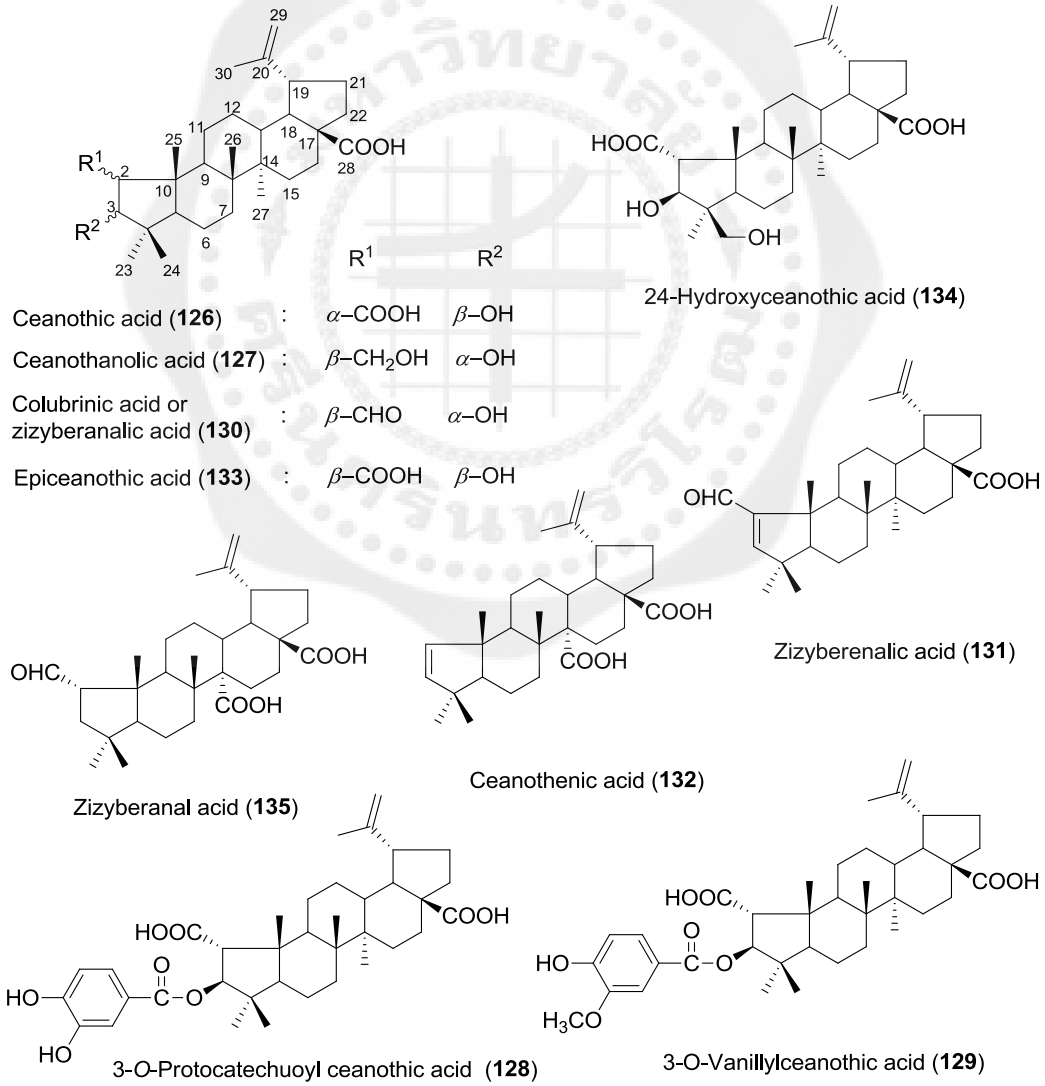

Figure 27 Structures of ceanothane–type triterpenes **126**–**135**

1.2.3 Ursane–type triterpene

The ursane–type triterpene is a series of 6–6–6–6–6 pentacyclic triterpene molecules, in which ring E is substituted with two vicinal methyl groups at C–19 and C–20.

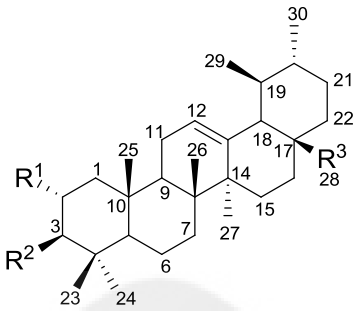

Figure 28 Basic structure of an ursane–type triterpene

Ursolic acid (**136**) *Z. rugosa* was isolated from the root of *Z. jujuba* Mill var. *spinosa* (Lee S. S., Lin and Chen, 1995), and from the fruits of *Z. jujube* (Guo et al., 2009).

2–α–Hydroxyursolic acid (**137**) was isolated from the root of *Z. jujuba* Mill var. *spinosa* (Lee S. S., Lin and Chen, 1995) and *Z. rugosa* (Kulshreshtha and Rastogi, 1972).

Ursonic acid or ursolonic acid (**138**) was isolated from the fruit of *Z. jujuba* (Huang et al., 2001).

Pomonic acid (**139**), pomolic acid (**140**) and corosolic acid (**141**), were obtained from the fruits of *Z. jujuba* var. *spinosa* (Guo et al., 2011a).

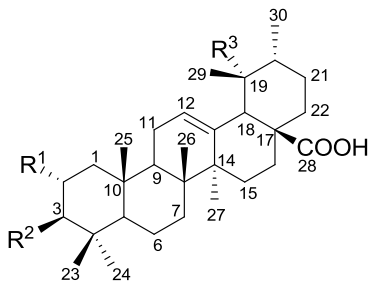

		R^1	R^2	R^3
Ursolic acid (**136**)	:	H	OH	H
2-α-Hydroxy ursolic acid (**137**)	:	OH	OH	H
Ursolonic acid **(138**)	:	H	=O	H
Pomonic acid (**139**)	:	H	=O	OH
Pomolic acid (**140**)	:	H	OH	OH
Corosolic acid (**141**)	:	OH	OH	H

Figure 29 Structures of ursane–type triterpenes **136**–**141**

1.2.4 Oleanane–type triterpene

The oleanane–type triterpenes is a series of 6–6–6–6–6 pentacyclic triterpenes, similar to the ursane type compounds, wherein ring E is substituted with two geminal methyl groups at C–20.

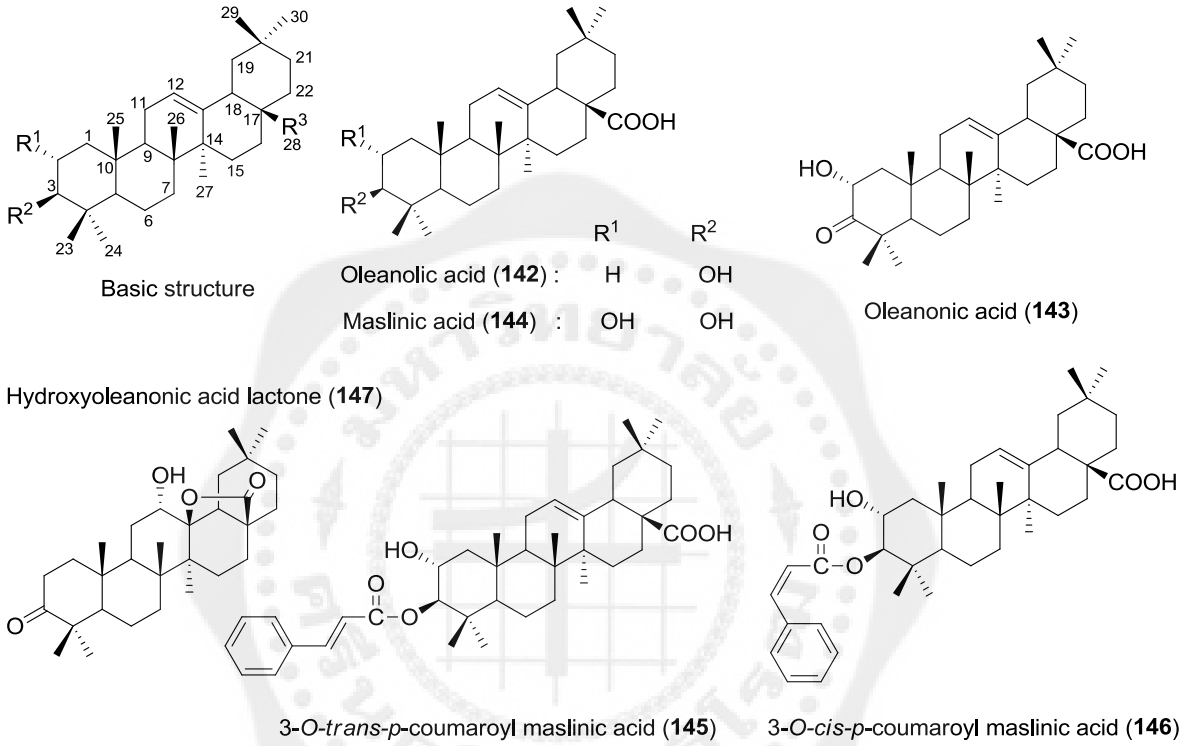

Figure 30 Basic backbone and structures of oleanane–type triterpenes **142**–**147**

Oleanolic acid or oleanic acid (**142**) was isolated from *Z. rugosa* (Kulshreshtha et al., 1972), the fruit of *Z. jujuba* Mill (Lee S. M. et al., 2004) and the fruits of *Z. jujuba* var. *spinosa* (Guo et al., 2011a)

Oleanonic acid (**143**) (Lee S. M. et al., 2004; Huang et al., 2001; Yagi et al., 1978), maslinic acid (**144**) and its derivertives, 3–*O*–*trans*–*p*–coumaroyl maslinic acid (**145**) and 3–*O*–*cis*–*p*–coumaroyl maslinic acid (**146**) (Lee S. M. et al., 2004; Yagi et al., 1978), were obtained from the fruit of *Z. jujuba* Mill.

Hydroxyoleanonic acid lactone (**147**) was isolated from the fruits of *Z. jujuba* var. *spinosa* (Guo et al., 2011a).

1.2.5 Dammarane–type saponin

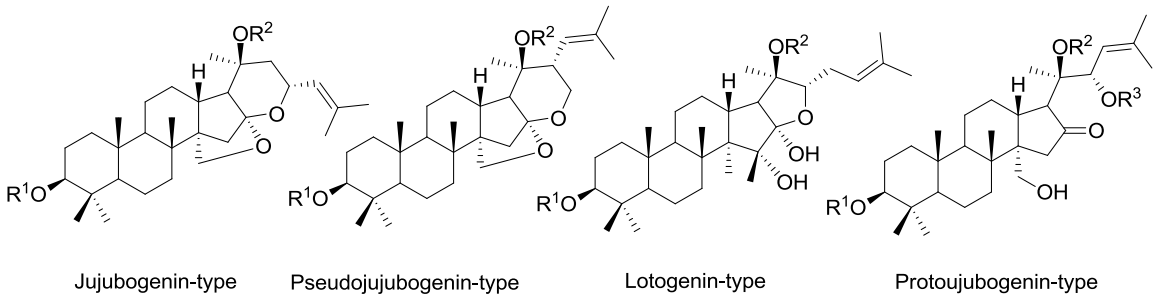

Figure 31 Some basic structures of dammarane–type saponin

Dammarane–type triterpene is a series of 6–6–6–5–6 or 6–6–6–5–5 pentacyclic triterpenes classified into five subgroups according to their aglycone units including jujubogenin (**148**) (Yoshikawa et al., 1997), pseudojujubogenin (**149**) (Ganapaty et al., 2006), protojujubogenin (**150**) (Wang J. Z. and Yang, 2008), lotogenin (**151**) (Renault et al., 1997) and joazeirogenin (**152**) (Schuhly et al., 2000) Sub–types.

1.2.5.1 Jujubogenin saponin

Jujubogenin type saponins is most common dammarane–type compounds containing the same aglycone core namely jujubogenin (**148**) (Yoshikawa et al., 1997).

Jujubosides A (**153**) and B (**154**) were isolated from the seeds of *Z. jujube* (Otsuka et al., 1978).

Jujuboside B_1 (**155**) was isolated from *Z. jujube* (Inoue, Ogihara and Yamasaki, 1978; Otsuka et al., 1978).

Zizyphus saponins I–III (**156**–**158**) were isolated from *Zizyphy fructus* or *Z. jujuba* (Okamura; et al., 1981).

Three triterpenoid saponins were isolated from the bark of *Z. joazeiro* and characterized as jujubogenin 3–*O*–α–*L*–arabinofuranosyl–(1→2)–[β–*D*–glucopyranosyl(1→3)]– α–*L*–arabinopyranoside (**159**), its 4'''–*O*–sulfate (**160**) and 3'',4'''–di–*O*–sulfate (**161**) (Higuchi et al., 1984).

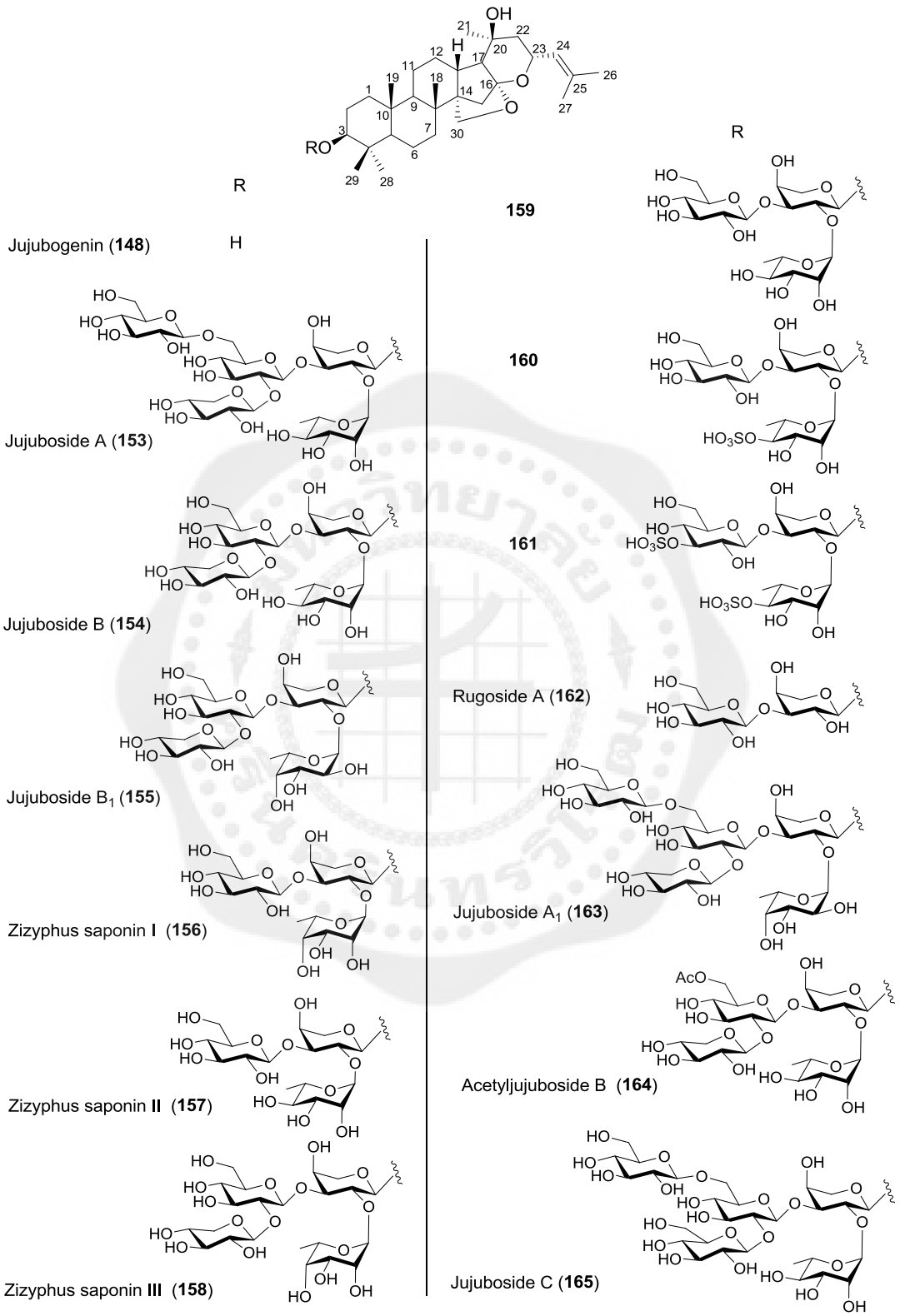

Figure 32 Structures of jujubogenin (**148**) dammarane saponins **153**–**165**

Rugoside A (**162**) was isolated from the bark of *Z. rugosa*, and its structure was established as jujubogenin 3–*O*–*D*–glucosyl–(1→3)–*L*–arabinopyranoside (Pandey V. B. and Tripathi, 1993).

Three saponins jujuboside A_1 (**163**), acetyljujuboside B (**164**), and jujuboside C (**165**) were isolated from Zizyphi Spinosi Semen, the Seeds of *Z. jujuba* MILL. var. *spinosa* HU (Yoshikawa et al., 1997).

A known saponin 3*β*–{{*O*–[*O*–[*α*–*L*–arabinofuranosyl–(1→2)–*O*–[*β*–D–glucopyranosyl–(1→3)]]–*α*–*L*–arabinonopyranosyl}oxy}jujubogenin (**166**) from *Z. joazeiro* stem bark (Schuhly et al., 2000).

Three jujubogenin glycosides of dammarane–type saponins were isolated from the leaves of *Z. lotus* (Maciuk et al., 2004). Their structures were elucidated as 3–*O*–*α*–*L*–Rhamnopyranosyl–(1→6)–*β*–*D*–glucopyranosyl jujubogenin–20–*O*–(2,3,4–*O*–triacetyl)–*α*–*L*–rhamnopyranoside (**167**), 3–*O*–*α*–*L*–rhamnopyranosyl–(1→6)–*β*–*D*–glucopyranosyl jujubogenin–20–*O*–*α*–*L*–rhamnopyranoside (**168**) and 3–*O*–*α*–*L*–rhamnopyranosyl–(1→2)–[(4–sulfo)–*β*–*D*–glucopyranosyl–(1→3)]–*α*–*L*–arabinopyranosyl jujubogenin (**169**) were isolated from *Z. lotus* (Maciuk et al., 2004).

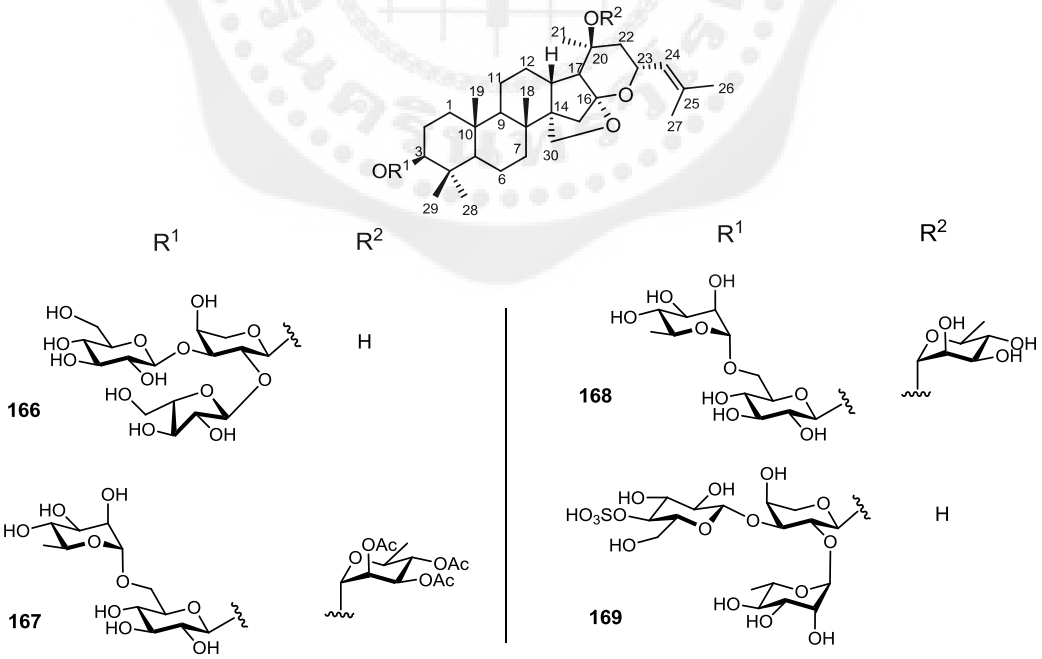

Figure 33 Structures of saponins **166**–**169**

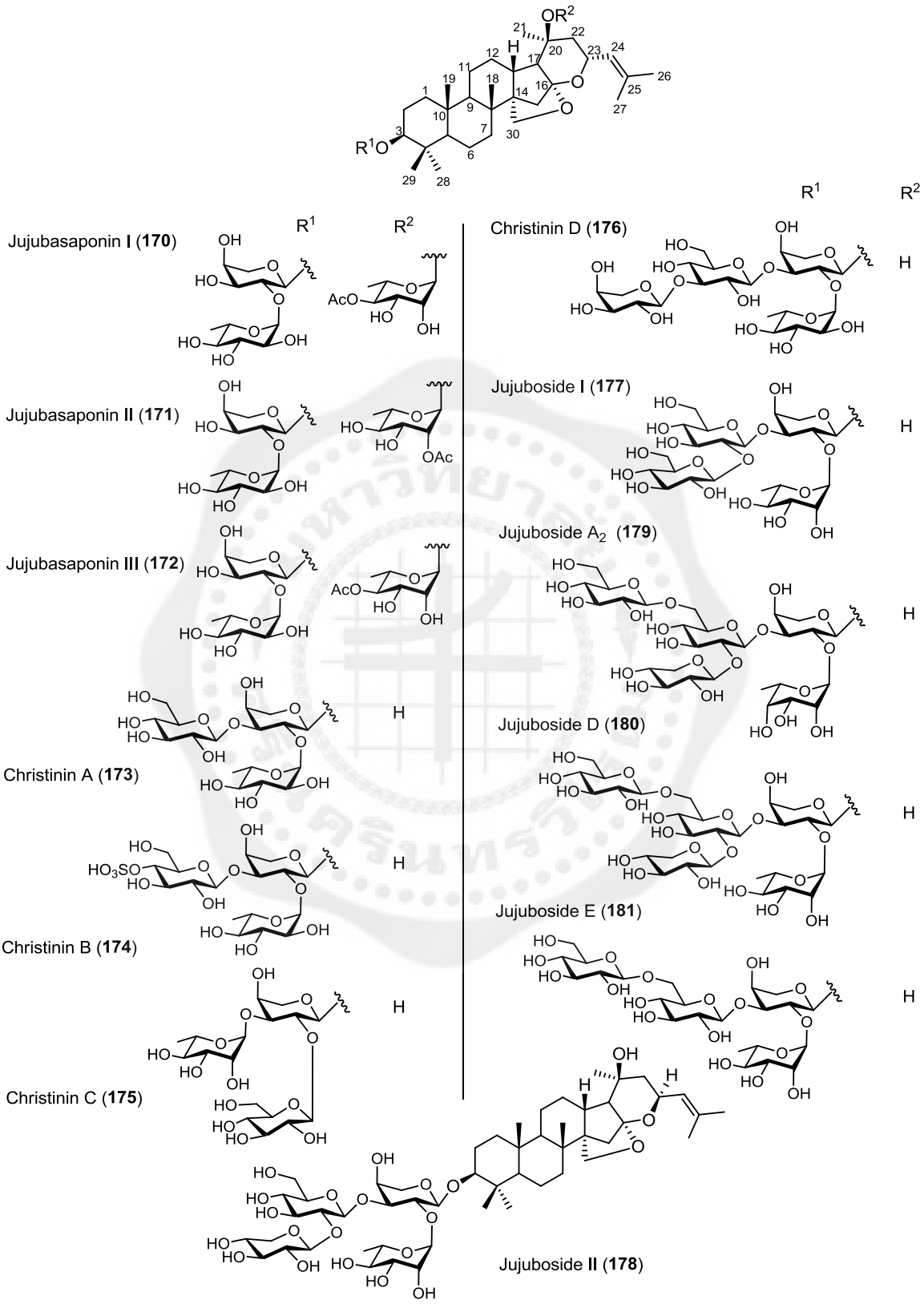

Figure 34 Structures of saponins **170**–**181**

Jujubasaponins I–III (**170**–**172**) were isolated from the fresh leaves of *Z. jujuba* (Yoshikawa, Shimono and Arihara, 1991).

Christinins A (**173**), B (**174**), C (**175**), and D (**176**) were isolated the leaves of *Z. spina–christi* (Mahran et al., 1996).

Jujubosides I–II (**177**–**178**), were isolated from Ziziphi Spinosae Semen or dried and ripe seeds of *Z. jujuba* Mill. var. *spinosa*. The H–23 of jujuboside II (**178**) was determined to have an uncommon α–orientation (Wang Y. et al., 2013).

Jujuboside A_2 (**179**) (Lee S. Y. et al., 2013) as well as two recent dammarane–type saponins named as jujubosides D (**180**) and E (**181**) (Yu, Wang X. S. and Hu, 2014) were isolated from Semen Ziziphi Spinosae or the seeds of *Z. jujuba* var. *spinosa*.

1.2.5.2 Pseudojujubogenin saponin

Some saponins carry pseudojujubogenin (**149**) aglycone that is an isomer of jujubogenin (**148**) in which the isobutenyl group is attached to C–22 instead of C–23 (Ganapaty et al., 2006).

Pseudojujubogenin 3–*O*–*β*–*D*–glucopyranoside (**182**) was isolated from the leaves (Ganapaty et al., 2006) and the stem bark (Rambabu et al., 2011) of *Z. glabrata* Heyne or *Z. trinervia* Roxb, as well as from the roots of *Z. xylopyra* (Rambabu, Ramana and Ganapaty, 2010).

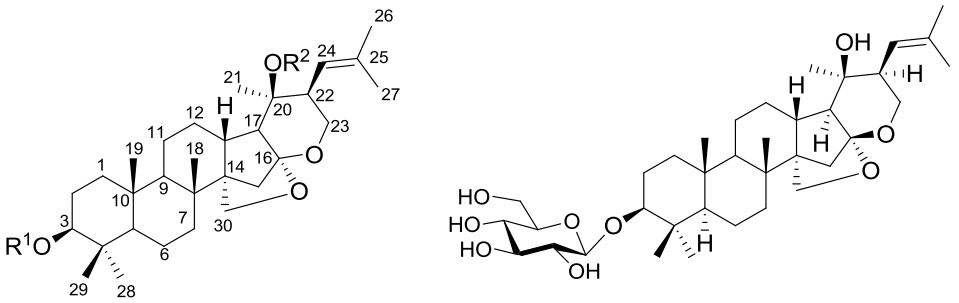

Pseudojujubogenin (**149**) : $R^1 = R^2 = H$ 3-*O*-*β*-*D*-Glucopyranosyl pseudojujubogenin (**182**)

Figure 35 Structures of 3–*O*–*β*–*D*–glucopyranosyl pseudojujubogenin (**182**)

1.2.5.3 Protojujubogenin saponin

A group of keto–dammarane saponin namely protojujubogenin (**150**) (Wang J. Z. and Yang, 2008) comprise a 16–keto and/or a 23–glucosyl moiety in their chemical structure.

Protojujubosides A, B, and B_1 (**183**–**185**) (Matsuda et al., 1999) and jujuboside G (**186**) (Wang J. Z. and Yang, 2008) were isolated from Zizyphi spinosi Semen, the seeds of *Z. jujuba* MILL. var. *spinosa* HU.

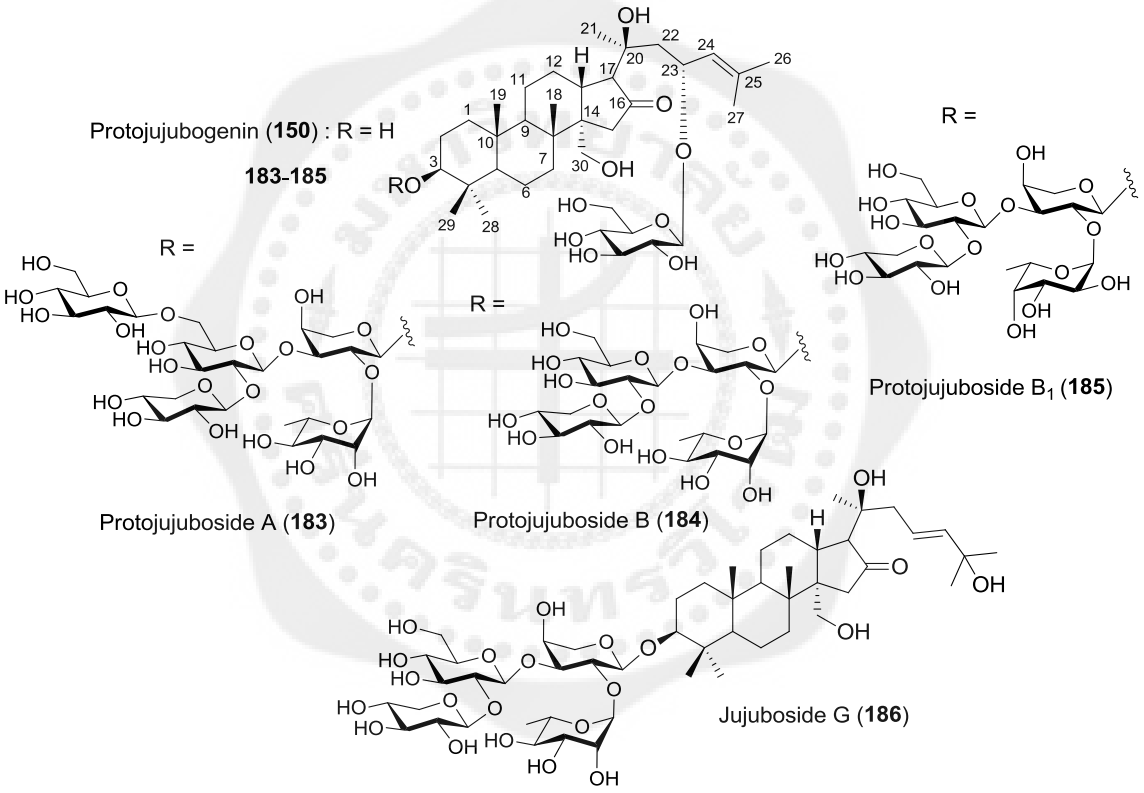

Figure 36 Basic structures of protojujubogenin saponins **183**–**186**

1.2.5.4 Lotugenin saponin

A group of dammarane saponins containing the same aglycone core namely lotugenin (**151**) was identified as (15*R*, 16*R*, 20*R*, 22*R*)–16β,22–epoxydammar–24–ene–38,15α,16α,20β–tetraol (Renault et al., 1997) (Figure 38).

Two lotugenin type saponins were isolated from the root bark of *Z. lotus* and their structures were identified as lotoside I (**187**) or 3–*O*–α–*L*–rhamnopyranosyl(1→2)–[β–*D*–glucopyranosyl(1→3)]–β–*D*–galactopyranosyl lotogenin and lotoside II (**188**) or 3–*O*–α–*L*–rhamnopyranosyl(1→2)–[β–*D*–glucopyranosyl(1→3)]–β–*D*–glucopyranosyl lotogenin (Renault et al., 1997).

Jujubasaponins IV–VI (**189**–**191**), saponins related to the lotogenin type, were isolated from the fresh leaves of *Z. jujuba* (Yoshikawa, Shimono and Arihara, 1992).

Lotoside A (**192**) was obtained from the stem bark of the *Z. joazeiro* (Schuhly et al., 2000).

3–*O*–α–*L*–Rhamnopyranosyl–(1→2)–[(4–sulfo)–β–*D*–glucopyranosyl–(1→3)]–β–*D*–galactopyranosyl–(20*R*,22*R*)–16β,22:16α,30–diepoxydammar–24–ene–3β,20–diol (**193**), a sulfated derivative of jujubasaponin IV (**190**), was isolated from the leaves of *Z. lotus* (Maciuk et al., 2004).

Jujubosides III–IV (**194**–**195**) were isolated from *Ziziphi Spinosae* Semen or dried and ripe seeds of *Z. jujuba* Mill. var. *spinosa* (Wang Y. et al., 2013).

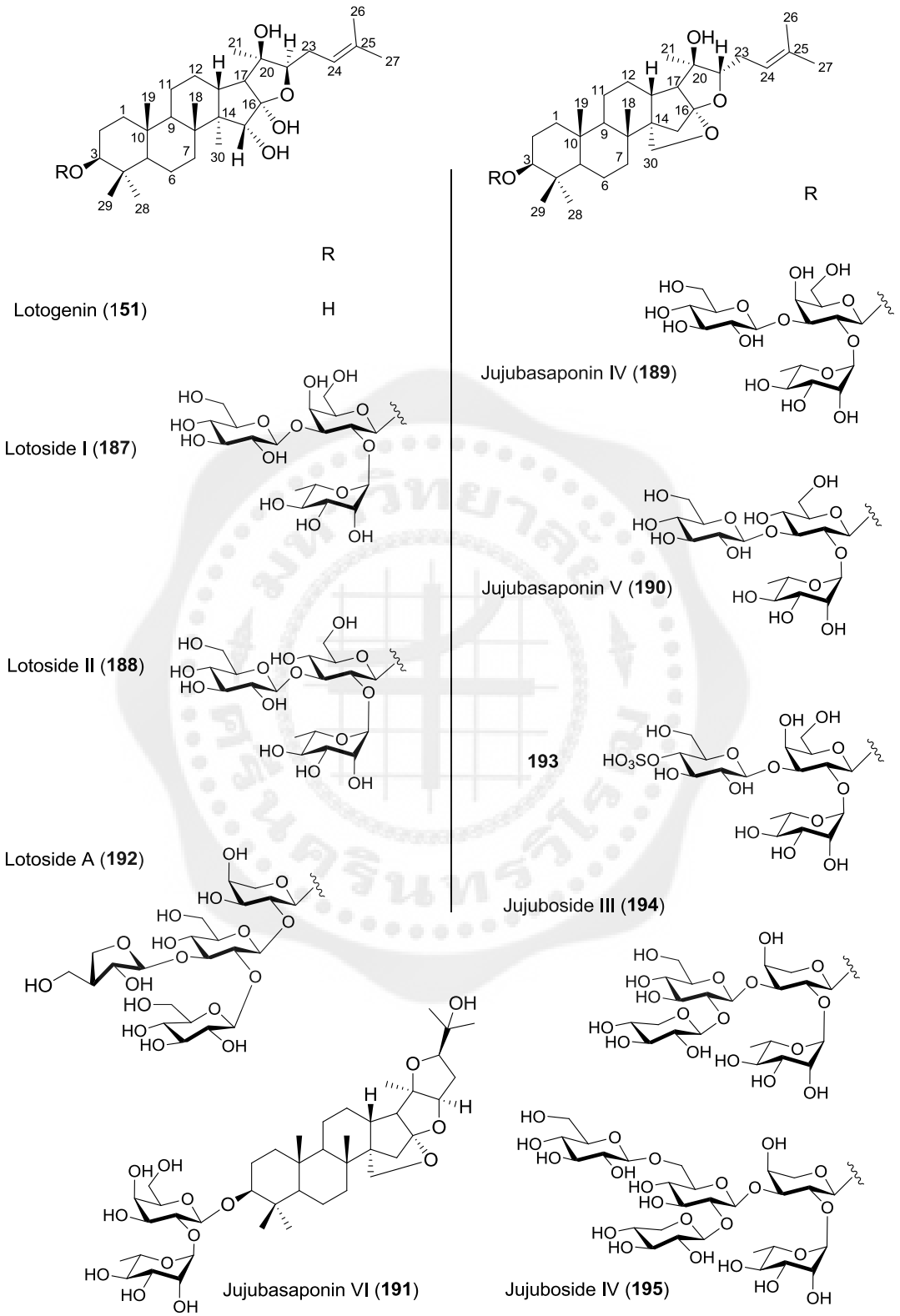

Figure 37 Basic structures of lotugenin (**151**) and saponins **187**–**195**

1.2.5.5 Joazeirogenin saponin

Saponins with an aglycone skeleton classified as 16,22–epoxy–24–methylidenedammarane–3*β*,15*α*,16*α*,20*β*–tetrol are named as joazeirogenin (**152**) (Schuhly et al., 2000).

Two respresentatives of this family, joazeirosides A (**196**) and B (**197**), were isolated from *Z. joazeiro* stem bark (Schuhly et al., 2000).

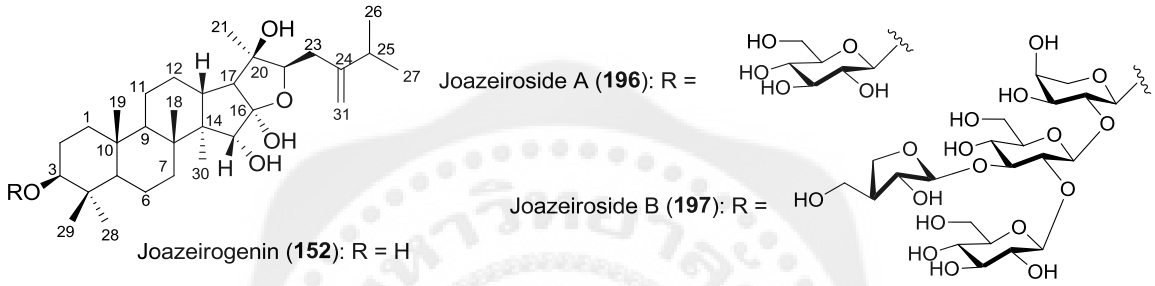

Figure 38 Structures of joazeirogenin (**152**), joazeirosides A (**196**) and B (**197**)

1.2.6 Other triterpenes

Cecropiacic acid (**198**) (Lontsi et al., 1987), an unusual 2,3–seco–ursane type triterpene, was isolated from the fruits of *Z. jujuba* var. *spinosa* (Guo et al., 2011a).

Zizimauritic acids A–C (**199**–**201**), three novel nortriterpenes consisting of a unique A–nor–E–seco spiro–lactone ceanothane–type triterpene skeleton, were isolated from the *Z. mauritiana* roots. A backbone planar structure was elucidated as 19,21–seco–19,20–ene–21,28–lactone ceanothenic acid, forming a spiro γ–methoxyl–γ–lactone at C–17 (Ji et al., 2012).

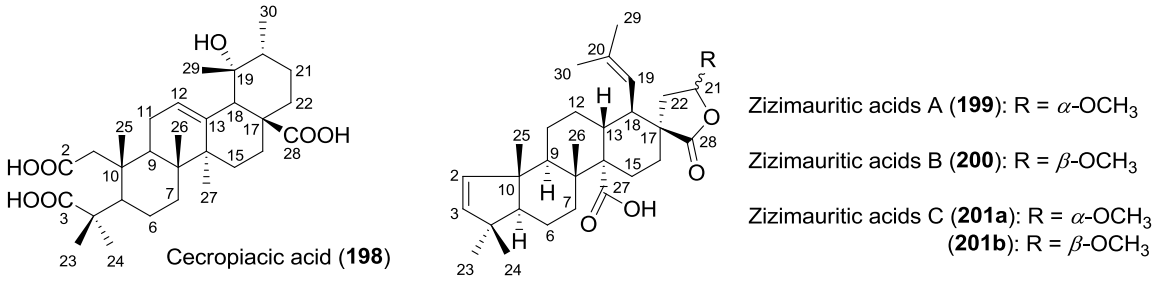

Figure 39 Structures of compounds **198**–**201**

1.2.7 Bioactivities of triterpenes and saponins

Zizimauritic acid B (**200**) exhibited most potent cytotoxicities against A549, BGC–823, Hela cell lines with the IC_{50} values 5.05, 6.24 and 5.36 μg/mL, respectively. Zizimauritic acids A (**199**) and C (**201**) showed an inhibitory effect on the growth of *Staphylococcus aureus* with the IC_{50} values 2.17 and 12.79 μg/mL, respectively (Table 3) (Ji et al., 2012).

Table 3 IC_{50} values (μg/mL) for cytotoxicities on three cancer cell lines, antibacterial and antifungal activities

Compounds	A549[a]	BGC–823[b]	Hela[c]	*SA*[d]	*CA*[e]
Zizimauritic acid A (**199**)	9.37	8.80	6.06	2.17	>10
Zizimauritic acid B (**200**)	5.05	6.24	5.36	>20	>10
Zizimauritic acid C (**201**)	11.94	10.06	9.25	12.79	>10
Taxol	0.02	0.01	0.38	–	–
Ampicillin	–	–	–	0.04	–
Miconazole nitrate	–	–	–	–	0.16

[a]Human lung carcinoma; [b]Gastric cancer cell line; [c]Immortal cell line; [c]*Staphylococcus aureus*; [d]*Candida albicans*

Jujubosides A (**153**), B (**154**), A_1 (**163**) and C (**165**), and acetyljujuboside B (**164**), found to be inhibitor of histamine release from rat peritoneal exudate cells induced by antigen–antibody reaction (Table 4) (Yoshikawa et al., 1997).

Pseudojujubogenin–3–*O*–*β*–*D*–glucopyranoside (**182**) exhibited antimicrobial activity against *Bacillus pumilus*, *Staphylococcus aureus*, *Escherichia coli* and *Proteus vulgaris* with MICs value of 51.2, 102.2, 12.8, 25.6 μg/mL, respectively (Ganapaty et al., 2006).

The inhibitory activity of jujuboside A (**153**), jujuboside A_1 (**163**), jujuboside C (**165**), jujuboside D (**180**) and jujuboside E (**181**) against lipoxygenase was determined. They exhibited as potent inhibitors of lipoxygenase (Table 5) (Yu, Wang and Hu, 2014).

Table 4 Inhibitory effects of jujubosides A (**153**), B (**154**), A_1 (**163**) and C (**165**), and acetyljujuboside B (**164**) on the histamine release

Compounds	Concentration	% Inhibition
Jujuboside A (**153**)	10^{-4}	46.9
Jujuboside B (**154**)	10^{-5}	32.0
Jujuboside A_1 (**163**)	10^{-4}	30.3
Acetyljujuboside B (**164**)	10^{-4}	14.5
Jujuboside C (**165**)	10^{-4}	71.4
Alexanox	10^{-4}	61.2
	10^{-5}	11.8

Table 5 Inhibitory effects of jujubosides A (**153**), A_1 (**163**), C (**165**), D (**180**) and E (**181**) against lipoxygenase

Compounds	IC_{50} (μM)
Jujuboside A (**153**)	61.2
Jujuboside A_1 (**163**)	71.3
Jujuboside C (**165**)	48.9
Jujuboside D (**180**)	56.7
Jujuboside E (**181**)	53.9
Baicalein	21.4

Jjujuboside A (**153**) exhibited moderate acetylcholinesterase (AchE) inhibitory activity with an inhibition value of 46.2% at a concentration of 1 μM compared with tacrine (59.0%) (Wang B. et al., 2013). It has been proven to be a hypnotic–sedative compound that may serve as a potential therapeutic agent for the treatment of Alzheimer's disease (Liu et al., 2014).

Jujuboside B (**154**) exhibited cytotoxicity against AGS human gastric cancer cells, HCT 116 human colon cancer cells, and Chang hepatic normal cells with IC_{50} values of 107, 114, and 182 μM, respectively. The IC_{50} values indicate a more potent

cytotoxicity effect against cancer cells versus normal cells. Mechanistic studies showed that the antitumor mechanism of jujuboside B (**154**) induced apoptosis and autophagy in AGS and HCT 116 human cancer cells and also effectively suppressed tumor growth in a nude mouse xenograft model bearing HCT 116 cells (Xu M.–Y. et al., 2014).

1.3 Flavonoid and glycosides

1.3.1 Flavonoids and phenolic compounds

Three flavonoids, quercetin (**202**), catechin (**203**), and epicatechin (**204**), together with ten phenolic compounds, cinnamic acid (**205**), *p*–coumaric acid (**206**), caffeic acid (**207**), ferulic acid (**208**), chlorogenic acid (**209**), *p*–hydroxybenzoic acid (**210**), protocatechuic acid (**211**), gallic acid (**212**), vanillic acid (**213**), and ellagic acid (**214**) (Figure 41) were found in the jujube fruit (*Ziziphus jujuba* Mill.) (Gao et al., 2012a; Gao et al., 2012b).

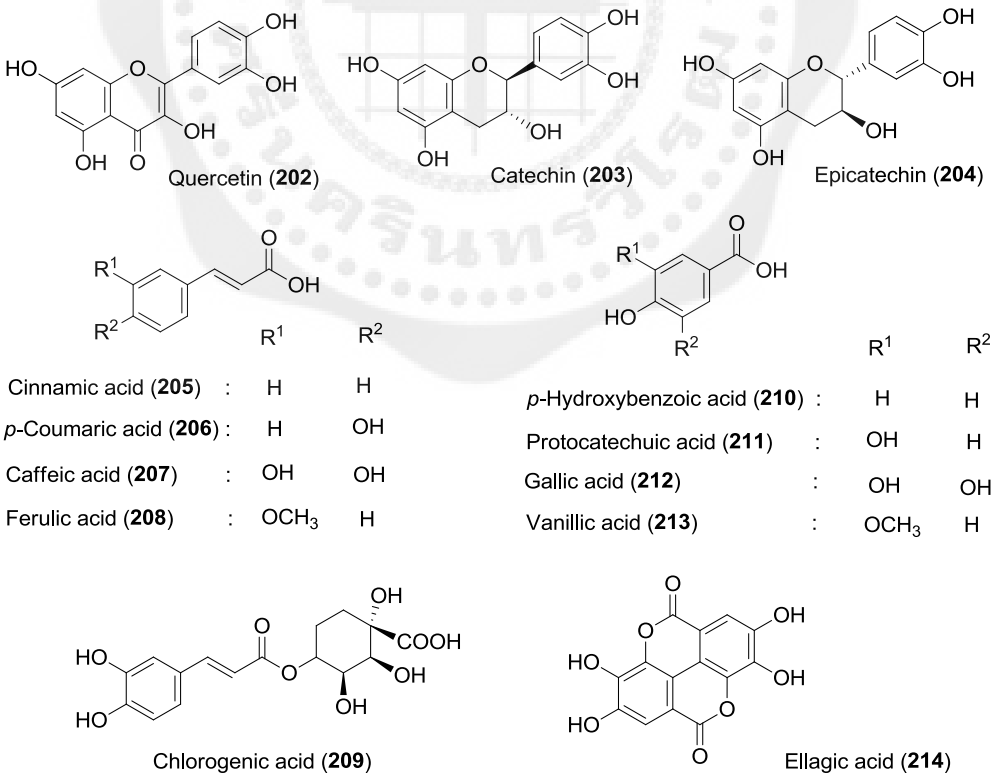

Figure 40 Structures of flavonoids and phenolic compounds **202**–**214**

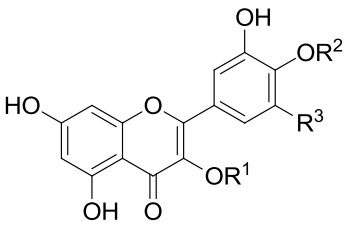

	R^1	R^2	R^3
Quercetol 4'-*O*-α -*L*-rhamnopyranosyl-3-*O*-α -*L*-rhamnopyranosyl-(1''''-6''')-β-*D*-glucopyranoside (**215**)	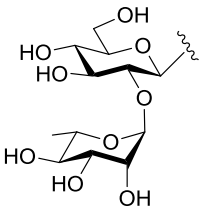	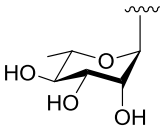	H
Myricetin-3-O-[β-xylopyranosyl-(1-2)-α-rhamnopyranoside]-4'-*O*-α-rhamnopyranoside or Bayarin (**216**)	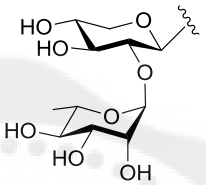	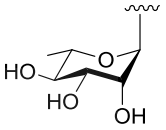	OH
Quercitrin (**217**)	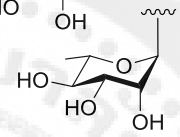	H	H
Isoquercitrin or quercitin 3-*O*-β-*D*-glucoside (**218**)	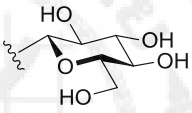	H	H
Quercitrin 3-*O*-*D*-arabinosyl-(1-2)-α-*L*-rhamnoside (**219**)	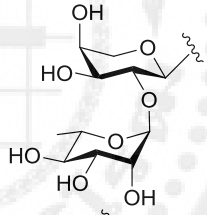	H	H
quercetin-3-O-[β-xylopyranosyl-(1-2)-α-rhamnopyranoside]-4'-*O*-α-rhamnopyranoside (**220**)	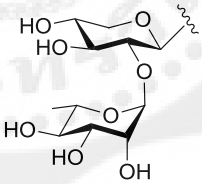	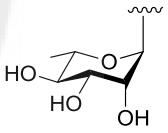	H
quercetin-3-O-β-xylopyranosyl-(1-2)-α-rhamnopyranoside (**221**)	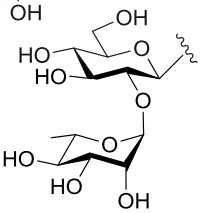	H	H
Rutin or quercetin-3-*O*-rutinoside (**222**)	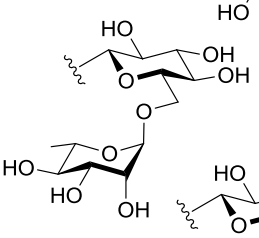	H	H
Quercetin-3-*O*-β-galactopyranoside (**223**)	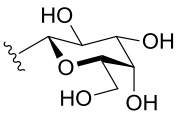	H	H

Figure 41 Structures of flavonoid *O*–glycosides **215**–**223**

1.3.2 Flavonoid *O*–glycosides

Two new flavonol glycoside quercetol 4'–*O*–α–*L*–rhamnopyranosyl–3–*O*–α–*L*–rhamnopyranosyl–(1""–6''')–*β*–*D*–glucopyranoside (**215**) (Maciuk et al., 2003) and a flavonol triglycoside, bayarin (**216**) or myricetin–3–*O*–[*β*–xylopyranosyl–(1→2)–*α*–rhamnopyranoside]–4'–*O*–*α*–rhamnopyranoside (Devkota, Watanabe and Yahara, 2013), were obtained from the leaves of *Z. lotus* and from the aerial parts of *Z. incurva* Roxb., respectively.

Quercitrin (**217**), isoquercitrin or quercitin 3–*O*–*β*–D–glucoside (**218**) and quercitin 3–*O*–*D*–arabinosyl–(1→2)–*α*–L–rhamnoside (**219**) (Figure 42), were isolated from the leaves of *Z. cambodiana* (Li X. et al., 2007).

Six known flavonoid glycosides were isolated from the aerial parts of *Z. incurva* Roxb for the first time. They were identified as quercetin–3–*O*–[*β*–xylopyranosyl–(1→2)–*α*–rhamnopyranoside]–4'–*O*–*α*–rhamnopyranoside (**220**), quercetin–3–*O*–*β*–xylopyranosyl–(1→2)–*α*–rhamnopyranoside (**221**), rutin (**222**), quercetin–3–*O*–*β*–glucopyranoside (**218**) and quercetin–3–*O*–*β*–galactopyranoside (**223**) (Figure 42) (Devkota, Watanabe and Yahara, 2013).

1.3.3 Flavonoid *C*–glycosides

A group of spinosin (**224**) derivatives, such as three new acylated flavonoid *C*–glycosides, 6'''–(–)–phaseoylspinosin (**225**), 6'''–(3'''',4'''',5''''–trimethoxyl)–(*E*)–cinnamoylspinosin (**226**) and 6'''–(4''''–*O*–*β*–*D*–glucopyranosyl)–benzoylspinosin (**227**) were isolated from *Z. mauritiana* seeds (Wang B. et al., 2013).

3,5'–Di–*C*–*β*–glucopyranosyl phloretin (**228**) was isolated from the aerial parts of *Z. incurva* Roxb. (Devkota, Watanabe and Yahara, 2013).

1.3.4 Recent bioactivities of flavonoids and glycosides

Compounds **217**–**219** exhibited neuraminidase inhibitory activity with IC_{50} 7.89, 9.87, 4.82 μM, respectively (Li X. et al., 2007).

Compounds **225** and **226** displayed a moderate AChE inhibitory activity with inhibition values of 24.9% and 33.9%, respectively, at a concentration of 1 μM, wherein tacrine (59.0%) was used as a positive control (Wang B. et al., 2013).

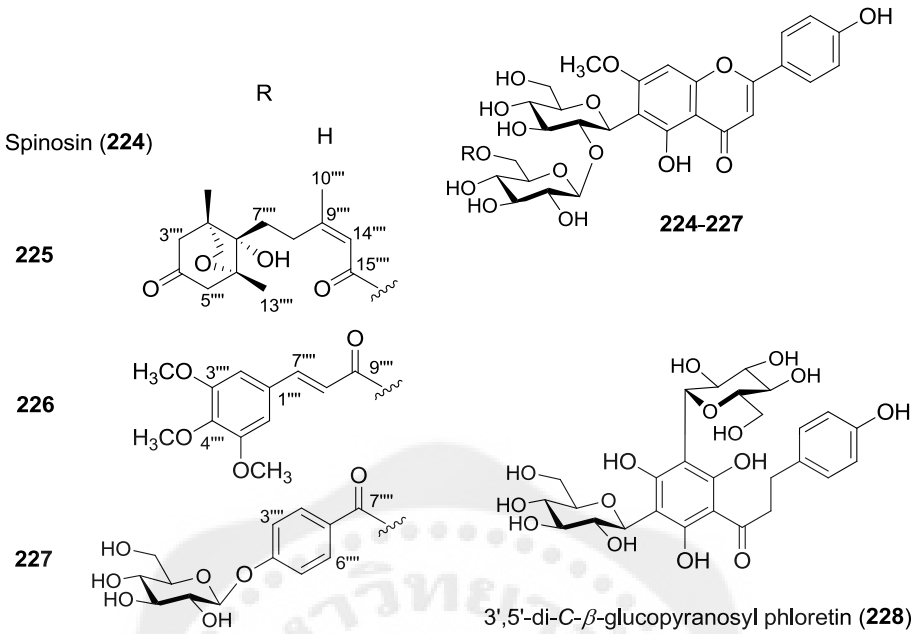

Figure 42 Structures of flavonoids *C*–glycosides **224**–**228**

1.4 Simultaneous analysis of bioactive constituents from *Ziziphus* plants

Chemical investigation of *Ziziphus* plants revealed the presence of many bioactive compounds such as cyclopeptide alkaloids, flavonoids, triterpenes and saponins. Many studies focused on the analytical methods for the determination of the triterpenic acids, saponins and flavonoids in *Ziziphus* plants and their seeds, fruits and leaves, using high–performance liquid chromatography (HPLC). A HPLC technique was developed and validated for detection of those compounds by comparison with several known species, especially commercial fruit of *Z. jujuba*.

Guo et al., have reported a reverse–phase high–performance liquid chromatography (HPLC) method for the simultaneous characterization and quantitation of eleven triterpenic acids [betulinic acid (**1**), alphitolic acid (**117**), betulonic acid (**123**), ceanothic acid (**126**), epiceanothic acid (**133**), ursolic acid (**136**), ursonic acid or ursolonic acid (**138**), pomonic acid (**139**), oleanolic acid or oleanic acid (**142**) and maslinic acid (**144**) (Figure 42)] in chloroform extracts of jujube fruits (*Z. jujube* and *Z. jujuba* var. *spinosa*). This was achieved by using an evaporative light scattering detector (ELSD) and electrospray ionization–mass spectrometry (ESI–MS) (Guo et al., 2010). Guo et al., have also reported

on the method development for leaves of *Z. jujuba* and *Z. jujuba* var. *spinosa* from different sources. The determinations were based on HPLC coupled with photo diode array and electrospray ionization tandem mass spectrometry detection (HPLC–PDA–ESI–MS/MS). As a result, fourteen constituents, including three flavonoids, two saponins and nine triterpenic acids, were identified or tentatively characterized. The naturally occurring compounds betulinic acid (**1**), alphitolic acid (**105**), ceanothic acid (**114**), zizyberanalic acid (**118**), ceanothenic acid (**120**), epiceanothic acid (**121**), 2α–hydroxyursolic acid (**125**), oleanolic acid (**129**), maslinic acid (**131**), zizyphus saponins I (**142**) and II (**143**) and quercetin–3–*O*–rutinoside (**204**) were selected as the chemical markers and were determined using HPLC coupled with evaporative light scattering detection (ELSD) method. The separation was carried out on a C18 column with 0.2% acetic acid and acetonitrile as the mobile phase under gradient elution (Guo et al., 2011b).

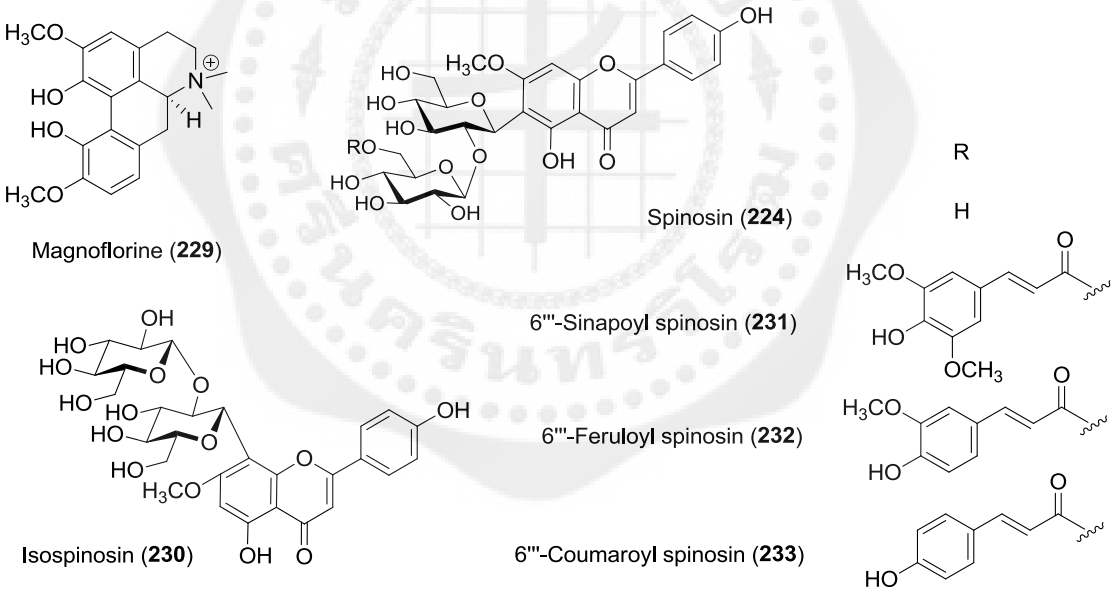

Figure 43 Structures of compounds **229**–**233**

Liao et al. (2012) have established a HPLC method with diode array detector (DAD), ELSD and ESI–MS for the simultaneous determination of nine representative metabolites from *Z. jujuba* var. *spinosa* including an alkaloid [magnoflorine (**229**)], five flavonoids [spinosin (**224**), isospinosin (**230**), 6'''–sinapoyl spinosin (**231**), 6'''–feruloyl spinosin (**232**), and 6'''–coumaroyl spinosin (**233**) (Figure 44)], three saponins [jujuboside A

(**139**), jujuboside A_2 (**164**), and jujuboside B (**154**) (Figure 32)]. The optimal chromatographic conditions were obtained on an ODS column and the mobile phase was composed of water and methanol with 0.1% formic acid using a gradient elution system. The verified method was successfully applied to the quantitative determination of representative metabolites in commercial fruits of *Z. jujuba* and *Z. mauritiana* from different markets. The analytical results showed that the contents of the nine analytes vary significantly with sources and species (Liao et al., 2012).

2. Structural modification of some naturally derived compounds

Several naturally occurring compounds exhibited less potent bioactivities because of their limited solubility in aqueous medium and/or stability. There are several routes that can be used to improve these issues, such as structural modification into water soluble salts, polyhydroxy groups and glycosides. Glycoside is a particularly important analogue that is involved the pharmacological activities due to an increased stability and/or solubility of various organic compounds, for example vitamins, terpenoids and phenolic compounds. There are many routes for the production of glycosides, e.g. biotransformations (such as cultured cells or enzymes) or chemical reactions on pharmaceuticals, aroma chemicals, and food additives (Hamada and Shimoda, 2013).

This study will be focused on the glycosylation of betulinic or 3–hydroxy–lup–20(29)–en–28–oic acid (**1**) and α–mangostin (**234**), bioactive naturally occurring compounds (aglycones) available in our laboratory. .

2.1 Glycosylation of betulinic acid

Betulinic acid (**1**) is the major widely distributed pentacyclic lupane–type triterpene in *Ziziphus* plants. Our lab uses betulinic acid found in Thai *Z. oenoplia*, *Z. cambodiana* and *Z. mauritiana*. It has been reported as anti–HIV (Kashiwada et al., 2000), antiplasmodial (Ziegler et al., 2004; Suksamrarn et al., 2006), antituberculosis (Cantrell et al., 2001; Suksamrarn et al., 2006) and anticancer (You et al., 2003) agents. Zuco et al. (2012) have proved that betulinic acid (**1**) is selective against cancer cells without affecting

normal cells. However, the medical uses of betulinic acid as therapeutic agents are limited because of their poor aqueous solubility and pharmacokinetic properties including absorption, distribution, metabolism and elimination (Udeani et al., 1999). In order to overcome these issues, modification of betulinic acid (**1**) and its related compounds [lupeol (**114**) and betulin (**115**)] into their glycosides would be of high interest. Previous synthetic and medicinal chemistry studies of betulinic acid derivatives revealed that betulinic acid (**1**) properties can be improved upon the addition of a sugar moiety at either C–3 and/or C–28. Importantly, it has been reported that betulinic acid glycosides have higher aqueous solubility than betulinic acid (Thibeault et al., 2007; Abdu et al., 2012) and also enhance pharmacokinetics properties (Thibeault et al., 2007).

For instance, glycosylations of betulinic acid was reported by Pichette's group. The synthesis of several saponins derived from three lupine–type triterpenes, betulinic acid (**1**), lupeol (**114**) and betulin (**115**), was based on six different natural sugar residues (*D*–glucose, *L*–rhamnose, *D*–arabinose, *D*–galactose, *D*–mannose and *D*–xylose) as follows.

Gauthier et al. (2006), reported the synthesis of *β*–*D*–glucopyranoside, *α*–*L*–rhamnopyranoside, and *α*–*D*–arabinopyranoside through glycosylation of betulinic acid (**1**) (Scheme 6), lupeol (**114**) (Scheme 8) and betulin (**115**) (Scheme 9) with trichloroacetimidate (TCA) glycosyl donors (**235**–**237**) (Scheme 6). Acceptors **1** and **115** were protect their functional groups at C–28 with allyl– and acetyl groups, respectively. The glycosylations were performed at rt in CH_2Cl_2 under catalysis of a Lewis acid, trimethylsilyl trifluoromethanesulfonate (TMSOTf). The protecting groups (benzoyls) were subsequently removed by using 0.25 N NaOH in MeOH/THF/H_2O (1:2:1). The C–28 acid function of betulinic acid was regenerated in the presence of tetrakistriphenyl phosphine palladium catalyst and pyrolidine in dry THF to give the desired saponins (Scheme 6). The glycosides were tested *in vitro* for cytotoxicity against cancer cell lines (A549, DLD–1 and B16–F1) and healthy (WSI) cell line. The results show that the 3–*O*–*α*–*L*–rhamnopyranosyl derivative (**239**) exhibited 8–12 fold higher sensitivity against cancer cell–lines with IC_{50} 2.6–3.9 μM, than that to the normal cells (IC_{50} 31 μM) (Table 6) (Gauthier et al., 2006).

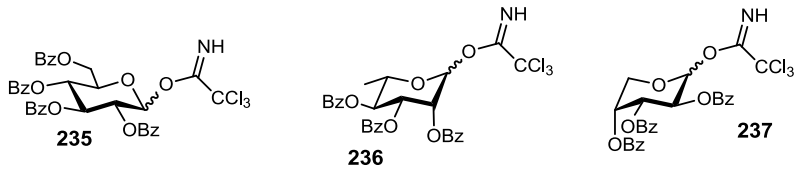

Figure 44 Trichloroacetimidate (TCA) glycosyl donors **235**–**237**

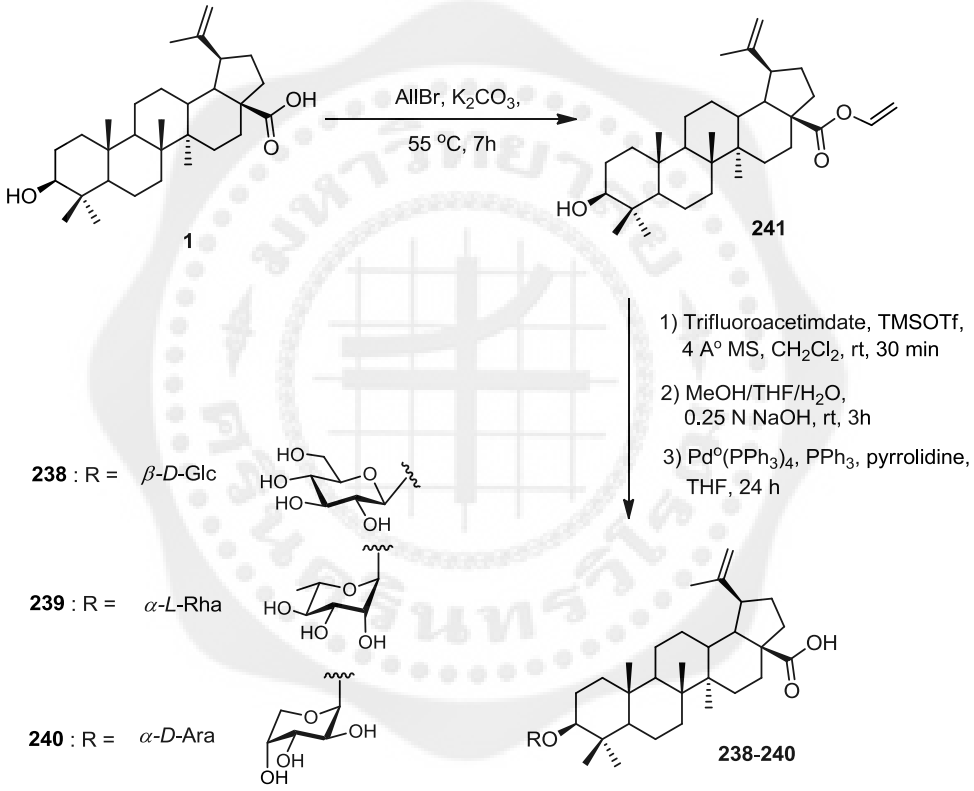

Scheme 6 Synthesis of betulinic acid glycosides **238**–**240**

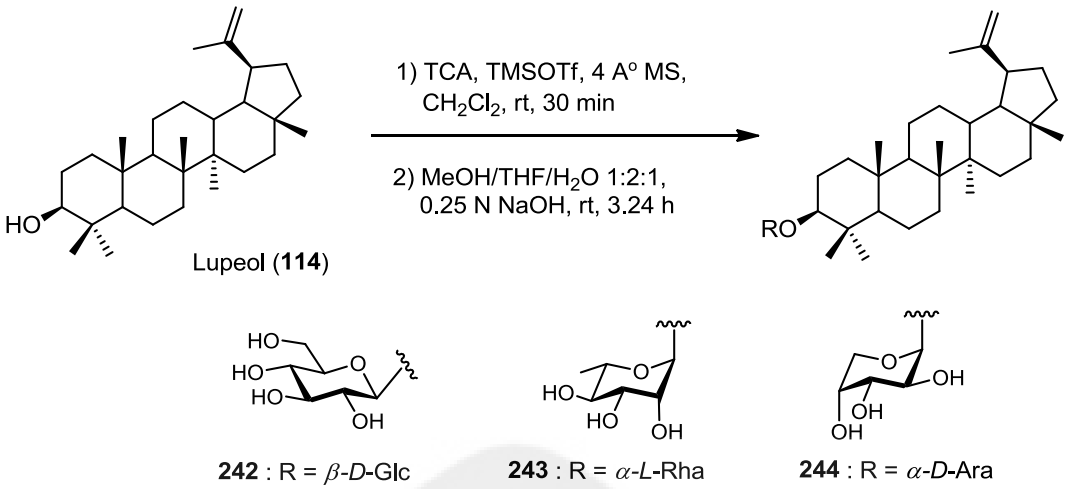

Scheme 7 Synthesis of lupeol glycosides **242**–**244**

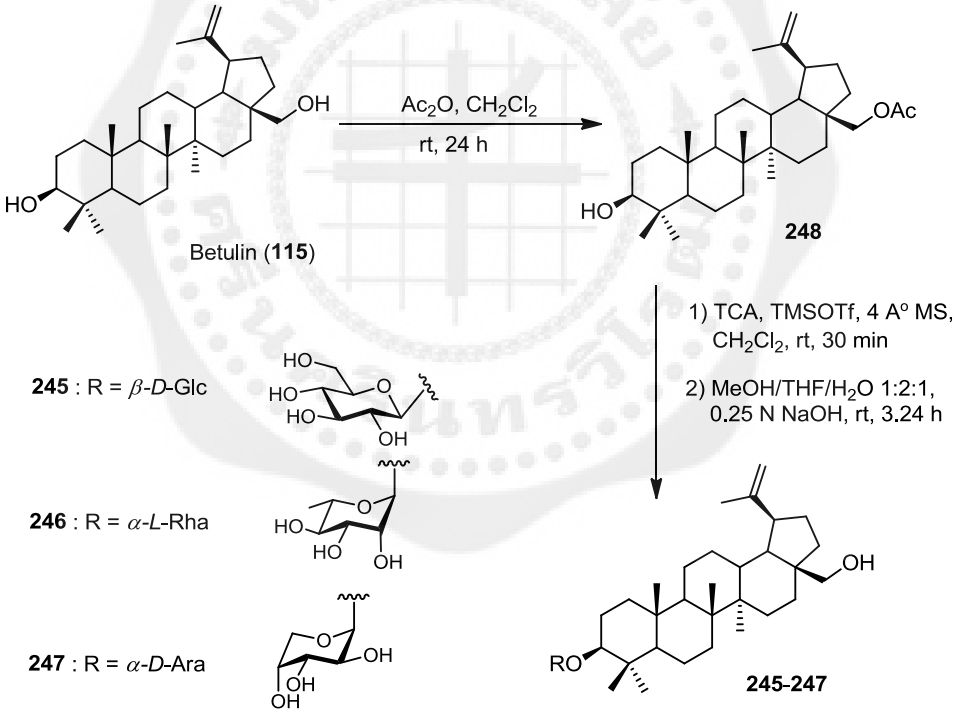

Scheme 8 Synthesis of betulin glycosides **245**–**247**

Noteworthy, from the *in vitro* cytotoxic results and the study of structure–activity relationships (SAR), Gauthier et al. have concluded that glycoside **239** exerted a stronger activity than betulinic acid (**1**) against tested cancerous cell lines (Table 6). The 3–

O–glycosylation of betulin (**115**) decreased the activity. The 3–*O*–β–*D*–glucosyl derivative of lupeol (**242**) enhanced the activity of its aglycone. The 3–*O*–α–*L*–rhamnosylation decreases the activity of lupeol (**114**) and betulin (**115**) except for betulinic acid (**1**). The 3–*O*–α–*D*–arabinosylation enhanced the activity of betulinic acid (**1**) and lupeol (**114**). The 3–*O*–glycosylation of betulinic acid (**1**) increased the selectivity against tested cancerous cell lines and enhanced the activity in the case of *L*–rhamnose and *D*–arabinose (Gauthier et al., 2006).

Table 6 Cytotoxicity of saponins **238**–**240** and **242**–**247**

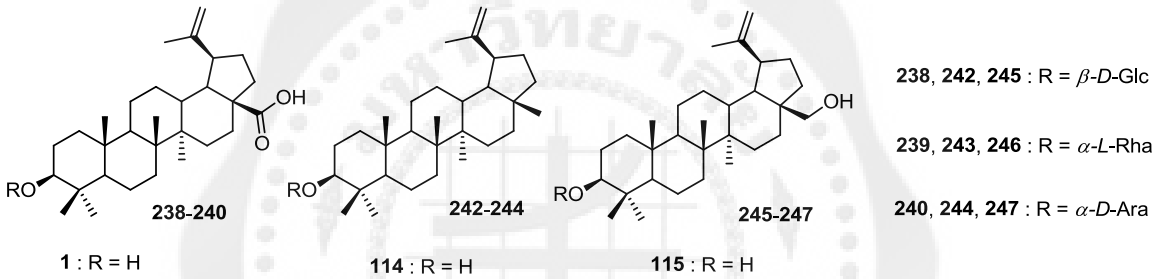

Compounds	IC_{50} (μM)			
	A549[a]	DLD–1[b]	B16–F1[c]	WS1[d]
Betulinic acid (**1**)	10.3	15.0	16.1	12
Lupeol (**114**)	165	125	104	63
Betulin (**115**)	3.80	6.6	13.8	3.58
238	>178	32	49	> 178
239	2.6	3.9	3.9	31
240	10	17	11	47
242	14	14	15.0	13.3
243	>178	>178	>178	>178
244	28	50	27	15.8
245	>200	>200	>200	>200
246	22	50	18	33
247	41	63	38	59
Etoposide[e]	1.2	27	–	34

[a] Human lung carcinoma; [b] Human colorectal adenocarcinoma; [c] mice melanoma; [d] Human normal skin;

[e] Reported by Gauthier et al., 2009

Thibeault et al. (2007), have described the synthesis of a series of 3–*O*–*β*–monodesmosidic saponins derived from lupane–type triterpenes betulinic acid (**1**) and betulin (**115**) based on six different natural sugar residues (*D*–glucosyl, *L*–rhamnosyl, *D*–arabinosyl, *D*–galactosyl, *D*–mannosyl and *D*–xylosyl) using glycosyl donors **235**–**237** and **249**–**251**. A series of glycosides were synthesized according to the reaction sequence shown in Scheme 10. Germanicane–type aglycones, allobetulin (**252**) and 28–oxoallobetulin (**253**) were obtained by the Wagner–Meerwein rearrangement of betulin (**115**) and betulinic acid (**1**), respectively, by the action of $Fe(NO_3)_3/SiO_2$ (1:4) in refluxing CH_2Cl_2. Then aglycones **252** and **253** were coupled with each trichloroacetimidate donor. Series of synthetic saponins derived from allobetulin (**254**–**259**) and 28–oxoallobetulin (**260**–**265**) have been studied for their *in vitro* anticancer activity against A549, DLD–1 and WS1 cell lines. The structure–activity relationship (SAR) study confirmed that glycosides of allobetulin (**252**) and 28–oxoallobetulin (**253**) generally decreased anticancer activity of betulinic acid (**1**) and betulin (**115**). All synthesized saponins have been calculated for their lipophilicity and aqueous solubility. The theoretical results showed that glycosides were shown to be more soluble in polar solvents (DMSO, MeOH) than their corresponding aglycone. These results were in agreement with their log*P* values smaller than 5 (Thibeault et al., 2007).

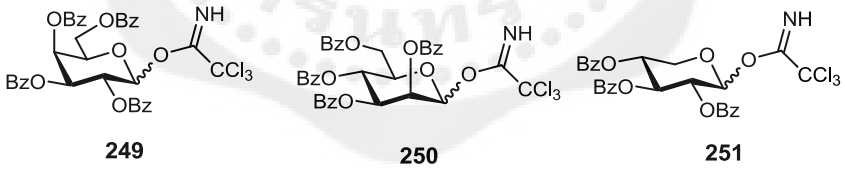

Figure 45 Trichloroacetimidate (TCA) sugar donors **249**–**251**

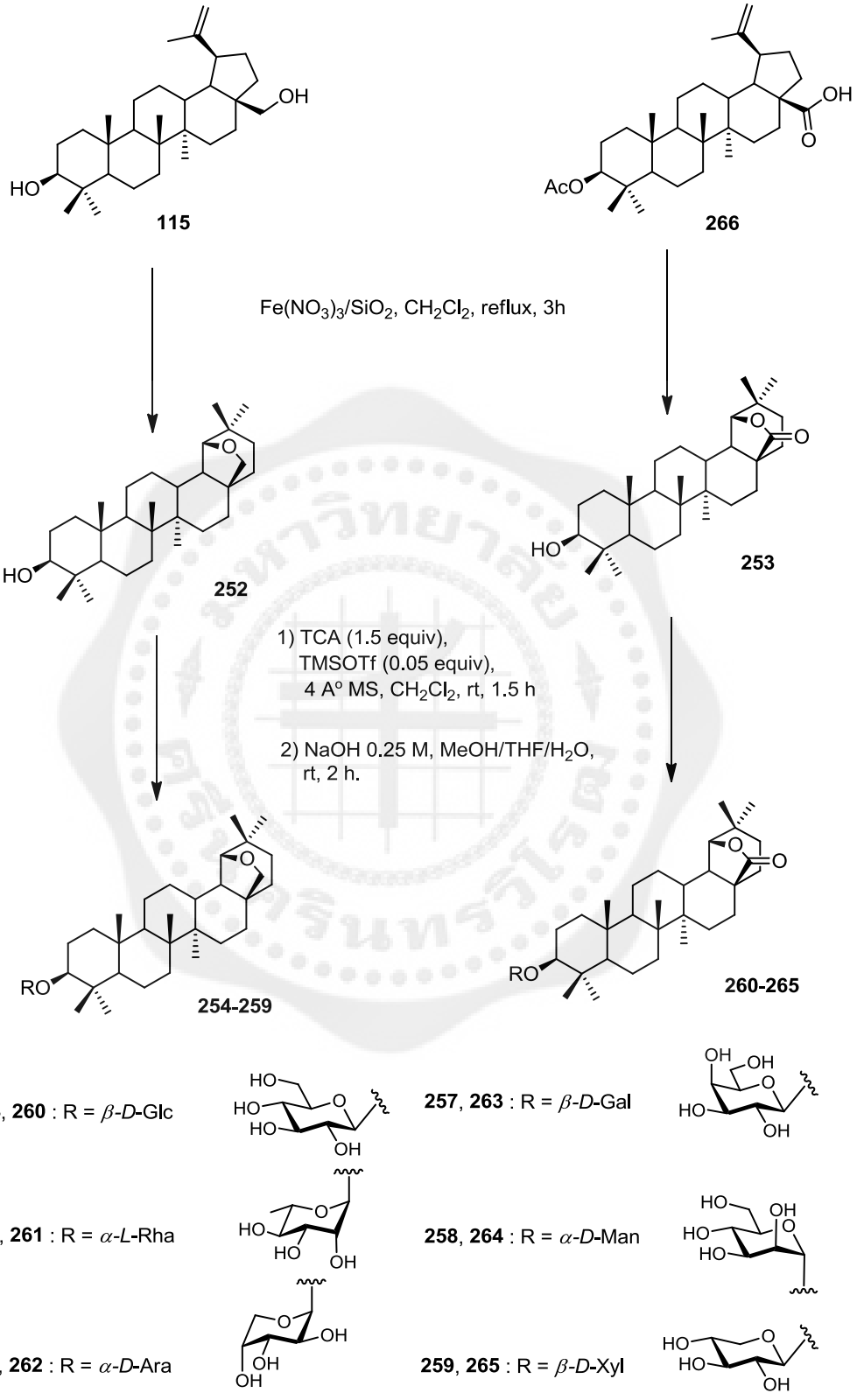

Scheme 9 Synthesis of saponins **254**–**265**

Table 7 Cytotoxicity of synthetic saponins **254**–**265**

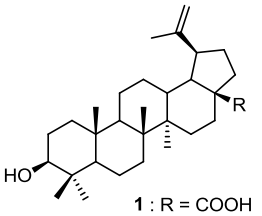

1 : R = COOH
114 : R = CH_2OH
115 : R = CH_3

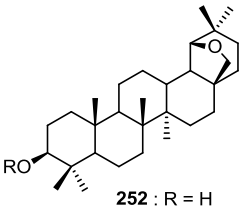

252 : R = H
254, **260** : R = β-*D*-Glc
255, **261** : R = α-*L*-Rha
256, **262** : R = α-*D*-Ara

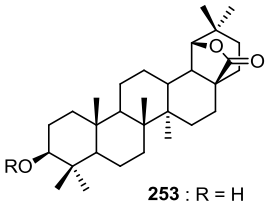

253 : R = H
257, **263** : R = β-*D*-Gal
258, **264** : R = α-*D*-Man
259, **265** : R = β-*D*-Xyl

Compounds	IC_{50} (μM)			log*P*	log*S*
	A549[a]	DLD–1[b]	WS1[c]		
Betulinic acid (**1**)	10.3	15.0	12	6.31	–6.91
Betulin (**115**)	3.80	6.6	3.58	6.06	–6.70
Lupeol (**114**)	165	125	63	–	–
Allobetulin (**252**)	>75	>75	>75	6.24	–7.44
28–oxoallobetulin (**253**)	>75	>75	>75	5.55	–6.83
254	31	40	40	3.95	–6.61
255	>75	>75	>75	4.71	–6.94
256	>75	>75	>75	4.73	–6.97
257	30	40	40	4.17	–6.30
258	>75	>75	>75	3.99	–6.67
259	>75	>75	>75	4.67	–6.96
260	>75	>75	>75	3.32	–6.31
261	>75	>75	>75	4.09	–6.56
262	>75	>75	>75	4.00	–6.64
263	>75	>75	>75	3.40	–6.29
264	>75	>75	>75	3.34	–6.16
265	>75	>75	>75	3.92	–6.57
Etoposide[d]	1.2	27	34	–	–

[a] Human lung carcinoma; [b] Human colorectal adenocarcinoma; [c] Human normal skin;

[d] Reported by Gauthier et al., 2009

Gauthier et al., also described the *O*–glycosylation of betulinic acid (**1**) and 28–oxoallobetulin (**253**) at the C–3 position. The chacotriosidesaponins (**266**–**267**) were evaluated *in vitro* for their anticancer (A549, DLD–1, MFC7, PC–3 and WS1 cell lines) and haemolytic activities. Chacotriosidesaponin **266** decreased the cytotoxicity of betulinic acid (**1**), whereas, chacotriosidesaponin **267** exhibited more potent cytotoxicity than that of the corresponding aglycone **253** against all cancer cell lines with IC_{50} range of 3.8–18 μM. Remarkably, the anticancer activity profile of chacotriosidesaponin **267** against human colorectal adenocarcinoma (DLD–1), human breast adenocarcinoma (MCF7), human prostate adenocarcinoma (PC–3) and human normal skin fibroblasts (WS1)was stronger than that of **1**. Haemolytic activity against red blood cells of saponins was also reported. Chacotriosidesaponin **267** exhibited haemolytic activity more than 10–fold in comparison with chacotriosidesaponin **265** and **1** (Table 8) (Gauthier et al., 2009).

Although the glycosylations of lupane–type triterpenes betulinic acid (**1**), lupeol (**114**) and betulin (**115**) have been reported, most of previous studies have been focusing on describing the cytotoxicity of synthetic saponins. The other bioactivities such as antibacterial, antiviral, antidiabetic and antiacetylcholinesterase are also of interest. In addition, methodology development, especially for the selectivity of glycosylation, should be considered.

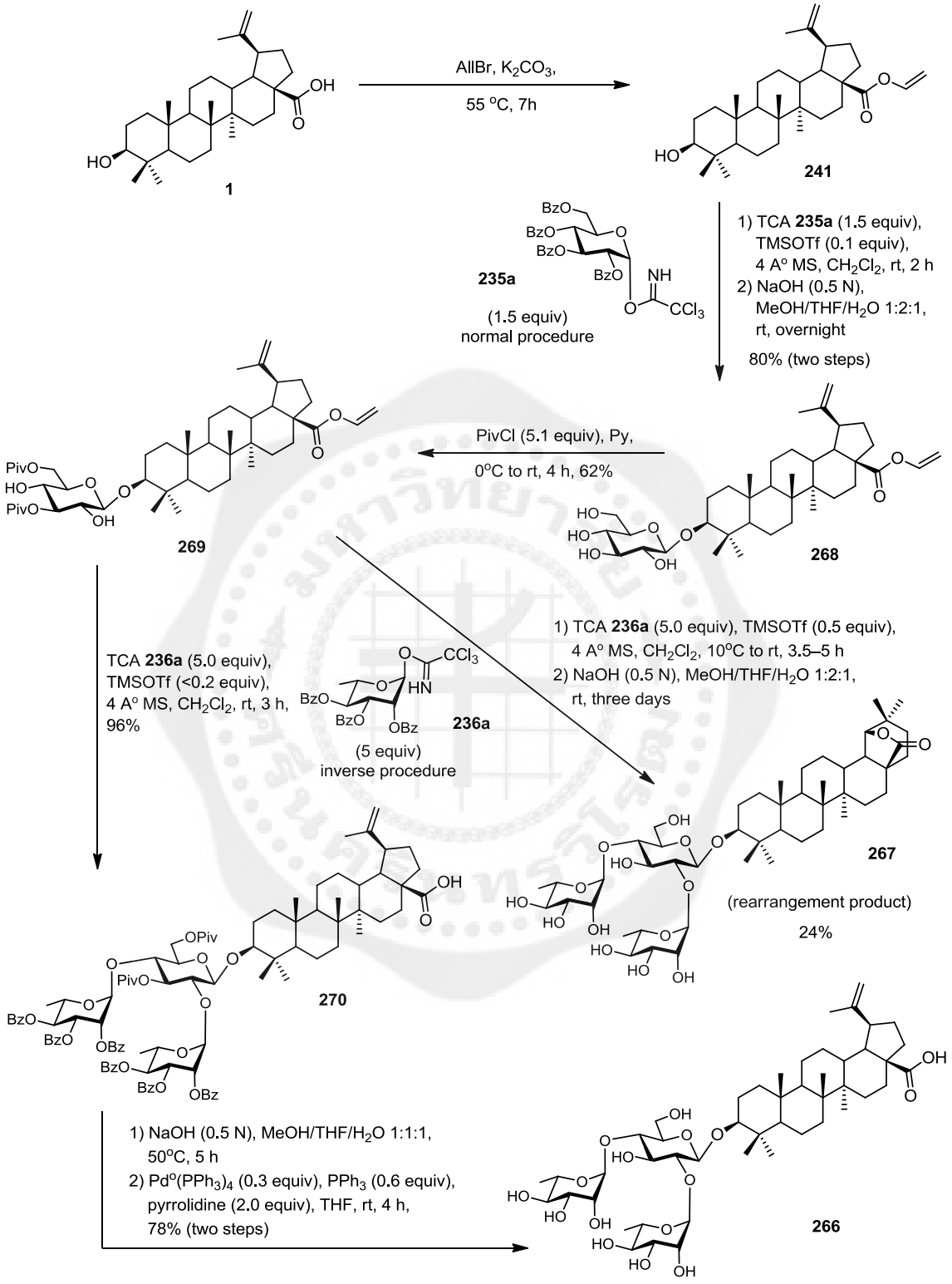

Scheme 10 Synthesis of saponins **266**–**267**

Table 8 Cytotoxicity of (IC_{50}) and haemolytic (HD_{50}) activities of triterpenenes **1**, **114**, **115** and chacotriosidesaponins **266**–**267**

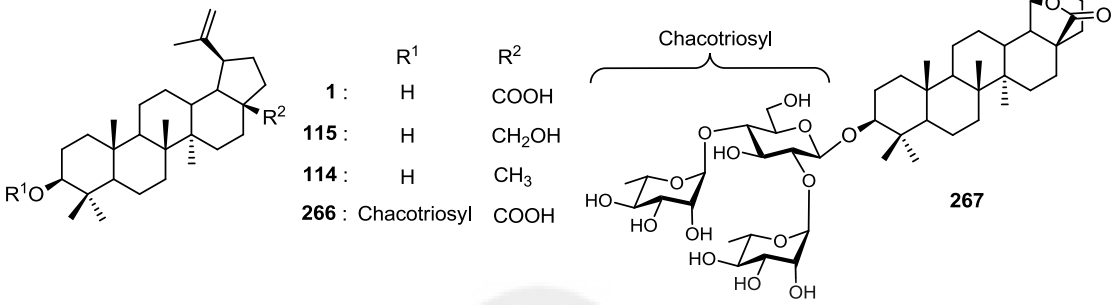

Compounds	IC_{50} (μM)					HD_{50}
	A549[a]	DLD–1[b]	MCF7	PC–3	WS1[d]	(μmol L^{-1})
Betulinic acid (**1**)	10.3	15.0	41	40	12	>100
Lupeol (**114**)	>50	>50	>50	>50	>50	>100
Betulin (**115**)	3.80	6.6	NT[g]	NT[g]	3.58	>100
Allobetulin (**252**)	>50	>50	>50	>50	>50	>100
28–Oxyallobetulin (**253**)	>50	>50	>50	>50	>50	>100
266	>50	>50	>50	>50	>50	>100
267	13	14	18	10	3.8	8.0
Etoposide[e]	1.2	27	–	–	34	–
PBS	–	–	–	–	–	>100
Saponin	–	–	–	–	–	7.4 (μg mL^{-1})

[a]Human lung carcinoma; [b]Human colorectal adenocarcinoma; [c]Human breast adenocarcinoma; [d]Human prostate adenocarcinoma; [e]WSI: Human normal skin; [f]Reported by Gauthier et al., 2009; [g]Not tested.

2.2 Glycosylation of α–mangostin

It is well known that *Garcinia* xanthones is famous for its antibacterial properties. α–Mangostin is the major metabolite, which can be isolated in gram–scale from mangosteen plant (*Garcinia mangostana*). It has been reported to possess a broad spectrum of biological activities including anti–HIV (Chen et al., 1996), anti–inflammatory (Nakatani et al., 2002), antiallergy (Nakatani et al., 2002), antituberculosis (Suksamrarn et al., 2003), cytotoxicity (Suksamrarn et al., 2006), antiproliferative (Krajarng et al., 2012), antibacterial (Sakagami et al., 2005), antioxidant (Jung et al., 2006), antifungal (Kaomongkolgit et al., 2009), enhancement of immune system (Tang et al., 2009), and analgesic activity (Cui et al., 2010).

However, aqueous solubility of α–mangostin is low. In order to overcome this, modification of α–mangostin to its glycosides is of interest. A thorough search of the literature showed that there are only three articles that describe the synthesis of mangostin glucosides.

Pai et al. have reported on the preparation of 3,6–di–O–*β*–*D*–glucopyranosyl mangostin (**272**). The synthesis started from the preparation of α–acetobromoglucose using Fischer's procedure (Fischer, 1911). The diglucoside **271** was then synthesized according to a procedure reported by Nagarajan and Parmar (1977). Product was then shaken with NaOMe in methanol followed by neutralization with ethanolic acetic acid to yield the product as 3,6–di–*O*–glucosyl mangostin (**272**), see Scheme 11. This analogue showed activity as the central nervous system depressant in mice and rats at doses of ≥100 mg/kg (i.p.) and also produced significant rise in blood pressure of dogs (Pai et al., 1979).

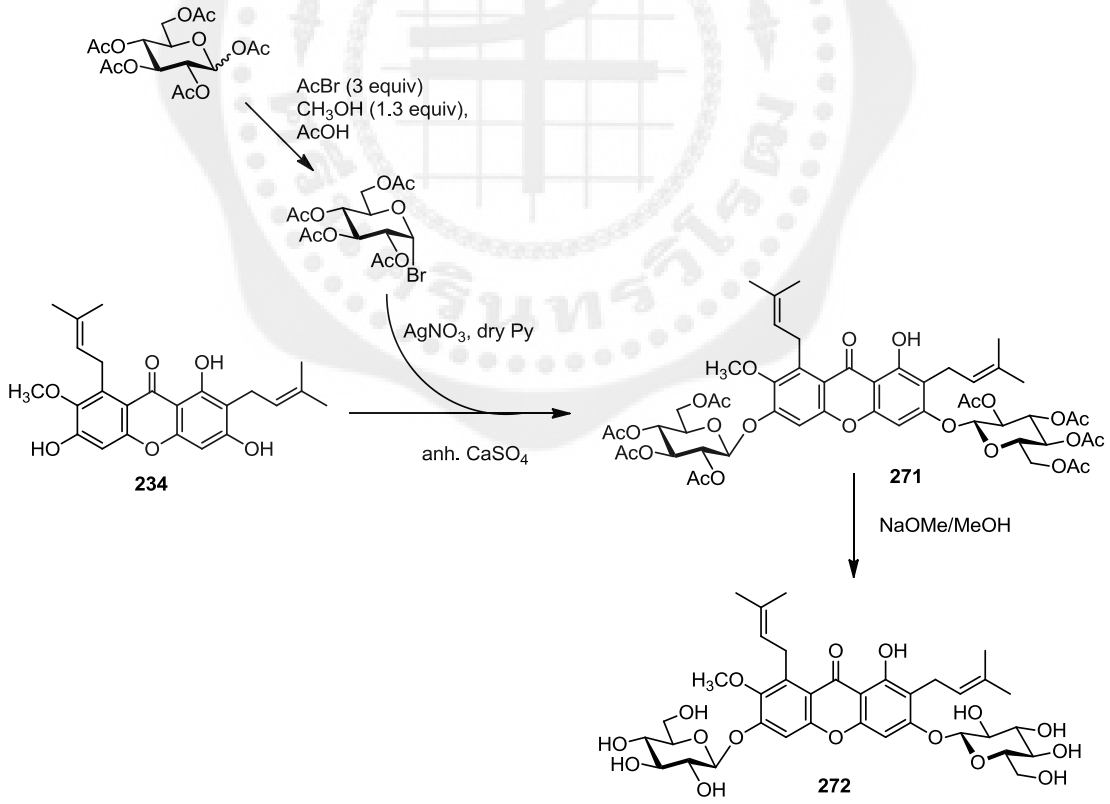

Scheme 11 Synthesis of glycosyl *α*–mangostin analogues

In 2008, α–mangostin glycosides were synthesized using the previously developed procedure (Pai et al., 1979) and then used as standards to identify naturally–occurring xanthone glycosides in mangosteen fruit (Jaratrungtawee et al., 2008). However, their biological activities have not been yet described.

In 2014, the enzymatic synthesis of α–mangostin glycosides has been reported by using two enzymatic systems for the synthesis of UDP–α–*D*–glucose and UDP–α–*D*–2–deoxyglucose and combined with a glycosyltransferase (GT) from *Bacillus licheniformis* DSM–13. Two series of glucosyl– and 2–deoxyglucosyl mangostin derivatives (**275**–**277**) glycosylated at C–3 and/or C–6 position were obtained. All compounds were evaluated for their antibacterial activity against Gram–positive bacteria by agar diffusion bioassay against *Micrococcus luteus, Bacillus subtilis and Staphylococcus aureus*. Analogue **274** showed the most effective antibacterial activity with diameter of zone of inhibition of 28, 11.5 and 12.5 mm, respectively; see Table (Le et al., 2014).

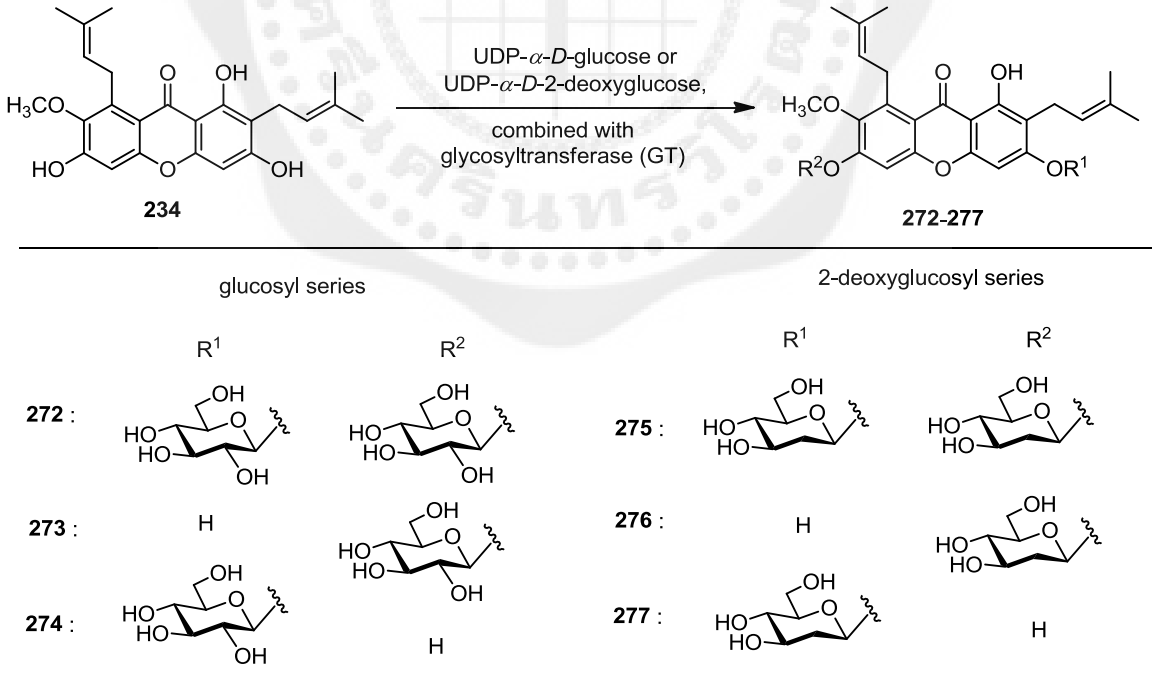

Scheme 12 Structures of α–mangostin glycosides obtained by enzymatic synthesis

Table 9 Zone of inhibition measured in the antibacterial activity assay of α–mangostin and its glycoside derivatives by agar diffusion bioassay against Gram–positive bacteria

Bacteria	Diameter of zone of inhibition (mm)						
	234	**272**	**273**	**274**	**275**	**276**	**277**
M. luteus	11	16	10.5	28	8.7	6.5	6.5
B. subtilis	9	0	7.5	11.5	8	8	8.5
S. aureus	9	0	6.5	12.5	6.5	6.5	6.5

As α–mangostin (**234**) has been investigated as a therapeutic agent, synthetic and medicinal chemistry studies of α–mangostin have continued. α–Mangostin displays low minimum inhibitory concentration (Koh et al., 2013) due to its hydrophobic nature of the xanthone core. To enhance its aqueous solubility, glycosyl analogues with improved hydrophilicity are required.

This work is dedicated to studying glycosylation of two glycosyl acceptors, betulinic (**1**) acid and α–mangostin (**234**). These targets represent certain challenges from the perspective of the glycosylation reaction, which required fine tuning of the reaction conditions to achieve excellent stereoselectivity, regioselectivity, and yields. Each of the natural products has been derivatized with glycosides of the *D*–glucosyl, *D*–galactosyl, *D*–mannosyl series using new methods for chemical glycosylation developed in the Demchenko lab (Yasomanee and Demchenko, 2012; Nigudkar, Stine and Demchenko, 2014; Pistorio, Yasomanee and Demchenko, 2014). Glycosyl acceptor **234** was glycosylated to its mono– or *di*–*O*–substituted derivatives at C–3 or C–6. All synthetic glycosides will be tested *in vitro* and/or *in vivo* as prodrug candidates with improved hydrophilic property.

CHAPTER 3

EXPERIMENTAL

Plant materials

The root bark of *Z. cambodiana* was collected from Chamni District, Buriram Province, Thailand, in March, 2007. A voucher specimen (Wicharn Wisetsri 001) was identified by James F. Maxwell and has been deposited at the CMU Herbarium, Faculty of Science, Chiang Mai University, Thailand.

The roots of *Z. oenoplia* (L.) Mill. var. *brunoniana* (Cl. Ex Brand.) Tard was collected from Nangrong District, Buriram Province, Thailand, in May 2013 and a voucher specimen, (Napaporn Charoenram 001) is deposited at the CMU Herbarium, Faculty of Science, Chiang Mai University, Thailand.

The roots of *Z. oenoplia* Mill. var. *oenoplia* was collected from Taklee District, Nakornsawan Province, Thailand, in April 2011 and a voucher specimen, (001) is deposited at the Department of Chemistry, Faculty of Science, Srinakharinwirot University, Thailand.

General experimental procedures

Melting points were measured using a Griffin melting point apparatus.

UV spectra were recorded in MeOH on Shimadzu UV–2401PC UV–VIS Recording Spectrophotometer.

IR spectra were obtained from Perkin Elmer FT–IR Spectrum BX spectrophotometer by using potassium bromide (KBr) disc or $CHCl_3$ film.

Optical rotation spectra were taken in MeOH on a JASCO–1020 digital polarimeter.

^{1}H and ^{13}C NMR spectra were recorded on a Bruker Avance 300 spectrometer, equipped with an Aspect 3000 computer, at 300 and 75 MHz, respectively, using $CDCl_3$, DMSO–d_6, pyridine–d_5 and methanol–d_4 as solvents. TMS was calibrated as references at 0.00 ppm for both ^{1}H and ^{13}C NMR spectra.

Electrospray ionization (ESI) mass spectra were determined on Thermo Finnigan LC–Q and a Bruker micrOTOF mass spectrometer.

Column chromatography was performed on Si gel 60 (Merck 1.07729, particle size < 0.063 mm or SiliCycle, SILIAFLASH G60, particle size 70–230 mesh) and Sephadex LH–20.

TLC was carried out on Merck precoated silica gel (60 F254) on aluminum plates and compounds were spotted on TLC, visualized under UV light (at wavelengths of 254 and 365 nm) and then reacted with anisaldehyde–H_2SO_4 followed by heating.

Extraction and isolation procedures

Extraction of the dried root bark of *Z. cambodiana*

The air–dried root bark of *Z. cambodiana* (10.0 kg) was extracted with EtOAc (3 x 20 L) at 50 ^{o}C for each 48 hours and then with MeOH (3 x 20 L) at 50 ^{o}C for each 48 hours. Each extract was evaporated under reduced pressure at 50 ^{o}C to afford EtOAc I and MeOH extracts for 144 g and 1.5 kg, respectively. The extraction procedure is shown in Scheme 13.

The EtOAc extract

The EtOAc extract 80.0 g (144 g) was fractionated on a quick column chromatography, eluting with a gradient system (hexane, CH_2Cl_2, EtOAc, MeOH), to provide nine major fractions (A–I) to give a major product of betulinic acid (**1**) and monitored by TLC (Scheme 14).

Fraction C (2.1 g, 80–20% (v/v) CH_2Cl_2–hexane, CH_2Cl_2, 10% EtOAc–CH_2Cl_2) was further chromatographed, eluting with EtOAc–CH_2Cl_2 and sixteen subfractions (C1–C16) were collected, to give lupeol (**32**) (colorless needles, 25 mg), betulin aldehyde (**33**) (sss4517, colorless amorphous solids, 68 mg) and betulin (**115**) (sss3972, colorless amorphous solids, 48 mg, 2% (v/v) EtOAc–CH_2Cl_2) from subfractions C3–C4, C6 and C9, respectively.

Fraction F (8.9 g, 10–30% (v/v) EtOAc–CH_2Cl_2 and 5% MeOH–EtOAc) was subjected to column chromatography employing solvent gradient EtOAc–CH_2Cl_2 and eight subfractions (F1–F8) were collected. Subfraction F5 (2.0 g, 10% (v/v) EtOAc–CH_2Cl_2 and 1% (v/v) MeOH–EtOAc) was further chromatographed, eluting with EtOAc–CH_2Cl_2, and nine subfractions (F5.1–F5.9) were collected. Subfraction F5.6 (4 mg, 30% (v/v) EtOAc–CH_2Cl_2) and 7 (69 mg, 30–40% (v/v) EtOAc–CH_2Cl_2) were combined (73 mg) was further chromatographed, eluting with CH_2Cl_2–EtOAc to have six subfractions (F5.6.1–F5.6.6), and

compound **A** was yielded as colorless amorphous solid (sss3096, 48 mg, 10% (v/v) EtOAc–CH_2Cl_2) from subfraction F5.6.4. Subfraction F5.8 (21 mg, 50–100% (v/v) EtOAc–CH_2Cl_2) was further subjected to CC (EtOAc– CH_2Cl_2) to give six subfractions (F5.8.1– F5.8.6). Subfraction F5.8.5 was selected for Sephadex LH–20 column (MeOH) to give compound **B** as colorless amorphous solids (sss3155, 7 mg). Subfraction F7 (535 mg, 5–40% (v/v) MeOH–EtOAc) was further chromatographed (MeOH–CH_2Cl_2) to obtained six subfractions (F7.1–F7.6) and compound **C** (sss4402, 16 mg, 2% MeOH–CH_2Cl_2) as colorless needles from subfraction F7.3.

The MeOH extract

Detannification: A portion of MeOH extract (225 g) was detannified by extracted with 1% (w/v) NaCl/EtOAc (Wall et al., 1996). The combination of EtOAc extract was evaporated in vacuum, and the resulting residue (12 g) was chromatographed on a silica gel to yield six fractions (A–F), Scheme 15.

Fraction B (1.2 g, CH_2Cl_2) was separated on silica gel column eluted with EtOAc–CH_2Cl_2 to provided seventeen fractions (B1–B17). Subfraction B12 yielded compound **D** as colorless needles (sss4732, 29 mg, 10% (v/v) EtOAc–CH_2Cl_2) after reCC (EtOAc–CH_2Cl_2). Subfraction B13 (56 mg, 10% (v/v) EtOAc–CH_2Cl_2) was chromatographed to yield compound **I** as colorless amorphous solid (sss4733, 18 mg) after subjected to LH–20 column (50% (v/v) MeOH–CH_2Cl_2). Subfraction B14 (19 mg, 11–12 % (v/v) EtOAc–CH_2Cl_2) was subjected to two step of LH–20 column (50% (v/v) MeOH–CH_2Cl_2) to give colorless needles of compound **E** (sss4759, 35 mg) and of compound **F** (sss4734, 7.0 mg), from the first and second column, respectively.

Fraction C was separated on silica gel column (EtOAc–CH_2Cl_2) to give nine subfractions (C1–C9). Subfraction C5 (11–12 % (v/v) EtOAc–CH_2Cl_2) yield compound **G** as a colorless amorphous solid (sss4767, 19 mg, 10 % (v/v) EtOAc–CH_2Cl_2) after filtered and then the solid was washed with MeOH. Subfraction C6 (103 mg, 15–20% (v/v) EtOAc–CH_2Cl_2) yielded compound **A** as colorless amorphous solids (sss4770, 21 mg) after processed as same as compound **G**.

Traditional CC: A portion of MeOH extract 30.7 g was fractionated by a quick column chromatography, eluting with 50% (v/v) EtOAc–CH_2Cl_2 then increased polarity by using EtOAc, MeOH and H_2O up to 50% (v/v) H_2O–MeOH to yield four fractions (A–D) on the basis of TLC analysis, Scheme 16.

Fraction A (820 mg, 50–100% (v/v) EtOAc–CH_2Cl_2) was applied to silica gel column eluted with MeOH–CH_2Cl_2 gradient system to yield 10 subfractions (A1–A10). Subfraction A2 was purified by CC over silica gel (eluted with MeOH–CH_2Cl_2 gradient system) and sephadex LH–20 (eluted with MeOH) to yield compound **H** as colorless needles (sss4449, 11.4 mg).

Fraction B (10.9 g, 40–60% (v/v) MeOH–EtOAc) was chromatographed on a silica gel to give six subfractions (B1–B6). Subfraction B2 (162 mg, 100% (v/v) CH_2Cl_2) was subjected to CC (EtOAc–CH_2Cl_2) to give compound **I** as colorless needles (sss4634, 16 mg, 8–10% (v/v) EtOAc–CH_2Cl_2) and lotusanine B as colorless amorphous solid (sss4635, 13 mg, 10–11% (v/v) EtOAc–CH_2Cl_2).

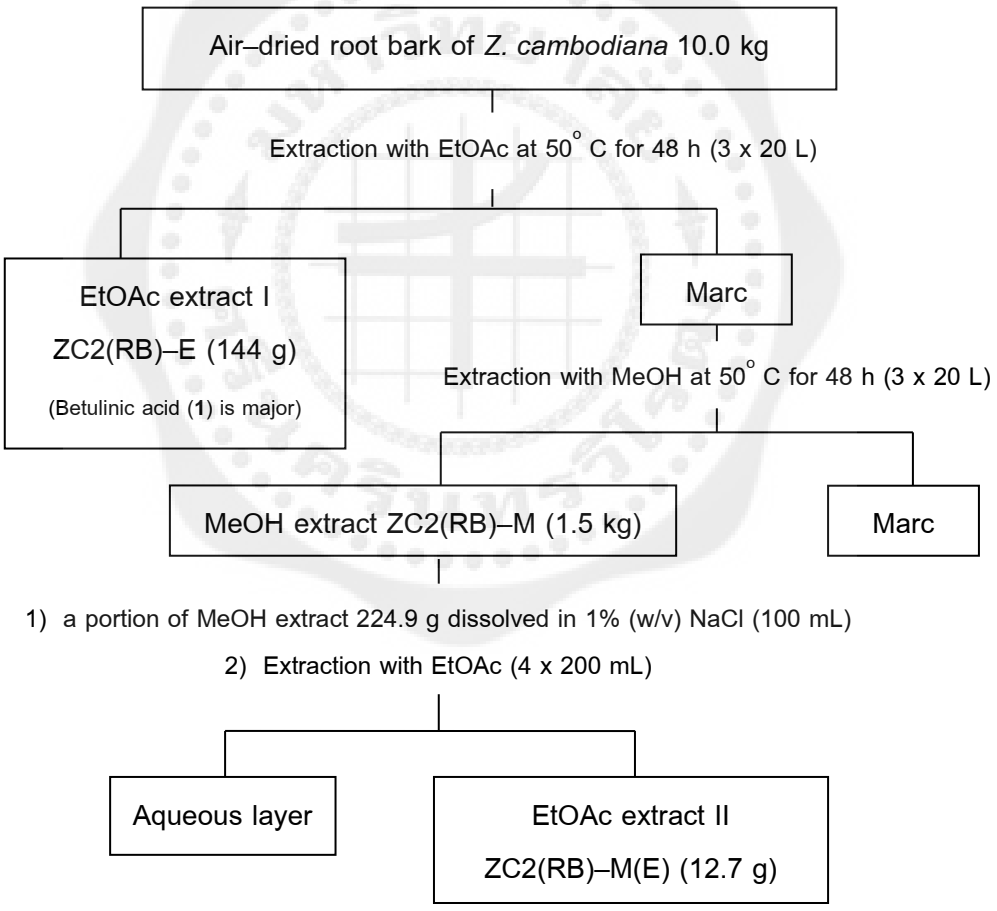

Scheme 13 Extraction procedure of the root bark of *Z. cambodiana*

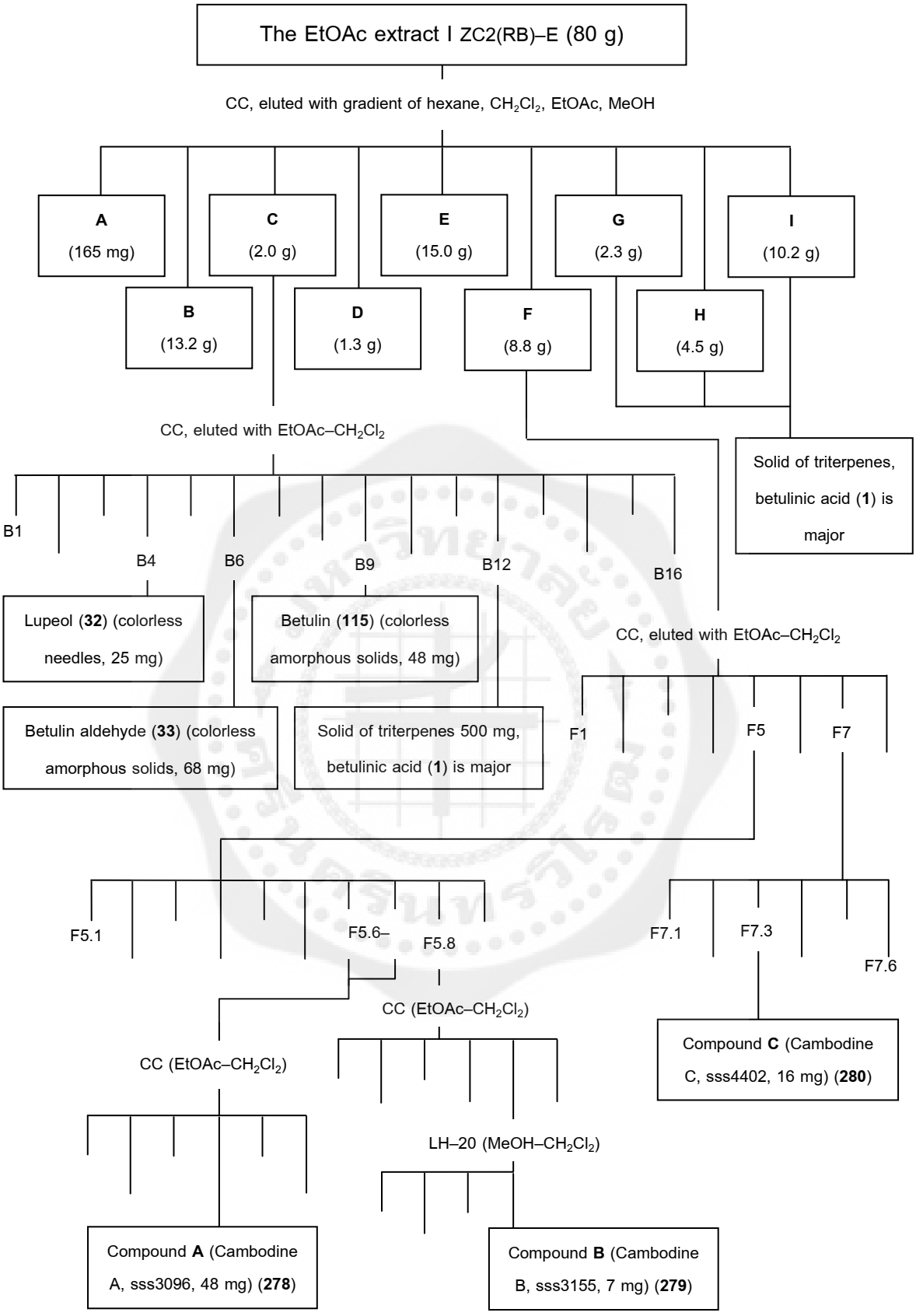

Scheme 14 Isolation of compounds from the EtOAc extract I of *Z. cambodiana* root bark

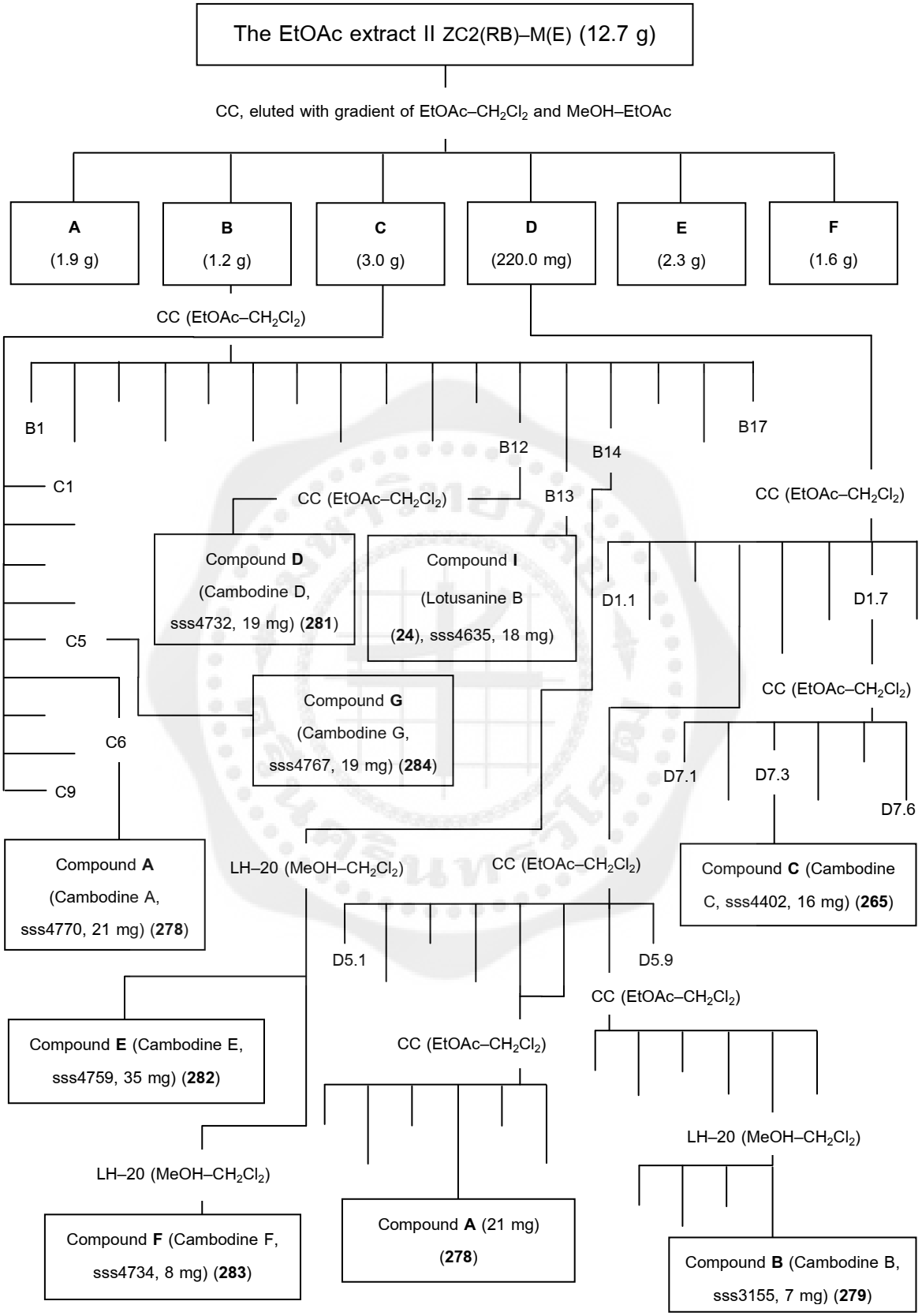

Scheme 15 Isolation of compounds from the EtOAc extract II of *Z. cambodiana* root bark

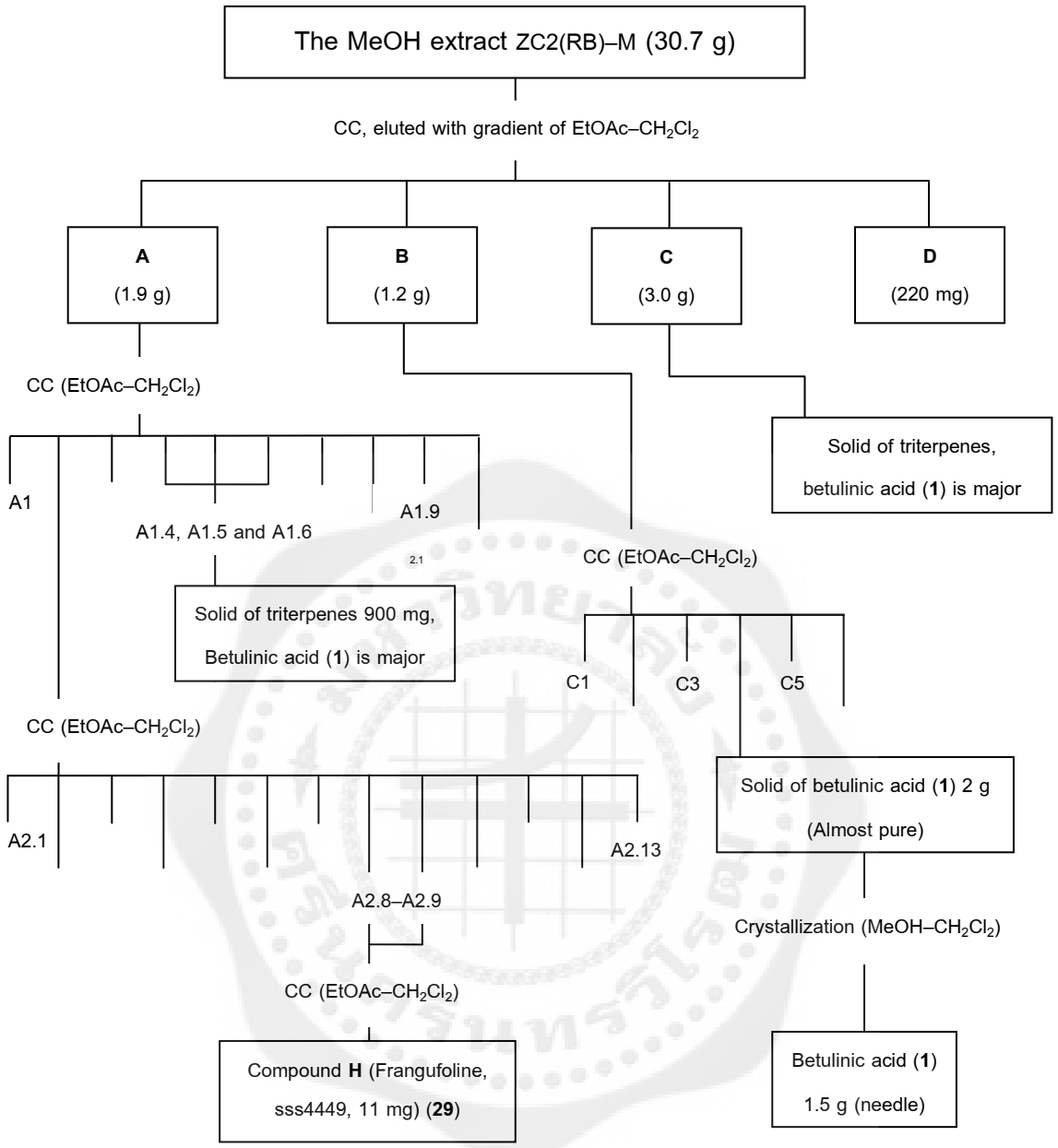

Scheme 16 Isolation of compounds from the MeOH of *Z. cambodiana* root bark

Cambodine A

Colorless amorphous solid, mp 248–249 $^{\circ}$C; $[\alpha]_D^{27}$: –161.6456 (*c* 0.3160, MeOH); UV (MeOH) λ_{max} (log ε) : end absorption band; CD (MeOH) [θ] (nm) : +7.60(220), –35.66(236), +5.71(283); IR (KBr) ν_{max}: 3289, 2963, 1636, 1508, 1455, 1241, 1019 and 697 cm^{-1}; for ^{1}H– and ^{13}C NMR spectra : *see* Table 15 and 16; HRTOFMS (APCI^{+}) *m/z* 680.3808 $[M+H]^{+}$ (calcd 680.3806 for $C_{40}H_{49}N_5O_5$ + H).

Cambodine B

Colorless amorphous solid, mp 140–141 °C; $[\alpha]_D^{28}$: –107.4 (*c* 0.2000, MeOH); UV (MeOH) λ_{max} (log ε) : end absorption band; CD (MeOH) [θ] (nm) : –9.30(224), –36.46(240) and +6.67(279); IR ($CHCl_3$) ν_{max} : 3447, 3289, 3065, 3031, 2924, 2852, 2797, 1653, 1519, 1507, 1455, 1291, 1228, 1168, 1053, 1012, 758 and 699 cm^{-1}; for ^{1}H– and ^{13}C NMR spectra : *see* Table 11 and 13; HRTOFMS ($APCI^+$) *m/z* 617.2751 $[M+H]^+$ (calcd 617.2785 for $C_{37}H_{36}N_4O_5$ + H).

Cambodine C

Colorless needles, mp 225–227 °C; $[\alpha]_D^{27}$: –198.89 (*c* 0.190, $CHCl_3$); UV (MeOH) λ_{max} (log ε) : end absorption band; CD (MeOH) [θ] (nm) : +15.46(220), –41.88(236) and +6.44(280); IR (KBr) ν_{max}: 3261, 2966, 2934, 1631, 1539, 1512, 1458, 1242, 1027 and 701 cm^{-1}; for ^{1}H– and ^{13}C NMR spectra : *see* Table 15 and 17; ESIMS *m/z* 668.3 $[M+H]^+$, *m/z* 666.5 $[M–H]^-$; HRTOFMS ($APCI^+$) *m/z* 668.38079 $[M+H]^+$ (calcd 668.38116 $C_{39}H_{49}N_5O_5$ + H).

Cambodine D

Colorless needles, mp 205–207 °C; $[\alpha]_D^{23}$: –131.3 (*c* 0.2050, MeOH) ; UV (MeOH) λ_{max} (log ε) : end absorption band; CD (MeOH) [θ] (nm) : –8.47(224), –46.45(244) and +3.98(286); IR ($CHCl_3$) ν_{max}: 3446, 3289, 3036, 1682, 1670, 1656, 1624, 1507, 1291, 1228, 1158, 1000, 752 and 699 cm^{-1}; for ^{1}H– and ^{13}C NMR spectra : *see* Table 11 and 14; ESIMS *m/z* 533.2 $[M+H]^+$, *m/z* 531.3 $[M–H]^-$; HRTOFMS ($APCI^+$) *m/z* 555.2929 $[M+Na]^+$ (calcd 555.29418 for $C_{31}H_{40}N_4O_4$ + Na).

Cambodine E

Colorless needles, mp 135–137 °C; $[\alpha]_D^{27}$: –169.3 (*c* 0.2060, MeOH) ; UV (MeOH) λ_{max} (log ε) : end absorption band; CD (MeOH) [θ] (nm) : –14.47(220), –88.99(243), and +4.25(286); IR ($CHCl_3$) ν_{max}: 3446, 3289, 3036, 1682, 1670, 1656, 1624, 1507, 1291, 1228, 1158, 1000, 752 and 699 cm^{-1}; for ^{1}H– and ^{13}C NMR spectra : *see* Table 11 and 12; ESIMS *m/z* $[M+H]^+$ 601.2 (15), *m/z* 599.4 $[M–H]^-$; HRTOFMS ($APCI^+$) *m/z* 623.2606 $[M+Na]^+$ (calcd 623.26288 for $C_{37}H_{36}N_4O_4$ + Na).

Cambodine F

Colorless needles, mp 216–218 °C ; $[\alpha]_D^{27}$: –130.9 (*c* 0.2030, MeOH) ; UV (MeOH) λ_{max} (log ε) : end absorption band; CD (MeOH) [θ] (nm) : –16.80(213), –46.29(236) and +9.76(282); IR ($CHCl_3$) ν_{max}: 3391, 3267, 3065, 3032, 2962,2927, 2875, 2855, 2797, 1685, 1647, 1559, 1541, 1507, 1456, 1337, 1233, 1170, 1012, 758 and 699 cm^{-1}; for ^1H– and ^{13}C NMR spectra : *see* Table 15 and 18; ESIMS *m/z* 694.8 $[M+H]^+$, *m/z* 692.3 $[M–H]^-$; HRTOFMS ($APCI^+$) *m/z* 716.3792 $[M+Na]^+$ (calcd 716.3782 for $C_{41}H_{51}N_5O_5$ + Na).

Cambodine G

Colorless needles, solid, mp 261–163 °C ; $[\alpha]_D^{26}$: –440.0 (*c* 0.2030, $CHCl_3$) ; UV (MeOH) λ_{max} (log ε) : 217(4.28), 223(4.22), 279(4.18) and 300(*sh*) nm ; CD (MeOH) [θ] (nm) : –13.25(220), –49.11(237) and –3.95(282); IR ($CHCl_3$) ν_{max}: 3420, 3276, 3065, 3032, 2967, 2934, 2877, 1636, 1613, 1508, 1452, 1418, 1288, 1242, 1201, 1173, 987, 855, 820, 763, 705 and 681 cm^{-1}; for ^1H– and ^{13}C NMR spectra: *see* Table 19; ESIMS *m/z* 587.4 $[M+H]^+$, *m/z* 585.4 $[M–H]^-$; HRTOFMS ($APCI^+$) *m/z* 609.3033 $[M+Na]^+$ (calcd 609.30474 for $C_{34}H_{42}N_4O_5$ + Na).

Frangufoline

Colorless needles, mp 216–218 °C ; $[\alpha]_D^{27}$: –218.59 (*c* 0.2060, $CHCl_3$) ; UV (MeOH) λ_{max} (log ε) : end absorption band; IR ($CHCl_3$) ν_{max}: 3446, 3266, 2956, 2923, 2852, 1645, 1632, 1521, 1508, 1237, 1125 and 701 cm^{-1}; ^1H– and ^{13}C NMR data: *see* Table 20; ESIMS *m/z* 535.5 $[M+H]^+$, *m/z* 533.3 $[M–H]^-$ ($C_{31}H_{42}N_4O_4$ 534.69).

Lotusanine B

Colorless amorphous solid, mp 185–187 °C ; $[\alpha]_D^{23}$: –117.7 (*c* 0.2070, $CHCl_3$) ; UV (MeOH) λ_{max} (log ε) : 216 (4.45), 224 (4.35), 279 (4.26) and 305 (*sh*) nm ; IR ($CHCl_3$) ν_{max}: 3449, 3261, 3056, 3030, 2966, 2934, 1685, 1631, 1539, 1512, 1382, 1242, 1230, 746, 713 and 701 cm^{-1}; ^1H– and ^{13}C NMR data: *see* Table 21; ESIMS *m/z* 619.5 $[M–H]^-$ ($C_{37}H_{40}N_4O_5$ 620.30).

Extraction of the root of *Z. oenoplia* Mill. var. *brunoniana*

The air–dried root of *Z. oenoplia* Mill. var. *brunoniana* (5.0 kg) was extracted with MeOH (5 L at rt for 7 days each) and then with MeOH (2 x 5 L at rt for 7 days each). Each extract was evaporated under reduced pressure at 50 ^{o}C to afford EtOAc and MeOH extracts for 29.6 g and 587.6 g, respectively. The extraction procedure is shown in Scheme 17.

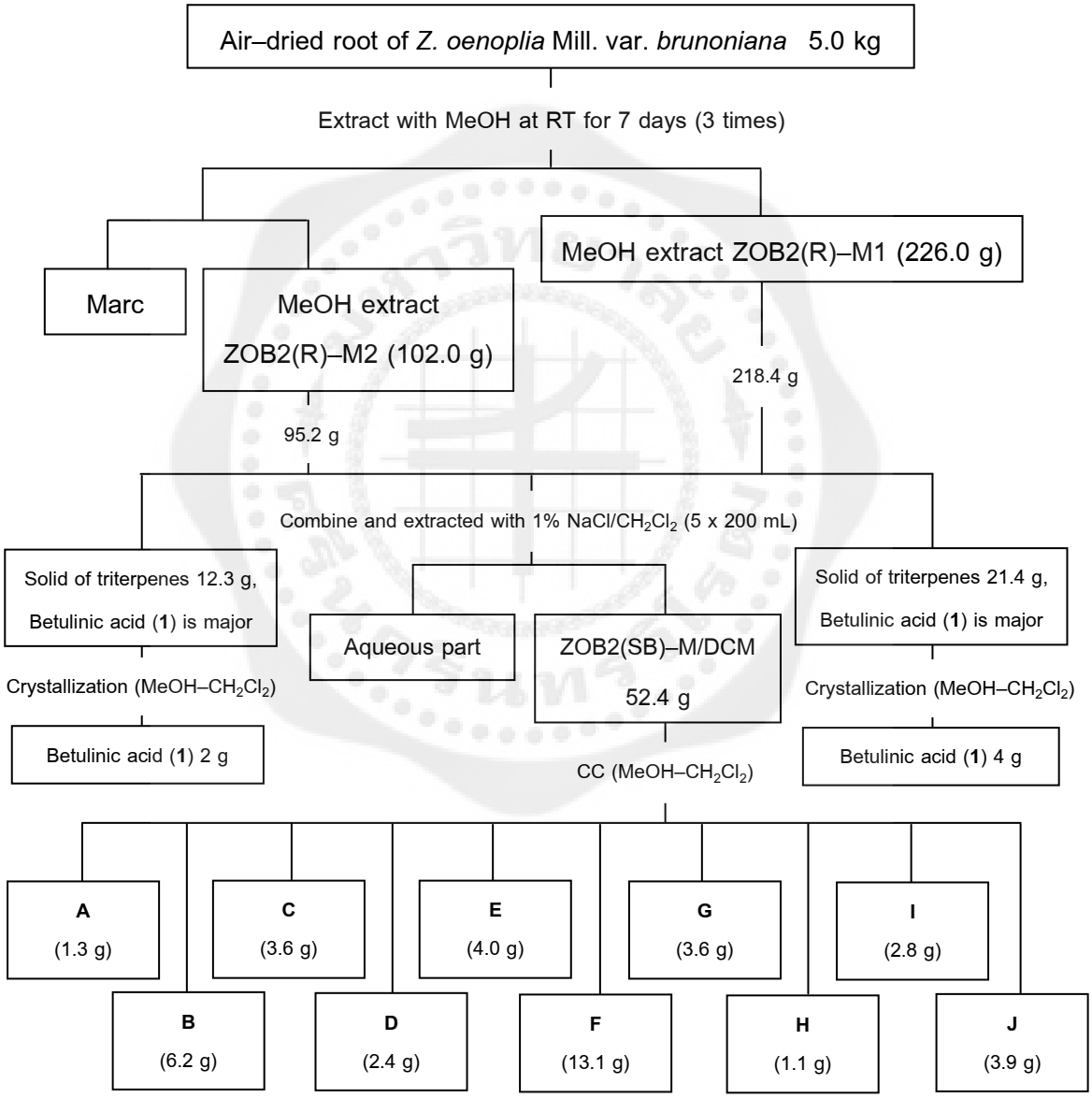

Scheme 17 Extraction procedure of *Z. oenoplia* Mill. var. *brunoniana* root

Extraction of the root of *Z. oenoplia* Mill. var. *oenoplia*

The air–dried root of *Z. oenoplia* var. *oenoplia* (3.5 kg) was extracted with EtOAc (3 x 5 L at rt for 7 days each) and then with MeOH (4 x 5 L at rt for 7 days each). Each extract was evaporated under reduced pressure at 50 ^{o}C to afford EtOAc and MeOH extracts for 28.3 g and 407.0 g, respectively. The extraction procedure is shown in Scheme 15.

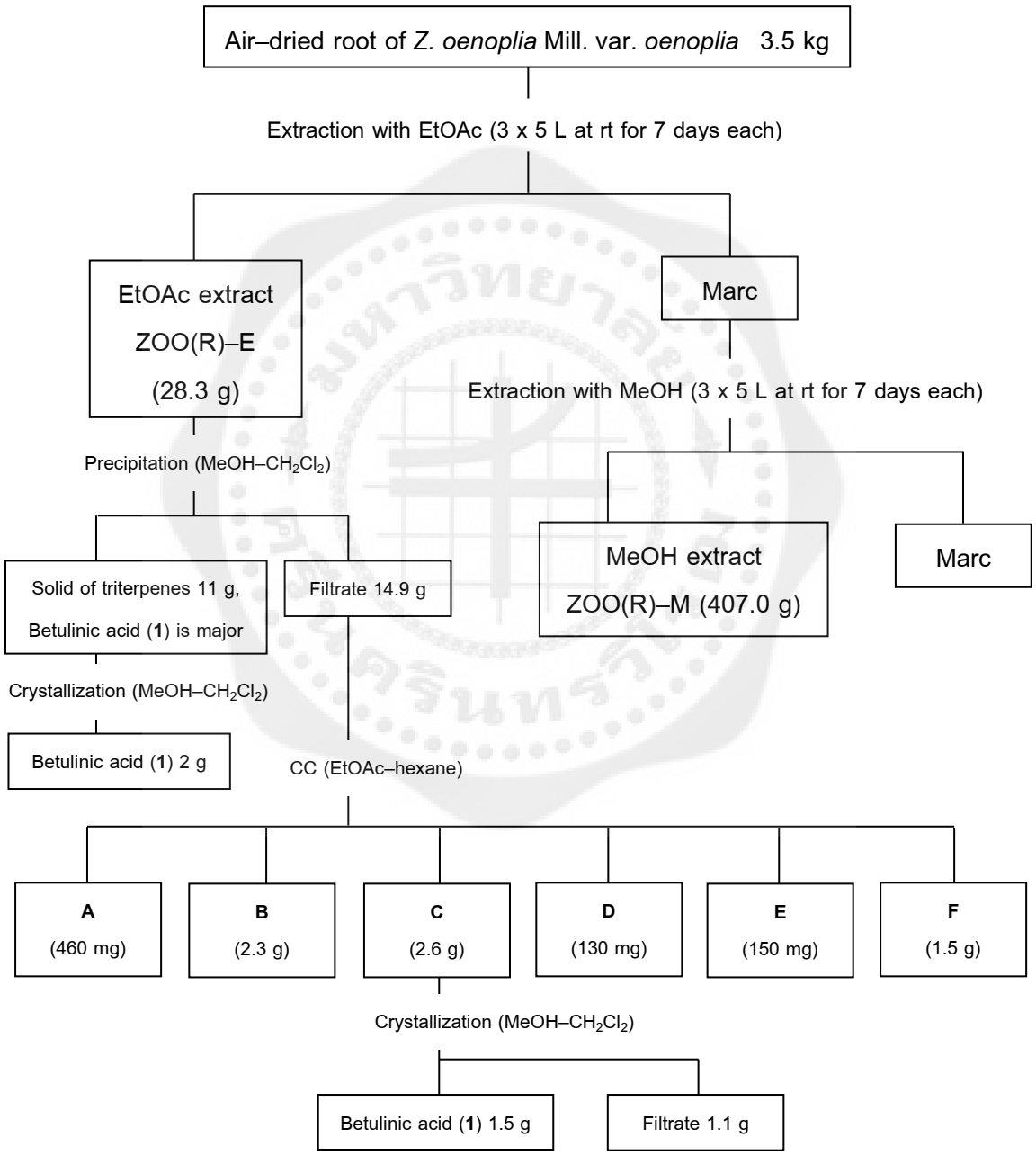

Scheme 18 Extraction procedure of *Z. oenoplia* Mill. var. *oenoplia* root

Bioassay procedure

The antiplasmodial activity was evaluated agents the *P. falciparum* (K1, multidrug resistant strain) using the method reported by Trager and Jensen (1976). The *in vitro* antiplasmodial activity was determined by means of the microculture radioisotope technique according to the method of Desjardins et al. (1979). The half maximal inhibitory concentration (IC_{50}) was measured by the *in vitro* uptake of 3[*H*]–hypoxanthine by *P. falciparum*. Dihydroartemisinin was used as the standard drug for antiplasmodial test, exhibited an IC_{50} value of 4.2 nM.

The antimycobacterial activity was assessed against *M. tuberculosis* H37Ra using the Microplate Alamar Blue Assay (Collins and Franzblau, 1997). The standard drugs Isoniazid and kanamycin sulfate, exhibited the respective MIC of 0.4 and 4.2 μM.

Structural modification of some naturally derived compounds: Glycosylation

Glycosylation of betulinic acid

Isolation of starting material

Betulinic acid (**1**) was obtained from *Ziziphus* plants. Several solid fractions of triterpenes which contained betulinic acid as the major component were combined and crystalized in MeOH–CH_2Cl_2 to yield 11 g of colorless needles and 44 g of white powder.

Synthesis of 28–*p*–methoxybenzyl betulinic acid (1′)

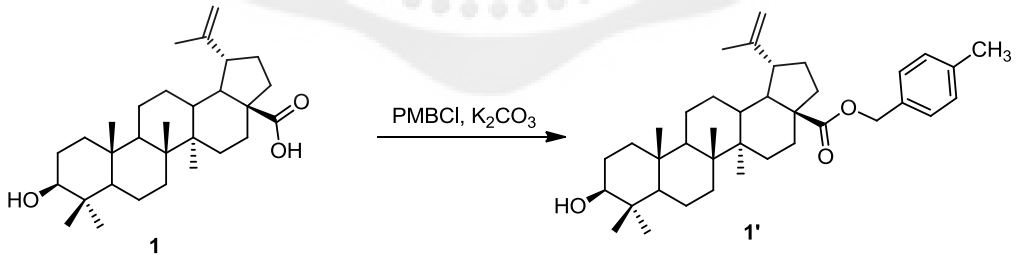

To a stirred mixture of **1** (1 g, 2.19 mmol) and K_2CO_3 (600 mg, 4.38 mmol) in DMF was added 4–methoxybenzyl chloride (PMBCl, 1.48 mL, 21.90 mmol). The reaction mixture was left stirring at room temperature for 1 hour. The resulting mixture was extracted with EtOAc (3 x 20 mL), washed with water (10 mL). The organic phase was separated, dried over Na_2SO_4 and concentrated. The residue was purified by column chromatography using gradient EtOAc–hexane to yield product **1′** (1.27 g, 99%).

28–*p*–Methoxybenzyl betulinic acid (1′): Colorless needles, mp 91–93 °C $[\alpha]_D^{28}$ = +13.2 (*c* 1.0 $CHCl_3$); ^{1}H NMR ($CDCl_3$, 300 MHz): 7.30*br d* (8.3 Hz, 2H, H–3′, H–7′), 6.88*br d* (8.3 Hz, 2H, H–4′, H–6′), 5.08*d* (11.9 Hz, 1H, CH_2PMP), 5.02*d* (11.9 Hz, 1H, CH_2PMB), 4.71*s* (1H, 29_a), 4.58*s* (1H, 29_b), 3.80s (3H, OCH_3), 3.17*dd* (10.7, 5.3 Hz, 1H, H–3), 3.01*td* (10.1, 5.1 Hz, 1H, H–19), 2.22*m* (1H), 2.16*td* (12.3, 2.7 Hz, 1H), 1.86*m* (2H), 1.67*s* (3H, H–30), 0.95*s* (3H, H–27), 0.93*s* (3H, H–23), 0.79*s* (3H, H–26), 0.75*s* (3H, H–25), 0.74*s* (3H, H–24), 0.65s (8.7 Hz, 1H, H–5), 1.60–0.84 (all *m*, 20 remaining protons); ^{13}C NMR (*see* supplementary data).

Synthesis of 3,3–difluoroxindole [HOFox, 3,3–difluoroindolin–2–one (285)]

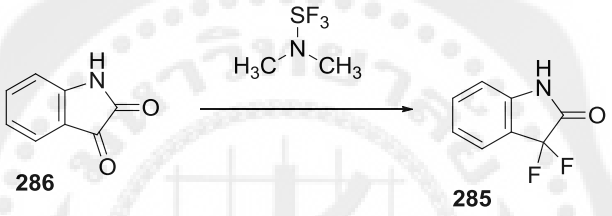

The title compound was obtained from the reaction of Isatin (**286**) and diethylaminosulfur trifluoride (DAST) as described by Zhu, Zhang and Hu (2010).

Synthesis of 3,3–difluoro–3*H*–indol–2–yl 3,4,6–tri–*O*–acetyl–2–*O*–benzyl–*β*–*D*–glucopyranoside (287)

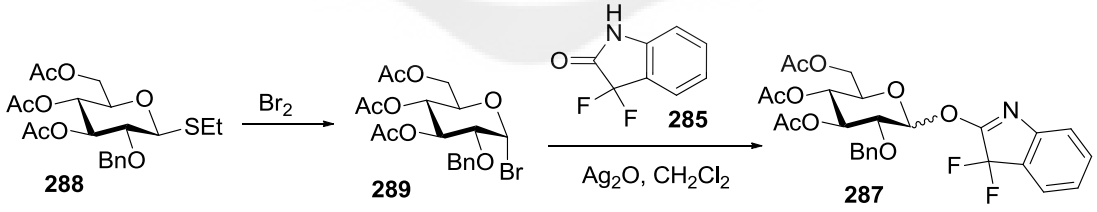

Compound **287** was synthesized according to method described by Nigudkar, Stine and Demchenko (2014).

Synthesis of 3–*O*–(3,4,6–tri–*O*–acetyl–*α*–*D*–glucopyranosyl) 28–*p*–methoxy–benzyl betulinic acid (290)

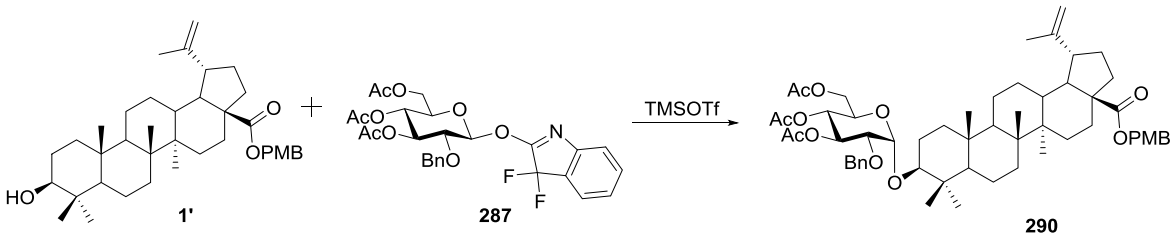

To a mixture of donor 287 (119 mg, 0.2180 mmol), acceptor **1′** (100 mg, 0.1736 mmol), and 4 Å molecular sieves in Et_2O/CH_2Cl_2 was added TMSOTf (3.69 μL, 0.0191 mmol) at –30 °C. After that, the reaction mixture was slowly warmed to rt until reaction complete in 30 min. The solid was filtered off, rinsed with DCM, and the combined filtrate was washed with $Na_2S_2O_3$ and water. The organic phase was separated, dried with anh.$MgSO_4$ and concentrated under reduced pressure. The crude residue was purified by column chromatography (EtOAc–hexane) to afford the title compound as a colorless foam in 77% yield (128 mg).

3–*O*–(3,4,6–Tri–*O*–acetyl–*α*–*D*–glucopyranosyl) 28–*p*–methoxybenzyl betulinic acid (290): colorless foam, $[\alpha]_D^{28}$= +58.9 (*c* 0.1 $CHCl_3$) ^{1}H NMR ($CDCl_3$, 300 MHz): aromatic protons showed at 7.27–7.19*m* (7H) and 6.81*d* (8.5 Hz), 5.31*t* (9.5 Hz, 1H, H–3′), 5.01*d* (11.9 Hz, 1H, CH_2PMB), 4.96*d* (11.9 Hz, 1H, CH_2PMB), 4.94*d* (2.6 Hz, 1H, H–1′), 4.87*t* (9.5 Hz, 1H, H–4′), 4.65*s* (1H, H–29_a), 4.52*s* (1H, H–29_b), 4.17*dd* (12.1, 4.3 Hz, 1H, H–6_a′), 4.07*br dd* (4.3, 1.5 Hz, 1H, H–5′), 3.96*br dd* (12.1, 1.5 Hz, 1H, H–6_b′), 3.50*dd* (9.5, 3.6 Hz, 1H, H–2′), 3.06*dd* (11.3, 4.0 Hz, 1H, H–3), 2.94*td* (10.1, 4.0 Hz, 1H, H–19), 2.17*br d* (9.2 Hz, 1H), 2.08*td* (9.0, 2.0 Hz, 1H), 1.99*s* (3H, OAc), 1.95*s* (3H, OAc), 1.92*s* (3H, OAc), 1.78*m* (2H), 1.60*s* (3H, H–30), 0.91*s* (3H, H–27), 0.85*s* (3H, H–23), 0.78*s* (3H, H–26), 0.74*s* (3H, H–25), 0.68*s* (3H, H–24), 0.57*d* (8.8 Hz, 1H, H–5), 1.55–0.71 (all *m*, 19 remaining protons); ^{13}C NMR ($CDCl_3$, 300 MHz): (see appendix); $C_{57}H_{78}O_{12}$ 954.5493

Deprotection of 3–*O*–(3,4,6–tri–*O*–acetyl–*α*–*D*–glucopyranosyl) 28–*p*–methoxybenzyl betulinic acid (290)

Deprotection of 3,4,6–tri–*O*–acetyl–*α*–*D*–glucopyranosyl 28–*p*–methoxybenzyl betulinic acid was carried out using Na(s) in dry NH_3 according to the Birch reduction procedure (Birch, 1944). After that extracted with *n*–BuOH/H_2O, the organic layer

was combined and evaporated. The crude residue was purified by column chromatography MeOH–hexane to afford the title compound as a white amorphous solid in 50% yield (40 mg).

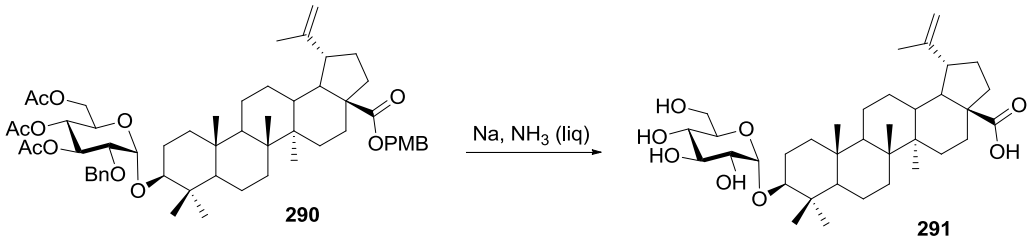

3–*O*–*α*–*D*–Glucopyranosyl betulinic acid (291): colorless amorphous solid. IR (KBr) ν_{max} cm^{-1} : 3407, 2930, 1696, 1457, 1143, 1069, 1024 and 877; $[\alpha]_D^{26}$ (*c* 0.1 MeOH); ^{1}H NMR (300 MHz, $CDCl_3$): 4.96*d* (3.6 Hz, 1H, H–1′), 4.70*s* (1H, $H29_a$), 4.59*s* (1H, $H–29_b$), 3.96*br dd* (10.4, 2.0 Hz, 1H, H–3′), 3.91*d* (2.0 Hz, 1H, H–4′), 3.81*dd* (10.1, 3.5 Hz, 1H, $H–6_a′$), 3.74*dd* (10.4, 3.6 Hz, 1H, H–2′), 3.69*m* (1H, H–5′), 3.67*m* (1H, $H–6_b′$), 3.22*dd* (11.4, 4.0 Hz, 1H, H–3), 3.02*td* (10.6, 4.2 Hz, 1H, H–19), 1.90*m* (2H), 1.69*s* (3H, H–30), 1.01*s* (3H, H–27), 1.00*s* (3H, H–23), 0.96*s* (3H, H–26), 0.88*s* (3H, H–25), 0.83*s* (3H, H–24), 0.76*d* (8.3 Hz, 1H, H–5), (all *m*, 19 remaining protons); ^{13}C NMR (75 MHz, methanol–d_4): 180.0 (1C, C–28), 151.9 (1C, C–29), 98.3 (1C, C–1′), 96.6 (1C), 96.3 (1C), 85.7 (1C), 84.3 (1C), 73.3 (1C, C–5′), 72.5 (1C, C–3′), 71.7 (1C, C–2′), 70.7 (1C, C–4′), 69.2 (1C, C–6′), 62.4 (1C), 57.4 (1C), 56.3 (1C), 52.5 (1C), 51.2 (1C), 51.0 (1C), 50.1 (1C), 43.5 (1C), 41.9 (1C), 32.7 (1C), 38.7 (1C), 38.2 (1C), 35.6 (1C), 32.3 (1C), 30.7 (1C), 29.7 (1C), 23.2 (1C), 19.4 (1C), 18.4 (1C), 17.8 (1C), 17.5 (1C), 15.8 (1C), 15.4 (1C), 14.3 (1C). HRMS *m/z* 641.3880 (calcd 641.4023 for $C_{36}H_{58}O_8$ + Na).

Synthesis of 3,3–difluoro–3*H*–indol–2–yl 4,6—di–*O*–benzoyl—2,3–di–*O*–benzyl–*α*–*D*–galactopyranoside (292)

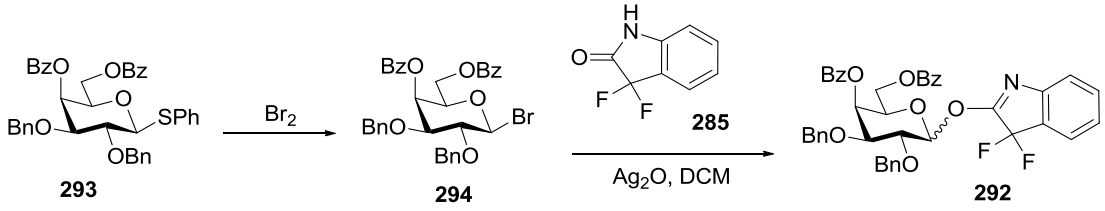

Phenyl 4,6–di–*O*–benzoyl–2,3–di–*O*–benzyl–1–thio–*α*–*D*–galactopyranoside (**293**) was first converted into reactive intermediate bromide **294**. For this purpose, a

solution of Br_2 in CH_2Cl_2 (19 mL, 0.12 mL of Br_2 in 20 mL of CH_2Cl_2) was added dropwise to a mixture of **292** (500 mg, 0.7575 mmol) (Pistorio, Yasomanee and Demchenko, 2014) and 3 Å molecular sieves (3 Å MS) in CH_2Cl_2. The resulting mixture was stirred for 5 min at rt then concentrated and co–evaporated with dry CH_2Cl_2 and dried in vacuum for 2 hours. The residue containing crude bromide **294** was dissolved in CH_2Cl_2 (20 mL), HOFox (124 mg, 0.7571 mmol) and Ag_2O (263 mg, 1.514 mmol) were added and the resulting mixture was stirred at rt for 1 hour. After that, the solid was filtered off and rinsed with DCM. The combined filtrate was washed with water. The organic phase was separated, dried, and concentrated. The crude residue was purified by column chromatography (EtOAc–hexane) to afford the title compound as a white foam in 41% yield (226 mg).

3,3–Difluoro–3*H*–indol–2–yl 4,6—di–*O*–benzoyl—2,3–di–*O*–benzyl–*α*–*D*– galactopyranoside (292): colorless foam; $[\alpha]_D^{28}$ = +22.6 (*c* 1.0 $CHCl_3$); ^{1}H NMR (300 MHz, $CDCl_3$): aromatic protons at 8.80*d* (7.1 Hz, 2H), 8.13*d* (7.1 Hz, 2H), 7.60*t* (7.3 Hz, 1H) and 7.55–7.16*m* (19H), 5.93*d* (9.5 Hz, 1H, H–1′), 5.91*d* (3.3 Hz, 1H, H–4′), 4.87*d* (11.4 Hz, 2H, CH_2Ph), 4.83*d* (13.7 Hz, 1H, CH_2PMB), 4.80*d* (13.7 Hz, 1H, CH_2PMB), 4.60*d* (11.4 Hz, 2H, CH_2Ph), 4.56*dd* (11.3, 7.1 Hz, 1H, H–6_a′), 4.42*dd* (11.3, 5.9 Hz, 1H, H–6_b′), 4.25*br dd* (7.1, 5.9 Hz, 1H, H–5′), 4.03*t* (9.5 Hz, 1H, H–2′), 3.48*dd* (9.5, 3.3 Hz, 1H, H–3′); ^{13}C NMR (75 MHz, $CDCl_3$): $C_{42}H_{35}F_2NO_8$ 719.23.

Synthesis of 4,6–di–*O*–benzoyl–2,3–di–*O*–benzyl–*α*–*D*–galactopyranosyl 28–*p*–methoxybenzyl betulinic acid (295)

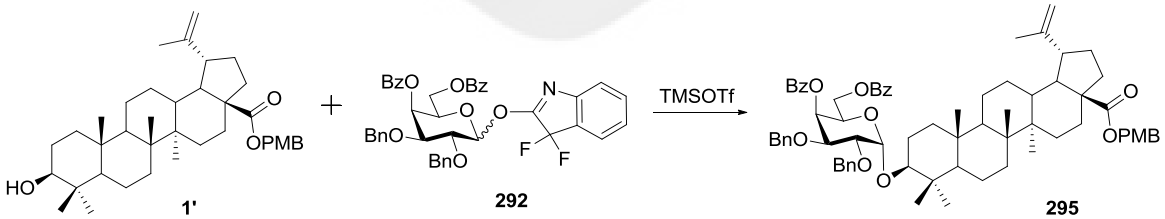

Compound **295** was synthesized according to method described before using donor **292** (137 mg, 0.1910 mmol), acceptor **1′** (100 mg, 0.1736 mmol) and CH_2Cl_2 to afford a product as a colorless foam in 98% yield (174 mg).

4,6–Di–*O*–benzoyl–2,3–di–*O*–benzyl–*α*–*D*–galactopyranosyl 28–*p*–methoxybenzyl betulinic acid (295): colorless amorphous solid. $[\alpha]_D^{28}$ = +62.8 (*c* 1.0 $CHCl_3$) ^{1}H NMR ($CDCl_3$, 300 MHz): aromatic protons at 8.01*m* (4H), 7.53*m* (2H), 7.41*m* (4H), 7.19–7.22*m* (12H) and 6.86*d* (8.6 Hz, 2H), 5.88*d* (3.0 Hz, 1H, H–4′), 5.14d (3.6 Hz, 1H, H–1′), 5.07*d* (11.9 Hz, 1H, CH_2PMB), 5.02*d* (11.9 Hz, 1H, CH_2PMB), 4.82*d* (11.1 Hz, 1H, CH_2Ph), 4.74*d* (11.1 Hz, 1H, CH_2Ph), 4.62*d* (12.0 Hz, 1H, CH_2Ph), 4.58*d* (12.0 Hz, 1H, CH_2Ph), 4.71*s* (1H, H–29_a), 4.56*s* (1H, H–29_b), 4.44*br dd* (9.7, 2.5 Hz, 1H, H–6_a′), 4.39*br dd* (3.5, 2.5 Hz, 1H, H–5′), 4.33*dd* (9.7, 3.5 Hz, 1H, H–6_b′), 4.07*dd* (10.0, 3.0 Hz, 1H, H–3′), 3.95*dd* (10.0, 3.6 Hz, 1H, H–2′), 3.14*dd* (11.6, 4.2 Hz, 1H, H–3), 3.00*td* (11.5, 6.2 Hz, 1H, H–19), 2.21*br d* (10.2 Hz, 1H), 2.13*td* (12.9, 3.3 Hz, 1H), 1.84*m* (2H), 1.67*s* (3H, H–30), 0.90*s* (6H, H–23, H–27), 0.79*s* (6H, H–25, H–26), 0.73*s* (3H, H–24), 0.54*d* (10.6 Hz, H–5), 1.77–0.64 (all *m*, 12 remaining protons); ^{13}C NMR ($CDCl_3$, 75 MHz): 175.8 (1C, C–28), 166.0 (1C), 165.8 (1C), 159.4 (2C), 150.6 (1C, C–20), 138.6 (1C), 138.1 (1C), 133.8 (1C), 132.4 (1C), 130.7 (1C), 129.7 (1C), 129.0 (1C), 128.6 (1C), 128.3 (1C), 127.6 (1C), 127.1 (1C), 126.7 (1C), 114.8 (1C), 114.5 (1C), 114.0 (1C), 113.5 (1C), 113.1 (1C), 113.0 (1C), 109.9 (1C), 94.1 (1C), 84.5 (1C), 76.0 (1C, C–5′), 75.3 (1C, C–3′), 74.6 (1C, C–2′), 72.8 (1C, C–4′), 71.8 (1C, C–6′), 68.8 (1C, OCH_3), 65.4 (1C), 56.3 (2C), 55.8 (1C), 55.1 (1C), 54.6 (1C), 47.5 (1C), 41.1 (1C), 40.6 (1C), 38.6 (1C), 37.3 (1C), 37.0 (1C), 31.3 (1C), 29.8 (1C), 29.3 (1C), 20.8 (1C), 19.2 (1C), 18.5 (1C), 18.1 (1C), 16.0 (1C), 15.5 (1C), 15.0 (1C); $C_{57}H_{71}O_9$ 1019.5673.

Debenzoylation of 4,6–di–*O*–benzoyl–2,3–di–*O*–benzyl—*α*–*D*–galactopyranosyl 28–*p*–methoxy–benzyl betulinic acid (295)

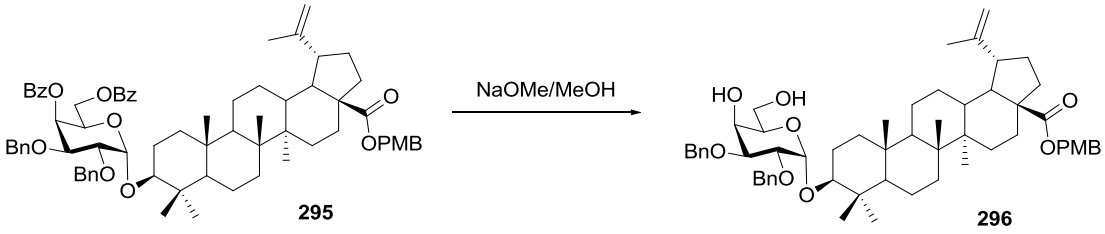

295 **296**

To a suspension of starting material **295** in MeOH NaOMe/MeOH was added until pH 10 and the resulting mixture was stirred at room temperature for 30 min. The reaction mixture was neutralized with Dowex (H^+) resin and stirred for 30 minutes. The resin was filtered off and rinsed with MeOH. The combined filtrate was concentrated and

the residue was purified by column chromatography using gradient of EtOAc–hexane to obtain 141 mg (81%) of 2,3–di–*O*–benzyl–α–*D*–galactopyranosyl 28–*p*–methoxybenzyl betulinic acid.

2,3–Di–*O*–benzyl–α–*D*–galactopyranosyl 28–*p*–methoxybenzyl betulinic acid (296): colorless amorphous solid; $[\alpha]_D^{28}$ = +32.6 (*c* 0.1 $CHCl_3$) ^{1}H NMR ($CDCl_3$: aromatic protons at 7.16–7.22*m* (12H) and 6.78*d* (8.6 Hz, 2H), 6.78*d* (8.6 Hz, 2H), 4.99d (11.9 Hz, 1H, CH_2PMB), 4.97*d* (4.2 Hz, 1H, H–1′), 4.92*d* (11.9 Hz, 1H, CH_2PMB), 4.69*d* (11.3 Hz, 2H, CH_2Ph), 4.63*d* (11.3 Hz, 2H, CH_2Ph), 4.64*s* (1H, H–29_a), 4.58*d* (11.9 Hz, 1H, CH_2Ph), 4.56*d* (11.9 Hz, 1H, CH_2Ph), 4.49*s* (1H, H–29_b), 4.01*brs* (1H, H–4′), 3.84*quin* (4.2 Hz, 1H, H–3′), 3.78*d* (4.2 Hz, 1H, H–2′), 3.77*m* (1H, H–5′), 3.60*m* (2H, H–6_a′, H–6_b′), 3.05*dd* (11.4, 3.8 Hz, 1H, H–3), 2.92*td* (11.0, 5.2 Hz, 1H, H–19), 2.27*d* (7.6 Hz, 1H), 2.06*td* (11.9, 3.3 Hz, 1H), 1.78*m* (2H), 1.57*s* (3H, H–30), 0.85*s* (3H, H–27), 0.82*s* (3H, H–27), 0.71*s* (6H, H–25, H–26), 0.65*s* (3H, H–24), 0.57*d* (7.9, 1H, H–5) 0.66–2.24 (all *m*, 12 remaining protons). ^{13}C NMR: 175.9 (1C, C–28), 159.4 (1C), 150.6 (1C, C–20), 138.5 (1C), 138.0 (1C), 131.0 (1C), 130.5 (1C), 129.5 (1C), 129.0 (2C), 128.8 (1C), 128.6 (1C), 128.3 (1C), 127.9 (1C), 127.4 (1C),127.2 (1C), 126.7 (1C), 109.5 (1C, C–29), 94.7 (1C, C–1′), 84.5 (1C), 83.3 (1C), 76.0 (1C, C–5′), 75.1 (1C, C–3′), 72.7 (1C, C–2′), 69.9 (1C, C–4′), 68.7 (1C, C–6′), 65.4 (1C), 56.4 (2C), 55.8 (1C), 54.7 (1C), 49.2 (1C), 47.5 (1C), 46.3 (1C), 42.3 (1C), 40.6 (1C), 38.6 (1C), 38.1 (1C), 37.0 (1C), 34.2 (1C), 31.1 (1C), 29.4 (1C), 28.4 (1C), 27.8 (1C), 19.1 (1C), 17.3 (1C), 16.6 (1C), 15.6 (1C), 15.3 (1C); $C_{58}H_{78}O_9$ 918.5646.

Hydrogenation of 3–*O*–(2,3–di–*O*–benzyl–α–*D*–galactopyranosyl) 28–*p*–methoxybenzyl betulinic acid (296)

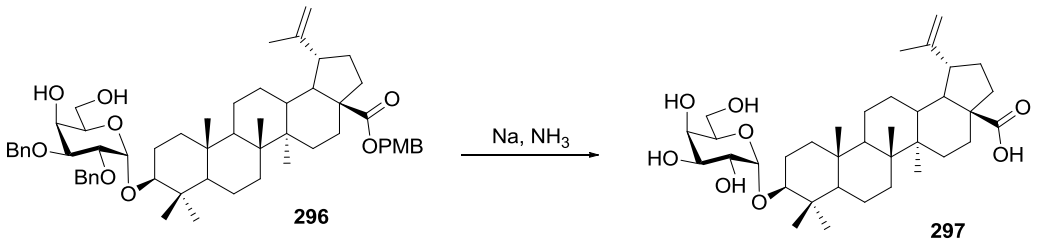

Deprotection of 3–*O*–(2,3–di–*O*–benzyl–α–*D*–galactopyranosyl) 28–*p*–methoxybenzyl betulinic acid was carried out with Na(s) in dry liquid NH_3 according to the Birch reduction procedure (Birch, 1944) to obtain compound **297** in 94% yield (58 mg).

3–*O*–*α*–*D*–Galactopyranosyl betulinic acid (297): white solid, mp 231–233 °C. IR (KBr) ν_{max} cm^{-1}: 3408, 2935, 1691, 1450, 1141, 1066, 1026 and 879; $[\alpha]_D^{26}$: +31.1 (c 0.1 CH_3OH); ^{1}H NMR (300 MHz, $CDCl_3$ + methanol–d_4): 4.87*d* (4.0 Hz, 1H, H–1′), 4.56*s* (1H, H–29_a), 4.43*s* (1H, 1H, H–29_b), 3,87*d* (1.8 Hz, 1H, H–4′), 3.79*br dd* (10.0, 1.8 Hz, 1H, H–3′), 3.64*dd* (10.0, 4.0 Hz, 1H, H–2′), 3.61*m* (2, H–5′, H–6_a′), 3.55*dd* (10.0, 2.9 Hz, 1H, H–6_b′), 3.05*dd* (11.7, 3.7 Hz, H–3), 2.85*m* (1H, H–19), 2.07*br t* (11.2 Hz, 2H), 1.78*m* (2H), 1.53*s* (3H, H–30), 0.82*s* (3H, H–27), 0.81*s* (3H, H–23), 0.78*s* (3H, H–26), 0.68*s* (3H, H–25), 0.63*s* (3H, H–24), 0.57*d* (8.9 Hz, 1H, H–5), 1.61–0.72 (all *m*, 24 remaining protons); ^{13} C NMR (75 MHz, $CDCl_3$ + methanol–d_4): HRFABMS *m/z* 641.3940 (calcd for $C_{36}H_{58}O_8Na$, 641.4023).

Synthesis of 3,3–difluoro–3*H*–indol–2–yl 2–*O*–benzyl–4,6–*O*–benzylidene–3–*O*–picoloyl–*D*–mannopyranoside (298)

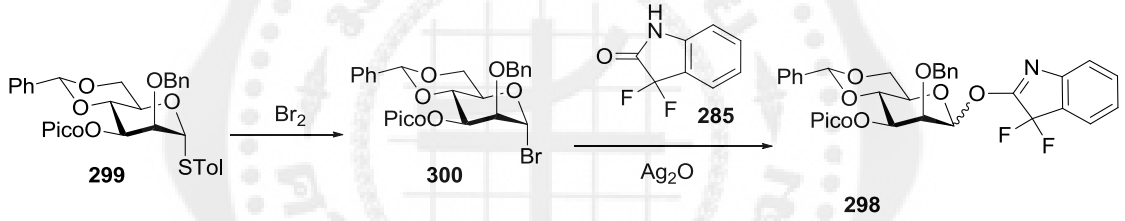

The OFox mannosyl donor **298** was synthesized follow previously described procedure (see the synthesis of **292**) using 300 mg of starting material **299** (0.5272 mmol). After column chromatography (EtOAc–hexane) the title compound was obtained as a white foam in 80% yield (244 mg).

3,3–Difluoro–3*H*–indol–2–yl 2–*O*–benzyl–4,6–*O*–benzylidene–3–*O*–picoloyl–*α*–*D*–mannopyranoside (298): colorless foam, $[\alpha]_D^{28}$ = +30.0 (*c* 1.0 $CHCl_3$) ^{1}H NMR ($CDCl_3$, 300 MHz): four protons of picoloyl group displayed at 8.79*br dd* (7.7, 3.8 Hz, 1H), 8.06*br dd* (7.8, 1.7 Hz, 1H), 7.80*ddd* (7.8, 7.7, 1.7 Hz, 1H), 7.47*ddd* (7.8, 7.8, 3.8 Hz, 1H), 7.45–7.12 (all *m*, 14 remaining aromatic protons), 6.41*br s* (1H), 5.71*dd* (10.5, 3.5 Hz, 1H, H–1), 5.62s (1H), 4.80*d* (11.8 Hz, 1H, CH_2Ph), 4.72*d* (11.8 Hz, 1H, CH_2Ph), 4.54*t* (10.5 Hz, 1H, H–4), 4.36*br dd* (3.5 Hz, 1H, H–2), 4.34*dd* (10.5, 4.6 Hz, 1H, H–6_a), 4.19*td* (10.5, 4.6 Hz, 1H, H–1), 3.89*t* (10.5 Hz, 1H, H–6_b); ^{13}C NMR ($CDCl_3$, 300 MHz): $C_{34}H_{28}F_2N_2O_7$ 614.1865

Synthesis of 3–*O*–(2–*O*–benzyl–4,6–*O*–benzylidene–3–*O*–picoloyl–*β*–*D*–mannopyranosyl) 28–*p*–methoxybenzyl betulinic acid (298)

The glycosylation was performed using the same procedure as that described for the synthesis of glucosides and galactosides. In this application donor **298** (137 mg, 0.1910 mmol) and acceptor **1′** (200 mg, 0.3472 mmol) were used to obtain the title compound that was purified by column chromatography (EtOAc–hexane) and obtained as a colorless foam in 60% yield (214 mg).

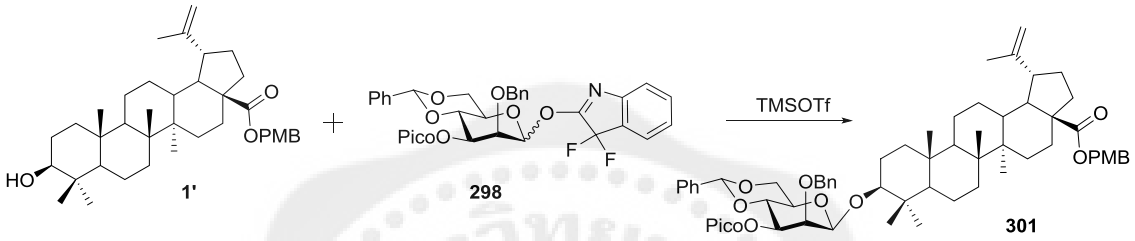

3–*O*–(2–*O*–Benzyl–4,6–*O*–benzylidene–3–*O*–picoloyl–*β*–*D*–mannopyranosyl) 28–*p*–methoxybenzyl betulinic acid (301): colorless foam, $[\alpha]_D^{28}$ = –38.6 (*c* 1.0 $CHCl_3$); ^{1}H NMR ($CDCl_3$, 300 MHz): aromatic protons at 8.79*br d* (2.9 Hz, 1H), 8.00*d* (7.7 Hz, 1H), 7.79*m* (1H), 7.45*m* (4H), 7.26*m* (2H), 7.18*br dd* (6.4, 3.6 Hz, 1H), 7.00*br dd* (6.8, 1.4 Hz, 1H) and 6.88*d* (8.6Hz, 1H), 5.62*s* (1H, H–1′), 5.59*s* (1H, –CHPh–), 5.25*dd* (9.8, 3.1 Hz, 1H, H–3′), 5.06*d* (11.9 Hz, 1H, CH_2PMB), 5.00*d* (11.9 Hz, 1H, CH_2PMB), 4.95*d* (7.4 Hz, 1H, CH_2Ph), 4.74*s* (1H, H–29$_a$), 4.70*m* (2H, H–5′, H–6$_a$′), 4.67*m* (1H, H–6$_b$′), 4.65*d* (7.4 Hz, 1H, CH_2Ph), 4.60*s* (1H, H–29$_b$), 4.38*br dd* (10.1, 9.8 Hz, 1H, H–2′), 4.24*d* (3.1 Hz, 1H, H–4′), 3.80*s* (3H, OCH_3), 3.16dd (10.6, 3.7 Hz, 1H, H–3), 3.02*d* (11.1, 5.5 Hz, H–19), 2.25*d* (9.3 Hz, 1H), 2.16*br t* (10.0 Hz, 1H), 1.68*s* (3H, H–30), 0.98*s* (3H, H–27), 0.94*s* (3H, H–23), 0.85*s* (3H, H–26), 0.82*s* (3H, H–25), 0.76*s* (3H, H–24), 1.86–0.76 (all *m*, 22 remaining protons); ^{13}C NMR ($CDCl_3$, 300 MHz): 175.3 (1C, C–28), 164.2 (1C), 159.4 (1C), 150.5 (1C, C–20), 149.8 (1C), 138.0 (1C), 137.1 (1C), 136.8 (1C), 130.0 (2C), 128.9 (1C), 128.6 (1C), 128.3 (1C), 128.4 (2C), 128.2 (1C), 128.1 (2C), 127.9 (2C), 127.8 (1C), 127.3 (1C), 126.8 (1C), 126.1 (2C), 125.5 (1C), 113.8 (2C), 109.5 (1C, C–29), 104.4 (1C), 101.6 (1C, C–1′), 91.4 (1C), 76.1 (1C, C–5′), 75.5 (1C, C–3′), 75.2 (1C, C–2′), 73.6 (1C, C–4′), 68.6 (1C, C–6′), 65.4 (1C), 56.4 (1C), 55.5 (1C), 55.2 (1C), 50.5 (1C), 49.4 (1C), 46.9 (1C), 42.3 (1C), 40.6 (1C), 39.0 (1C), 38.1 (1C), 36.9 (1C), 34.2 (1C), 32.0 (1C), 30.5 (1C), 29.4 (1C), 28.4 (1C), 25.5 (1C), 20.8 (1C), 19.3 (1C), 18.2 (1C), 16.0 (1C), 15.8 (1C), 14.6 (1C); $C_{64}H_{79}NO_{10}$ 1021.5704.

Picoloyl removal from 3–*O*–(2–*O*–benzyl–4,6–*O*–benzylidene–3–*O*–picoloyl–*β*–*D*–mannopyranosyl) 28–*p*–methoxy–benzyl betulinic acid (301)

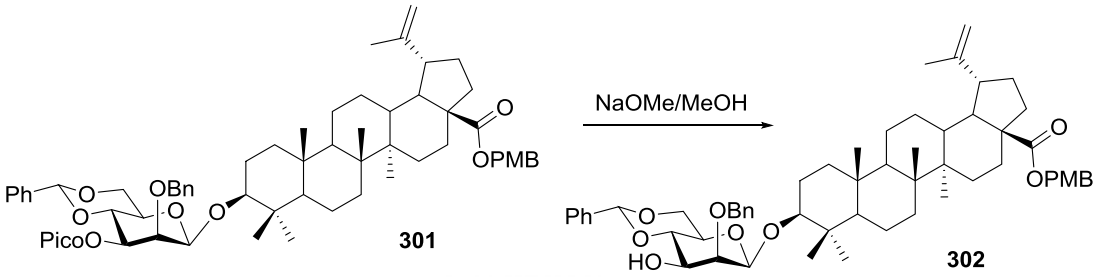

To a solution of starting material **301** (200 mg) NaOMe/MeOH was added until pH 10 and stirred at rt for 30 miniutes. The reaction was neutralized by adding of Dowex resin and stirred until reaction complete in 30 minutes. The mixture was filtered the concentrated and purified by column chromatography using gradient system of EtOAc–hexane to obtain product as colorless amorphous solid in 89% yield (162 mg).

3–*O*–(2–*O*–Benzyl–4,6–*O*–benzylidene–*β*–*D*–mannopyranosyl) 28–*p*–methoxybenzyl betulinic acid (302): colorless amorphous solid, $[\alpha]_D^{28}$ = –20.9 (*c* 1.0 $CHCl_3$); ^{1}H NMR ($CDCl_3$, 300 MHz): aromatic protons displayed at 7.48–7.27*m* (12 H) and 6.67*d* (8.6 Hz, 2H), 5.54*d* (8.6 Hz, 1H, H–1′), 5.50*s* (1H, –CHPh–), 5.11*d* (11.8 Hz, 1H, CH_2Ph), 5.05*d* (11.9 Hz, 1H, CH_2PMB), 5.01*d* (11.9 Hz, 1H, CH_2PMB), 4.75*dd* (5.7, 2.4 Hz, 1H, H–6_a′), 4.71*m* (1H, H–6_b′), 4.70*s* (1H, H–29_a), 4.62*d* (11.8 Hz, 1H, CH_2Ph), 4.61*m* (1H), 4.58*s* (1H, H–29_b), 4.25*m* (1H, H–3′), 3.94*d* (3.1 Hz, 1H, H–4′), 3.83*m* (1H), 3.79*s* (3H, OCH_3), 3.11*dd* (11.4, 4.7 Hz, 1H, H–3), 2.99*td* (10.0, 3.9 Hz, 1H, H–19), 2.40*d* (7.5 Hz, 1H), 2.23*d* (9.2 Hz, 1H), 2.41*m* (1H), 1.83*m* (2H), 1.6 5*s* (3H, H–30), 0.95*s* (3H, H–27), 0.91*s* (3H, H–23), 0.82*s* (3H, H–26), 0.85*s* (3H, H–25), 0.74*s* (3H, H–24),
^{13}C NMR ($CDCl_3$, 300 MHz): $C_{58}H_{76}O_9$ 916.5489.

Benzylidene removal from 3–*O*–(2–*O*–benzyl–4,6–*O*–benzylidene–*β*–*D*–mannopyranosyl) 28–*p*–methoxybenzyl betulinic acid (302)

To a solution of **302** (140 mg) in CH_2Cl_2/H_2O (9 mL) TFA (1 mL, 10%) was added and then stirred at rt. Crude product was further purified by CC (CH_2Cl_2–MeOH) product was obtained as a colorless amorphous solid in 69% yield (87 mg).

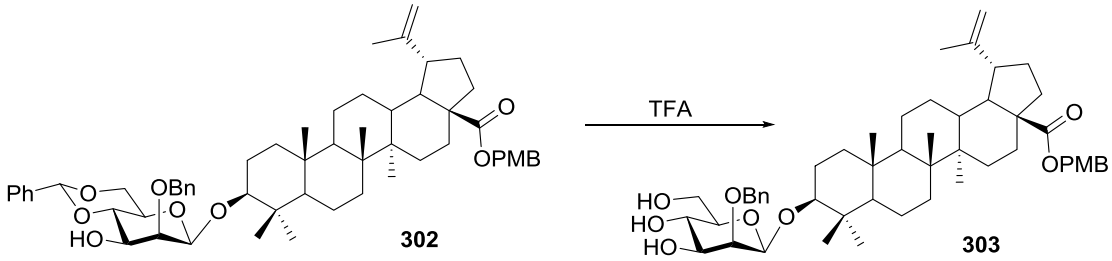

3–*O*–(2–*O*–benzyl–*β*–*D*–mannopyranosyl) 28–*p*–methoxybenzyl betulinic acid (303): **c**olorless amorphous solid, $[\alpha]_D^{28}$ = –20.9 (*c* 1.0 $CHCl_3$); ^{1}H NMR ($CDCl_3$, 300 MHz): aromatic protons displayed at 7.32*m* (5H), 7.06*d* (8.5 Hz, 2H), 6.79*d* (8.5 Hz, 2H), 5.07*d* (11.8 Hz, 1H, H–1′), 4.56*dd* (11.8, 2.9 Hz, 2H, H–2′, H–3′), 3.86m (1H, H–6_a′), 3.85*d* (2.9 Hz, 1H, H–4′), 3.84*s* (1H, H–29_a), 3.76*s* (3H, OCH_3), 3.75*m* (2H, H–5′, H–6_b′), 3.74*s* (1H, H–29_b), 3.59*m* (1H, H–3), 3.25*m* (1H, H–19), 3.10*m* (1H), 1.64s (3H, H–30), 0.96*s* (3H, H–27), 0.93*s* (3H, H–23), 0.89*s* (3H, H–26), 0.86*s* (3H, H–25), 0.83*s* (3H, H–24), 0.71–1.82 (all *m*, 20 remaining protons); ^{13}C NMR ($CDCl_3$, 300 MHz): see appendix (need more purification).

Debenzylation of 3–*O*–(2–*O*–benzyl–*β*–*D*–mannopyranosyl) 28–*p*–methoxy–benzyl betulinic acid (303)

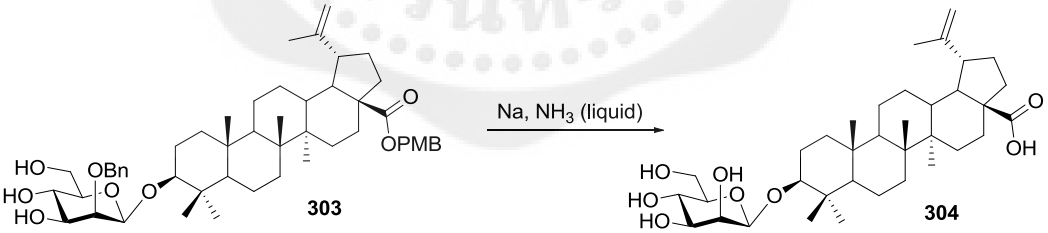

Debenzylation of 3–*O*–(2–*O*–benzyl–*β*–*D*–mannopyranosyl) 28–*p*–methoxy–benzyl betulinic acid was provided using Na(s) in dry liquid NH_3 according to Birch reduction procedure (Birch, 1944).

3–*O*–*β*–*D*–mannopyranosyl betulinic acid (304): **c**olorless amorphous solid, mp 230–232°C. IR (KBr) V_{max} cm^{-1} : 3411, 2931, 1695, 1453, 1146, 1069, 1023 and 877 ; $[\alpha]_D^{26}$: +22.7 (c 0.1 CH_3OH); ^{1}H NMR (300 MHz, pyridine–d_6): 5.44*d* (3.8 Hz, 1H, H–

1′), 4.92*s* (3H, 1H, H–29$_a$), 4.76*s* (3H, 1H, H–29$_b$), 4.56*m* (1H, H–1′), 4.54*m* (1H, H–6$_a$′), 4.49*m* (1H, H–5′), 4.43*dd* (10.9, 4.6 Hz, 1H, H–6$_b$′), 4.24*t* (9.7 Hz, 1H, H–3′), 4.14*dd* (9.7, 3.8 Hz, 1H, H–3′), 3.51*m* (1H, H–19), 3.41*dd* (11.1, 3.9 Hz, H–3), 2.70*br t* (11.2 Hz, 1H), 2.61*br d* (12.5 Hz, 1H), 1.78*s* (3H, H–30), 1.14*s* (3H, H–27), 1.03*s* (3H, H–23), 1.00*s* (3H, H–26), 0.79*s* (3H, H–25), 0.71*s* (3H, H–24), 0.66–2.24 (all *m*, 27 remaining protons); ^{13}C NMR (75 MHz, pyridine–d_6): 179.1 (1C, C–29), 151.4 (1C, C–20), 109.6 (1C, C–29), 98.1 (1C, C–1′), 96.7 (1C), 48.7 (1C), 83.1 (1C), 75.5 (1C, C–5′), 74.8 (1C, C–3′), 73.8 (1C, C–2′), 73.3 (1C, C–4′), 72.4 (1C, C–6′), 63.0 (1C), 56.7 (1C), 55.6 (1C), 50.8 (1C), 50.4 (1C), 50.0 (1C), 48.5 (1C), 47.2 (1C), 42.9 (1C), 41.1 (2C), 38.7 (1C), 37.4 (1C), 37.3 (1C), 34.8 (1C), 29.0 (1C), 21.1 (1C), 20.2 (1C), 19.8 (1C), 18.3 (1C), 16.9 (1C), 16.4 (1C), 16.3 (1C), 14.9 (1C). HRFABMS *m/z* 641.4139 (calcd for $C_{36}H_{58}O_8Na$, 641.4023).

Glycosylation of α–mangostin

Isolation of starting material

α–Mangostin (**234**) was isolated from mangosteen fruit hall as reported by Sudta (Sudta, 2011).

Synthesis of 6–*O*–benzoyl α–mangostin (234′)

α–Mangostin (5 g, 12.19 mmol) was dissolved in pyridine and stirred under Ar atmosphere for 15 min. A solution of benzoyl chloride (1.42 mL, 12.19 mmol) in pyridine (10 mL) was added to solution of starting material at 0 ^{o}C and stirred for 1.5 hour at rt. The reaction was quenched by the dropwise addition of MeOH. The reaction mixture was allowed to cool to rt, the volatiles were removed under the reduced pressure, and the residue was co–evaporated with toluene. The residue was dissolved in CH_2Cl_2 (30 mL) and washed with water (10 mL), 1 N HCl (10 mL), $NaHCO_3$ (10 mL), and water (2 x 10 mL). The organic layer was separated, dried, and concentrated. The residue was purified by column chromatography using gradient system of EtOAc–hexane to give **234′** (3.79 g, 61%) and its 3,6–di–*O*–benzoyl analogue (**234′′**, 2.44 g, 32%).

6–*O*–Benzoyl α–mangostin (234′): Yellow solid, mp 190–192 ^{o}C; IR (KBr) ν_{max} cm^{-1} : 3470, 2912, 1720, 1643, 1597, 1460, 1276, 1166, 1109, 823 and 705 ; ^{1}H NMR ($CDCl_3$, 300 MHz): 13.57*s* (1H, 1–OH), 8.23*d* (7.6 Hz, 2H, H–3′, H–7′), 7.68*t* (7.6 Hz, 2H,

H–5′), 7.54*br t* (7.6 Hz, 2H, H–4′, H–6′), 7.21*s* (1H, H–5), 6.25*s* (1H, H–4), 6.24*s* (1H, 3–OH), 5.27*t* (7.0 Hz, 1H, H–12), 5.22*t* (6.2 Hz, 1H, H–12), 4.15*d* (6.2 Hz, 2H, H–16), 3.74*s* (3H, 7–OCH_3), 3.44*d* (7.0 Hz, 2H, H–11), 1.82*s* (3H, H–19), 1.81*s* (3H, H–14), 1.75*s* (3H, H–20), 1.67*s* (3H, H–15).

Benzoylation of sugars

305-307

Each sugar (3 g, 16.6 mmol) was dissolved in pyridine and stirred under Ar atmosphere for 15 min, a solution of benzoyl chloride (1.22 mL, 116.5 mmol) in pyridine was added at 0 ^{o}C, and the resulting mixture was left for 16 h at room temperature. The reaction mixture was worked up as described as described for 6–*O*–benzoylation of α–mangostin. As a result, perbenzoylated derivatives (**305**–**307**) of glucose, galactose and mannose were obtained in 99% (11.55 g), 83% (9.72 g) and 99% (11.55 g) yields, respectively.

Synthesis of 2,3,4,6–tetra–*O*–benzoyl–α–glycopyranosyl bromides

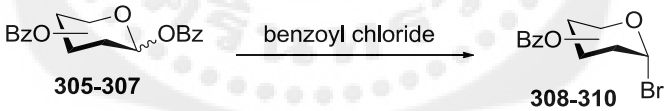

305-307 **308-310**

To a solution of each perbenzoylated sugar (**305**–**307**, 9 g, 13.6 mmol) in CH_2Cl_2 was added hydrogen bromide in acetic acid (HBr/AcOH) (6.80 mL, 115.2 mmol) dropwise and the resulting mixture was stirred under Ar atmosphere for 3 hours at rt. After that, the reaction mixture was diluted with CH_2Cl_2 and sequentially extracted with cold water (20 mL), $NaHCO_3$ (20 mL), and cold water (2 x 20 mL). The organic phase was separated, dries, and concentrated at room temperature. The residue was precipitated by the addition of excess hexanes. The white precipitate was filtered and dried to yield glucosyl– (**308**), galactosyl– (**309**) and mannosyl bromide donors (**310**) in 84% (11.81 g), 99% (13.92 g), and 99% (13.92 g), respectively.

Synthesis of 3,6–di–*O*–glycosyl–mangostins

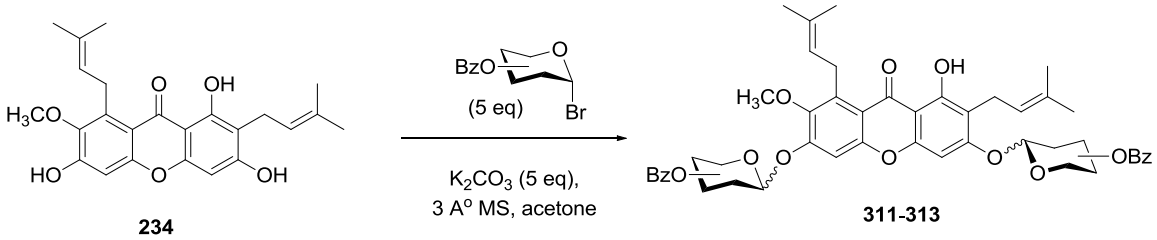

A glycosyl acceptor, α–mangostin (100 mg, 0.2439 mmol) was dissolved in acetone and stirred with 3 Å MS under Ar atmosphere for an hour. K_2CO_3 (168 mg, 1.2 mmol) was then added into solution and left stirring for half hour. Each glycosyl donor (803 mg, 1.2 mmol) was added in to reaction mixture at rt and then stirred at 60 ^{o}C (for only glucosylation and mannosylation) under reflux condition. The solution was filtered then evaporated and extracted with CH_2Cl_2/H_2O. The residue was concentrated and then subjected to column chromatography using EtOAc–hexane to yield 118 mg (31 %), 359 mg (94 %) and 222 mg (58 %) of glucosyl– (**311**), galactosyl– (**312**) and mannosyl mangostins (**313**), respectively.

3,6–di–*O*–(2,3,4,6–tetra–*O*–benzoyl–β–*D*–glucopyranosyl)–mangostin

(311): yellow needles, mp 120–122 ^{o}C. IR ($CHCl_3$) ν_{max} cm^{-1} : 2928, 1733, 1646, 1599, 1465, 1267, 1091, 1072, 754, 707; ^{1}H NMR ($CDCl_3$, 600 MHz): 13.25 (1H, 1–OH), aromatic protons at 7.81–7.93*m* (20H) and 7.17–7.41*m* (20H), 6.82*s* (1H, H–5), 6.38*s* (1H, H–4), 5.94*m* (2H, H–3′, H–3′′), 5.82*m* (4H, H–2′, H–2′′, H–4′, H–4′′), 5.53*d* (7.2 Hz, 1H, H–1′), 5.50*d* (7.3 Hz, 1H, H–1′), 5.06*t* (5.7 Hz, 1H, H–17), 4.98*t* (6.7 Hz, 1H, H–12), 4.73 *br dd* (12.4, 9.9 Hz, 2H, H–6_a′, H–6_a′′), 4.33 *m* (4H, , H–5′, H–5′′, H–6_b′, H–6_b′′), 3.94*d* (5.7 Hz, 2H, H–16), 3.56*s* (3H, 7–OCH_3, 3.19*d* (6.7 Hz, 2H, H–16), 1.69*s* (3H, H–19), 1.64*s* (3H, H–14), 1.56*s* (3H, H–20), 1.33*s* (3H, H–15). ^{13}C NMR (125 MHz): 182.0 (1C, C–9), 165.9 (2C), 165.7 (1C), 165.6 (1C), 165.0 (2C), 164.9 (2C), 160.4 (1C, C–3), 159.9 (1C, C–1), 154.5 (1C, C–6), 154.3 (2C, C–4a, C–10a), 144.8 (1C, C–7), 138.3 (1C, C–8), 133.6 (1C), 133.5 (3C), 133.4 (1C), 133.3 (1C), 133.0 (1C, C–18), 132.9 (1C, C–13), 131.9 (2C), 129.8 (8C), 129.7 (4C), 129.6 (4C), 129.3 (1C), 129.2 (1C), 128.9 (1C), 128.8 (1C), 128.7 (2C), 128.5 (1C), 128.4 (8C), 128.3 (6C), 128.2 (2C), 128.1 (1C), 122.6 (1C, C–17), 121.4 (1C, C–12), 113.9 (1C, C–8a), 112.8 (1C, C–2), 105.0 (1C, C–5), 102.7 (1C, C–9a), 98.2 (1C, C–1′), 98.0 (1C, C–1′′), 91.8 (1C, C–4), 72.8 (1C, C–5′), 72.7 (1C, C–5′′), 72.6 (1C, C–3′), 72.5

(1C, C–3′′), 71.5 (1C, C–2′), 71.4 (1C, C–2′′), 69.0 (1C, C–2′), 68.9 (1C, C–4′′), 62.8 (2C, C–6′, C–6′′), 61.1 (1C, 7–OCH_3), 26.1 (1C, C–20), 25.8 (1C, C–16), 25.4 (1C, C–15), 21.4 (1C, C–11), 18.0 (1C, C–19), 17.7 (1C, C–14). HRFABMS *m/z* 1589.4753 (calcd for $C_{92}H_{78}O_{24}Na$, 1589.4781).

3,6–di–*O*–(2,3,4,6–tetra–*O*–benzoyl–*β*–*D*–galactopyranosyl)–mangostin (312): yellow needles, mp 123–125 °C. IR ($CHCl_3$) ν_{max} cm^{-1}: 2917, 1731, 1643, 1599, 1451, 1270, 1094, 1067, 762, 707 ; ^{1}H NMR (600 MHz): 13.31*s* (1H, 1–OH), aromatic protons at 8.10*br s* (1H), 8.04*d* (7.6 Hz, 5H), 7.95*d* (7.4 Hz, 5H), 7.89*d* (7.6 Hz, 8H), 7.75*d* (7.8 Hz, 4H), 7.56*t* (7.3 Hz, 2H), 7.42*m* (10H) and 7.14–7.32*m* (9H), 6.89*s* (1H, H–5), 6.45*s* (1H, H–4), 6.10*dt* (8.9, 7.9 Hz, 2H, H–2′, H–2′′), 6.03*d* (3.1 Hz, 2H, H–4′, H–4′′), 5.68*dd* (8.9, 3.1 Hz, 2H, H–3′, H–3′′), 5.52*d* (7.9 Hz, 1H), 5.48*d* (7.9 Hz, 1H), 5.06*t* (5.5 Hz, 1H), 4.95*t* (7.9 Hz, 1H), 4.59*m* (2H, H–6_a′, H–6_a′′), 4.43*m* (2H, H–5′, H–5′′), 4.59*m* (2H, H–6_b′, H–6_b′′), 3.98*d* (5.5 Hz, 1H, H–16), 3.55*s* (3H, 7–OCH_3), 3.22*d* (7.9 Hz, 2H, H–11), 1.70*s* (3H, H–19), 1.68*s* (3H, H–14), 1.56*s* (3H, H–20), 1.30*s* (3H, H–15). ^{13}C NMR (125 MHz): 182.1 (1C, C–9), 165.9 (2C), 165.5 (2C), 165.4 (2C), 165.1 (1C), 165.0 (1C), 160.6 (1C, C–3), 160.0 (1C, C–1), 154.6 (1C, C–6), 154.5 (1C, C–10a), 154.4 (1C, C–4a), 144.8 (1C, C–7), 138.5 (1C, C–8), 133.7 (2C), 133.5 (1C), 133.4 (1C), 133.2 (1C), 133.1 (1C), 132.1 (1C, C–18), 131.9 (1C, C–13), 130.0 (3C), 129.9 (2C), 129.8 (3C), 129.7 (5C), 129.6 (2C), 129.3 (1C), 129.2 (1C), 128.9 (3C), 128.8 (1C), 128.7 (5C), 128.6 (2C), 128.5 (5C), 128.4 (4C), 128.3 (4C), 122.7 (1C, C–17), 121.5 (1C, C–12), 114.1 (1C, C–8a), 113.1 (1C, C–2), 105.2 (1C, C–9a), 103.2 (1C, C–5), 98.9 (1C, C–1′), 98.7 (1C, C–1′′), 91.9 (1C, C–4), 71.9 (1C, C–5′), 71.8 (1C, C–5′′), 71.5 (1C, C–3′), 71.3 (1C, C–3′′), 69.3 (1C, C–2′), 69.1 (1C, C–4′′), 67.6 (1C, C–4′, C–4′′), 61.7 (2C, C–6′, C–6′′), 61.2 (1C, 7–OCH_3), 26.2 (1C, C–20), 25.8 (1C, C–16), 25.4 (1C, C–15), 21.5 (1C, C–11), 18.1 (1C, C–19), 17.8 (1C, C–14). HRFABMS *m/z* 1589.4763 (calcd for $C_{92}H_{78}O_{24}Na$, 1589.4781).

3,6–di–*O*–(2,3,4,6–tetra–*O*–benzoyl–*α*–*D*–mannopyranosyl)–mangostin (313): yellow needles, mp 125–127 °C. IR ($CHCl_3$) ν_{max} cm^{-1}: 2961, 1731, 1643, 1599, 1451, 1267, 1097, 1067, 754, 707 ; ^{1}H NMR (300 MHz): 13.48*s* (1H, 1–OH), aromatic protons at 8.07–8.10*m* (4H), 7.92–7.96*m* (4H), 7.85–7.88*m* (8H), 7.61*m* (2H) and 7.25–7.52*m* (22H), 7.04*s* (1H, H–5), 6.59*s* (1H, H–4), 6.13*m* (4H, H–3′, H–3′′, H–4′, H–4′′), 5.95*dt* (10.2, 2.1 Hz, 2H, H–2′, H–2′′), 5.89*d* (10.2 Hz, 1H, H–1′), 5.88*d* (10.2 Hz, 1H, H–

1′′), 5.39*t* (6.5 Hz, H–12), 5.26*t* (6.5 Hz, H–17), 4.18*d* (6.6 Hz, H–16), 3.57*s* (3H, 7–OCH_3), 3.55*d* (6.5 Hz, H–11), 4.55*dd* (12.1, 5.7 Hz, 2H, H–6_a′, H–6_a′′), 4.52*dd* (8.6, 5.7 Hz, 2H, H–5′, H–5′′), 4.47*dd* (12.1, 8.7 Hz, 2H, H–6_b′, H–6_b′′), 1.93*s* (3H, H–14), 1.90*s* (3H, H–19), 1.79*s* (3H, H–15), 1.73*s* (3H, H–20). ^{13}C NMR (75 MHz): 182.2 (1C, C–9), 166.2 (1C), 166.0 (2C), 165.4 (3C), 165.3 (2C), 165.2 (1C, C–3), 160.3 (1C, C–1), 158.8 (1C, C–6), 154.5 (1C, C–10a), 153.6 (1C, C–4a), 144.5 (1C, C–7), 138.3 (1C, C–8), 133.7 (2C), 133.4 (2C), 133.2 (2C), 133.0 (2C), 132.6 (1C, C–16), 132.2 (1C, C–13), 130.6 (1C), 130.3 (1C), 130.0 (2C), 129.8 (4C), 129.7 (4C), 129.4 (3C), 129.3 (2C), 129.2 (1C), 129.0 (1C), 128.9 (2C), 128.8 (1C), 128.7 (2C), 128.6 (2C), 128.5 (5C), 128.4 (2C), 128.3 (6C), 127.3 (1C), 122.7 (1C, C–17), 122.1 (1C, C–12), 113.8 (1C, C–8a), 112.6 (1C, C–2), 105.0 (1C, C–5), 102.5 (1C, C–9a), 95.9 (1C, C–1′), 95.2 (1C, C–1′′), 92.3 (1C, C–4), 69.9 (2C, C–5′, C–5′′), 69.7 (2C, C–3′, C–3′′), 68.8 (1C, C–2′), 66.8 (1C, C–2′), 66.5 (2C, C–4′, C–4′′), 62.6 (3C, C–6′, C–6′′, 7–OCH_3), 26.3 (1C, C–20), 25.8 (2C, C–15, C–16), 21.5 (1C, C–11), 18.1 (2C, C–14, C–19). HRMS *m/z* 1589.4791 (calcd for $C_{92}H_{78}O_{24}Na$, 1589.4781).

Debenzoylation of 3,6–di–*O*–glycosyl–mangostins

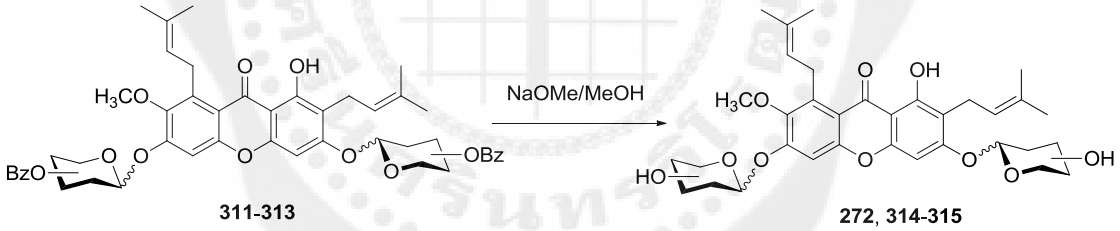

The reactions were provided using 80 mg, 200 mg and 170 mg of compounds **311**–**313**, respectively. To a suspension of starting material in MeOH, NaOMe/MeOH was added until pH 10 and stirred at rt for half hour. The reaction was neutralized by adding of Dowex resin and stirred until reaction complete in 30 minutes. The mixture was filtered the concentrated and purified by column chromatography using gradient system of EtOAc–hexane. Products were obtained as 36 mg (96 %) of 3,6–di–*O*–*β*–*D*–glucopyranosyl mangostin (**272**), 59 mg (63 %) of 3,6–di–*O*–*β*–*D*–galactopyranosyl mangostin (**314**) and 52 mg (65 %) of 3,6–di–*O*–*α*–*D*–mannopyranosyl mangostin (**315**).

3,6–di–*O*–*β*–*D*–glucopyranosyl mangostin (272): Yellow amorphous solid, mp 237–239 °C. $[\alpha]_D^{24}$ +27.4 (*c* 1.0, MeOH); Clog*P*: 0.87 ± 1.18; IR (KBr) ν_{max} cm^{-1} :

3395, 2917, 1646, 1602,1462, 1278, 1097, 1080, 828; ^{1}H– and ^{13}C NMR *see* Table 26. HRESIMS *m/z* 757.2410 (calcd for $C_{36}H_{46}O_{16}Na$, 757.2678).

3,6–di–*O*–*β*–*D*–galactopyranosyl mangostin (314): Yellow amorphous solid, mp 225–227 °C $[\alpha]_D^{24}$–72.7 (c 1.0, MeOH) Clog*P*: 0.87 ± 1.18; IR (KBr) ν_{max} cm^{-1}: IR (KBr) ν_{max} cm^{-1}: 3391, 2919, 1645, 1698,1462, 1276, 1097, 1084, 825; ^{1}H– and ^{13}C NMR *see* Table 26. HRFABMS *m/z* 757.2683 (calcd for $C_{36}H_{46}O_{16}Na$, 757.2684).

3,6–di–*O*–*α*–*D*–mannopyranosyl mangostin (315): Yellow–orange amorphous solid, mp 223–225 °C $[\alpha]_D^{25}$+48.4 (c 1.0, MeOH); Clog*P*: 0.87 ± 1.18; IR (KBr) ν_{max} cm^{-1}: 3384, 2923, 1687, 1646, 1588, 1462, 1275, 1086, 1050, 823; ^{1}H– and ^{13}C NMR *see* Table 26. HRESIMS *m/z* 757.2454 (calcd for $C_{36}H_{46}O_{16}Na$, 757.2684).

Synthesis of 6–*O*–glycosyl–6–*O*–benzoyl mangostins

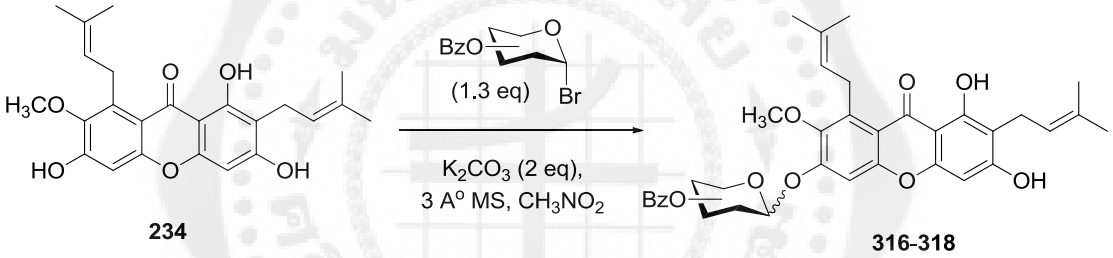

A glycosyl acceptor, *α*–mangostin (100 mg, 0.2439 mmol) was dissolved in CH_3NO_2 and stirred with 3 Å MS under Ar atmosphere for an hour. K_2CO_3 (67 mg, 0.4878 mmol) was then added into solution and left stirring for half hour. Each glycosyl donor was added in to reaction mixture and then stirred at rt until reaction complete. The solution was filtered then evaporated and extracted with CH_2Cl_2/H_2O. The residue was concentrated and then subjected to column chromatography using EtOAc–hexane to yielded 120 mg (50 %), 147 mg (61 %) and 142 mg (59 %) of glucosyl–, galactosyl– and mannosyl mangostin, respectively.

6–*O*–(2,3,4,6–tetra–*O*–benzoyl–*β*–*D*–glucopyranosyl)–mangostin (316): yellow needles, mp 108–110 °C. $[\alpha]_D^{26}$+31.5 (*c* 1.0, $CDCl_3$); Clog*P*: 14.93 ± 1.22; IR ($CHCl_3$) ν_{max} cm^{-1}: 3395, 2917, 1728, 1643, 1602, 1462, 1270, 1089, 1072, 757, 707 ; ^{1}H NMR (600 MHz): 13.69*s* (1H, 1–OH), aromatic protons at 7.92–7.96*m* (6H), 7.87*br d* (7.0 Hz, 2H) and 7.25–7.54*m* (12H), 6.98*s* (1H, H–5), 6.13*s* (1H, 3–OH), 6.06*s* (1H, H–4), 6.00*t*

(9.1 Hz, 1H, H–3′), 5.89*dd* (9.1, 7.1 Hz, 1H, H–2′), 5.77*t* (9.1 Hz, 1H, H–3′), 5.57*d* (7.1 Hz, 1H, H–1′), 5.28*t* (7.2 Hz, 1H, H–12), 5.12*t* (6.5 Hz, 1H, H–17), 4.73*dd* (11.5, 1.9 Hz, 1H, H–6_a′), 4.51*dd* (11.5, 6.5 Hz, 1H, H–6_b′), 4.43*dd* (6.5, 1.9 Hz, 1H, H–5′), 4.01*d* (6.5, 1H, H–16), 3.58*s* (3H, 7–OCH_3), 3.45*d* (6.5, 1H, H–11), 1.83*s* (3H, H–19), 1.77*s* (3H, H–14), 1.73*s* (3H, H–20), 1.61*s* (3H, H–15); ^{13}C NMR (125 MHz): 182.0 (1C, C–9), 166.0 (1C), 165.7 (1C), 165.2 (1C), 164.9 (1C), 161.7 (1C, C–3), 160.5 (1C, C–1), 154.9 (1C, C–6), 154.5 (1C, C–10a), 154.3 (1C, C–4a), 144.6 (1C, C–7), 138.2 (1C, C–8), 136.0 (1C), 133.6 (1C), 133.4 (2C), 133.2 (1C, C–18), 131.9 (1C, C–13), 129.9 (2C), 129.8 (2C), 129.7 (2C), 129.6 (2C), 129.2 (1C), 128.8 (1C), 128.5 (4C), 128.4 (2C), 128.3 (4C), 122.8 (1C, C–17), 121.3 (1C, C–12), 114.0 (1C, C–8a), 108.3 (1C, C–2), 103.7 (1C, C–9a), 103.0 (1C, C–5), 98.5 (1C, C–1′), 93.4 (1C, C–4), 72.9 (1C, C–5′), 72.5 (1C, C–3′), 71.4 (1C, C–2′), 69.1 (1C, C–4′), 62.9 (1C, C–6′), 61.1 (1C, 7–OCH_3), 26.1 (1C, C–20), 25.8 (2C, C–15, C–16), 21.4 (1C, C–11), 18.1 (1C, C–19), 17.9 (1C, C–14); HRFABMS *m/z* 1011.3223 (calcd for $C_{58}H_{52}O_{15}Na$, 1011.3204).

6–*O*–(2,3,4,6–tetra–*O*–benzoyl–*β*–*D*–galactopyranosyl)–mangostin

(317): yellow needles, mp 103–105 °C. $[\alpha]_D^{26}$ +70.6 (*c* 1.0, $CDCl_3$); Clog*P*: 14.93 ± 1.22**;** IR ($CHCl_3$) ν_{max} cm^{-1} : 3417, 2917, 1728, 1643, 1604, 1462, 1270, 1094, 1070, 754, 707 ; ^{1}H NMR (600): 13.69*s* (1–OH), aromatic protons at 8.10*d* (7.1 Hz, 2H), 8.00*d* (7.0 Hz, 2H), 7.92*d* (7.1 Hz, 2H), 7.80*d* (7.1 Hz, 2H), 7.92*t* (7.4 Hz, 1H) and 7.25–7.51*m* (11H), 7.03*s* (1H, H–5), 6.21*s* (1H, H–4), 6.19*dd* (10.3, 7.8 Hz, 1H, H–2′), 6.07*dd* (10.3, 7.8 Hz, 1H, H–4′), 6.06*s* (1H, 3–OH), 5.72*dd* (10.3, 3.4 Hz, 1H, H–3′), 5.53*d* (7.8 Hz, 1H, H–1′), 5.28*t* (7.0 Hz, 1H, H–12), 5.14*t* (6.5 Hz, 1H, H–17), 4.67*dd* (13.3, 6.8 Hz, 1H, H–6_a′), 4.60*dd* (6.8, 4.2 Hz, 1H, H–5′), 4.55*dd* (13.3, 4.2 Hz, 1H, H–6_b′), 4.03*d* (6.5 Hz, 2H, H–16), 3.56*s* (3H, 7–OCH_3), 3.45*d* (7.0 Hz, 2H, H–11), 1.83*s* (3H, H–19), 1.77*s* (3H, H–14), 1.73*s* (3H, H–20), 1.67*s* (3H, H–15); ^{13}C NMR (125 MHz): 182.0 (1C, C–9), 166.1 (1C), 165.5 (1C), 165.4 (1C), 165.1(1C), 161.7 (1C, C–3), 160.5 (1C, C–1), 154.9 (1C, C–6), 154.7 (1C, C–10a), 154.4 (1C, C–4a), 144.7 (1C, C–7), 138.5 (1C, C–8), 136.2 (1C), 133.4 (3C, C–18), 132.0 (1C, C–13), 130.0 (2C), 129.8 (2C), 129.7 (2C), 129.6 (2C), 129.1 (1C), 128.9 (1C), 128.7 (3C), 128.5 (3C), 128.4 (2C), 128.3 (2C), 122.8 (1C, C–17), 121.3 (1C, C–12), 114.0 (1C, C–8a), 108.4 (1C, C–2), 103.7 (1C, C–9a), 103.1 (1C, C–5), 99.2 (1C, C–1′), 93.4 (1C, C–4), 72.2 (1C, C–5′), 71.4 (1C, C–3′), 69.1 (1C, C–2′), 67.8 (1C, C–4′), 62.3 (1C, C–6′), 61.1

(1C, 7–OCH_3), 26.2 (1C, C–20), 25.8 (2C, C–15, C–16), 21.4 (1C, C–11), 18.1 (1C, C–19), 17.9 (1C, C–14); $C_{58}H_{52}O_{15}$; ESIMS *m/z* (–ve) 1397 (100), 409(83), (+ve) 989(33).

6–*O*–(2,3,4,6–tetra–*O*–benzoyl–*α*–*D*–mannopyranosyl)–mangostin (318): yellow needles, mp 101–103 °C. $[\alpha]_D^{26}$ +50.3 (*c* 1.0, $CDCl_3$); Clog*P*: 14.93 ± 1.22**;** IR ($CHCl_3$) ν_{max} cm^{-1} : 3406, 2967, 1731, 1643, 1588, 1465, 1267, 1105, 1070, 757, 707; ^1H NMR (600 MHz): 13.62*s* (1H, 1–OH), aromatic protons at 8.02*d* (7.6 Hz, 2H), 7.91*d* (7.6 Hz, 2H), 7.85*d* (7.7 Hz, 2H), 7.81*d* (8.7 Hz, 2H), 7.56*t* (7.3 Hz, 1H) and 7.12–7.39*m* (10H), 7.03*s* (1H, H–5), 6.28*s* (1H, 3–OH), 6.10*s* (1H, H–4), 6.09*br s* (2H, H–2′, H–4′), 5.77*s* (2H, H–1′, H–3′), 5.23*t* (7.0 Hz, 1H, H–12), 5.17*t* (6.1 Hz, 1H, H–17), 4.51*m* (3H, H–5′, H–6_a′, H–6_b′), 4.10*d* (6.1, 2H, H–5′), 3.93*s* (3H, 7–OCH_3), 3.39*d* (7.0, 2H, H–11), 1.82*s* (3H, H–19), 1.77*s* (3H, H–14), 1.70*s* (3H, H–20), 1.65*s* (3H, H–15); ^{13}C NMR (125 MHz): 182.0 (1C, C–9), 165.9 (1C), 165.5 (2C), 165.4(1C), 161.7 (1C, C–3), 160.6 (1C, C–1), 154.9 (1C, C–6), 154.5 (1C, C–10a), 153.3 (1C, C–4a), 144.4 (1C, C–7), 138.3 (1C, C–8), 135.6 (1C), 133.8 (1C), 133.6 (2C), 133.4 (1C), 133.0 (1C, C–18), 132.0 (1C, C–13), 129.9 (2C), 129.8 (2C), 129.7 (2C), 129.4 (2C), 129.3 (1C), 128.8 (2C), 128.7 (2C), 128.6 (1C), 128.5 (2C), 128.4 (2C), 128.2 (2C), 122.9 (1C, C–17), 121.4 (1C, C–12), 113.8 (1C, C–8a), 108.6 (1C, C–2), 104.0 (1C, C–9a), 102.5 (1C, C–5), 95.8 (1C, C–1′), 93.3 (1C, C–4), 70.3 (1C, C–5′), 70.0 (1C, C–3′), 69.7 (1C, C–2′), 66.3 (1C, C–4′), 62.5 (1C, C–6′), 61.5 (1C, 7–OCH_3), 26.3 (1C, C–20), 25.9 (1C, C–16), 25.8 (1C, C–15), 21.4 (1C, C–11), 18.2 (1C, C–19), 17.9 (1C, C–14); HRFABMS *m/z* 1011.3215 (calcd for $C_{58}H_{52}O_{15}Na$, 1011.3204).

Debenzoylation of 6–*O*–glycosyl–mangostin

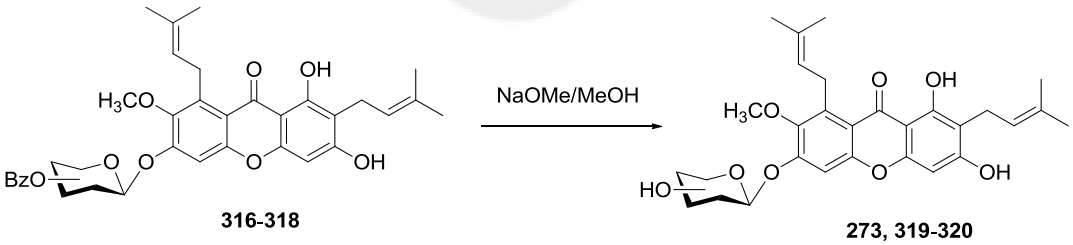

316-318 **273, 319-320**

The reactions were provided using 90 mg, 100 mg and 110 mg of compounds **316**–**318**, respectively. To a suspension of starting material in 5 mL MeOH, NaOMe/MeOH was added until pH 10 and stirred at rt for 30 min. The reaction was neutralized by adding of Dowex resin and stirred until reaction complete in 30 minutes. The

mixture was filtered the concentrated and purified by column chromatography using gradient system of MeOH–DCM to obtain 44 mg (88 %) of 6–*O*–*β*–*D*–glucopyranosyl mangostin (**273**), 35 mg (61 %) of 6–*O*–*β*–*D*–galactopyranosyl mangostin (**319**) and 26 mg (40 %) of 6–*O*–*α*–*D*–mannopyranosyl mangostin (**320**).

6–*O*–*β*–*D*–glucopyranosyl mangostin (273): Yellow amorphous solid, mp 184–186 °C; $[\alpha]_D^{24}$+70.1 (*c* 1.0, MeOH); Clog*P*: 3.04±1.17; IR (KBr) ν_{max} cm^{-1} : IR (KBr) ν_{max} cm^{-1} : 3368, 2917, 1643, 1604, 1462, 1273, 1078, 1053, 820; ^{1}H– and ^{13}C NMR *see* Table 28. HRESIMS *m/z* 595.2083 (calcd for $C_{30}H_{36}O_{11}Na$, 595.2149).

6–*O*–*β*–*D*–galactopyranosyl mangostin (319): Yellow amorphous solid, mp 188–190 °C; $[\alpha]_D^{25}$+25.1 (*c* 1.0, MeOH); Clog*P*: 3.04±1.17; IR (KBr) ν_{max} cm^{-1} : IR (KBr) ν_{max} cm^{-1} : 3368, 2926, 1647, 1604, 1465, 1276, 1083, 1040, 840; ^{1}H– and ^{13}C NMR *see* Table 28. HRFABMS *m/z* 595.2155 (calcd for $C_{30}H_{36}O_{11}Na$, 595.2149).

6–*O*–*α*–*D*–mannopyranosyl mangostin (320): Yellow–orange amorphous solid, mp 181–183 °C; $[\alpha]_D^{24}$+30.7 (*c* 1.0, MeOH); Clog*P*: 3.04±1.17; IR (KBr) ν_{max} cm^{-1} : IR (KBr) ν_{max} cm^{-1} : 3362, 2928, 1648, 1585, 1459, 1275, 1083, 1026, 823 ; ^{1}H– and ^{13}C NMR *see* Table 28. HRFABMS *m/z* 595.2158 (calcd for $C_{30}H_{36}O_{11}Na$, 595.2149).

Glycosylation to 3–*O*–glycosyl–6–*O*–benzoyl mangostins

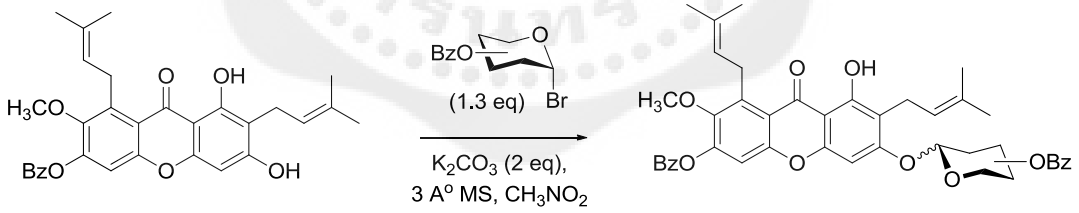

6–*O*–benzoyl mangostin (**234′**) was used as a glycosyl acceptor. Compound **234′** (100 mg, 0.1945 mmol) was dissolved in acetone and stirred with 3 Å MS under Ar atmosphere for an hour. K_2CO_3 (54 mg, 0.3891 mmol) was then added into solution and left stirring for half hour then. Each glycosyl donor (167 mg, 0.2528 mmol) was added in to reaction mixture at 60 °C then stirred until reaction complete. The solution was filtered then evaporated and extracted with CH_2Cl_2/H_2O. The residue was concentrated and then subjected to column chromatography using EtOAc–hexane to yield 146 mg (69 %),

146 mg (69 %) and 144 mg (68 %) of glucosyl– (**311**), galactosyl– (**322**) and mannosyl mangostins (**323**), respectively.

3–*O*–(2,3,4,6–tetra–*O*–benzoyl–*β*–*D*–glucopyranosyl)–6–*O*–benzoyl mangostin (321): yellow needles, mp 104–106 °C; $[\alpha]_D^{26}$ +108.7(*c* 1.0, $CDCl_3$); Clog*P*: 14.92 ± 1.22; IR ($CHCl_3$) ν_{max} cm^{-1} : 2928, 1733, 1632, 1599, 1451, 1264, 1091, 1067, 757, 707 ; ^{1}H NMR (300): 13.59*s* (1–OH), aromatic protons at 8.24*d* (7.1 Hz, 2H), 7.96*d* (7.0 Hz, 6H), 7.89*d* (7.1 Hz, 2H), 7.69*t* (7.4 Hz, 1H), 7.44–7.59*m* (6H) and 7.29–7.41*m* (8H), 7.03*s* (1H, H–5), 6.46*s* (1H, H–4), 6.03*t* (9.1 Hz, 1H, H–3′), 5.93*dd* (9.1, 7.1 Hz, 1H, H–2′), 5.76*t* (9.1 Hz, 1H, H–4′), 5.61*d* (7.1 Hz, 1H, H–1′), 5.18*t* (6.4 Hz, 1H, H–12), 5.14*t* (6.1 Hz, 1H, H–17), 4.73*br d* (9.9 Hz, 1H, H–6_a′), 4.54*m* (1H, H–6_b′), 4.50*m* (1H, H–5′), 4.04*d* (6.1 Hz, 2H, H–16), 3.62*s* (3H, 7–OCH_3), 3.38*d* (6.4 Hz, 2H, H–11), 1.77*s* (3H, H–19), 1.64*s* (3H, H–14), 1.59*s* (6H, H–20, H–15); ^{13}C NMR (75 MHz): 182.6 (1C, C–9), 166.0 (1C), 165.6 (1C), 165.2 (1C), 165.1 (1C), 164.2 (1C, C–3), 160.9 (1C, C–1), 155.1 (1C, C–6), 154.8 (1C, C–2′′), 154.6 (1C, C–10a), 153.5 (1C, C–4a), 144.8 (1C, C–7), 138.4 (1C, C–8), 133.9 (1C), 133.4 (3C), 132.3 (1C, C–18), 132.1 (1C, C–13), 130.6 (2C), 129.7 (3C), 129.7 (3C), 129.5 (2C), 129.4 (2C), 129.1 (1C), 128.9 (1C), 128.8 (1C), 128.7 (1C), 128.6 (2C), 128.5 (5C), 128.4 (4C), 122.6 (1C, C–17), 121.3 (1C, C–12), 116.3 (1C, C–8a), 113.9 (1C, C–2), 110.7 (1C, C–5′′), 102.8 (1C, C–9a), 100.4 (1C, C–5), 98.4 (1C, C–1′), 92.6 (1C, C–4), 72.4 (1C, C–5′), 71.3 (1C, C–3′), 70.7 (1C, C–2′), 69.1 (1C, C–4′), 63.0 (1C, C–6′), 61.1 (1C, 7–OCH_3), 26.2 (1C, C–20), 25.8 (1C, C–16), 25.6 (1C, C–15), 22.3 (1C, C–11), 18.1 (1C, C–19), 17.7 (1C, C–14); $C_{65}H_{56}O_{16}$ 1092; ESIMS *m/z* (–ve) 513(100), 409(25), 989(100), 990(72); (+ve) 1026(24), 1027(16).

3–*O*–(2,3,4,6–tetra–*O*–benzoyl–*β*–*D*–galactopyranosyl)–6–*O*–benzoyl mangostin (322): yellow needles, mp 98–100 °C; $[\alpha]_D^{23}$ +99.2 (*c* 1.0, $CDCl_3$); Clog*P*: 14.92 ± 1.22; IR ($CHCl_3$) ν_{max} cm^{-1} : 2912, 1731, 1635, 1602, 1462, 1259, 1094, 1072, 754, 707; ^{1}H NMR (300): 13.56*s* (1–OH), aromatic protons at 8.23*br d* (7.1 Hz, 1H), 8.09*m* (6H), 8.00*d* (7.6 Hz, 4H), 7.91*m* (4H), 7.79*m* (4H) and 7.22–7.70*m* (5H), 7.06*s* (1H, H–5), 6.41*s* (1H, H–4), 6.19*dd* (10.2, 7.8 Hz, 1H, H–2′), 6.07*d* (2.9 Hz, 1H, H–4′), 5.74*td* (10.2, 2.9 Hz, 1H, H–3′), 5.54*d* (7.8 Hz, 1H, H–1′), 5.16*t* (6.9 Hz, 1H, H–12), 5.13*t* (7.8 Hz, 1H, H–17), 4.65*m* (1H, H–6_a′), 4.56*m* (1H, H–5′), 4.43*dd* (10.7, 6.2 Hz, 1H, H–6_b′), 4.04*br d* (7.7 Hz, 2H, H–16), 3.58*s* (3H, 7–OCH_3), 3.36*d* (6.9 Hz, 2H, H–11), 1.75*s* (3H, H–19), 1.62*s* (3H,

H–14), 1.57*s* (3H, H–20), 1.54*s* (3H, H–15); ^{13}C NMR (75 MHz): 182.6 (1C, C–9), 166.1 (1C), 165.9 (1C), 165.2 (1C), 165.1 (1C), 164.6 (1C), 164.2 (1C, C–3), 160.9 (1C, C–1), 155.2 (1C, C–6), 154.8 (1C, C–2′′), 154.7 (1C, C–10a), 153.5 (1C, C–4a), 144.8 (1C, C–7), 138.4 (1C, C–8), 134.1(1C), 133.9 (1C), 133.3 (1C), 132.9 (1C), 132.3 (1C, C–18), 132.1 (1C, C–13), 130.7 (1C), 130.4 (1C), 130.2 (2C), 130.0 (1C), 129.9 (1C), 129.8 (1C), 129.5 (2C), 129.3 (2C), 129.2 (3C), 128.9 (2C), 128.7 (1C), 128.6 (2C), 128.5 (2C), 128.2 (2C), 127.4 (1C), 122.6 (1C, C–17), 121.4 (1C, C–12), 116.3 (1C, C–8a), 113.9 (1C, C–2), 107.0 (1C, C–5′′), 102.9 (1C, C–9a), 100.4 (1C, C–5), 99.1 (1C, C–1′), 92.9 (1C, C–4), 71.5 (1C, C–5′), 71.3 (1C, C–3′), 67.9 (1C, C–2′), 67.8 (1C, C–4′), 62.6 (1C, C–6′), 61.0 (1C, 7–OCH_3), 26.2 (1C, C–20), 25.7 (2C, C–16), 22.3 (1C, C–11), 18.0 (1C, C–19), 17.8 (1C, C–14); $C_{65}H_{56}O_{16}$ 1092; ESIMS *m/z* (–ve) 513(100), 514(32); (+ve) 1026(100), 1027(41), 1093(29), 989(14).

3–*O*–(2,3,4,6–tetra–*O*–benzoyl–*α*–*D*–mannopyranosyl)–6–*O*–benzoyl mangostin (323): yellow needles, mp 103–105 °C; $[\alpha]_D^{25}$ –7.6 (*c* 1.0, $CDCl_3$); Clog*P*: 12.46 ± 1.20; IR ($CHCl_3$) ν_{max} cm^{-1}: 2917, 1731, 1635, 1599, 1462, 1264, 1091, 1067, 757, 705; ^{1}H NMR (300): 13.57*s* (1–OH), aromatic protons at 8.24*d* (7.6 Hz, 2H), 8.11*d* (7.1 Hz, 2H), 8.00*d* (7.5 Hz, 2H), 7.94*d* (7.7 Hz, 2H), 7.81*d* (7.2 Hz, 2H) and 7.21–7.71*m* (15H), 7.07*s* (1H, H–5), 6.41*s* (1H, H–4), 6.20*dd* (10.2, 7.7 Hz, 1H, H–2′), 6.07*d* (3.3 Hz, 1H, H–4′), 5.75*td* (10.2, 3.3 Hz, 1H, H–3′), 5.55*d* (7.7 Hz, 1H, H–1′), 5.17*t* (6.7 Hz, 1H, H–12), 5.14*t* (7.4 Hz, 1H, H–17), 4.65*m* (1H, H–6_a′), 4.61*m* (1H, H–5′), 4.55*m* (1H, H–6_b′), 4.04*br d* (7.4 Hz, 2H, H–16), 3.59*s* (3H, 7–OCH_3), 3.36*d* (6.7 Hz, 2H, H–11), 1.75*s* (3H, H–19), 1.63*s* (3H, H–14), 1.59*s* (3H, H–20), 1.58*s* (3H, H–15); ^{13}C NMR (75 MHz): 182.6 (1C, C–9), 166.1 (1C), 165.4 (3C), 165.1 (1C), 164.2 (1C, C–3), 160.9 (1C, C–1), 155.2 (1C, C–6), 154.8 (1C, C–2′′), 154.7 (1C, C–10a), 153.5 (1C, C–4a), 144.8 (1C, C–7), 138.4 (1C, C–8), 133.9 (1C), 133.8 (1C), 133.6 (1C), 133.4 (1C), 132.3 (1C, C–18), 132.1 (1C, C–13), 130.2 (1C), 130.0 (1C), 129.9 (1C), 129.7 (3C), 129.6 (2C), 129.3 (1C), 129.1 (1C), 128.9 (2C), 128.8 (1C), 128.7 (4C), 128.6 (1C), 128.5 (2C), 128.4 (2C), 128.3 (2C), 122.6 (1C, C–17), 121.4 (1C, C–12), 116.3 (1C, C–8a), 113.9 (1C, C–2), 107.0 (1C, C–5′′), 102.9 (1C, C–9a), 100.5 (1C, C–5), 99.1 (1C, C–1′), 93.0 (1C, C–4), 72.4 (1C, C–5′), 72.3 (1C, C–3′), 69.1 (1C, C–2′), 67.9 (1C, C–4′), 62.1 (1C, C–6′), 61.1 (1C, 7–OCH_3), 26.2 (1C, C–20), 25.9 (1C, C–16), 25.6 (1C, C–15), 22.3 (1C, C–11), 18.1 (1C, C–19), 17.7 (1C, C–14); $C_{65}H_{56}O_{16}$ 1092; ESIMS *m/z* (–ve) 513(100), 514(36), 1026(9); (+ve) 1026(24), 1027(16).

Debenzoylation of 3–*O*–glycosyl–6–*O*–benzoyl mangostins

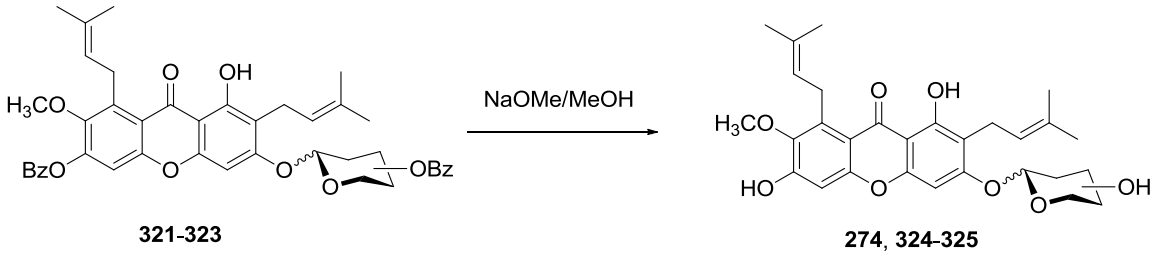

321-323 **274**, **324-325**

The reactions were provided using each 100 mg of compounds **321**–**323**, respectively. To a suspension of starting material in 5 mL MeOH, NaOMe/MeOH was added until pH 10 and stirred at rt for 30 min. The reaction was neutralized by adding of Dowex resin and stirred until reaction complete in 30 minutes. The mixture was filtered the concentrated and purified by column chromatography using gradient system of MeOH–CH_2Cl_2 to obtain 32 mg (56 %) of 6–*O*–*β*–*D*–glucopyranosyl mangostin (**274**) and each 31 mg (55 %) of 6–*O*–*β*–*D*–galactopyranosyl mangostin (**324**) and 6–*O*–*α*–*D*–mannopyranosyl mangostin (**325**).

3–*O*–*β*–*D*–glucopyranosyl mangostin (274): Yellow amorphous solid, mp 188–190 °C, $[\alpha]_D^{24}$+68.3 (*c* 1.0, MeOH); Clog*P*: 3.28 ± 1.14; IR (KBr) ν_{max} cm^{-1}: 3395, 2923, 1646, 1604, 1465, 1275, 1100, 1080, 825; ^{1}H– and ^{13}C NMR *see* Table 29. HRFABMS *m/z* 595.2081 (calcd for $C_{29}H_{34}O_{10}Na$, 595.2149).

3–*O*–*β*–*D*–galactopyranosyl mangostin (324): Yellow amorphous solid, mp 190–192 °C, $[\alpha]_D^{24}$–10.6 (*c* 1.0, MeOH); Clog*P*: 3.28 ± 1.14; IR (KBr) ν_{max} cm^{-1}: 3369, 2928, 1646, 1610, 1465, 1276, 1084, 1068, 825; ^{1}H– and ^{13}C NMR *see* Table 29. HRFABMS *m/z* 595.2095 (calcd for $C_{29}H_{34}O_{10}Na$, 595.2149).

3–*O*–*α*–*D*–mannopyranosyl mangostin (325): Yellow–orange amorphous solid, mp 184–186 °C, $[\alpha]_D^{25}$–10.8 (*c* 1.0, MeOH); Clog*P*: 4.67 ± 1.20; IR (KBr) ν_{max} cm^{-1}: 3390, 2923, 1648, 1607, 1588, 1462, 1273, 1086, 1056, 825; ^{1}H– and ^{13}C NMR *see* Table 29. HRFABMS *m/z* 595.2099 (calcd for $C_{29}H_{34}O_{10}Na$, 595.2149).

CHAPTER 4

RESULTS AND DISCUSSION

Cyclopeptide alkaloids from *Ziziphus* plants

The MeOH extract of *Z. cambodiana* root bark

In 2006, a new triterpene ester 3–*O*–vanillylceanothic acid (**31**), together with five known lupane constituents including lupeol (**32**), betulinaldehyde (**33**), betulinic acid (**34**), 2–*O*–*trans*–*p*–coumaroyl alphitolic acid (**35**) and alphitolic acid (**36**), and three ceanothane triterpenes, zizyberanalic acid (**37**), zizyberenalic acid (**38**) and ceanothic acid (**39**, Figure 13), were isolated from the EtOAc extract (80.0 g) of Thai *Z. cambodiana* root bark, which showed a purple coloration with anisaldehyde–H_2SO_4 reagent. Those compounds were evaluated for their antiplasmodial and antituberculosis activities (Table 2) (Suksamrarn et al., 2006). In 2011, three cyclopeptide alkaloids were isolated from fractionated part of MeOH extracts of *Z. cambodiana* root bark, which showed intense blue coloration with anisaldehyde–H_2SO_4 reagent indicating the presence of a cyclopeptide alkaloid (Suksamrarn et al., 2005).

This dissertiation describes a continuous study on the other portion of the MeOH extract obtained from *Z. cambodiana* root bark. The air–dried root bark of *Z. cambodiana* was extracted with EtOAc followed by MeOH to give the EtOAc– and MeOH extracts, respectively. The chemical screening of the extracts was monitored by TLC. The MeOH extract showed intense blue coloration with anisaldehyde–H_2SO_4 reagent, whereas a very weak blue color was detected during the EtOAc extract test. Therefore, the MeOH extract was selected for further chemical investigations. A large amount of tannin found in the methanolic solution was removed by extraction with 1% NaCl/EtOAc as described by Wall et al. (1996) before chromatographic separations. The EtOAc soluble fraction that showed the increase of blue coloration with anisaldehyde–H_2SO_4 reagent confirmed the presence of cyclopeptide alkaloids (Suksamrarn et al., 2005; and, Panseeta et al., 2011). The alkaloidal EtOAc soluble fraction was further chromatographed and resulted in the isolation of seven new (**A**–**G**), together with two known (**H** and **I**), 14–membered cyclopeptide alkaloids (Table 10).

Table 10 Isolated cyclopeptide alkaloids from *Z. cambodiana*

Compound	Name	Weight
A sss3096 ZC2(RB)–E–54/F4(12–13)	Cambodine A (**278**)	69 mg
B sss3155 ZC2(RB)–E–54/F4(12–13)	Cambodine B (**279**)	7 mg
C sss4402 ZC2(RB)–E–74/F3(41–45)	Cambodine C (**280**)	16 mg
D sss4732 ZC2(RB)–M2(E)–49/F12(144–169)	Cambodine D (**281**)	19 mg
E sss4759 ZC2(RB)–M2(E)–49/F14(201–259)s1	Cambodine E (**282**)	35 mg
F sss4734 ZC2(RB)–M2(E)–49/F14(201–259)s2	Cambodine F (**283**)	8 mg
G sss4767 ZC2(RB)–M2(E)–53/F5 (127–145)s1	Cambodine G (**284**)	19 mg
H sss4449 ZC2(RB)–M–40/F9 (88–90)	Frangufoline (**6**)	18 mg
I sss4635 ZC2(RB)–M–42/F8(86–118)	Lotusanine B (**24**)	18 mg

The NMR and mass spectroscopic data of all isolated compounds allowed for determining the structure of these macrocyclic cyclopeptides. Their UV spectra showed the end absorption band, which were consistent with the 14–membered type cyclopeptide, except for compounds **G** and **I**, which were composed of a coumaroyl group that showed UV absorption bands at around 220, 280 and 300 nm (Gonzalez et al., 1974). Their IR spectra exhibited diagnostic peaks for the amino (3261–3391 cm^{-1}), amido (1636–1685 cm^{-1}) and aryl ether (1221–1291 cm^{-1}) functions, suggesting that all isolates possessed a 14–membered cyclopeptide. The CD spectra showed intense negative and weak positive Cotton effects at around 220 and 280 nm, respectively, indicating the 5*S*, 8*S*, 9*S*–configurations in macrocyclic ring system (Gournelis, Laskaris and Verpoorte, 1998). Surprisingly, five of the new alkaloids (**A**–**B** and **C**–**F**) contained imidazolidinone ring. The new compounds can be further divided into three groups depending on their amino acid units including 4(14)–integerrine–type (**B**, **D** and **E**), 5(14)–scutianine A–type (**A**, **C** and **F**) and a neutral compound related to cyclopeptide alkaloid (**G**).

Among the isolated cyclopeptides, compound **E** was crystalized out and its x–ray crystallographic structure in particular its stereochemistry was determined.

Compounds form the 4(14)–integerrine–type cyclopeptide alkaloid series (B, D and E)

Three compounds were isolated and identified as cyclopeptides belong to this group (Table 1) consisting of styrylamine, *β*–hydroxyphenylalanine and showing different in ring–bound and terminal amino acid units.

Table 11 The NMR spectral data in $CDCl_3$ for compounds belong to 4(14)–integerrine–type cyclopeptide alkaloid (**B**, **D** and **E**)

Position	δ_H			δ_C		
	B (sss3155)	**D** (sss4732)	**E** (sss4759)	**B**	**D**	**E**
1	6.59 *br s*	6.46 *d* (7.6)	6.47 *d* (7.8)	121.2	117.8	116.9
2	6.59 *br s*	6.66 *dd* (9.5, 7.6)	6.37 *br t* (7.8)	125.2	125.4	125.6
3–NH	6.59 *br s*	6.50 *d* (9.5)	6.51 *d* (9.9)	–		–
4–CO	–	–	–	167.8	166.8	166.5
5	4.51 *dd* (8.5, 7.6)	4.01 *dd* (8.5, 4.4)	4.44 *ddd* (11.2, 8.1, 3.4)	57.5	59.3	55.4
6–NH	6.37 *d* (8.5)	5.81 *d* (8.5)	6.40 *d* (8.1)	–		–
7–CO	–	–	–	167.7	168.2	168.1
8	4.87 *d* (7.3)	5.09 *d* (7.6)	4.95 *d* (7.2)	57.8	57.9	57.6
9	5.90 *d* (7.3)	5.99 *d* (7.6)	5.91 *d* (7.2)	81.6	80.7	81.7
11	–	–	–	155.3	155.0	155.4
12	7.26 *m*	7.32 *m*	7.34 *m*	123.2	123.3	123.2
13	7.09 *m*	7.13 *m*	7.14 *m*	130.2	130.2	130.4
14	–	–	–	131.9	132.3	132.2
15	7.11 *m*	7.10 *m*	7.14 *m*	131.0	131.6	131.7
16	7.29 *m*	7.34 *m*	7.34 *m*	121.9	122.8	122.5
17	4.94 *d* (7.6)	2.16 *m*	3.40 *dd* (14.8, 3.4)	73.1	34.4	36.7
			2.61 *dd* (14.8, 11.2)			
18	7.24 *m*	1.17 *m*	7.09 *m*	126.9	23.9	128.8
19	7.03 *m*	0.81 *t* (6.3)	7.19 *m*	128.7	11.7	128.5
20	7.24 *m*	0.70 *d* (6.8)	7.07 *m*	128.7	16.5	127.1
21	–	–	–	136.0	136.2	136.0
22,22′	7.46 *m*	7.52 *dd* (7.7, 1.9)	7.46 *m*	128.2	127.8	128.2
23,23′	7.19 *m*	7.39 *m*	7.39 *m*	128.6	128.8	128.8
24	7.39 *m*	7.41 *m*	7.11 *m*	129.1	129.2	129.0
26–CO	–	–	–	172.1	172.8	172.3
27	2.69 *m*	2.48 *dd* (2.6,	2.39 *m*	66.5	70.4	66.1
28	2.67 *m*	1.29 *m*	2.66 *dd* (13.8, 8.9)	37.5	35.8	37.6
28a	–	1.08 *m*	–	138.1	24.7	138.2
29,29′	7.39 *m*	0.77 *t* (7.4)	7.00 *br d* (6.1)	129.1	11.9	129.1
30,30′	7.24 *m*	0.55 *d* (6.8)	7.26 *m*	128.2	14.7	128.2
31	7.47 *m*	–	7.22 *m*	126.3		126.2
33	3.66 *d* (4.3)	3.83 *br d* (3.9) [a]	3.56 *d* (4.7)	67.1	67.6	67.0
	2.70 *d* (4.3)	3.22 *br d* (4.9) [a]	2.43 *d* (4.7)			
NCH_3	1.64 *s*	2.11 *s*	1.48 *s*	39.8	41.1	39.5

[a] each H coupled with H–27 in COSY

Compound **E** (sss4759) was obtained as colorless needles, mp 135–137 ^{o}C. Based on the analysis of its HRTOFMS (*m/z* 623.2606, $[M + H]^+$, calcd 623.2628 for $C_{37}H_{36}N_4O_4$ + Na) and the ^{13}C NMR data, the molecular formula of **E** was established as $C_{37}H_{36}N_4O_4$.

The ^{13}C NMR and DEPT spectra showed no signals in the aliphatic amino acid region and indicated 37 signals attributable to one *N*–methyl, three methylenes, twenty five (including one oxygenated and two olefinic) methines, and five quaternary carbons, three of which corresponded to the carbonyl groups. The analysis of the ^{1}H, ^{13}C, DEPT and 2D NMR (COSY and HMQC) spectra of **E** suggested 4 structural units for an *p*–oxystyrylamine, *β*–hydroxyphenylalanine, phenylalanine and a derived *N*–methyl phenylalanine in a 1–methylimidazolidin–4–one ring.

Its EIMS data showed a base peak at *m/z* 509 (**326**) as well as an ion fragment at *m/z* 227 (**327**) (Scheme 19) indicating the presence of a 1–methylimidazolidin–4–one group as the terminal unit (Tschesche et al., 1977). This was supported by the presence of two geminal protons at δ_H 3.56*d* (*J* = 4.7 Hz, H_β–33) and δ_H 2.43*d* (*J* = 4.7 Hz, H_α–33) (δ_C 67.0), an NCH_3 at δ_H 1.48*s* (δ_C 39.5), a methine (H–27) at δ_H 2.39*m* (δ_C 66.1) in addition to a carbonyl carbon at δ_C 172.3 in its NMR data.

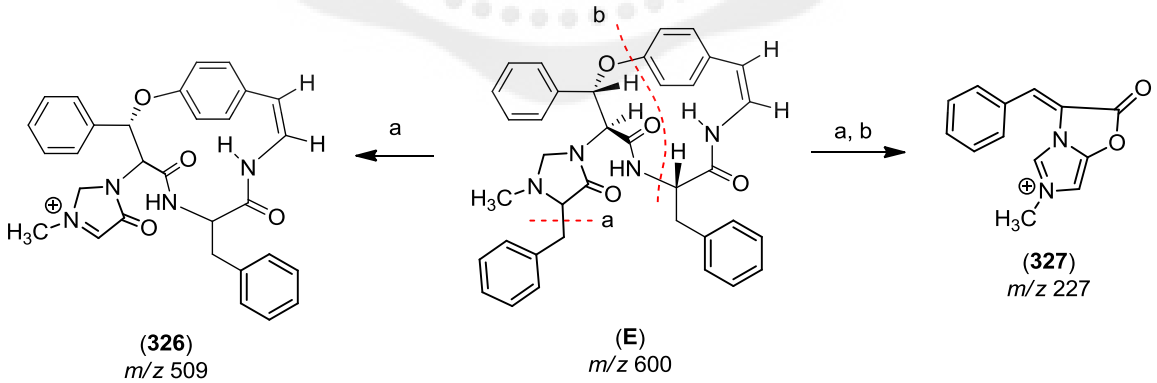

Scheme 19 EI fragments of compound **E**

The signal of a styrylamine *Z*–configure double bond in the AMX system showed at δ_H 6.47*d* (*J* = 7.8 Hz), 6.37*br t* (*J* = 7.8 Hz) and 6.51*d* (*J* = 9.9 Hz). The signal of olefinic proton H–2 at δ_H 6.37*br t* (*J* = 7.8 Hz) showed correlation to the signal at δ_H 4.44*ddd* (*J* = 11.2, 8.1, 3.4 Hz, H–5) in NOESY spectrum indicating the placement of the phenylalanine unit next to the styrylamine moiety (Table 12). The correlations of H–5 and of H–8 at δ_H 4.95*d* (*J* = 7.2 Hz) to carbonyl C–7 (δ_C 168.1) in the HMBC experiments displayed the connection of phenylalanine to β–hydroxyphenylalanine unit in the macrocyclic ring. The correlation of methine proton H–27 (δ_H 2.39, *m*) to carbonyl carbon signal at δ_C 172.3 (C–26) and δ_C 37.6 (C–28) in HMBC experiments indicated that imidazolidinone unit is connected to the β–hydroxyphenylalanine group.

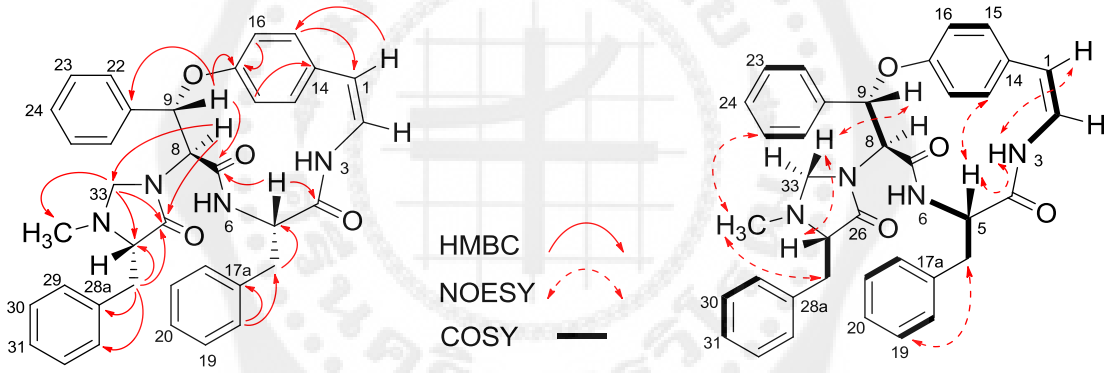

Figure 46 Selected HMBC, COSY and NOESY correlations for compound **E**

The 5*S*,8*S*,9*S*–configuration in the macrocyclic ring were assigned from an intense negative and a weak positive Cotton effects (CE) in the circular dichroism (CD) spectrum at 243 and 285 nm, respectively (Gournelis, Laskaris and Verpoorte, 1998). The β–hydroxyphenylalanine unit has the relative *erythro*–configuration based on the vicinal coupling constant (*J* = 7.2 Hz) between H–8 and H–9 (5.91*d*, *J* = 7.2 Hz) and the relatively upfield shifted ^{13}C NMR signal of C–9 (δ_C 81.1) compared with δ_C 80.7 of waltherine B (**23**) for the *erythro*–isomer (Morel et al., 1999), and of δ_C 86.3 of condaline A (**25**) for the *threo*–isomer (Morel et al., 2005). ^{1}H NMR chemical shifts of H–8 and H–9 were slightly different when compared to those of franganine (**7**) recorded in methanol–d_4 (δ_H 4.45*d*, *J* = 8.4 Hz

and δ_H 4.88*dd*, *J* = 2.0, 8.4 Hz) which was confirmed the absolute configuration by the analysis of NMR data and X–ray diffraction analysis of its methiodide salt (Caro et al., 2012). In addition, the strong NOESY interactions shown between pair of protons H_β–9/H_β–33, and H–27 with H_α–33, suggested the 27*S*–configuration in **E** (Figure 47). Similarly, ROESY interactions between those pair of protons in apetaline B (**105**) were also observed where its absolute stereochemistry was assigned as all *S* by chemical hydrolysis (Han J. et al., 2011).

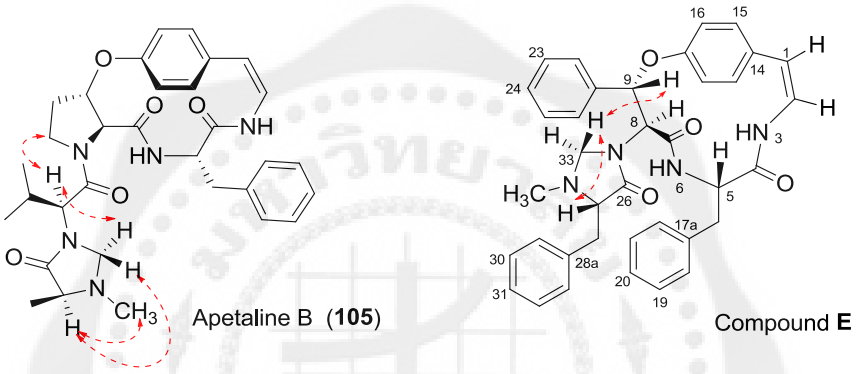

Figure 47 Comparison of ROESY correlations in apetaline B (**105**) and NOESY correlations in compound **E**

The analysis of the ORTEP diagram of the single–crystal structure of **E** consistent with *L–erythro* configuration between H–8 and H–9 and also confirmed the *S*–configuration both at H–5 and H–27, Figure 47. Based on this evidence, the stereochemistry of **E** was assigned all *S*–configuration and named as cambodine E. The anomalous hindered double bond of styrylamine unit was revealed by both experiments; due to this effect the cyclopeptide having the 14–membered ring showed the end absorption band (Gournelis, Laskaris and Verpoorte, 1998). The energy–minimized structure provided by MM2 calculations also deduced the stabilized conformation of integerrine–type cyclopeptide ring systems (Lin et al., 2003) which agreed with its crystal structure.

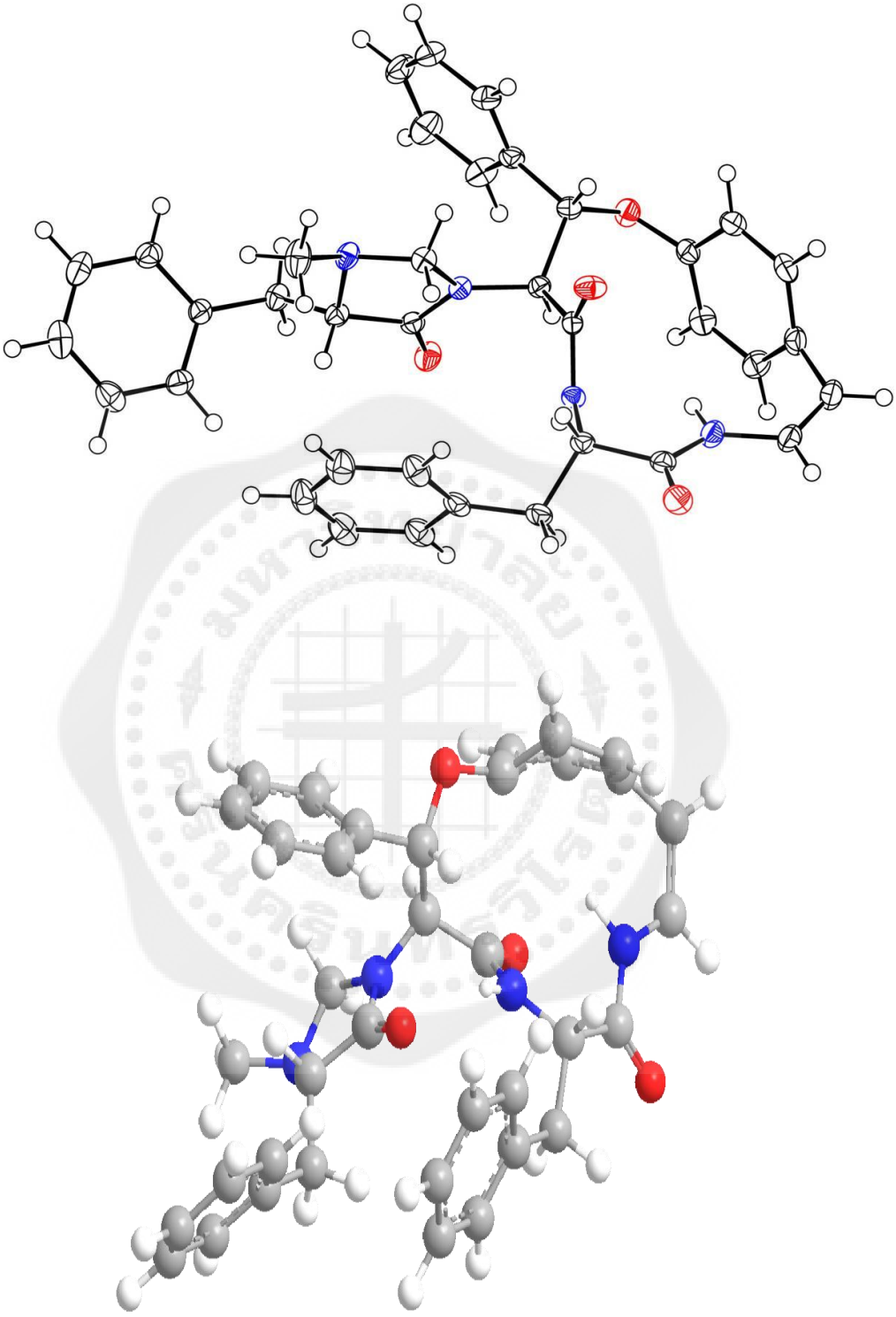

Figure 48 ORTEP plots of the X–ray crystal structure and energy–minimized structure by MM2 calculation of compound **E**

Table 12 ^{1}H–, ^{13}C– and 2D NMR data of compound **E** in $CDCl_3$

Position	δ_H	δ_C	HMBC correlations	NOESY correlations
1	6.47 *d* (7.8)	116.9	C–15	
2	6.37 *br t* (7.8)	125.6	–	–
3–NH	6.51 *d* (9.9)	–	–	H–1, H–2, H–5
4–CO	–	166.5	–	–
5	4.44 *ddd* (11.2, 8.1, 3.4)	55.4	C–4, C–7	H–3, H–13, H–17
6–NH	6.40 *d* (8.1)	–	–	–
7–CO	–	168.1	–	–
8	4.95 *d* (7.2)	57.6	C–7, C–9, C–26, C–33	H–9, H–12, H–22
9	5.91 *d* (7.2)	81.7	C–7, C–8, C–11, C–21	H–8, H–22, H$_\beta$ –33
11	–	155.4	–	–
12	7.34 *m*	123.2	C–11, C–14	H–8, H–9
13	7.14 *m*	130.4	C–11, C–14	–
14	–	132.2	–	–
15	7.14 *m*	131.7	C–1, C–11	–
16	7.34 *m*	122.5	C–11, C–15	–
17	3.40 *dd* (14.8, 3.4)	36.7	C–4, C–5, C–18, C–19	H–5, H–19
	2.61 *dd* (14.8, 11.2)			
17a	–	136.9	–	–
18,18′	7.09 *m*	128.8	C–17, C–17a, C–19	–
19,19′	7.19 *m*	128.5	C–17a, C–20	H–17
20	7.07 *m*	127.1	–	–
21	–	136.0	–	–
22,22′	7.46 *m*	128.2	C–21, C–24	H–9
23,23′	7.39 *m*	128.8	C–21, C–22	–
24	7.11 *m*	129.0	–	–
26–CO	–	172.3	–	–
27	2.39 *m*	66.1	*N*CH$_3$	H–30
28	2.66 *dd* (13.8, 8.9)	37.6	C–26, C–27, C–29, C–30	H–31, *N*CH$_3$
28a	–	138.2	–	–
29,29′	7.00 *br d* (6.1)	129.1	C–31, C–32	H–27, *N*CH$_3$
30,30′	7.26 *m*	128.2	C–29	H–28
31	7.22 *m*	126.2	C–29	–
33	3.56 *d* (4.7), β	67.0	C–26, C–27	H–9, H–22
	2.43 *d* (4.7), α			
*N*CH$_3$	1.48 *s*	39.5	–	H–23, H–24, H–28, H–30

Compound **B**, a colorless solid, mp 140–141 ^{o}C, was established as $C_{37}H_{36}N_4O_5$ from HRFABMS ion peak at *m/z* 617.2751 (calcd 617.2785 for $C_{37}H_{36}N_4O_5$ + H).

The ^{13}C NMR and DEPT spectra showed 37 signals consistent with one *N*–methyl, two methylenes, twenty six (including one oxygenated and two olefinic) methines and five quaternary carbons, three of which corresponded to the carbonyl groups. The analysis of the ^{1}H and the ^{13}C NMR spectroscopic data of **B** compared with those of **E** demonstrated the difference only in the ring–bound β–hydroxyphenylalanine in **B** and phenylalanine in **E**. This was supported by the presence of two geminal protons at δ_H 3.66 *d* (*J* = 4.3 Hz, H$_\beta$–33) and δ_H 2.70*d* (*J* = 4.3 Hz, H$_\alpha$–33) (δ_C 67.1), an *N*CH$_3$ at δ_H 1.63*s* (δ_C 39.8), a methine δ_H 2.69*m* (δ_C 66.5) in addition to a carbonyl carbon at δ_C 172.1 (C–26) in its NMR data.

The weak correlation between NH–3 (δ_H 6.59*br s*) and H–5 (δ_H 4.51*dd*, *J* = 8.5 and 7.6 Hz) and strong correlation of NH–3 to NH–6 (δ_H 6.37*d*, *J* = 8.5 Hz) in NOESY experiments displayed that the β–hydroxyphenylalanine unit is attached to the styrylamine moiety. The HMBC correlations of H–5, H–6 and H–9 (δ_H 5.90*d*, *J* = 7.3 Hz) to carbonyl at δ_C 167.7 (C–7) indicated the connection between two β–hydroxyphenylalanine units in the macrocyclic ring. The correlations of H–8 to C–26 (δ_c 172.1) in HMBC spectrum and NOE effects of H–8 to H–33 (δ_H 3.56*d*, *J* = 4.7 Hz, β and δ_H 2.43*d*, *J* = 4.7 Hz, α), display the connection between terminal imidazolidinone unit and macrocyclic ring at C–8. The HMBC correlations of both protons H–33 to *N*CH$_3$ (δ_c 39.8) and of *N*CH$_3$ (δ_H 1.64 *s*) to C–33 (δ_C 67.1) were also observed.

The analysis of its ^{1}H and ^{13}C NMR as well as coupling constant ($^{3}J_{8,9}$ = 7.3 Hz) compared to **E** confirmed 8*S*,9*S*–*erythro*–configuration. Strong NOE enhancements between two pairs of protons H$_\beta$–9 with H$_\beta$–33 and between H–27 (δ_H 2.93*m*) with H$_\alpha$–33, suggested the 27*S*–configuration. Above results were consistent with its Cotton effects in CD spectrum that showed strong negative and weak positive signals at 240 and 279 nm, respectively (Gournelis, Laskaris and Verpoorte, 1998).

Table 13 ^{1}H–, ^{13}C– and 2D NMR data of compound **B** in $CDCl_3$

Position	δ_H	δ_C	HMBC correlations	NOESY correlations
1	6.59 *br s*	121.2	C–2, C–14	–
2	6.59 *br s*	125.2	C–14	–
3–NH	6.59 *br s*	–	–	H–5, H–18
4–CO	–	167.8	–	–
5	4.51 *dd* (8.5, 7.6)	57.5	C–4, C–7	NH–3, H–6, H–17, H–18
6–NH	6.37 *d* (8.5)	–	–	H–5, H–8, H–17
7–CO	–	167.7	–	–
8	4.87 *d* (7.3)	57.8	C–7, C–9, C–26, C–33	H–6, H–9, H–22
9	5.90 *d* (7.3)	81.6	C–7, C–8, C–11	H–8, H–22, H–23, Hβ –33
11	–	155.3	–	–
12	7.26 *m*	123.2	–	–
13	7.09 *m*	130.2	–	–
14	–	131.9	–	–
15	7.11 *m*	131.0	–	H–16
16	7.29 *m*	121.9	C–1, C–12, C–13, C–14, C–15	H–16
17	4.94 *d* (7.6)	73.1	C–5	H–5, H–18
17a	–	139.0	–	–
18,18′	7.24 *m*	126.9	C–17, C–17a	H–5, H–17
19,19′	7.03 *m*	128.7	C–20	–
20	7.24 *m*	128.7	C–19	–
21	–	136.0	–	–
22,22′	7.46 *m*	128.2	–	H–8, H–9, Hα –33
23,23′	7.19 *m*	128.6	–	H–9
24	7.39 *m*	129.1	–	–
26–CO	–	172.1	–	–
27	2.69 *m*	66.5	–	H–28a, Hα –33
28	2.67 *m*	37.5	C–30	H–27
28a	–	138.1	–	–
29,29′	7.39 *m*	129.1	–	H–28a, H–28b, *N*CH_3
30,30′	7.24 *m*	128.2	–	*N*CH_3
31	7.47 *m*	126.3	C–30	–
33	3.66 *d* (4.3), β	67.1	–	H–9, H–22, H–27
	2.70 *d* (4.3), α			
NCH_3	1.64 *s*	39.8	C–27, C–33	H–30, H–31

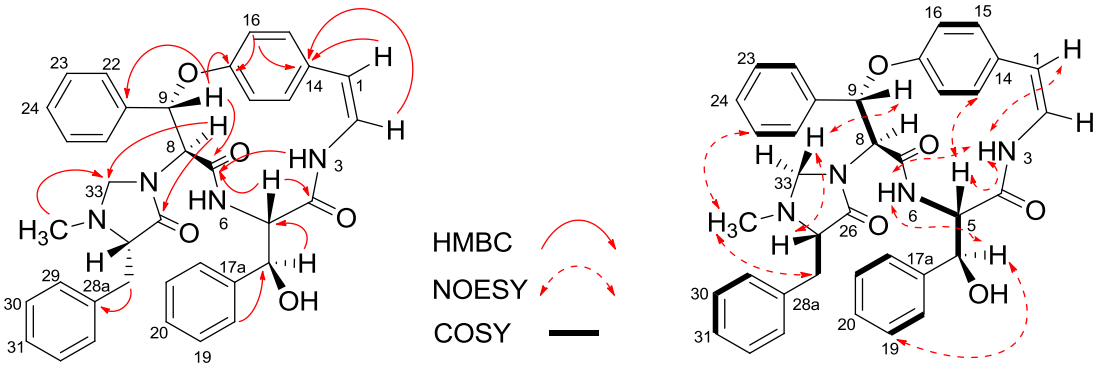

Figure 49 Selected HMBC COSY and NOESY correlations of compound **B**

The configuration of C–17 was assigned by the comparison of its NMR data with those of related compounds. Its NMR (in $CDCl_3$, 300 MHz) displayed ^{1}H upfield at δ_H 4.94*d* (*J* = 7.6 Hz) and ^{13}C downfield at δ_C 73.1, consistent with those of 8,9,17–*tris*–*epi*–scutiaene E (**61**), 17–*epi*–scutianene E (**62**) (in DMSO–d_6, 400 MHz) bearing *L*–*erythro* ($J_{5,17}$ = 4.6 Hz) 5*S*,17*S*–configuration. The NMR chemical shifts and coupling constants showed an instant difference from *L*–*threo* ($J_{5,17}$ = 1.8 Hz) 5*S*,17*R*–configuration in scutianene E (**60**) [at δ_H 5.15 $J_{5,17}$ = 1.8 Hz (δ_C 69.8)] (Maldaner et al., 2011). Therefore, **B** was assigned to have all *S*–configuration and named cambodine B.

Compound **D** (sss4732) was isolated as colorless needles, mp 205–207 °C. On the basis of its HRTOFMS *m/z* 555.2929 (calcd 555.29418 for $C_{31}H_{40}N_4O_4$ + Na) in combination with analysis of the ^{13}C NMR spectrum, the molecular formula of compound **D** was established as $C_{31}H_{40}N_4O_4$.

The ^{13}C NMR and DEPT spectra of compound **D** indicated 31 signals consistent with four methyls, one *N*–methyl, three methylenes, seventeen methines (including one oxygenated and two olefinic) and three quaternary carbons, three of which corresponded to carbonyl groups. Analysis of the ^{1}H, ^{13}C, DEPT and 2D NMR (COSY and HMQC) spectra of compound **D** showed that it is composed of 4 units including *p*–

oxystyrylamine group, *β*–hydroxyphenylalanine unit, isoleucine and derived *N*–methyl isoleucine to be imidazolidinone moiety.

Intense NOE enhancements of NH–3 (δ_H 6.50*d*, *J* = 9.5 Hz) to H–2 (δ_H 6.66*dd*, *J* = 9.5, 7.6 Hz) and NH–6 (δ_H 5.81*d*, *J* = 8.5 Hz) demonstrated the connection of the isoleucine to styrylamine unit. Correlations of H–5 (δ_H 4.01*dd*, *J* = 8.5, 4.4 Hz) and H–8 (δ_H 5.09*d*, *J* = 7.6 Hz) to C–7 (δ_H 168.2) in HMBC spectrum showed that the *β*–hydroxyphenylalanine moiety is attached to the isoleucine unit. A strong HMBC correlation of H–8 and C–33 (δ_c 67.6), H–33 (δ_H 3.83*br d*, *J* = 3.9 Hz, H$_\beta$–33 and δ_H 3.22*br d*, *J* = 4.9 Hz, H$_\alpha$–33) to C–26 (δ_c 172.8) confirmed the attachment of terminal imidazolidinone to macrocyclic ring at C–8 (δ_c 57.9). The correlations of H–33 to *N*CH$_3$ (δ_c 41.1) and of *N*CH$_3$ (δ_H 2.11 s) to H–33 in HMBC experiment were also observed.

The analysis of its CD spectrum exhibited CE including intense negative and weak positive signals at 244 and 286 nm, respectively, demonstrated that compound **D** has a 5*S*,8*S*,9*S*–configuration (Gournelis, Laskaris and Verpoorte, 1998). A strong correlation in the NOESY spectrum between H$_\beta$–9 and H$_\beta$–33, and between H–27 and H$_\alpha$–33, suggested the 27*S*–configuration corresponding to those correlations of compounds **B** and **E**. These evidences led to the conclusion that compound **D** has all *S*–configuration and it was named cambodine D.

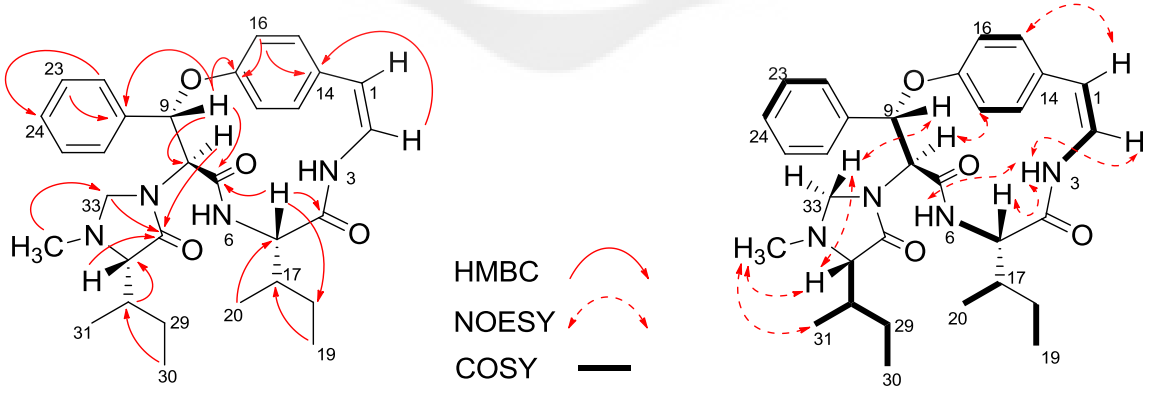

Figure 50 Selected HMBC COSY and NOESY correlations of compound **D**

Table 14 ^{1}H–, ^{13}C– and 2D NMR data of compound **D** in $CDCl_3$

Position	δ_H	δ_C	HMBC correlations	NOESY correlations
1	6.46 *d* (7.6)	117.8	C–2	H–15
2	6.66 *dd* (9.5, 7.6)	125.4	C–1, C–14	H–2
3–NH	6.50 *d* (9.5)	–	–	H–2, NH–6
4–CO	–	166.8	–	–
5	4.01 *dd* (8.5, 4.4)	59.3	C–4, C–7, C–17, C–18, C–20	–
6–NH	5.81 *d* (8.5)	–	–	NH–3, H–8
7–CO	–	168.2	–	–
8	5.09 *d* (7.6)	57.9	C–7, C–9, C–26	NH–6, H–9, H–12, H–22
9	5.99 *d* (7.6)	80.7	C–7, C–8, C–11, C–21, C–22	H–8, H–12
11	–	155.0	–	–
12	7.32 *m*	123.3	C–11	H–8, H–9
13	7.13 *m*	130.2	C–11, C–15	–
14	–	132.3	–	–
15	7.10 *m*	131.6	C–11, C–13, C–14	H–1
16	7.34 *m*	122.8	C–11	–
17	2.16 *m*	34.4	H–18	H–18, H–19
18	1.17 *m*, 0.88 m	23.9	–	H–17
19	0.81 *t* (6.3)	11.7	C–17	H–17
20	0.70 *d* (6.8)	16.5	C–5, C–17, C–18	–
21	–	136.2	–	–
22,22′	7.52 *dd* (7.7, 1.9)	127.8	C–24	H–8, H–33
23,23′	7.39 *m*	128.8	C–21, C–22	–
24	7.41 *m*	129.2	–	–
26–CO	–	172.8	–	–
27	2.48 *dd* (2.6, 1.3)	70.4	C–26, *N*CH_3	H–28, H–29, H–31
28	1.29 *m*	35.8	C–27	H–27, H–31
29	1.08 *m*	24.7	–	H–31
30	0.77 *t* (7.4)	11.9	C–28, C–29	–
31	0.55 *d* (6.8)	14.7	C–28, C–29	H–27, H–29, *N*CH_3
33	3.83 *br d* (3.9)[a] β	67.6	C–26, *N*CH_3	H–22
	3.22 *br d* (4.9)[a] α			
NCH_3	2.11 *s*	41.1	C–33	H–28, H–31

[a] each H coupled with H–27 in COSY

Compounds that belong to 5(14)–scutianine A–type cyclopeptide alkaloid

Three compounds were isolated and identified to be cyclopeptides that belong to the title group, which consists of *β*–hydroxyphenylalanine as a B unit. Units A, C, D and E are *N*–methyl phenylalanine, isoleucine, styrylamine moiety and phenylalanine.

Table 15 NMR spectral data for compounds that belong to 5(14)–scutianine A–type cyclopeptide alkaloid

Position	δ_H			δ_C		
	A [a] 3096	**C** [b] 4402	**F** [b] 4734	**A** [a]	**C** [b]	**F** [b]
1	6.58 *d* (7.5)	6.44 *d* (7.1)	6.45 *d* (7.4)	125.1	117.5	117.5
2	6.29 *br d* (7.5)	6.65 *dd* (9.6, 7.1)	6.65 *dd* (9.2, 7.4)	125.4	125.5	125.4
3–NH	–	6.73 *d* (9.6)	6.52 *d* (9.2)	–	–	–
4–CO	–	–	–	168.8	167.2	167.2
5	3.80 *br dd* (7.0, 5.0)	4.08 *dd* (8.3, 4.1)	3.98 *dd* (8.0, 4.2)	58.3	59.3	59.3
6–NH	–	6.19 *d* (8.3)	5.92 *d* (8.0)	–	–	–
7–CO	–	–	–	170.7	171.0	171.0
8	4.70 *br dd* (9.4, 7.8)	4.78 *dd* (8.9, 6.7)	4.70 *dd* (8.4, 8.0)	56.6	56.7	57.2
9	5.84 *d* (7.8)	6.10 *d* (6.7)	5.92 *d* (8.0)	81.1	81.5	81.6
11	–	–	–	154.8	155.1	155.2
12	7.03 *m*	ca 7.32	7.35 *dd* (8.4, 2.1)	130.7	123.1	122.9
13	7.15 *m*	ca 7.15	7.17 *m*	120.4	130.1	130.1
14	–	–	–	132.0	132.5	132.2
15	7.17 *m*	ca 7.11	7.12 *m*	122.2	131.9	131.8
16	7.05 *m*	ca 7.34	7.40 *dd* (8.4, 2.3)	129.5	122.6	122.5
17	1.76 *m*	ca 2.11	2.04 *m*	35.4	35.2	35.3
18	1.05 *m*	1.25 *m*	1.15 *m*	23.8	23.9	23.9
19	0.71 *t* (7.0)	0.84 *t* (7.2)	0.79 *t* (7.2)	11.7	11.9	11.9
20	0.64 *d* (6.6)	0.75 *d* (6.8)	0.67 *d* (6.9)	15.3	15.8	16.4
21	–	–	–	137.3	136.8	137.2
22,22′	7.46 *d* (7.7)	7.51 *dd* (7.5, 1.0)	7.67 *br d* (7.1)	128.1	128.1	128.2
23,23′	7.29 *br dd* (7.7, 7.3)	7.40 *m*	7.48 *br t* (7.4)	128.5	128.8	128.8
24	7.30 *d* (7.3)	7.45 *m*	7.31 *m*	128.5	128.9[a]	128.9
25–NH	8.03 *d* (9.4)	6.84 *d* (8.9)	8.73 *d* (8.4)	–	–	–
26–CO	–	–	–	167.5	170.9	170.0
27	4.34 *dd* (9.9, 6.1)	4.20 *dd* (4.8, 10.4)	3.49 *dd* (12.0, 4.4)	54.9	54.7	63.0
28	2.66 *m*	2.88 *dd* (14.2, 4.8)	2.31 *m*	34.2	36.6	33.2
28a	–	–	–	135.1	136.3	136.6
29,29′	6.96 *br t* (6.7)	6.98 *dd* (8.4, 2.1)	6.93 *dd* (7.6, 1.1)	128.5	128.9[a]	129.2
30,30′	7.13 *m*	7.18 *m*	7.22 *m*	128.1	128.6	128.5
31	7.08 *m*	7.22 *m*	7.24 *m*	126.9	127.0	127.0
33–CO	–	–	–	167.5	174.2	174.8
34	2.64 *m*	2.50 *d* (4.0)	2.57 *s*	70.8	69.1	71.0
35	1.43 *m*	1.51 *m*	1.50 *m*	35.3	37.6	36.5
36	1.07 *m*	0.86 *m*	1.28 *m*	24.7	24.2	24.8
37	0.69 *t* (7.2)	0.65 *t* (6.0)	0.85 *t* (7.3)	10.9	11.7	12.2
38	0.49 *d* (6.7)	0.62 *d* (6.9)	0.77 *d* (6.8)	14.1	15.5	14.9
40	4.23 *br d* (5.0), 3.31 *m*	–	2.41 *br d* (5.4)	66.8	–	78.9
41	–	–	0.92 *d* (5.4)	–	–	19.5
NCH_3	2.32 *s*	2.11 *s*	1.85 *s*	41.1	36.5	39.6

NMR spectra were recorded in: [a] $CDCl_3$ and few drops of methanol–d_4 or [b] $CDCl_3$

Compound **A** (sss3096) was obtained as a colorless amorphous solid, mp 248–249 ^{o}C, and established to be $C_{40}H_{49}N_5O_5$ on the basis of ^{13}C NMR and HRTOFMS (APCI^{+}) mass spectrum, which displayed an intense $[M+H]^{+}$ signal at *m/z* 680.3808 (calcd 680.3806 for $C_{40}H_{49}N_5O_5$ + H).

The ^{13}C NMR and DEPT spectra displayed resonances consistent with 40 signals attributable to four methyls, one *N*–methyl, four methylenes, twenty three methines (including one oxygenated and two olefinic) and four quaternary carbons, four of which corresponded to the carbonyl groups.

The analysis of the ^{1}H, ^{13}C, DEPT and 2D NMR (COSY and HMQC) spectra of compound **A** displayed 5 units including *p*–oxystyrylamine group, *β*–hydroxy–phenylalanine, isoleucine, phenylalanine and *N*–methyl phenylalanine with methylimidazolidinone ring. Its EIMS spectra showed a fragmentation pattern with the characteristic base peak at *m/z* 155, 525 and 622 indicating the presence of the terminal methylimidazolidinone unit (Tschesche, Elgamal and Eckhardt, 1977).

The analysis of its EIMS spectra demonstrated a fragmentation pattern as characteristic base peak at *m/z* 155 (**328**) and a fragment at *m/z* 622 (**329**) indicated the presence of a terminal 1–methylimidazolidin–4–one group (Scheme 20) (Tschesche et al., 1977). The presence of a 1–methylimidazolidin–4–one moiety was also deduced by its ^{1}H and ^{13}C NMR data. The ^{1}H NMR spectrum showed the presence of methylene protons (H–40) at δ_H 4.23*br d* (*J* = 5.0 Hz) and δ_H 3.31*m* which correlated with a downfield carbon at δ_H 66.8 similar to those of **E**.

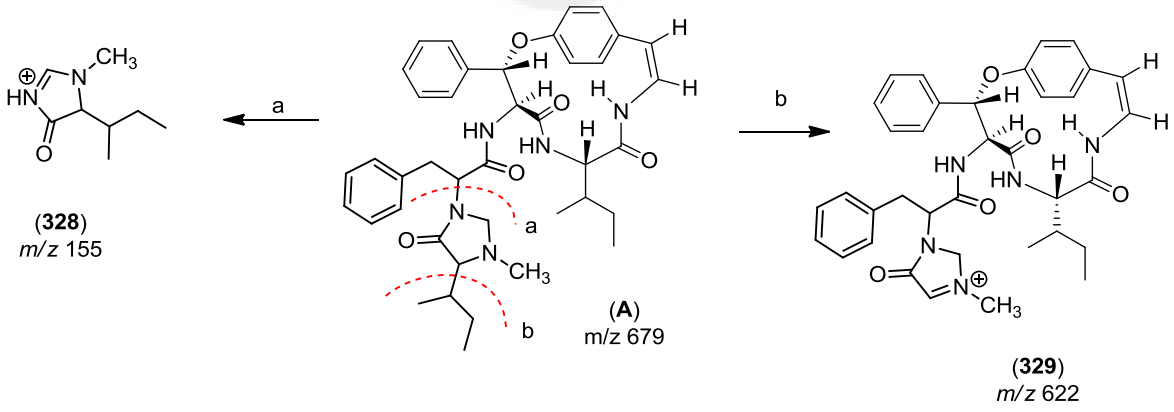

Scheme 20 EI fragments of compound **A**

Table 16 ^{1}H–, ^{13}C– and 2D NMR data of compound A in $CDCl_3$ + methanol–d_4

Position	δ_H (300 MHz)	δ_C (75 MHz)	HMBC correlations	NOESY correlations
1	6.58 *d* (7.5)	125.1	C–2, C–14	H–2, H–15
2	6.29 *br d* (7.5)	125.4	C–1	H–1, H–5, H–15
3–NH	–	–	–	–
4–Co	–	168.8	–	–
5	3.80 *br dd* (7.0, 5.0)	58.3	C–4, C–7, C–17, C–18, C–20	H–6, H–13, H–17, H–18, H–20
6–NH	–	–	C–5, C–7	H–5, H–8, H–9, H–20
7–CO	–	170.7	–	
8	4.70 *br dd* (9.4, 7.8)	56.6	C–7, C–9, C–26	NH–6, H–22, NH–25
9	5.84 *d* (7.8)	81.1	C–7, C–8, C–21, C–22	H–12, H–22, H–23
11	–	154.8	–	–
12	7.03 *m*	130.7	–	H–9
13	7.15 *m*	120.4	C–11	H–5
14	–	132.0	–	–
15	7.17 *m*	122.2	C–11, C–13	H–1, H–2
16	7.05 *m*	129.5	C–11, C–14	–
17	1.76 *m*	35.4	–	H–5, H–20
18	1.05 *m*	23.8	–	–
19	0.71 *t* (7.0)	11.7	C–17, C–18	–
20	0.64 *d* (6.6)	15.3	C–5, C–17, C–18	H–17
21	–	137.3	–	–
22,22′	7.46 *d* (7.7)	128.1	C–9, C–21, C–23, C–24	H–8, H–9
23,23′	7.29 *br dd* (7.7, 7.3)	128.5	C–22	H–9
24	7.30 *d* (7.3)	128.5	C–22	–
25–NH	8.03 *d* (9.4)	–	–	H–8, H–27
26	–	167.5	–	–
27	4.34 *dd* (9.9, 6.1)	54.9	C–26, C–28	NH–25, H–28b, H–30, H–40a
28	28a, 2.66 *m,* β	34.2	C–27, C–29	H–27, H–30
	28b, 2.59 *m,* α			
28a	–	135.1	–	–
29,29′	6.96 *br t* (6.7)	128.5	C–28, C–32	H–27, H–28
30,30′	7.13 *m*	128.1	C–32	–
31	7.08 *m*	126.9	C–31	–
33–CO	–	167.5	–	–
34	2.64 *m*	70.8	C–34	H–36, H–38, H–39, NCH$_3$
35	1.43 *m*	35.3	–	H–35, H–39
36	1.07 *m,* 0.95 *m*	24.7	–	–
37	0.69 *t* (7.2)	10.9	C–36, C–37	–
38	0.49 *d* (6.7)	14.1	C–35, C–36	H–35, H–36, H–40b,
40	4.23 *br d* (5.0), β, 3.31 *m,* α	66.8	C–34, C–35	H–28a, NCH$_3$
NCH$_3$	2.32 *s*	41.1	C–35, C–40	H–36, H–39, H–40a

^{1}H NMR showed the signal for *Z*–olefinic protons of styrylamine unit at δ_H 6.58*d* (*J* = 7.5 Hz, H–1) and δ_H 6.29*br d* (*J* = 7.5 Hz, H–2). Proton at δ_H 3.80*br dd* (*J* = 7.0, 5.0 Hz, H–5) correlated with the carbonyl signal at δ_C 168.8 (C–4) in the HMBC spectrum revealing the connection of styrylamine moiety and isoleucine group. The correlation of the methine proton at H–5 to carbonyl C–7 (δ_C 170.7) supported that the isoleucine unit was attached to the β–hydroxyphenylalanine group. The HMBC correlation of H–8 (δ_H 4.70*br dd*, *J* = 9.4 Hz, 7.8 Hz) with the carbonyl carbon signal at δ_C 167.5 (C–26) allowed the placement of the intermediate phenylalanine group next to the β–hydroxyphenylalanine moiety. The correlation of H–40β (δ_H 4.23*d*, *J* = 5.0 Hz) in the NOESY experiment displayed the connection between phenylalanine unit and terminal methylimidazolidinone moiety. The correlation of *N*CH$_3$ (δ_H 2.32 *s*) and C–40 (δ_C 66.8) in the HMBC spectrum and the NOE effect of *N*CH$_3$ to H–34 (δ_H 2.64 *m*) were also observed.

Its 5*S*,8*S*,9*S*–configuration was assigned by CD spectra that showed intense negative and weak positive CE at 236 and 283 nm, respectively (Gournelis, Laskaris and Verpoorte, 1998). The intense NOE enhancement between H–8 and H–25 (8.03*d*, *J* = 9.4 Hz) compared to those of H–9 confirmed the α–orientation of H–27 (4.34*dd*, *J* = 9.9, 6.1 Hz). Due to different orientation (27*S*,35*S*–configuration) of H$_\alpha$–27 and H$_\beta$–35, no NOESY correlation was observed between these protons. Thus, the structure of **A** was established as a new cyclopeptide alkaloid possessing all *S*–configuration and it was named cambodine A.

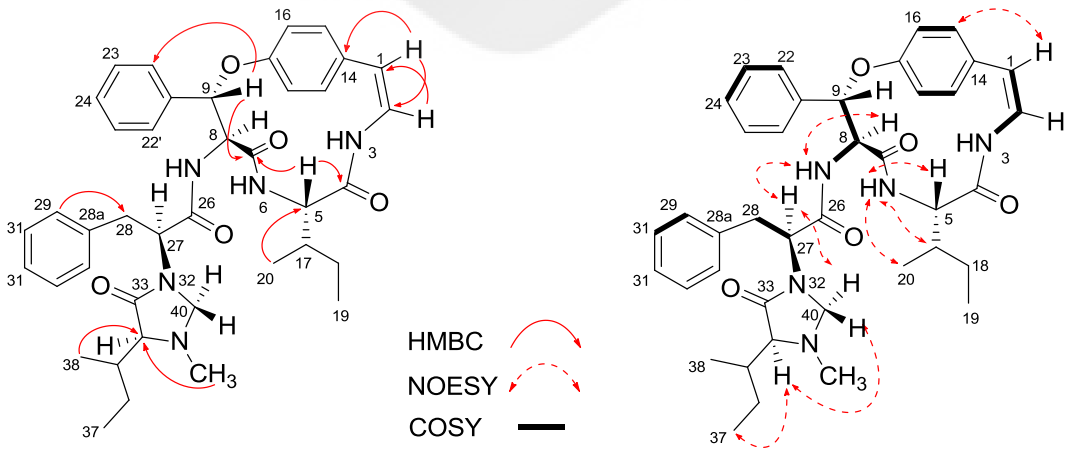

Figure 51 Selected HMBC COSY and NOESY correlations of compound **A**

Compound **C** (sss4402), colorless needles, mp 225–227 ^{o} C and the molecular formula $C_{39}H_{49}N_5O_5$ was deduced by ^{13}C NMR and HRTOFMS at *m/z* 668.38079 $[M+H]^+$ (calcd 668.38116 $C_{39}H_{49}N_5O_5$ + H).

The ^{13}C NMR and DEPT spectra indicated 39 signals attributable to four methyls, one *N*–methyl, three methylenes, twenty three methines (including one oxygenated and two olefinic) and four quaternary carbons, four of which corresponded to the carbonyl groups. The ^{1}H NMR spectrum of **C** displayed signals corresponding to *Z*–olefinic protons of styrylamine at δ_H 6.44*d* (*J* = 7.1 Hz, H–1) and 6.65*dd* (*J* = 9.6 Hz, 7.1, H–2), a number of aromatic, methine, methylene and methyl protons including a singlet corresponding to the *N*–methyl protons at δ_H 2.11. From the COSY and HMQC spectra of compound **C** and its comparison with the reported values led to a conclusion for the presence of *p*–oxystyrylamine group, β–hydroxyphenylalanine, isoleucine, phenylalanine and *N*–methyl isoleucine units.

Comparison of the ^{1}H and the ^{13}C NMR spectroscopic data of compound **C** with those of compounds **A** and **F** indicated that **C** possessed a similar unit to that of other structures except for the lack of the methylimidazolidinone moiety at terminal *N*–methyl isoleucine unit. The signal for *p*–oxystyrylamine proton at NH–3 (δ_H 6.73*d*, *J* = 9.6 Hz) showed a weak NOESY correlation to the signal at δ_H 4.08 (*dd*, 8.3, 4.1, H–5) and the HMBC correlations of the resonance at δ_H 6.65 (H–2) to C–14 (δ_C 132.5) and of H–1 (δ_H 6.44) to C–2 allowed the placement of the isoleucine moiety next to the styrylamine group. The HMBC correlations of NH–6 (δ_H 6.19*d*, *J* = 8.3 Hz) to C–7 (δ_C 171.0), and H–8 (δ_H 4.78*dd*, *J* = 8.9, 6.7 Hz) to C–7 (δ_C 171.0), C–11 (δ_C 155.1) and C–21 (δ_C 136.8) revealed the connection of isoleucine to β–hydroxyphenylalanine fragments in the macrocyclic ring. The β–hydroxyphenylalanine moiety was as assigned to have the *erythro* relative configuration by the vicinal coupling constant (*J* = 6.7 Hz) between H–8 and H–9 (δ_H 6.10*d*, *J* = 6.7 Hz) (Gournelis, Laskaris and Verpoorte, 1998).

NOE enhancements displayed a correlation between NH–25 (6.84*d*, *J* = 8.9 Hz) and H–27 (4.20*m*) in the NOESY spectrum, and the HMBC spectrum showed a correlation of the H–8 with the carbonyl carbon signal at δ_C 170.9 (C–26), H–27 to C–28a (δ_C 136.3). These data supported that the phenylalanine unit is attached to the β–hydroxyphenylalanine moiety at NH–25 (6.85*d*, *J* = 8.9 Hz). HMBC correlations of H–27

with the carbonyl carbon signal at δ_C 174.2 (C–33) and NOESY correlation of *N*–methyl proton at δ_H 2.11 with H–34 (δ_H 2.50 *d,* 4.0) demonstrated that the *N*–methyl isoleucine unit was attached to phenylalanine at N–32. HMBC correlations of H–33 to ^{13}C signals at δ_C 15.5 (C–38), δ_C 24.2 (C–36) and δ_C 37.6 (C–35), of H–37 (δ_H 0.65) to C–35 and NOESY correlation of NCH_3 to the signal at δ_H 0.62 (H–38) were also observed.

Its CD spectrum of compound **C** showed intense negative CE 236 nm and weak positive at 280 nm, corroborating the 5*S*,8*S*,9*S*–configuration (Gournelis, Laskaris and Verpoorte, 1998).

The ^{1}H and ^{13}C NMR spectroscopic data of the intermediate phenylalanine and the basic end *N*–methylisoleucine units were similar to that of the *N*–methylisoleucine moiety in paliurine B (**27**) (Lin et al., 2000). Terminal unit *N*–methylisoleucine in **27** was determined to be *L*–configuration by NMR comparison to a model dipeptide, *L*–Phe(OEt)–*L*–Ile($N(CH_3)_2$). The strong NOE enhancements between H–8 and NH–25, NH–25/H–27 and no correlation between H–27 (4.20*dd*, *J* = 4.8, 10.4 Hz) and H–34 (2.50*d*, *J* = 4.0 Hz) in the same experiment substantiated the β–orientation of H–34 (*S*–configuration). From the above evidences compound **C** has found to be a new compound with all *S*–configuration and named cambodine C.

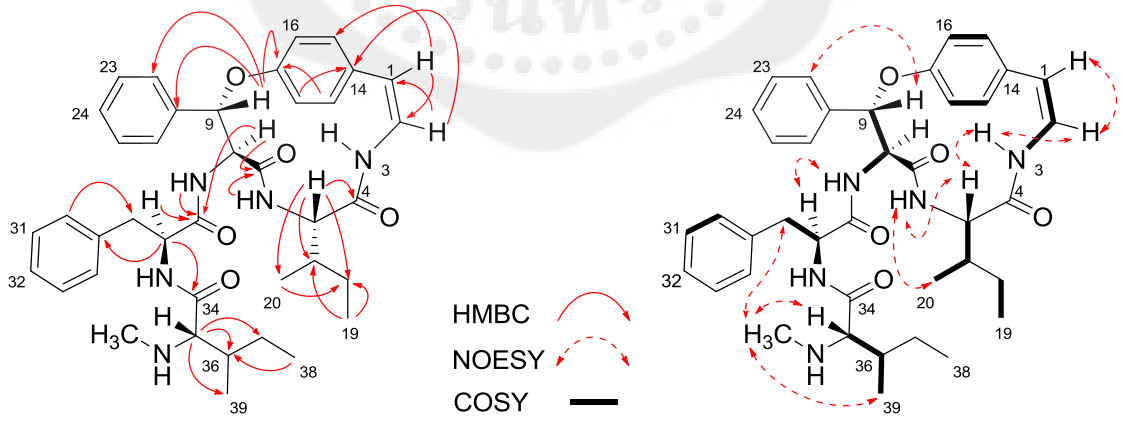

Figure 52 Selected HMBC COSY and NOESY correlations of compound **C**

Table 17 ^{1}H–, ^{13}C– and 2D NMR data of compound **C** in $CDCl_3$

Position	δ_H (300 MHz)	δ_C (75 MHz)	HMBC correlations	NOESY correlations
1	6.44 *d* (7.1)	117.5	C–2, C–14, C–15	H–2, NH–3
2	6.65 *dd* (9.6, 7.1)	125.5	C–1, C–14	H–1, H–3, H–5
3–NH	6.73 *d* (9.6)	–	–	H–2, H–5, NH–6
4–CO	–	167.2	–	–
5	4.08 *dd* (8.3, 4.1)	59.3	C–4, C–7, C–17, C–18,	NH–3, H–6, H–17
6–NH	6.19 *d* (8.3)	–	C–5, C–7	NH–3, H–5, H–8, H–20
7	–	171.0	–	
8	4.78 *dd* (8.9, 6.7)	56.7	C–7, C–9, C–26	NH–6, H–23, NH–25
9	6.10 *d* (6.7)	81.5	C–7, C–8, C–11, C–21, C–22, C–22′	H–22, H–22′, H–23
11	–	155.1	–	–
12	ca 7.32	122.6	C–11, C–14	–
13	ca 7.15	130.1	C–11, C–15	–
14	–	132.5	–	–
15	ca 7.11	131.9	C–13	–
16	ca 7.34	123.1	C–11	–
17	ca 2.11	35.2	–	H–5
18	1.25 *m*	23.9	C–29	–
19	0.84 *t* (7.2)	11.9	C–17, C–18	–
20	0.75 *d* (6.8)	15.8	C–5, C–17, C–18	H–6,
21	–	136.8	–	–
22,22′	7.51 *dd* (7.5, 1.0)	128.1	C–9, C–21, C–23	H–9
23,23′	7.40 *m*	128.8	–	H–8
24	7.45 *m*	128.9	C–23	–
25–NH	6.84 *d* (8.9)	–	C–7, C–26	H–8, H–27
26–CO	–	170.9	–	–
27	4.20 *dd* (4.8, 10.4)	54.7	C–26, C–28, C–29, C–34	NH–25, H–28, H–30, H–31
28	2.88 *dd* (14.2, 4.8)	36.6	C–26, C–27, C–29	H–27, H–30, H–31, *N*CH_3
	2.45 *dd* (14.2, 10.4)			
28a	–	136.3	C–28	–
29,29′	6.98 *dd* (8.4, 2.1)	128.9	C–26, C–28, C–34, *N*CH_3	H–27, H–28
30,30′	7.18 *m*	128.6	C–27, C–34	H–27, H–28
31	7.22 *m*	127.0	–	–
33	–	174.2	–	–
34	2.50 *d* (4.0)	69.1	C–36, C–37, C–39, *N*CH_3	H–36, H–39, *N*CH_3
35	1.51 *m*	37.6	–	H–35, H–39
36	0.86 *m*	24.2	C–38	–
37	0.65 *t* (6.0)	11.7	C–36, C–37	–
38	0.62 *d* (6.9)	15.5	C–35, C–36	H–35, H–36, *N*CH_3
NCH_3	2.11 *s*	36.5	C–26	H–28, H–39, H–35

[a] Assignments confirmed by 1H–1H COSY and NOESY

[b] Assignments confirmed by DEPT, HMQC and HMBC

Compound **F** (sss4734) was obtained as colorless needles, mp 216–218 ^{o}C. On the basis of the positive ion HRTOFMS at *m/z* 716.3792 (calcd 716.3782 for $C_{41}H_{51}N_5O_5$ + Na) in combination with analysis of the ^{13}C NMR spectrum, the molecular formula of **F** was established to be $C_{41}H_{51}N_5O_5$.

The ^{13}C NMR and DEPT spectra indicated 41 signals attributable to five methyls, one *N*–methyl, three methylenes, twenty four methines (including one oxygenated and two olefinic) and four quaternary carbons, four of which corresponded to the carbonyl groups.

The analysis of the ^{1}H, ^{13}C, DEPT and 2D NMR (COSY and HMQC) spectra of **F** displayed 4 units. A comparison of the spectra with those of compound **A** suggested that **F** has a skeleton similar to that of **A** except for the 1–methylimidazolidin–4–one unit which was replaced with 1,2–dimethylimidazolidin–4–one. The ^{1}H NMR spectrum showed the presence of a methine proton (H–40) at δ_H 2.41*br d* (*J* = 5.4 Hz) which correlated with a high downfield carbon at δ_C 78.9 (C–40). The COSY correlation between this methine and a doublet methyl (H–41) at δ_H 0.92*d* (*J* = 5.4 Hz) was observed.

The analysis of its EIMS spectra demonstrated a fragmentation pattern as a characteristic base peak at *m/z* 169 (**330**) and a fragment at *m/z* 636 (**331**) were observed on its EIMS spectra. These EI fragments demonstrated the presence of a terminal 1,2–dimethylimidazolidin–4–one group (Scheme 21) (Tschesche et al., 1977).

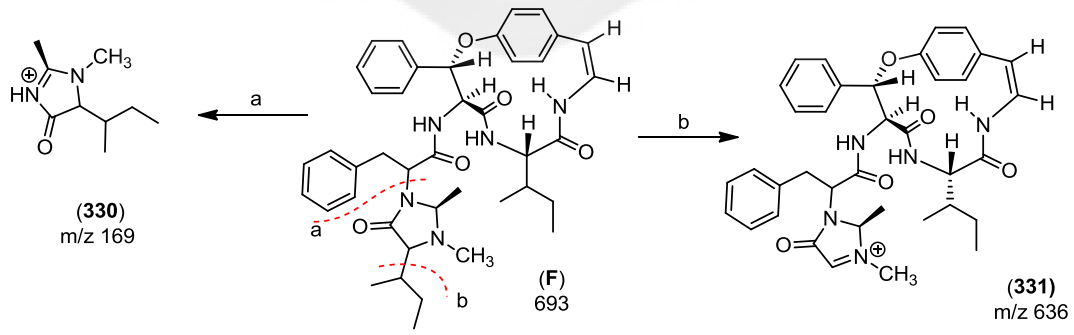

Scheme 21 EI fragments of compound **F**

NOE enhancements of H–2 (δ_H 6.65*dd*, *J* = 9.2, 7.4 Hz) to NH–3 (δ_H 6.52*d*, *J* = 9.2 Hz) and H–5 (δ_H 3.98*dd*, *J* = 8.0, 4.2 Hz) showed that the isoleucine unit is placed next to styrylamine unit. HMBC correlation of NH–6 (δ_H 5.92*d*, *J* = 8.0 Hz) and H–8 (δ_H 4.70*dd*, *J* = 8.4, 8.0 Hz) to carbonyl at δ_C 171.0 (C–7) displayed the placement of the isoleucine unit next to β–hydroxyphenylalanine in the macrocyclic ring. The correlations of H–8 to NH–25 (δ_H 8.73*d*, *J* = 8.4 Hz) in the NOESY spectrum and to C–26 (δ_C 170.0) in the HMBC experiment allowed placing a connection between the phenylalanine unit and β–hydroxyphenylalanine of the macrocyclic ring at C–8. The correlation between two methine protons H–8 and H–40 (δ_H 2.41*br d*, *J* = 5.4 Hz) in NOESY experiment exhibited the connection of the phenylalanine unit and the terminal imidazolidinone moiety. The correlation of H–40 to C–41 (δ_C 19.5) and that of H–41 (0.92*d*, *J* = 5.4 Hz) to C–40 (δ_C 78.9) and *N*CH_3 (δ_C 39.6) in the HMBC spectrum and that NOE enhancement between H–40 and *N*CH_3 were also observed. The configuration of the macrocyclic ring was assigned as 5S,8S,9S proved by its CD spectrum which showed intense negative and weak positive CE at 236 and 282 nm, respectively.

The intense NOE enhancement between H–8 and H–25 compared to that of H–9 revealed the α–orientation of H–27 (27*S*). The intense NOE effect observed between H–27 and H–40 was consistent with 27α– and 40α–orientations (27*S*,40*S*–configurations) of those protons. Its ^{1}H and ^{13}C NMR data at C–34 (δ_C 71.0) and H–34 (δ_H 2.57 s) were agreeable with those of **1** and **3**, which were assigned to be 35*S*. Those evidences led to the conclusion that **6** possessed 5*S*,8*S*,9*S*,27*S*,35*S*,40*S*–configuration and it was named cambodine F. This is the first isolation of a cyclopeptide alkaloid comprising the 1,2–dimethylimidazolidin–4–one unit.

Table 18 ^{1}H–, ^{13}C– and 2D NMR data of compound **F** in $CDCl_3$

Position	δ_H (300 MHz)	δ_C (75 MHz)	HMBC correlations	NOESY correlations
1	6.45 *d* (7.4)	117.5	C–2, C–15	–
2	6.65 *dd* (9.2, 7.4)	125.4	C–14	NH–3
3–NH	6.52 *d* (9.2)	–	–	H–2, H–5
4–CO	–	167.2	–	–
5	3.98 *dd* (8.0, 4.2)	59.3	C–4, C–7	NH–3, NH–6
6–NH	5.92 *d* (8.0)	–	–	H–5, H–17, H–20, H–42
7–CO	–	171.0	–	–
8	4.70 *dd* (8.4, 8.0)	57.2	C–9	H–9, H–12, H–22, NH–25
9	5.92 *d* (8.0)	81.6	C–7, C–21, C–22	H–8, H–22
11	–	155.2	–	–
12	7.35 *dd* (8.4, 2.1)	122.9	C–16	H–8
13	7.17 *m*	130.1	–	–
14	–	132.2	–	–
15	7.12 *m*	131.8	C–13	H–16
16	7.40 *dd* (8.4, 2.3)	122.5	C–12	H–15
17	2.04 *m*	35.3	–	NH–6, H–18
18	1.15 *m*	23.9	–	H–17
	0.80 *m*			
19	0.79 *t* (7.2)	11.9	C–17, C–18	–
20	0.67 *d* (6.9)	16.4	C–5, C–17, C–18	NH–6
21	–	137.2	–	–
22,22′	7.67 *br d* (7.1)	128.2	–	H–8, H–23, NH–25
23,23′	7.48 *br t* (7.4)	128.8	–	H–22
24	7.31 *m*	128.9	–	–
25–NH	8.73 *d* (8.4)	–	–	H–8, H–22, H27, H–28
26	–	170.0	–	–
27	3.49 *dd* (12.0, 4.4)	63.0	–	NH–25, H–35, H–41
28	2.31 *m*	33.2	C–29, C–30	H–30
28a	–	136.6	–	–
29,29′	6.93 *dd* (7.6, 1.1)	129.2	C–28	H–28, H–32
30,30′	7.22 *m*	128.5	–	–
31	7.24 *m*	127.0	–	H–30
33–CO	–	174.8	–	–
34	2.57 *s*	71.0	C–34	H–27, H–30, H–37, H–38, H–42,
35	1.50 *m*	36.5	–	–
36	1.28 *m*	24.8	–	H–35
37	0.85 *t* (7.3)	12.2	C–36, C–37	H–35
38	0.77 *d* (6.8)	14.9	C–35, C–36, C–37	–
39	2.41 *br d* (5.4)	78.9	C–42, *N*CH_3	H–27, *N*CH_3
41	0.92 *d* (5.4)	19.5	C–41	NH–6
NCH_3	1.85 *s*	39.6	C–35, C–41	H–35, H–41

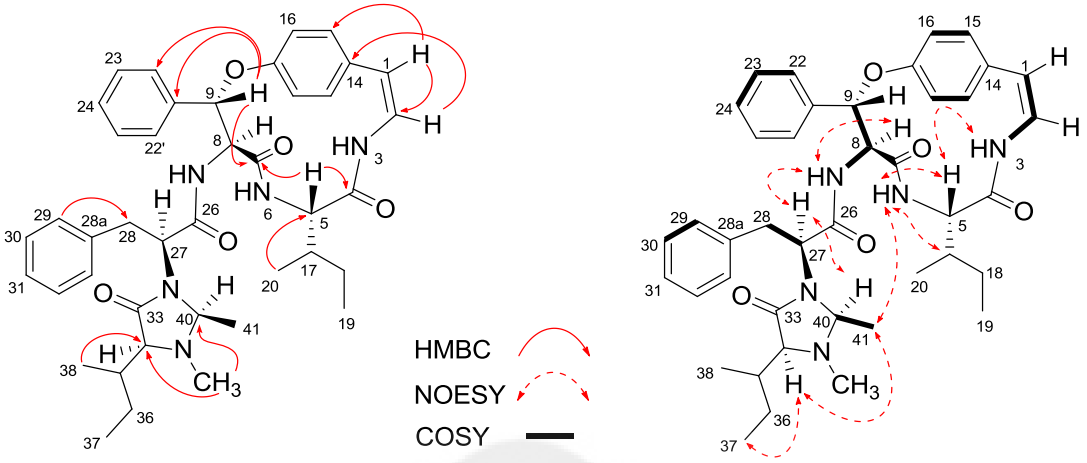

Figure 53 Selected HMBC COSY and NOESY correlations of compound **F**

Neutral compound related to the 14–membered ring cyclopeptide alkaloid

Only one compound was isolated and identified to be the cyclopeptide of the title group that consists of a neutral moiety and coumaroyl as the terminal unit (Table 1).

Compound **G** (ssss4767) was obtained as colorless needles, mp 261–263 ^{o}C. Its molecular formula was established as $C_{34}H_{42}N_4O_5$ from HRTOFMS at *m/z* 609.3033, $[M + H]^+$ (calcd 609.30474 for $C_{34}H_{42}N_4O_5$ + Na).

Unlike other new compounds, compound **G** showed UV (MeOH) absorption bands at λ_{max} 217, 223 and 279 nm due to its coumaroyl moiety (Gonzalez Sierra, et al., 1974). The ^{1}H NMR spectrum of **G** exhibited signals for *trans*–double bonds at δ_H 6.75*d* (*J* = 15.4 Hz, H–32) and δ_H 7.77*d* (*J* = 15.4 Hz, H–33), which were assigned to the *trans*–coumaroyl protons, H–32 (δ_C 117.0) and H–33 (δ_C 144.1), respectively. A *Z*–double bond showed signals at δ_H 6.35*d* (*J* = 7.5 Hz, H–1) and 6.68*dd* (*J* = 10.1, 7.5, H–2). Also present were the signals corresponding to four methylene groups, three methyl doublets, one methyl triplet, a number of aromatic, methine and methylene protons, including NH signals at δ_H 6.54*d* (*J* = 10.1 Hz, NH–3), 6.05*d* (*J* = 8.0, NH–6), 8.33*d* (*J* = 9.2, NH–24). The ^{13}C NMR and DEPT spectra of **G** showed 34 carbon resonances for four methyls (δ_C 12.0, 15.8, 14.6 and 20.4), four methylenes (δ_C 23.7, 25.1, 25.9 and 47.2), nineteen methines (two of which were olefinic carbons at δ_C 115.6 and 125.5), three quaternary

aromatic carbons (δ_C 123.1, 131.7 and 134.6), and four carbonyl carbons (δ_C 166.6, 167.0, 171.1 and 171.6).

Table 19 ^{1}H–, ^{13}C– and 2D NMR data of compound **G** in $CDCl_3$

Position	δ_H	δ_C	HMBC correlations	NOESY correlations
1	6.35 *d* (7.5)	115.6	C–2, C–14	–
2	6.68 *dd* (10.1, 7.5)	125.5	C–1, C–14	–
3–NH	6.54 *d* (10.1)	–	–	H–5
4–CO	–	167.0	–	–
5	4.02 *dd* (8.0, 3.6)	55.7	C–4, C–7, C–18, C–20	H–2, NH–6, H–17, H–20
6–NH	6.05 *d* (8.0)	–	C–7	H–5, H–20
7–CO	–	171.6	–	–
8	4.44 *dd* (9.2, 6.9)	59.4	C–7, C–9	NH–6, H–21, NH–24
9	5.02 *dd* (6.9, 1.7)	81.5	C–7, C–22	H–12, H–21, H–22
11	–	155.9	–	–
12	7.20 *dd* (8.5, 2.7)	123.1	C–11, C–14	H–9
13	7.05 *d* (8.5)	123.1	C–11	–
14	–	131.7	–	–
15	7.05 *d* (8.5)	130.3	C–1, C–11	–
16	7.11 *dd* (8.5, 2.7)	131.9	C–11	–
17	2.20 *m*	34.8	–	H–5, H–19, H–20
18,18′	0.96 *m*	23.7	C–19, C–20	–
19,19′	0.84 *t* (7.1)	12.0	C–17	H–17
20	0.72 *d* (6.9)	15.8	C–17, C–18	H–5, NH–6, H–17
21	1.97 *m*	29.1	C–23	H–9
22	0.80 *d* (6.6)	14.6	C–9, C–21	H–9, H–23
23	1.20 *d* (6.7)	20.4	C–21	H–22
24–NH	8.33 *d* (9.2)	–	C–25	H–8, H–26
25–CO	–	171.1	–	–
26	4.70 *d* (7.4)	59.4	C–28, C–29	NH–24, H–27, H–28
27	27a 2.53 *m,* 27b 1.80 *m*	25.9	–	H–26, H–28
28,28′	2.13 *m*	25.1	–	H–27
29,29′	29a 3.70 *quin* (8.7), 29a 3.67 *quin* (8.7)	47.2	C–27	H–32, H–33
31–CO	–	166.6	–	–
32	6.75 *d* (15.4)	117.0	C–31, C–33, C–34	H–29, H–33
33	7.77 *d* (15.4)	144.1	C–31, C–32, C–34	H–29, H–32, H–35
33a	–	134.6	–	–
34	7.58 *dd* (7.8, 3.7)	128.1	C–33	H–33
35	7.42 *br dd* (7.8, 2.6)	128.9	–	–
36	7.42 *br dd* (3.7, 2.6)	129.9	–	–

The analysis of the COSY and HMQC spectra of **G** and its comparison with the reported values led us to a conclusion for the presence of styrylamine units, *β*–hydroxyluecine, isoleucine, proline and coumaroyl group. The signal for *p*–oxystyrylamine NH–3 (δ_H 6.54*d*, *J* = 10.1 Hz) showed weak NOESY correlation to signal at δ_H 4.02*dd* (*J* = 8.0, 3.6 Hz, H–5) and olefinic proton H–1 (δ_H 6.35*d*, *J* = 7.5 Hz) to H–5 allowed the placement of an isoleucine moiety next to the styrylamine group. The correlations of H–8 (δ_H 4.44*dd*, *J* = 9.2, 6.9 Hz) to NH–6 (δ_H 6.05*d*, *J* = 8.0 Hz) in the NOESY and of H–5 (δ_H 4.02*dd*, *J* = 8.0, 3.6 Hz) to C–7 (δ_C 171.6) in the HMBC experiments described the connection of isoleucine to *β*–hydroxyluecine fragments in the macrocyclic ring. The HMBC of H–26 (δ_H 4.70*d*, *J* = 7.4 Hz) with the carbonyl carbon signal at δ_C 171.1 (C–25) indicated that proline unit connected to *β*–hydroxyluecine group. The correlations of H–29 ($\delta_{H\alpha}$ 3.70*quin*, *J* = 8.7 Hz and $\delta_{H\beta}$ 3.67*quin*, *J* = 8.7 Hz) and H–32 (δ_H 6.75*d*, *J* = 15.4 Hz) in the NOESY spectrum established that the coumaroyl moiety is placed next to the proline unit.

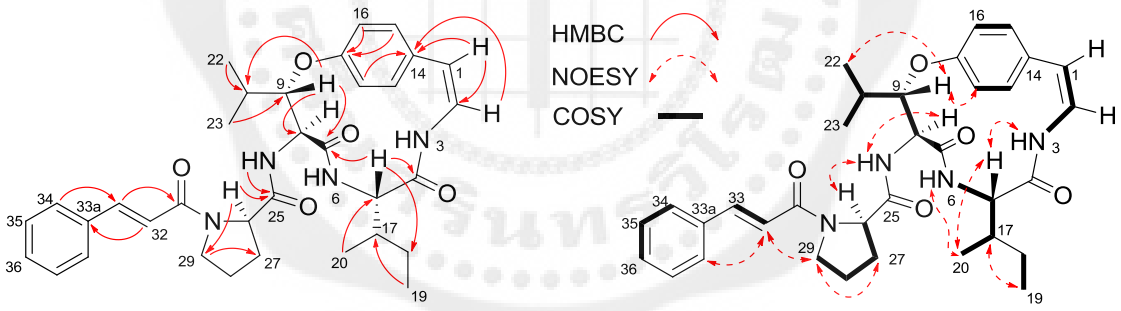

Figure 54 Selected HMBC COSY and NOESY correlations of compound **G**

The CD spectrum of **G** displayed an intense negative CE bands at 237 nm and coupling constants consistent with the 5*S*,8*S*,9*S*–configuration of the 14–membered ring nucleus (Gournelis, Laskaris and Verpoorte, 1998). The C–26 (δ_C 59.4) of the proline unit was assigned by the comparison of its ^{1}H and ^{13}C NMR spectra with those of amaiouine (**63**) (de Oliveira et al., 2009). The result showed that *S*–configuration in both structure possessed the same orientation confirmed by NMR signals at δ_C 59.4 and δ_H 4.70*d* (*J* = 7.4 Hz) for **G**, and δ_C 59.0 and δ_H 3.90*d* (*J* = 6.9 Hz) for **63**. Therefore,

compound **G** was determined to be a new cyclopeptide alkaloid attached to coumaroyl group and it was named cambodine G.

Known alkaloids

On a combination of their MS, 1D and 2D NMR, and comparison to the reported data, two known compounds **H** and **I** were identified as frangufoline (Devi et al., 1987) or sanjoinine A (Han B. H. and Park M. H. 1987) and lotusanine B (Abu–Zarga et al., 1995), respectively. Herein we report complete ^{1}H– and ^{13}C NMR assignments for both compounds and the establishment of the configuration of **I**.

Compound **H** (ssss4449) was obtained as colorless needles, mp 216–218 ^{o}C. Its molecular formula was established as $C_{31}H_{42}N_4O_4$ from ESIMS *m/z* 535.5 $[M+H]^+$, *m/z* 533.3 $[M–H]^-$ ($C_{31}H_{42}N_4O_4$ 534.69).

Connections among the structural subgroups were provided by analysis of its HMBC and NOESY spectra (Figure 54). The NOE correlations were observed for styrylamine proton at δ_H 6.46 (NH–3) to H–5 (δ_H 4.04) of leucyl proton together with HMBC correlations of H–2 (δ_H 6.67) to C–1 (δ_C 115.6) and C–14 (δ_C 131.8), and H–1 (δ_H 6.36) to C–2 (δ_C 125.6), C–14 and C–15 (δ_C 131.7) indicating that the leucine amino acid was attached to the styrylamine unit. HMBC correlations from H–8 and H–9 to β–OH–leucine carbonyl C–7 (δ_C 171.6) confirmed the connection between the ring–bound leucine unit and β–OH–leucine amino acids. A strong NOE enhancement displayed in the NOESY spectrum between the proton at δ_H 4.50 (H–8) and NH–24 (δ_H 7.90) of *N*,*N*–dimethylphenylalanine unit, and HMBC correlation observed between NH–24 and terminal carbonyl C–25 (δ_C 172.6) confirmed that the *N*,*N*–dimethylphenylalanine unit is attached to the β–OH–leucine unit. Furthermore, the NOE correlation of the *N,N*–dimethyl proton δ_H 2.25 to H–8, and HMBC correlations of H–26 to C–25, and *N,N*–dimethyl carbon, of H–27 to C–25 and of H–29 and H–30 to C–28, supported the placement of *N*–methyl phenylalanine as the end amino acid (Table 20). These evidences led to a conclusion that the structure of compound **H** was frangufoline.

Table 20 Comparison of ^{1}H– and ^{13}C NMR data of compound **H** with frangufoline (**6**)

Position	δ_H		δ_C	
	I (300 MHz)	**6** (500 MHz)	**I** (75 MHz)	**6** (125 MHz)
1	6.36 *d* (7.5)	6.38 *d* (7.7)	115.6	123.1
2	6.67 *dd* (10.6, 7.5)	–	125.6	125.9
NH–3	6.46 *d* (10.6)	–	–	–
CO–4	–	–	167.4	167.6
5	4.04 *ddd* (11.3, 7.8, 3.3)	4.05 *m*	52.6	52.7
NH–6	5.78 *d* (7.8)	–	–	–
CO–7	–	–	171.6	171.5
8	4.50 *dd* (7.3, 10.0)	4.65 *m*	55.2	55.4
9	5.0 *d* (7.3, 1.5)	4.92 *dd* (7.5,1.9)	81.7	81.9
11	–	–	155.9	156.2
12	7.13 *dd* (8.1, 2.6)	7.00–7.50 *m*	123.0	122.8
13	7.04 *m*	7.00–7.50 *m*	130.2	115.9
14	–	–	131.8	131.8
15	7.07 *m*	7.00–7.50 *m*	131.7	130.3
16	7.19 *m*	7.00–7.50 *m*	122.7	132.0
17	α 1.69 *m* , β 1.23–1.29[a] (signal overlapped)	3.10 *m*	39.1	39.4
18	0.60–0.65[a]	2.02 *m*	23.1	24.5
19	0.65 *d* (6.5)	1.24 *d* (6.8)	24.3	20.6
20	0.60 *d* (6.5)	1.14 *d* (6.8)	20.4	23.1
21	3.16–3.23[a] (signal overlapped with H–21, H–27)	2.05 *m*	29.3	29.4
22	1.28 *d* (6.7)	0.71 *d* (6.6)	20.3	15.1
23	1.01 *d* (6.7)	0.57 *d* (6.6)	15.0	20.4
NH–24	7.90 *d* (10.0)	–	–	–
CO–25	–	–	172.6	172.7
26	3.16–3.23[a] (signal overlapped with H–21, H–27)	–	70.4	70.6
27	α 3.16–3.23[a] (signal overlapped with H–21, H–26) β 2.85 *dd* (15.8, 8.3)	3.34 *br d* (14.8)	30.6	30.9
27a	–	–	140.3	140.4
28,28′	7.26 *m*	–	128.5	128.6
29,29′	7.25 *m*	–	128.9	129.0
30	7.22 *m*	–	126.1	126.2
NMe_2	2.25 *s*	2.97*s* , 2.85*s*	41.8	41.9

[a] Assignments confirmed by COSY.

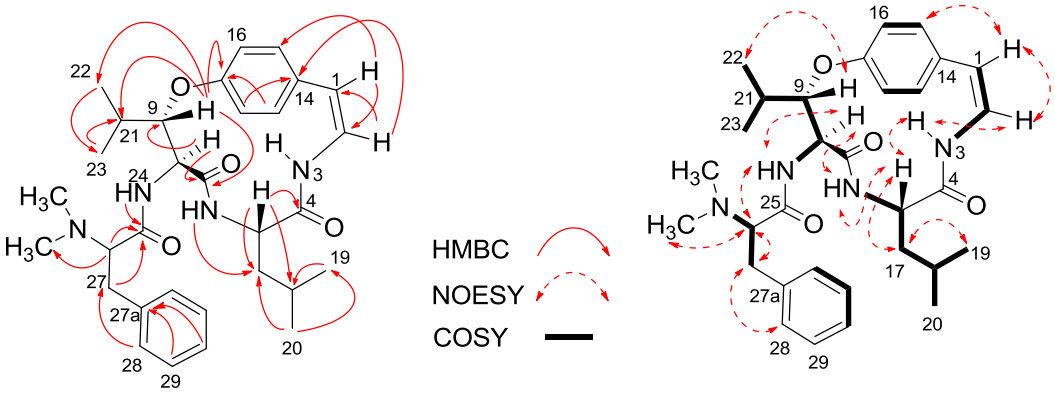

Figure 55 Selected HMBC, COSY and NOESY correlations for compound **H**

The *Z*–geometry of the double bond was established on the basis of the coupling constant value (Morel et al., 1999) of 7.5 Hz for H–1 (6.36*d*, *J* = 7.5 Hz) and H–2 (6.67*dd*, *J* = 10.6, 7.5 Hz). The coupling constant value of 10.6 Hz between H–2 and NH–3 (6.46*d*, *J* = 10.6 Hz) protons and a weak NOE interaction observed among them indicated *trans*–coplanar orientation of these two protons (Morel et al., 1999). The NH–6 (5.78*d*, *J* = 7.8 Hz) and H–5 (4.04*ddd*, *J* = 11.3, 7.8, 3.3 Hz) protons showed the coupling constant of 7.8 Hz and a small NOE cross peak was observed between both protons suggesting they were in the opposite orientation. In contrast, strong NOE enhancement observed between NH–6 and H–8 (4.50*dd*, *J* = 7.3, 10.0 Hz) indicated that these protons reside on the same side. The vicinal coupling constant value 7.3 Hz of the methine protons H–8 and H–9 (5.0*d*, J = 7.3, 1.5 Hz) indicated a *trans*– configuration (Gournelis, Laskaris and Verpoorte, 1998) together with weak NOE effect observed between these two protons in its NOESY spectrum further supported the *trans*– relationship between H–8 and H–9.

The ^{1}H and ^{13}C NMR chemical shifts, together with the coupling constant of H–8/H–9 (*J* = 7.3 Hz), for compound **H** followed the similar values to those of frangufoline. A comparison of its NMR data with those of franganine (**7**), which was assigned as all *S* absolute configuration by X–ray diffraction analysis of franganine methiodide salt (**7′**) (Caro et al., 2012), along with its levorotatory optical rotation $[\alpha]_D^{27}$ – 218° (Giacomelli et al., 2004), led to a conclusion that this cyclopeptide also has all *S*–configuration (Figure 17) (Lomchoey, 2011).

Frangufoline (**6**) (Zarga et al., 1995) or daechuine S1 (Han B. H., Park and Han Y.N. 1989) or Sanjoinine A (Han B. H., Park and Han Y. N., 1990) was isolated from several *Ziziphus* plants, such as the hexane extract of the seeds of *Z. vulgularis* var. *spinosus* (Han B. H., Park and Han Y. N., 1990).

Compound **I** (sss4635) was obtained as colorless needles, mp 185–187 ^{o}C and gave violet–blue coloration with anisaldehyde–H_2SO_4 reagent. On the basis of its ESIMS *m/z* 619.5 $[M–H]^-$, a molecular formula of **I** was established as $C_{37}H_{40}N_4O_5$ with support of its ^{13}C NMR spectrum. The UV absorption maxima at 216, 224 and 279 nm were found, which was consistent with the 14–membered type cyclopeptide alkaloid with coumaroyl moiety (Zarga et al., 1995; Han B. H., Park and Han Y. N. 1990; Gonzalez et al., 1974). Their IR spectra exhibited diagnostic peaks for amine (3277 cm^{-1}), amide (1624–1646 cm^{-1}) and aryl ether (1238 cm^{-1}) functions.

The ^{1}H, ^{13}C NMR (Table 21, Figure 56), DEPT and HMQC spectra of compound **I** indicated the presence of 31 carbon resonances, which provided signals for four methyls, four methylenes, twenty three methines and eight quaternary carbons including four carbonyl carbons. The ^{1}H NMR spectrum ($CDCl_3$ 300 MHz) of **I** exhibited signals for *trans*–double bonds at 6.69*d* (*J* = 15.4 Hz, H–32) and 7.73*d* (*J* = 15.4 Hz, H–33), which were assigned to the *trans*–coumaroyl protons, C–32 (δ_C 116.9) and C–33 (δ_C 144.1), respectively, and the carbonyl carbon (CO–31) of coumaroyl group displayed at δ_C 166.5 (de Oliveira et al., 2009). The C–26 methine proton of the proline appeared as a doublet at 4.16*d* (*J* = 7.6 Hz) and three methylene group of proline showed at δ_H 2.26*m* (H_α–27), 1.56*m* (H_β–27), 2.13*m* (H–28), 3.70*quin* (*J* = 8.7 Hz, H_α–29) and 3.67*quin* (*J* = 8.7 Hz, H_β–29). Two sets of doublets corresponding to methyl protons of β–OH–leucine H–22 and H–23 showed at δ_H 1.14*d* (*J* = 6.7 Hz) and 0.69*d* (*J* = 6.6 Hz), respectively. The C–8 (δ_C 55.1) and C–9 (δ_C 81.8) methine protons appeared as double doublets at δ_H 4.32*dd* (*J* = 9.4, 6.9 Hz) and 4.94*dd* (*J* = 6.9, 1.6 Hz), respectively, which were due to the α– and β–protons of the β–OH–leucine, respectively. The C–5 methine proton appeared at δ_H 4.62*ddd* (*J* = 11.0, 7.9, 4.1 Hz) and the C–17 methylene protons of the phenylalanine showed at δ_H 3.42 (*dd*, 16.0, 4.0, H_α–17) and δ_H 2.75*dd* (*J* = 16.0, 11.0 Hz, H_β–17). The

H–1 olefinic proton identified as a doublet at δ_H 6.36*d* (*J* = 7.6 Hz), the second olefinic proton at C–2 (δ_C 125.5) and NH–3 appeared at δ_H 6.73*dd* (*J* = 10.4, 7.6 Hz) and 6.56*d* (*J* = 10.4 Hz), respectively. The doublets of NH protons were exhibited at δ_H 6.09*d* (*J* = 7.9 Hz, NH–6), 8.09*d* (*J* = 9.4 Hz, NH–24). Moreover, the unambiguous assignment of all protons of compound **I** was made by a series of 2D NMR experiments reported in Table 21.

Connections among four subgroups were provided by analysis of its HMBC and NOESY spectra. The NOESY correlations were observed for styrylamine proton at δ_H 6.56 (NH–3) to H–5 (δ_H 4.62) of phenylalanine proton together with HMBC correlations of H–2 (δ_H 6.73) to C–1 (δ_C 115.5) and C–15 (δ_C 131.8), and H–1 (δ_H 6.36) to C–2 (δ_C 125.5), C–14 (δ_C 136.6) and C–15 indicating that phenylalanine amino acid is attached to the styrylamine unit. HMBC correlations from H–8 and H–9 to *β*–OH–leucine carbonyl C–7 (δ_C 171.1) confirmed the connection between the ring–bound leucine unit and *β*–OH–leucine amino acid. The NOESY correlations of H–29 (δ_H 3.58) to *trans*–double bond proton H–32 (δ_H 6.69) supported that the *trans*–coumaroyl utit is connected to the *N*–proline unit. The strong NOE effects between the proton at δ_H 8.09 (NH–24) to H–8 (δ_H 4.32) and H–26 confirmed that the *N*–coumaroylproline unit is attached to the *β*–OH–leucine amino acid (Figure 55). These evidences led to the conclusion that the structure of compound **I** deduced to be lotusanine B.

Lotusanine B (**21**) was isolated from the C_6H_6 extract of the whole plant (except the roots) of *Z. lotus* (Abu–Zarga et al., 1995).

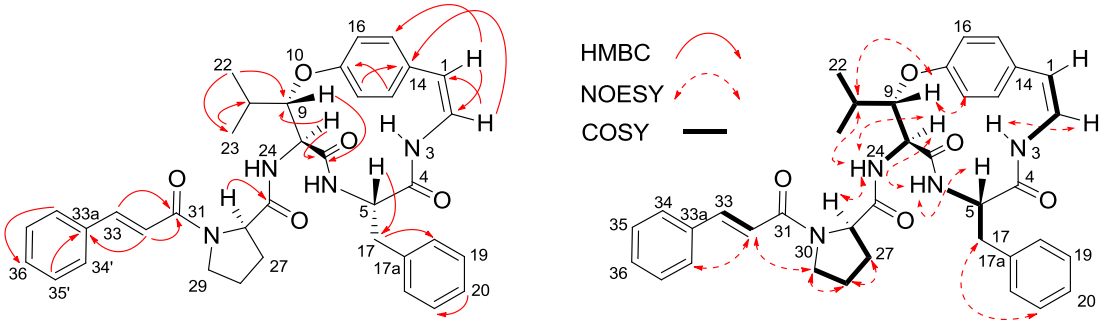

Figure 56 Selected HMBC, COSY and NOESY correlations for compound **I**

Table 21 ^{1}H–, ^{13}C– and 2D NMR data of compound **I** in $CDCl_3$

Position	δ_H	δ_C	HMBC correlations	NOESY correlations
1	6.36 *d* (7.6)	115.5	C–2, C–15	–
2	6.73 *dd* (10.4, 7.5)	125.5	C–1, C–15	NH–3, H–5,
NH–3	6.56 *d* (10.4)	–		H–2
4	–	166.9	–	–
5	4.62 *ddd* (11.0, 7.9, 4.1)	53.4		NH–3, NH–6, H–17, H–19
NH–6	6.09 *d* (7.9)	–	–	H–5, H–17
CO–7	–	171.1	–	–
8	4.32 *dd* (9.4, 6.9)	55.1	C–7, C–9	H–21, NH–24
9	4.94 *dd* (6.9, 1.6)	81.8	C–8	H–21, H–22, H–23
11	–	156.0	–	–
12	7.22 *m*[a]	123.4	C–14	–
13	7.04 *m*[a]	126.5	C–11	–
14	–	136.6	–	–
15	7.05 *m*[a]	131.8	C–16	–
16	7.17 *m*[a]	123.4		–
17	α 3.42 *dd* (16.0, 4.0)	35.9	C–17a, C–18	H–19
	β 2.75 *dd* (16.0, 11.0)			
17a	–	136.6	–	–
18,18′	7.27 *m*[a]	128.2	–	–
19,19′	7.07 *m*[a]	128.0	–	H–5, H–17
20	7.02 *m*[a]	130.1	C–19	
21	1.82 *ddd* (6.7, 6.6, 1.6)	29.0	–	H–8, H–9, H–22, H–23,
				NH–24, H–32
22	1.14 *d* (6.7)	14.5	C–9, C–21, C–23	H–21, H–23
23	0.69 *d* (6.6)	20.4	C–9, C–21, C–22	H–21, H–22, H–32
NH–24	8.09 *d* (9.4)	–	–	H–21, H–26, H–32
CO–25	–	171.4		
26	4.16 *d* (7.6)	59.1	C–25	NH–24, H–27
27	27α 2.26 *dd* (12.2, 4.4)	25.8	–	H–26, H–28
	27β 1.56 *m*			
27a	2.03 *m*	24.9	–	H–27, H–29
29	3.58 *m*	47.1	–	H–28, H32
31	–	166.5	C–31, C–32, C–33	
32	6.69 *d* (15.4)	116.9	C–30, C–31, C–33,	H–29, H–33, H–35
			C–34, C–35	
33	7.73 *d* (15.4)	144.1	–	H–21, H–23, NH–24, H–31
33a	–	134.6	–	–
34	7.56 *dd* (5.9, 2.0)	128.5	C–37	H–32
35	7.41 *t* (3.5, 2.9)	128.9	C–34	H–32
36	7.02 *m*	130.3	C–35, C–36	–

[a] Assignments confirmed by DEPT, HMQC and HMBC.

The comparison of ^{1}H and ^{13}C NMR data (Table 22) of the cyclic part of compound **I** with lotusanine B (**21**) (Abu–Zarga et al., 1995) showed similar chemical shifts in both compounds, except for C–1 [compound **I**: δ_C 115.5, δ_H 6.36*d* (*J* = 7.6 Hz); lotusanine B: δ_C 130.9, δ_H 6.02*d* (*J* = 7.8 Hz) (Abu–Zarga et al., 1995)] (Table 8). However, the comparison of ^{1}H and ^{13}C NMR data at C–1 of compound **I** with waltherine A (**332**) [δ_C 119.0, δ_H 6.40*d* (*J* = 7.0 Hz)], a cyclopeptide with the same cyclic part as **I**, gave the similar result (Morel et al., 1999). Moreover, the chemical shift of C–27 at 59.1 ppm was corrected to be 29.1 ppm in lotusanine B (**24**) (Abu–Zarga et al., 1995) by Tan and Zhou (2006) and this was comparable to our data (Lomchoey, 2011).

The stereochemistry of compound **I** was determined by comparison of the corresponding chemical shifts with those of amaiouine (**63**), a cyclopeptide with related structure to that of compound **I** (de Oliveira et al., 2009). The X–ray analysis of amaiouine confirmed all *S* configuration at amino acid residues in its structure. The levorotatory optical rotation $[\alpha]_D^{27}$ = –117° similar to amaiouine $[\alpha]_D^{25}$ = –87° (de Oliveira et al., 2009) also suggested that compound **I** posesses all *S* configuration as shown in Figure 19.

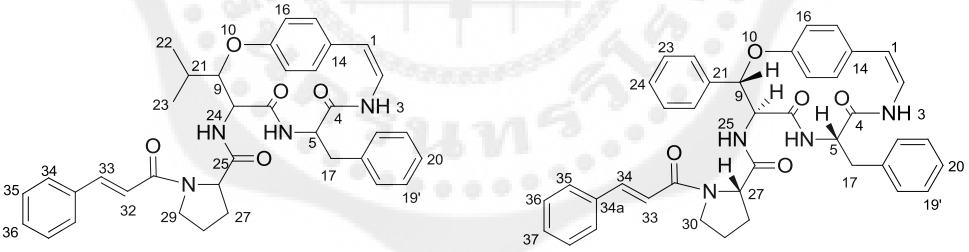

Lotusanine B (**21**)

Amaiouine (**63**)

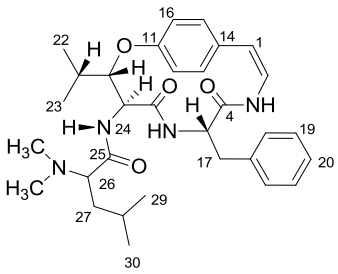

Waltherine A (**332**)

Figure 57 Structures of lotusanine B (**21**), amaiouine (**63**) and waltherine A (**332**)

Table 22 Comparison of ^{1}H– and ^{13}C NMR data of compound **I** with lotusanine (**24**)

Position	δ_H		δ_C	
	I (300 MHz)	**24** (500 MHz)	**I** (70 MHz)	**24** (125 MHz)
1	6.36 *d* (7.6)	6.02 *d* (7.8)	115.5	130.9
2	6.73 *dd* (10.4, 7.5)	6.32 *d* (7.6)	125.5	131.8
NH–3	6.56 *d* (10.4)	–	–	–
4	–	–	166.9	166.6
5	4.62 *ddd* (11.0, 7.9, 4.1)	4.30 *dd* (9.2, 6.7)	53.4	53.9
NH–6	6.09 *d* (7.9)	–	–	–
CO–7	–	–	171.1	167.7
8	4.32 *dd* (9.4, 6.9)	4.60 *m*	55.1	55.2
9	4.94 *dd* (6.9, 1.6)	5.00 *dd* (6.6, 1.9)	81.8	81.9
11	–	–	156.0	156.0
12	7.22 *m*[a]	7.38–7.54 *m*	123.4	123.5
13	7.04 *m*[a]	7.38–7.54 *m*	126.5	117.1
14	–	7.38–7.54 *m*	136.6	126.6
15	7.05 *m*[a]	7.38–7.54 *m*	131.8	123.4
16	7.17 *m*[a]	7.38–7.54 *m*	123.4	130.1
17	α 3.42 *dd* (16.0, 4.0)	7.38–7.54 *m*	35.9	36.0
	β 2.75 *dd* (16.0, 11.0)			
17a	–	–	136.6	131.8
18,18'	7.27 *m*[a]	7.38–7.54 *m*	128.2	128.8
19,19'	7.07 *m*[a]	7.38–7.54 *m*	128.0	129.0
20	7.02 *m*[a]	7.38–7.54 *m*	130.1	125.5
21	1.82 *ddd* (6.7, 6.6, 1.6)	1.80 *m*	29.0	28.9
22	1.14 *d* (6.7)	0.66 *d* (6.6)	20.4	14.0
23	0.69 *d* (6.6)	1.12 *d* (6.6)	14.5	19.7
NH–24	8.09 *d* (9.4)	–	–	–
CO–25	–	–	171.4	171.5
26	4.16 *d* (7.6)	3.39–3.55 *m*	59.1	59.1
27	27α 2.26 *dd* (12.2, 4.4)	3.39–3.55 *m*	25.8	59.1[b]
	27β 1.56 *m*			
28	2.03 *m*	3.39–3.55 *m*	24.9	28.1
29	3.58 *m*	3.39–3.55 *m*	47.1	47.2
CO–31	–	–	166.5	171.4
32	6.69 *d* (15.4)	6.68 *d* (15.4)	116.9	128.2
33	7.73 *d* (15.4)	7.72 *d* (15.4)	144.1	144.1
33a	–	–	134.6	136.7
34	7.56 *dd* (5.9, 2.0)	7.3– 7.54 *m*	128.5	128.1
35	7.41 *t* (3.5, 2.9)	7.3– 7.54 *m*	128.9	130.9
36	7.02 *m*	7.3– 7.54 *m*	130.3	126.6

[a] Assignments confirmed by DEPT, HMQC and HMBC.

[b] Data were corrected to 59.1 ppm by Tan and Zhou (Tan and Zhou, 2006).

All isolated compounds were tested for their *in vitro* biological properties. Only cambodine F exhibited antiplasmodial activity against *P. falciparum* (Trager and Jensen, 1976) with the IC_{50} values of 6.1 μM (4.23 μg/mL), probably due to a specific 1,2–dimethylimidazolidin–4–one moiety. Cambodines B and C, and lotusanine B showed antimycobacterial effect against *M. tuberculosis* with the IC_{50} values of 50, 100 and 50 μg/mL, respectively (Collins and Franzblau, 1997). This report also confirmed *in vitro* antiplasmodial and antimycobacterial activities of cyclopeptide alkaloids we have previously described (Suksamrarn et al., 2005; Panseeta et al., 2011). In addition, compounds cambodine C–E exhibited cytotoxic activity against human lung cancer cell lines (NCI) at values of IC_{50} 12.77, 19.57 and 21.05 μg/mL, respectively. All compounds were nontoxic to Vero cell except for cambodine **E**, which exhibited cytotoxicity to this cell line with IC_{50} 25.72 μg/mL.

Table 23 Bioactivities of cyclopeptide alkaloids (μg/mL)

Compound	Bioactivities			
	M. Tuberculosis	*P. falciparum*	NCI–H187	Vero cells
Cambodine A	inactive	inactive	inactive	nontoxic
Cambodine B	50	inactive	inactive	nontoxic
Cambodine C	inactive	100	12.77	nontoxic
Cambodine D	inactive	inactive	19.57	nontoxic
Cambodine E	inactive	inactive	21.05	25.72
Cambodine F	inactive	4.23 (6.1 μM)	inactive	nontoxic
Cambodine G	inactive	inactive	inactive	nontoxic
Frangufoline	inactive	inactive	inactive	nontoxic
Lotosanine B	50	inactive	inactive	nontoxic
Isoniazid	0.4 μM	–	–	–
Kanamycin sulfate	4.2 μM	–	–	–
Dihydroartemisinin	–	4.2 nM	–	–

The roots of *Z. oenoplia* (L.) Mill. var. *brunoniana*

Betulinic acid (**1**) was participated from the MeOH extract and further crystalized in MeOH–CH_2Cl_2 to yield colorless needles (6 g). The filtrate containing betulinic acid was concentrated and combined with other solid parts from other *Ziziphus* plants and then crystalized from MeOH–CH_2Cl_2.

The roots of *Z. oenoplia* Mill. var. *oenoplia*

Betulinic acid (**1**) was obtained in 3.5 g as a major product from EtOAc extract (28.3 g). A solid of triterpenes which contained almost pure betulinic acid was combined with solids from other *Ziziphus* plants.

A combination of solid parts of *Ziziphus* triterpenes was then crystalized from MeOH–CH_2Cl_2 and recrystallized from the same solvent mixture for a few times to obtain a white powder in a combined amount of 44 g.

Structural modification of some naturally derived compounds

Not all naturally occurring compounds are bioactive, but many bioactive compounds show low activity levels because of their limited solubility in aqueous medium and/or stability. Glycosylation offers a convenient approach to increase pharmacological activity, stability, and solubility of natural products without inducing toxic byproducts at target cells. Moreover, sugar moiety of natural product may contribute to specific interactions with the biological target (Diaz et al., 2010).

This work describes a structural modification of natural products to enhance their hydrophilicity.

Glycosylation of betulinic acid

Betulinic acid (**1**) was crystalized from a combined solid parts from *Ziziphus* plant. Previous synthetic and medicinal chemistry studies of betulinic acid derivatives reported that (specify) properties of **1** can be improved upon the addition of a sugar moiety at either C–3 and/or C–28 position. Importantly, it has been reported that glycosides of **1** have higher aqueous solubility than unmodified betulinic acid and the glycosylation can also

enhance pharmacokinetics properties (Gauthier et al., 2006; Abdu et al., 2012). The *O*–glycosyl residue at C–2 as along with free carboxyl group at C–28 of **1** was found to be an important structural determinant for enhancing its cytotoxicity (Thibeault et al., 2007). However, no previous study described the synthesis and investigation of α–gluco, α–galacto and β–mannoside of **1**.

In glycosylation the leaving group (LG) employed at the anomeric carbon of a glycosyl donor. Generally, the glycosylation mechanism starts when adding an electrophilic promoter (P). Lewis acid will activate the LG to form donor–promoter complex, and then transform into;

a) for a non–participating at C–2 (Scheme 22) such as *O*–benzyl, the glycosyl carbocation which exists in its stabilized resonance form, oxacarbenium ion. The subsequent nucleophilic attack of the glycosyl acceptor (ROH) is possible mainly from both the bottom face of the sugar ring, leading to the formation of α–(1,2–*cis*) linkage as major product.

b) for a participating at C–2 (Scheme 22) such as *O*–benzoyl, upon dissociation of the leaving group, a short lived positively charged species is formed and which is immediately transformed into more stable, lower–energy acyloxonium ion by intramolecular attack. The subsequent direct nucleophilic attack on C–1 is the route to the β–(1,2–*trans*) glycoside product (Mydock and Demchenko, 2010).

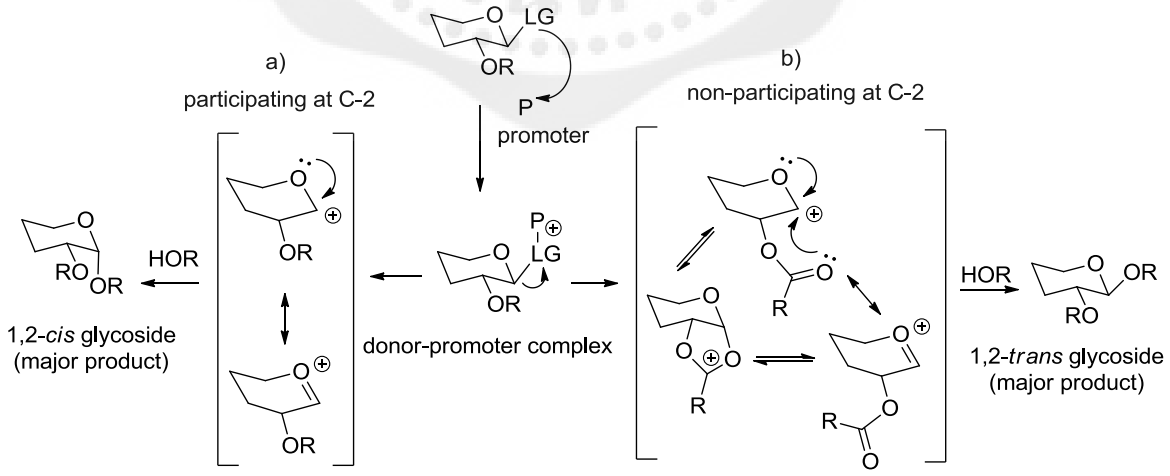

Scheme 22 General mechanisms of glycosylation

In order to obtain a series of 1,2–*cis*–linked glycosides we developed a series of new glycosyl donors based on highly reactive OFox imidates developed by the Demchenko lab for glycosylation of sugar acceptors (Nigudkar, Stine and Demchenko, 2014). In application to mannosylation we also employed 3–*O*–picoloyl group that is known to assist in β–glycosylations via so–called H–bond–mediated aglycone delivery (HAD) (Pistorio, Yasomanee and Demchenko 2014). The general outline of this concept is shown in Scheme 23.

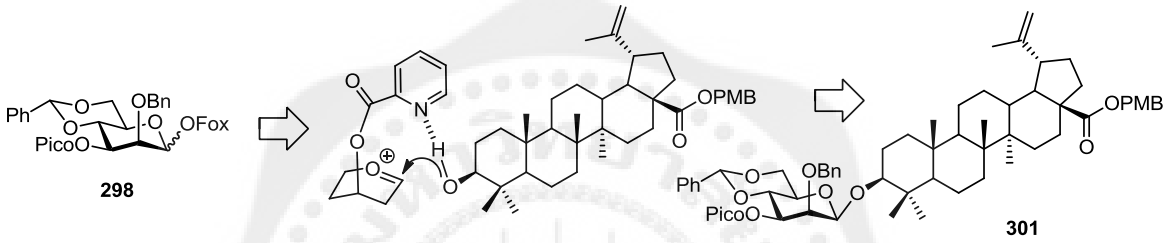

Scheme 23 3–*O*–Picoloyl–assisted β–*D*–mannosylation

The synthesis was started from the protection of 28–carboxyl of **1** (1 g, 2.19 mmol) with PMBCl (1.48 mL, 21.90 mmol) to yield ester **1′** (1.27 g, 99%). To establish the most suitable reaction conditions, ester **1′** was initially coupled with known glycosyl donors **288**, **293** and **298** in the presence of trimethylsilyl trifluoromethanesulfonate (TMSOTf, 0.11 equiv.) as a Lewis acid promoter at –30 ^{o}C to rt (Scheme 24). To our surprise only glycosylation of OFox donor **298** was effective. Therefore, donors **288** and **293** were converted to their corresponding OFox donors **287** and **292**, respectively. Aglycone acceptors **1′** was successfully glycosylated with all OFox donors in the presence of TMSOTf (0.11 equiv) at –30 ^{o}C to rt (Scheme 25).

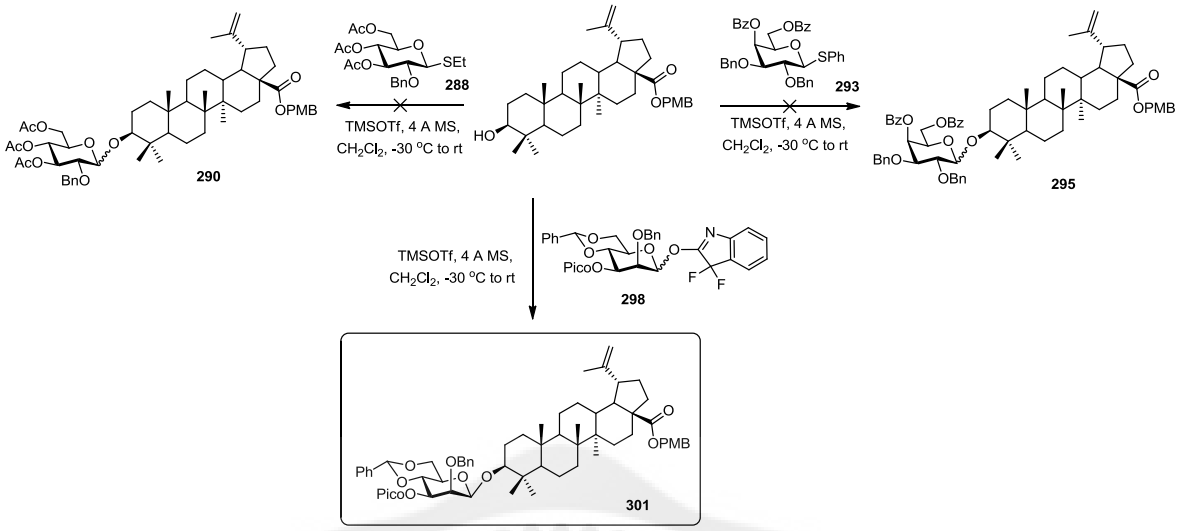

Scheme 24 Condition studies of the synthesis of betulinic acid saponins

The structures of synthetic betulinic acid glycosides were elucidated mainly by the analysis of their NMR and MS spectroscopic data. The presence of the sugar region at δ_H 3.5–5.5 ppm in the ^{1}H–NMR spectra confirmed the attachment of the sugar moiety to lupane scaffold (*see* appendix). The α–glycosidic bond in 3–*O*–α–*D*–gluco– and 3–*O*–α–*D*–galactopyranosyl betulinic acid (**291** and **297**, respectively) was confirmed by small vicinal coupling constants between H–1′ and H–2′ ($^3J_{1,2}$) of 3.6 and 4.0 Hz in **291** and **297**, respectively (Yasomanee and Demchenko 2012). Hydrophilicity of synthetic saponins was evaluated from their Clog*P* which was predicted by ACD/ChemSketch Freeware (Osterberg and Norinder 2001). All synthetic saponins display log*P* value of 6.97 (Table 25). The result showed that the sugar moiety enhances hydrophilicity of betulinic acid which showed log*P* of 6.61 (Elusiyan, et al., 2011).

Their biological activity will be further evaluated.

Table 24 Calculated log*P* of betulinic acid saponins

Entry	Compound	Clog*P*
1	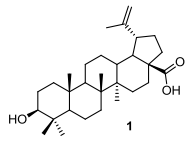 **1**	8.94±0.39
2	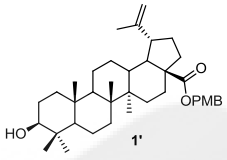 **1'**	11.62±0.42
3	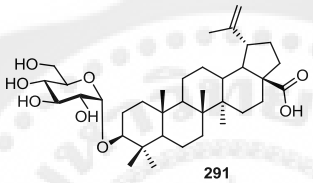 **291**	6.97±0.44
4	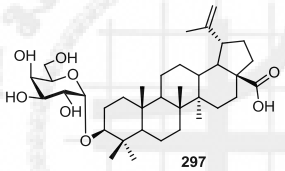 **297**	6.97±0.44
5	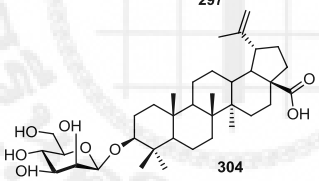 **304**	6.97±0.44

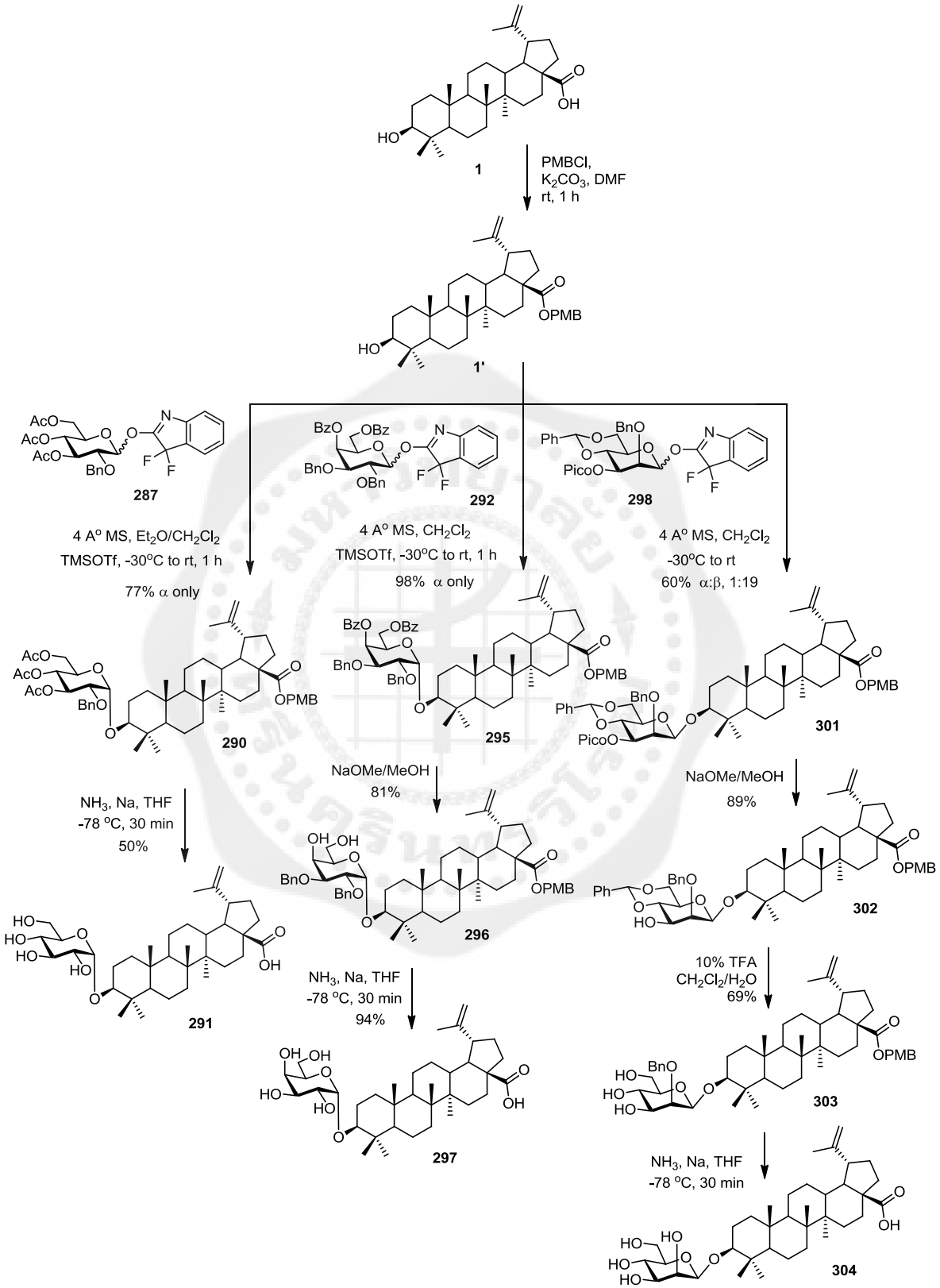

Scheme 25 Overall synthetic sequences of betulinic acid saponins

Glycosylation of α–mangostin

A series of mangostin glycosides was synthesized by the structural modification of OH at C–3 (3–*O*–glycoside), C–6 (6–*O*–glycoside) and bis–glycosylation (3,6–di–*O*–glycoside). The screening of reaction conditions showed that the glycosylation at phenolic OH of **234** can be accomplished with glycosyl bromide donors in the presence of a weak base (Pai et al., 1979).

Due to the intramolecular hydrogen bond between the hydroxyl group at C–1 and C–8 carbonyl group, the C–1 hydroxyl moiety is less reactive (Hyz et al., 2011). We first targeted the preparation of per–benzoylated glycopyranosyl mangostin derivatives. To control the regioselectivity of glycosylations the molar ratio between the donor and acceptor components of the reaction was investigated (Sudta et al., 2013).

In order to obtain 6–*O*–monoglycosylated products (**316**–**318**), molar ratio of each corresponding donor was established to be 1.3 equiv. under high dilution using CH_3NO_2 as the solvent. These conditions were shown to effectively slow down the glycosylation of **234**. It is noteworthy that glucosylation in CH_3NO_2 under various reaction conditions gave only 6–*O*–monoglycosylated product **316** (50% yield), whilst a trace amount of the starting material **234** was also observed on TLC. Even in the presence of the excess base yielded **316** as the major product (Table 24). In this work, we demonstrated that *O*–glucosylation reaction showed exclusive regioselection towards the hydroxyl group at C–6 position. When excess donor was used the formation of 3,6–di–*O*–glucoside (**311**) was observed. Interestingly, the reaction in the presence of excess base (10 equiv) and excess donor (5 equiv) under reflux condition gave 6–*O*–benzoyl mangostin (**234′**). Fortunately, unlike other alkylation of **234**, the 3–*O*–mono glycoside was not observed for all glycosylations probably due to the steric effect of the neighboring 2–prenyl group. Using the same reaction conditions, 6–*O*–mono galactoside (**317**) was obtained in 61% yield. However, 6–*O*–mono mannoside (**318**) was not observed when CH_3NO_2 was used as the solvent. A similar mannosylation reaction in acetone was much more effective and gave the desired product **318** in 59% yield.

To obtain 3,6–di–*O*–substituted glycosides, the treatment of **234** with appropriate donors (**308**–**310**) was carried out using excess donor (5 equiv) and excess K_2CO_3 (5 equiv) under reflux condition. This approach led to complete substitution and afforded the desired 3,6–di–*O*–substituted products (**311**–**313**) in good yields. In particular,

the galactosylation reaction was the most effective, which was reflected in a much higher yield of 94% for the disubstituted product in comparison to that of glycosylation with donors of the gluco (31%) and manno series (58%).

Table 25 Condition study for the synthesis of α–mangostin perbenzoylated glycosides

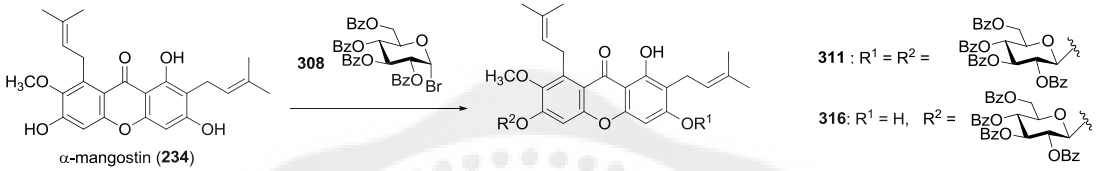

Entry	Donor, equiv	K_2CO_3, equiv	Solvent	Temp (^{o}C), Time (d, h)	Product, 3,6–*O*–di	Product, 6–*O*–mono	di/mono (w/w)
1	1.3	2	CH_3NO_2	rt to 60 ^{o}C, 5 d	–	**316**, 50[a]	mono only
2	3	8	CH_3NO_2	rt, 18 h	**311**, 31	**316**, 32	1.7/1
3	5	5	CH_3NO_2	rt to 60 ^{o}C, 3 d, 21 h	**311**, 23	**316**, 35	1/1
4	1.3	5	Acetone	rt to 60 ^{o}C, 17 h	–	**316**, 10[a]	mono only
5	5	8	Acetone	rt to 60 ^{o}C, 5 d, 20 h	**311**, 23	**316**, 41	1/1.1
6	5	10	Acetone	rt to 60 ^{o}C, 3 d, 17 h	nonglucosyl product **234′**, 40		6–*O*–Bz only
7	5	8	CH_3NO_2	rt to 60 ^{o}C, 1 d, 21 h	–	**316**, 42[a]	NA
8	5	8	CH_3CN	rt to 60 ^{o}C, 1 d, 21 h	–	**316**, 33[a]	NA
9	5	8	THF	rt to 60 ^{o}C, 5 d, 20 h	No reaction		NA
10	5	8	DMF	55 to 100 ^{o}C, 1 d, 21 h	No reaction		NA

[a] Reaction was not complete, α–mangostin showed on TLC

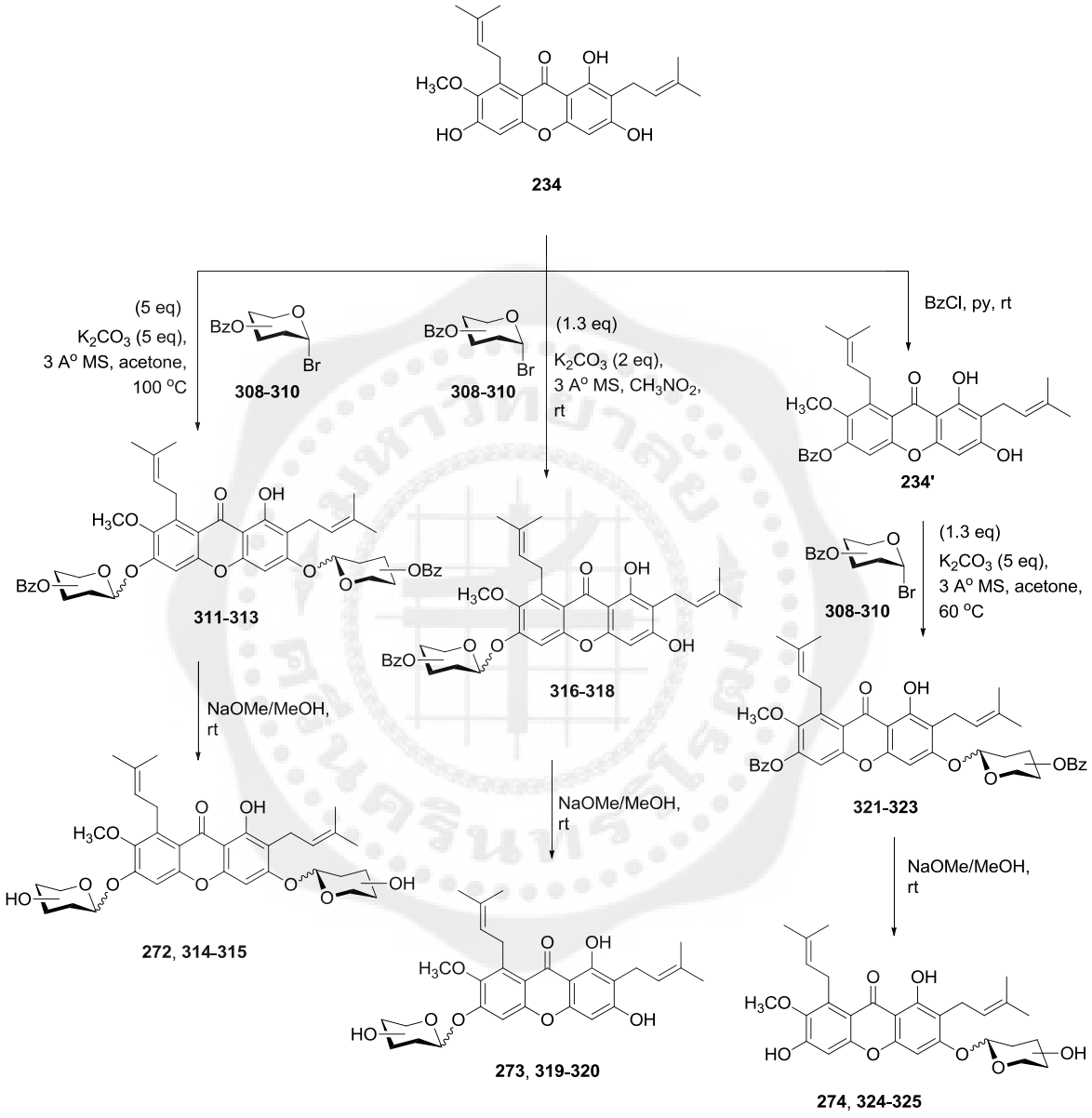

Scheme 26 Synthesis of α–mangostin glycosides

Table 26 Synthesis of α–mangostin perbenzoylated glycosides

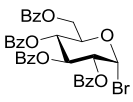
308

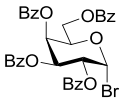
309

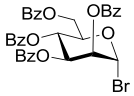
310

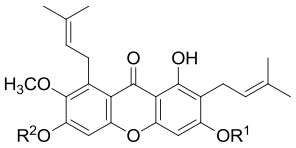

234 : $R^1 = R^2 = H$
234': $R^1 = H$, $R^2 = Bz$

Entry	Donor	Acceptor	Product			Temp (^{o}C), Time (d, h)	%Yield, ratio α/β
			No.	R^1	R^2		
1	**308**	**234**	**311**	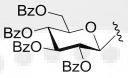	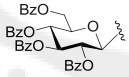	rt to 60 ^{o}C, 3 d, 21 h	31[a], β only
2	**309**	**234**	**312**	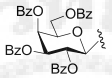	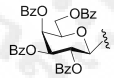	rt, 2 d, 17 h	94, β only
3	**310**	**234**	**313**	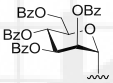	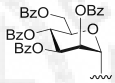	rt to 60 ^{o}C, 4 d 19 h	58, α only
4	**308**	**234**	**316**	H	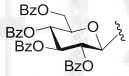	rt to 60 ^{o}C, 5 d	50[a], β only
5	**309**	**234**	**317**	H	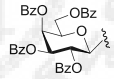	rt, 2 d, 20 h	61, β only
6	**310**	**234**	**318**	H	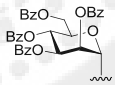	rt, 6 d, 18 h	59, α only
7	**308**	**234'**	**321**	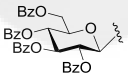	H	60 ^{o}C, 2 d, 12 h	69, β only
8	**309**	**234'**	**322**	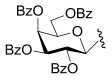	H	60 ^{o}C, 18 h	69, β only
9	**310**	**234'**	**323**	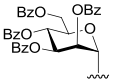	H	60 ^{o}C, 19 h	68, α only

[a] 3,6–*O*–di–glucosyl analogue was obtain as minor product for all glucosylation conditions of α–mangostin

Table 27 Debenzoylation of perbenzoylated analogues and calculated log*P* of glycopyranosyl α–mangostins

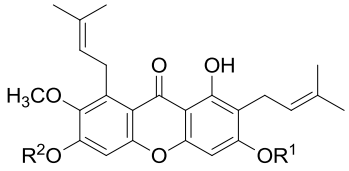

Entry	Product	R^1	R^2	%Yield	ClogP
1	**272**	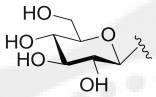	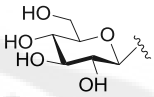	96	0.87±1.18
2	**314**	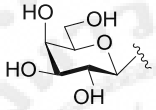	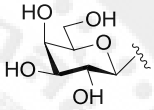	63	0.87±1.18
3	**315**	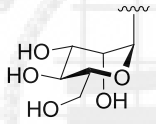	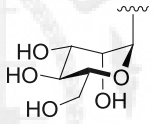	65	0.87±1.18
4	**273**	H	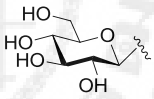	88	3.04±1.17
5	**319**	H	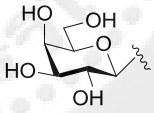	61	3.04±1.17
6	**320**	H	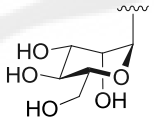	40	3.04±1.17
7	**274**	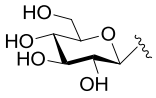	H	56	3.28±1.14
8	**324**	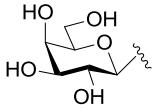	H	55	3.28±1.14
9	**325**	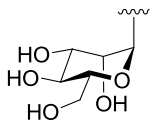	H	55	3.28±1.14

In case of 3–*O*–mono glycosylation, acceptor **234** was first converted to 6–*O*–benzoyl mangostin (**234′**). Acceptor **234′** was then glycosylated with 1.3 equiv donor in the present of K_2CO_3 (2 equiv) in acetone at reflux to afford a series of 3–*O*–mono glycosylated product in good yields ranging from 50% to 61%. It should be noted that experiments performed at high dilution gave 3,6–di–*O*–benzoyl mangostin (**234′′**) as a minor product.

All synthetic perbenzoylated glycosides were deprotected by the treatment with NaOMe/MeOH to obtain α–mangostin glycosides in good yields (40–96%). The structures of synthetic glycosides were elucidated mainly by analysis of their NMR and MS spectroscopic data. The presence of a down field singlet of hydrogen bonded signal and the presence of an additional sugar region at δ_H 3.5–5.5 ppm in the ^{1}H–NMR spectra confirmed the structure of α–mangostin glycosides (Tables 25–27).

Hydrophilicity of synthetic glycosides was evaluated from their Clog*P*, an ACD/ChemSketch Freeware was selected to predict Clog*P* (Osterberg and Norinder 2001). All synthetic mangostin glycosides displayed log*P* value of 0.87±1.18, 3.04±1.17 and 3.28±1.14 for 3,6–di–*O*–, 6–*O*–mono– and 3–*O*–monoglycosides, respectively (Table 25). The result showed that sugar moiety improves hydrophilicity of the α–mangostin scaffold which was measured log*P* of 6.4 (Koh et al., 2013) and Clog*P* of 5.44±1.13 predicted by ACD/ChemSketch.

Biological activities of all synthetic glucosyl mangostin analogues will be further investigated.

Table 28 ^{1}H– and ^{13}C NMR data of 3,6–di–*O*–glycosyl mangostin analogues

Position	δ_H (pyridine–d_5, 300 MHz)			δ_C (pyridine–d_5 , 75 MHz)		
	272	**314**	**315**	**272**	**314**	**315**
1	–	–	–	161.1	161.1	160.4
2	–	–	–	113.3	113.3	112.3
3	–	–	–	162.9	163.0	161.3
4	7.01*s*	7.08*s*	7.09*s*	93.6	93.7	93.9
4a	–	–	–	155.8	155.8	155.4
5	7.37*s*	7.42*s*	7.48*s*	103.0	102.5	102.3
6	–	–	–	157.4	157.5	156.0
7	–	–	–	145.4	145.4	144.9
8	–	–	–	137.8	137.7	137.1
8a	–	–	–	113.4	113.3	112.9
9	–	–	–	183.2	183.2	182.8
9a	–	–	–	105.2	105.2	104.8
10a	–	–	–	155.9	155.9	155.4
11	3.85*dd* (13.2, 7.4)	3.81*dd* (12.8, 7.0)	3.59*br dd* (6.8)	22.8	22.8	22.2
	3.69*dd* (13.2, 7.4)	3.65*dd* (12.8, 7.0)				
12	5.73*t* (7.4)	5.68*t* (7.0)	5.55*t* (6.8)	123.7	123.7	124.7
13	–	–	–	131.9	131.7	131.2
14	1.86*s*	1.82*s*	1.84*s*	18.6	18.5	18.8
15	1.60*s*	1.59*s*	1.62*s*	26.4	26.4	26.2
16	4.37*d* (5.9)	4.35*d* (6.0)	4.34*br dd* (6.8)	26.5	26.5	26.2
17	5.59*t* (5.9)	5.57*td* (6.0)	5.57*t* (6.8)	124.8	124.9	125.2
18	–	–	–	131.9	131.7	131.3
19	1.89*s*	1.88*s*	1.88*s*	18.8	17.5	19.1
20	1.73*s*	1.73*s*	1.71*s*	27.1	27.1	18.8
7–OCH_3	3.95*s*	3.89*s*	3.75*s*	61.6	61.6	60.2
1–OH	14.13*s*	14.11*s*	14.09*s*	–	–	–
	glucosyl	galactosyl	mannosyl			
1′	5.84*d* (7.3)	5.79*d* (7.6)	6.30*d* (5.3)	102.2	103.1	101.7
2′	4.39[a] *m*	4.86*br t* (7.6)	4.83*m*	75.4	72.7	71.7
3′	4.54[a] *m*	4.43*br dd* (7.6, 3.0)	4.80*m*	79.2	76.0	73.0
4′	4.44[a] *m*	4.67*br t* (3.0)	4.86*m*	71.6	70.7	68.5
5′	4.36[a] *m*	4.52*m*	4.46*m*	79.7	78.5	77.5
6′	4.42*m*, 4.21*m*	4.42*m*	4.58*m*, 4.39*m*	62.8	62.9	62.8
	glucosyl	galactosyl	mannosyl			
1′′	5.79*d* (7.3)	5.73*d* (7.6)	6.30*d* (5.3)	101.9	103.0	101.3
2′′	4.39[a] *m*	4.86*br t* (7.6)	4.83*m*	75.2	72.5	71.7
3′′	4.54*m*	4.43*br dd* (7.6,	4.80*m*	79.1	75.9	73.0
4′′	4.44[a] *m*	4.67*br t* (3.0)	4.86*m*	71.5	70.7	68.5
5′′	4.36[a] *m*	4.52*m*	4.46*m*	79.7	78.3	77.0
6′′	4.42 [a] *m*, 4.21*m*	4.42*m*	4.58*m*, 4.39*m*	62.8	62.8	62.8

[a] Signal overlapped with same sign, chemical shifts were determined by COSY and their coupled protons

Table 29 ^{1}H– and ^{13}C NMR data of 6–*O*–glycosyl mangostin analogues

Position	δ_H (300 MHz)			δ_C (75 MHz)		
	273[a]	**319**[b]	**320**[b]	**273**[a]	**319**[b]	**320**[b]
1	–	–	–	159.9	159.4	160.1
2	–	–	–	110.3	109.4	110.5
3	–	–	–	162.1	162.1	162.7
4	6.22*s*	6.45*s*	6.19*s*	92.1	91.0	91.9
4a	–	–	–	154.7	153.3	153.6
5	6.86*s*	7.10*s*	6.94*s*	101.4	100.6	101.3
6	–	–	–	154.7	154.4	164.2
7	–	–	–	143.2	142.8	143.4
8	–	–	–	137.5	135.4	136.7
8a	–	–	–	113.0	111.1	112.3
9	–	–	–	181.6	180.4	181.2
9a	–	–	–	102.9	101.5	102.4
10a	–	–	–	154.7	153.5	154.0
11	3.30[a] *d* (7.0)	3.62*d* (6.7)	3.35*d* (5.6)	21.0	20.3	21.0
12	5.19*t* (7.0)	5.55*t* (6.7)	5.27*t* (5.6)	122.0	120.9	122.3
13	–	–	–	131.4	129.3	129.1
14	1.74*s*	1.87*s*	1.70*s*	17.3	16.3	17.3
15	1.59*s*	1.69*s*	1.54*s*	25.3	24.2	25.2
16	4.02[c] *d* (6.4)	4.32*d* (6.4)	3.99*br d* (4.9)	25.4	24.3	25.3
17	5.13*t* (6.4)	5.41*t* (6.4)	5.14*t* (4.9)	122.8	122.5	122.9
18	–	–	–	131.5	129.3	129.2
19	1.75*s*	1.87*s*	1.70*s*	17.7	16.6	17.5
20	1.60*s*	1.70*s*	1.56*s*	25.8	24.7	25.6
7–OCH_3	3.74*s*	3.77*s*	3.56*s*	61.1	59.3	60.3
1–OH	13.46[d] *s*	13.98*s*	13.41[b] *s*	–	–	–
	glucosyl	galactosyl	mannosyl			
1′	4.49*d* (7.4)	5.36*d* (7.6)	5.61*s*	100.5	100.6	98.6
2′	3.56*m*	4.50*t* (7.6)	4.23*br s*	72.8	69.7	70.0
3′	3.48*m*	*ca*4.06[e] *dd* (7.6, 2.8)	4.19*m*	75.9	73.1	71.0
4′	3.71*m*	4.36*d* (2.8)	4.19*m*	69.5	68.1	66.6
5′	3.88*br d* (13.2)	*ca*4.05[f] *dd* (6.6, 4.4)	3.67*m*	76.3	75.8	74.0
6′	4.09*m*	*ca*4.27[f] (11.6, 6.6)	3.90*br dd* (12.4,	61.3	60.5	61.0
		4.13*dd* (11.6, 4.4)	4.0), 3.83*m*			

[a] NMR spectra were recorded in $CDCl_3$ + 20 drops of methanol–d_4

[b] NMR spectra were recorded in $CDCl_3$ + 10 drops of pyridine–d_5

[c] Signal overlapped with methanol, chemical shift and coupling constant were determined by COSY correlation

[d] Weak signal showed at reported chemical shift

[e,f] Signal overlapped with same sign, chemical shifts and coupling constants were determined by COSY and their coupled proton

Table 30 ^{1}H– and ^{13}C NMR data of 3–*O*–glycosyl mangostin analogues

Position	δ_H ($CDCl_3$ + pyridine–d_5)			δ_C ($CDCl_3$ + pyridine–d_5)		
	274	**324**	**325**	**274**	**324**	**325**
1	–	–	–	159.9	159.7	160.1
2	–	–	–	109.9	109.7	110.1
3	–	–	–	162.6	162.4	162.6
4	6.39*s*	6.96*s*	6.30*s*	91.1	91.4	91.8
4a	–	–	–	153.7	153.5	153.7
5	6.92*s*	7.21*s*	7.03*s*	101.5	100.8	101.2
6	–	–	–	154.6	154.6	154.2
7	–	–	–	143.1	143.0	143.4
8	–	–	–	136.1	135.8	136.6
8a	–	–	–	111.8	111.5	112.2
9	–	–	–	180.9	180.8	181.1
9a	–	–	–	101.8	101.8	102.3
10a	–	–	–	154.0	153.8	154.0
11	3.54*d* (6.7)	3.54*d* (6.6)	3.45*br d* (6.1)	20.7	20.6	20.9
12	5.48*t* (6.7)	5.47*t* (6.6)	5.38*br t* (6.1)	121.3	121.6	122.2
13	–	–	–	130.2	129.9	130.5
14	1.85*s*	1.85*s*	1.81*s*	16.5	16.7	17.1
15	1.69*s*	1.69*s*	1.65*s*	24.2	24.7	25.1
16	4.19*d* (6.7)	*ca*4.17[a] *d* (5.4)	4.07*br d* (10.7)	25.3	24.7	25.1
17	5.34*t* (6.7)	5.35*t* (5.4)	5.24*br t* (10.7)	122.9	122.7	123.1
18	–	–	–	130.2	129.9	130.5
19	1.85*s*	1.85*s*	1.83*s*	17.7	17.0	17.4
20	1.69*s*	1.69*s*	1.69*s*	25.6	25.0	25.5
7–OCH_3	3.76*s*	3.75*s*	3.66*s*	61.0	59.7	60.2
1–OH	13.79*s*	13.81*s*	13.60	–	–	–
	glucosyl	galactosyl	mannosyl			
1′	5.26*d* (6.9)	5.20*d* (7.6)	5.72*s*	99.0	100.3	98.6
2′	3.95*m*	4.32*br t* (7.6)	4.35*br s*	71.8	70.0	69.8
3′	4.18*m*	*ca*3.57[b] *br dd* (7.6, 2.7)	4.28*br d* (8.2)	73.6	73.3	71.3
4′	4.00*m*	4.25*d* (2.7)	3.74*d* (8.2)	68.6	68.4	66.7
5′	3.87*m*	*ca*3.91[b] *br dd* (6.4, 4.1)	4.03*m*	75.6	76.1	75.1
6′	3.91*m*, 3.83*m*	*ca*4.18[a] *br dd* (11.8, 6.4), 4.02*dd* (11.8, 4.1)	4.03*m*, 3.88 *br d* (10.0)	59.2	60.9	61.1

[a,b] Signal overlapped with same sign chemical shifts and coupling constants were determined by COSY and their coupled protons, respectively.

CHAPTER 5
CONCLUSIONS

Phytochemical investigation of Thai *Z. cambodiana* root bark native to Thailand led to isolation of seven new cyclopeptide alkaloids named cambodines A–G (**278**–**284**). All new compounds were divided into three groups depend on their amino acid units including 4(14)–integerrine–type (**279**, **281** and **282**), 5(14)–scutianine A–type (**278**, **280** and **283**) and neutral compound related to cyclopeptide alkaloid (**284**). In addition, cambodine E (**282**) was isolated and its structure was determined by x–ray crystallography. Moreover, two known cyclopeptides 4(14)–frangulanine–type cyclopeptide alkaloid, frangufoline (**6**), and neutral compound related to 14–membered cyclopeptide alkaloids, lotusanine B (**24**) were isolated (Figure 57). Herein, we isolated five of the new alkaloids (**278**–**279** and **282**–**283**) are constructed imidazolidinone ring which was previously reported as only four compounds. Cambodine F (**284**) was found to possessed the 1,2–dimethylimidazolidin–4–one cyclopeptide was also reported for the first time. This is the first isolation of a 5(14)–scutianine A–type cyclopeptide, cambodines A (**278**) and F (**283**), with imidazolidinone group.

All isolated compounds were tested for their *in vitro* biological properties. Only cambodine F (**283**) exhibited antiplasmodial activity against *P. falciparum* (Trager and Jensen, 1976) with the IC_{50} values of 6.1 μM (4.23 μg/mL), probably be due to a specific 1,2–dimethylimidazolidin–4–one moiety. Cambodines B (**279**) and C (**280**), and lotusanine B (**24**) showed antimycobacterial effect against *M. tuberculosis* with the IC_{50} values of 50, 100 and 50 μg/mL, respectively (Collins and Franzblau, 1997). This report also reinforced the *in vitro* antiplasmodial and antimycobacterial activities of cyclopeptide alkaloids we have previously reported (Suksamrarn S et al., 2005; Panseeta et al., 2011). In addition, compounds **281**–**283** exhibited cytotoxic activity against human lung cancer cell lines (NCI–H187) at values of IC_{50} 12.77, 19.57 and 21.05 μg/mL, respectively. All compounds were found to be nontoxic to Vero cells except cambodine E (**282**), which exhibited cytotoxicity to this cell line with IC_{50} 25.72 μg/mL.

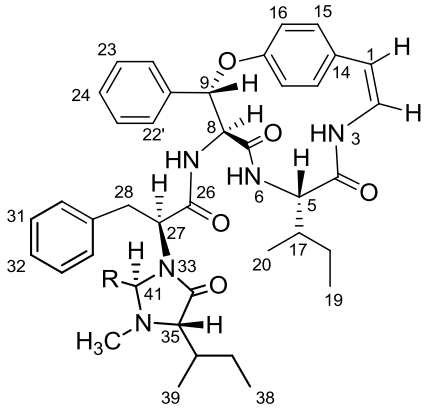

Cambodine A (**278**): R = H
Cambodine F (**283**): R = CH_3

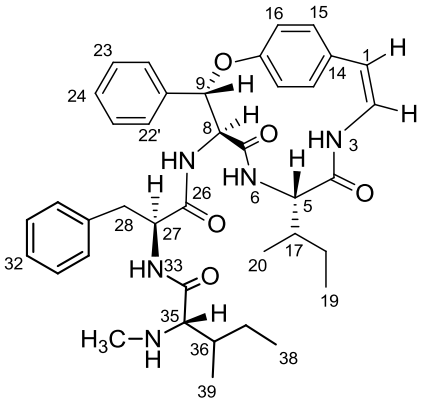

Cambodine C (**280**)

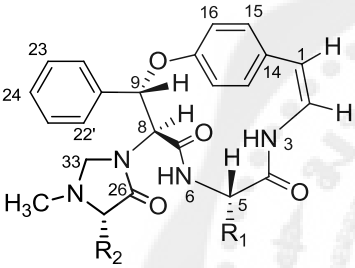

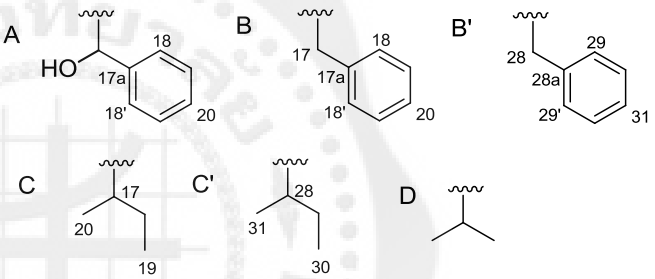

Cambodine B (**279**): R_1 = A, R_2 = B'
Cambodine D (**281**): R_1 = C, R_2 = C'
Cambodine E (**282**): R_1 = B, R_2 = B'

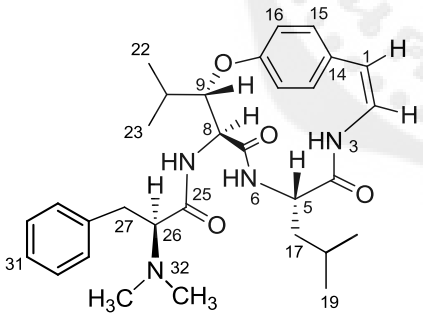

Frangufoline (**6**)

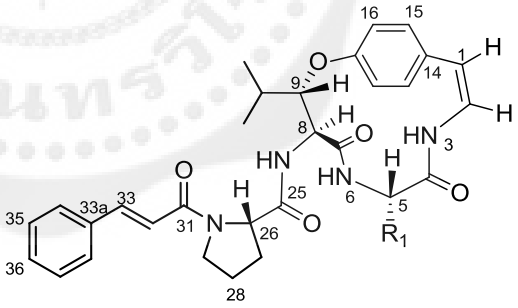

Cambodine G (**284**): R = C
Lotusanine B (**24**): R = B

Figure 58 Cyclopeptide alkaloids from Thai *Z. cambodiana*

This work also describes *O*–glycosylation of two importabt natural compounds, betulinic acid (**1**) and α–mangostin (**234**) using three natural sugars, *D*–glucose, *D*–galactose and *D*–mannose. Glycosyl acceptor **1** was α–*O*–glycosylated at C–3 using OFox donors. Glycosyl acceptor **234** was mono– or di–*O*–glycosylated at C–3 or C–6 positions (Figure 58). To improved hydrophilic property, all synthetic glycosides were calculated their log*P* by ACD/ChemSketch. The results showed Clog*P* of all synthetic glycosides are smaller than their aglycones led to the conclusion that glycosides enhance their aglycone's hydrophilicity. Biological activities of all synthetic glucosyl mangostin analogues will be further investigated.

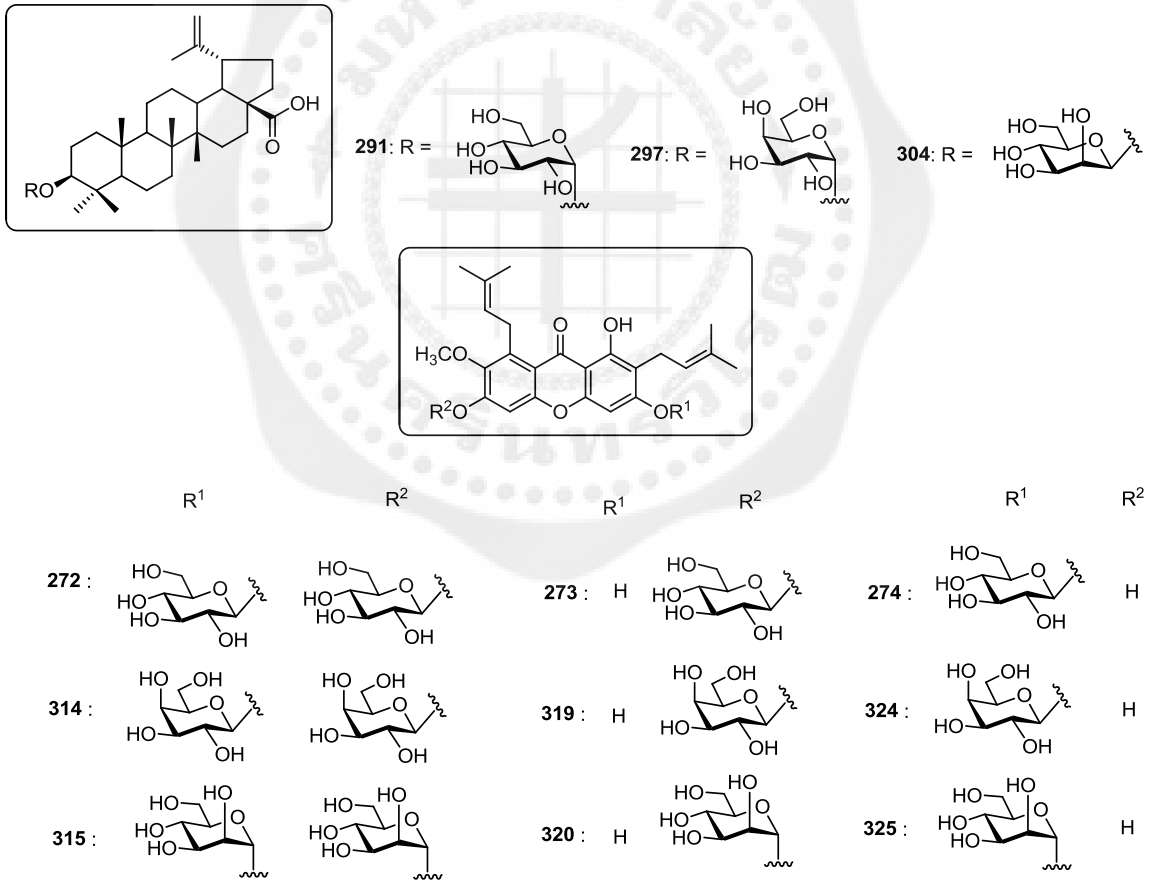

Figure 58 Synthetic glycosides

BIBLIOGRAPHY

BIBLIOGRAPHY

Abdu, H.; Ahmad, F. B., H.; Ismail, I. S., Betulinic acid glycosides: A Review. *Orient. J. Chem.* **2012,** *28*, 1123–1133.

Abu–Zarga, M.; Sabri, S.; Al–Aboudi, A.; Ajaz, M. S.; Sultana, N.; Rahman, A.–U., New Cyclopeptide Alkaloids from *Zizyphus lotus*. *J. Nat. Prod.* **1995,** *58*, 504–511.

Acharya, S. B.; Tripathi, S. K.; Tripathi, Y. C.; Pandey, V. B., Some pharmacological studies on *Ziziphus rugosa* saponins. *Indian J. Pharmacol*. **1988**, *20*, 200–202.

Arai, M. A.; Tateno, C.; Hosoya, T.; Koyano, T.; Kowithayakorn, T.; Ishibashi, M., Hedgehog/GLI–mediated transcriptional inhibitors from *Zizyphus cambodiana*. *Bioorg. Med. Chem*. **2008,** *16*, 9420–9424.

Aunchai, N. Study on the chemical constituents of *Ziziphus oenoplia* (Linn.) Mill. root [Dissertation M.Sc. Biological Chemistry]. Bangkok: Srinakharinwirot University; **2002**. pp. 38–77.

Auvin, C.; Lezenven, F.; Blond, A.; Augeven–Bour, I.; Pousset, J.–L.; Bodo, B.; Camara, J., Mucronine J, a 14–Membered Cyclopeptide Alkaloid from *Zizyphus mucronata*. *J. Nat. Prod.* **1996**, *59*, 676.

Bhattachachryya, B.; Johri, B. M., In: *Flowering plants: Taxonomy and phylogeny*. New Delhi: Narosa Publishing House; **1998**, pp. 326–328.

Birch, A. J., Reduction by dissolving metals. Part I *J. Chem. Soc.*, **1944**, 430–436.

Boulos, L., In: *Medicinal Plants of North Africa.* Reference Publications, Michigan. **1983**, p. 153.

Bruneton, J., In: *Pharmacognosy, Phytochemistry and Medicinal Plants*. Intercept. Ltd. England, U.K. **1999**.

Bunyapraphatsara, N.; Chokechaijaroenporn, O., In: *Thai medicinal plants*. Vol. 4. Bangkok: Mahidol University and National Center for Genetic Engineering and Biotechnology. **2000**, pp. 291–292.

Bunyapraphatsara, N.; Chokechaijaroenporn, O., In: *Thai medicinal plants*. Vol. 3. Bangkok: Mahidol University and National Center for Genetic Engineering and Biotechnology. **1999**, pp. 328–329.

Cantrell, C. L.; Franzblau, S. G.; Fischer, N. H., Antimycobacterial plant terpenoids. *Planta Med.* **2001**, *67*, 685–694.

Caro, M. S. B.; de Oliveira, L. H.; Ilha, V.; Burrow, R. A.; Dalcol, I. I.; Morel, A. F., Absolute configuration of franganine. *J. Nat. Prod.* **2012,** *75*, 1220–1222.

Chauhan, J. S.; Srivastava, S. K., Chemical investigation of the stem of *Zizyphus mauritiana* (N.O. Rhamnaceae). *Proc. Natl. Acad. Sci*. India, Sect A **1978**, *48*, 6.

Chen, S. X.; Wan, M.; Loh, B. N., Active constituents against HIV–1 protease from Garcinia mangostana. *Planta Med*. **1996**, *62*, 381–382.

Cho, T. S.; Ro, J. Y.; Hong, S. S., *Korean J. Pharmacol*. **1976**, *18*, 17.

Choudhary, M. I.; Adhikari, A.; Rasheed, S.; Marasini, B. P.; Hussain, N.; Kaleem, W. A.; Atta–ur–Rahman, Cyclopeptide alkaloids of *Ziziphus oxyphylla* Edgw as novel inhibitors of *α*–glucosidase enzyme and protein glycation. *Phytochemistry Lett.* **2011,** *4*, 404–406.

Collins, L., Franzblau, S. G., Microplate alamar blue assay versus BACTEC 460 system for high–throughput screening of compounds against *Mycobacterium tuberculosis* and *Mycobacterium avium*. *Antimicrob. Agents Chemother*. **1997**, *41*, 1004–1009.

Cristau, P.; Temal–Laïb, T.; Bois–Choussy, M.; Martin, M.–T.; Vors, J.–P.; Zhu, J., Total synthesis of mauritines A, B, C, and F: Cyclopeptide alkaloids with a 14–membered paracyclophane Unit. *Chem. Eur. J.* **2005,** *11*, 2668–2679.

Cui, J.; Hu, W.; Cai, Z.; Liu, Y.; Li, S.; Tao, W.; Xiang H., New medicinal properties of mangostins: analgesic activity and pharmacological characterization of active ingredients from the fruit hull of (*Garcinia mangostana* L.). *Pharmacol. Biochem. Behav.* **2010**, *95*, 166–172.

de Oliveira, P. L.; Tanaka, C. M. A.; Kato, L. I.; da Silva, C. C.; Medina, R. P.; Moraes, A. P.; Sabino, J. R.; de Oliveira, C. I. M. A., Amaiouine, a cyclopeptide alkaloid from the leaves of *Amaioua guianensis*. *J. Nat. Prod.* **2009,** *72*, 1195–1197.

Desjardins, R. E.; Canfield, C. J.; Haynes, J. D.; Chulay J. D., Quantitative assessment of antimalarial activity in vitro by a semiautomated microdilution technique. *Antimicrob. Agents Chemother*. **1979**, *16*, 710–718.

Devkota, H. P.; Watanabe, T.; Yahara, S., Flavonoids and saponins from *Zizyphus incurva*. *Nat. Prod. Res.* **2013,** *27*, 697–701.

Diaz, J. G.; de Paz, P. P.; Herz, W., New water soluble flavone and xanthone glycosides from Hypericum canariense L. *Phytochem. Lett.* **2010,** *3*, 171–175.

Digel. M.; Morel, A.; Layer, H.; Biermann, J.; Voelter, W., Peptide alkaloids from *Discaria febrifuga* Mart. *Hoppe Seylers Z Physiol Chem*. **1983**, *364*, 1641–1643.

El–Seedi, H.; Zahra, M.; Goransson, U.; Verpoorte, R., Cyclopeptide alkaloids. *Phytochem. Rev.* **2007,** *6*, 143–165.

Elusiyan, C. A.; Msagati, T. A. M.; Shode, F. O.; Mamba, B. B., Measurements of distribution coefficients and lipophilicity values for oleanolic acid and betulinic acid extracted from indigenous plants by hollow fibre supported liquid membrane. *Bull. Chem. Soc. Ethiop.* **2011,** *25*, 321–332.

Ganapaty, S.; Thomas, P. S.; Ramana, K. V.; Karagianis, G.; Waterman, P. G. Dammarane and ceanothane triterpenes from *Zizyphus glabrata*. *Z. Naturforsch* **2006,** *61b*, 87–92.

Gao, Q. H.; Wu, C. S.; Wang, M.; Xu, B. N.; Du, L. J. Effect of drying of jujubes (*Ziziphus jujuba* Mill.) on the contents of sugars, organic acids, *α*–tocopherol, *β*–carotene and phenolic compounds. *J. Agric. Food Chem*. **2012**a, *60*, 9642–9648.

Gao, Q. H.; Wu, C. S.; Yu, J. G.; Wang, M.; Ma, Y. J.; Li, C. L., Textural characteristic, antioxidant activity, sugar, organic acid, and phenolic profiles of 10 promising jujube (*Ziziphus jujuba* Mill.) selections. *J. Food Sci*. **2012**b, 1218–1225.

Gardner, S.; Sidisunthorn, P.; Anusarnsunthorn. V. In: *A Field Guide to Forest Trees of Northern Thailand*. Bangkok: Kobfai Publishing Project. **2000**, p.130.

Gauthier, C.; Legault, J.; Lebrun, M.; Dufour, P.; Pichette, A. Glycosidation of lupane–type triterpenoids as potent in vitro cytotoxic agents. *Bioorg. Med. Chem.* **2006,** *14*, 6713–6725.

Gauthier, C.; Legault, J.; Piochon, M.; Lavoie, S.; Tremblay, S.; Pichette, A., Synthesis, cytotoxicity, and haemolytic activity of chacotrioside lupane–type neosaponins and their germanicane–type rearrangement products. *Bioorg. Med. Chem.* **2009,** *19*, 2310–2314.

Giacomelli, S. R.; Maldaner, G.; Gonzaga, W. A.; Garcia, C. M.; da Silva, U. F.; Dalcol, I. I.; Morel, A. F., Cyclic peptide alkaloids from the bark of *Discaria americana*. *Phytochemistry* **2004,** *65*, 933–937.

Giacomelli, S. R.; Missau, F. C.; Mostardeiro, M. A.; da Silva, U. F.; Dalcol, I. I.; Zanatta, N.; Morel, A. F., Cyclopeptides from the Bark of *Discaria americana*. *J. Nat. Prod.* **2001,** *64*, 997–999.

Gournelis, D. C.; Laskaris, G. G.; Verpoorte, R., In: *Progress in the Chemistry of Organic Natural Products*; Herz, H. F. W., Kirby, G. W., Moore, R. E., Tamm, C., Eds.; Springer: New York, **1998**, pp. 1–179.

Goyal, M.; Sasmal, D.; Nagori, B. P., Review on ethnomedicinal uses, pharmacological activity and phytochemical constituents of *Ziziphus mauritiana* (*Z. jujuba* Lam., non Mill). *Spatula DD* **2012**, *2*, 107–116.

Guo, S.; Duan, J.–a.; Tang, Y.; Qian, Y.; Zhao, J.; Qian, D., Triterpenoids from the fruits of *Ziziphus jujuba* var. *spinosa*. *Biochem. Sys. Ecol.* **2011**a**,** *39*, 880–882.

Guo, S.; Duan, J.–a.; Tang, Y.; Qian, Y.; Zhao, J.; Qian, D.; Su, S.; Shang, E., Simultaneous qualitative and quantitative analysis of triterpenic acids, saponins and flavonoids in the leaves of two *Ziziphus* species by HPLC–PDA–MS/ELSD. *J. Pharm. Biomed. Anal.* **2011**b**,** *56*, 264–270.

Guo, S.; Duan, J.–a.; Tang, Y.; Su, S.; Shang, E.; Ni, S.; Qian, D., High–performance liquid chromatography–Two wavelength detection of triterpenoid acids from the fruits of *Ziziphus jujuba* containing various cultivars in different regions and classification using chemometric analysis. *J. Pharm. Biomed. Anal.* **2009**a**,** *49*, 1296–1302.

Guo, S.; Duan, J.–A.; Tang, Y.–P.; Yang, N.–Y.; Qian, D.–W.; Su, S.–L.; Shang, E.–X., Characterization of Triterpenic Acids in Fruits of *Ziziphus Species* by HPLC–ELSD–MS. *J. Agric. Food Chem.* **2010,** *58*, 6285–6289.

Guo, S.; Tang, Y. P.; Duan, J. A.; Su, S. L.; Ding, A. W. Two new terpenoids from fruits of *Ziziphus jujube. Chinese Chem. Lett.* **2009**b, *20*, 197–200.

Hamada, H.; Shimoda, K. The high functionality of glycosylation using plant suspension cells. *TCIMAIL* **2013***, 151*, 1–6.

Han, B. H.; Park, M. H., Sedative activity and the active components of *Ziziphi fructus*. *Arch. Pharm. Res.* **1987**, *10*, 208–211.

Han, B. H.; Park, M. H.; Wah, S. T., Structure of daechualkaloid A, a new pyrrolidine alkaloid of novel skeleton from *Zizyphus jujuba* var. *inermis*. *Tetrahedron Lett.* **1987**, *28*, 3957–3958.

Han, J.; Ji, C.–J.; He, W.–J.; Shen, Y.; Leng, Y.; Xu, W.–Y.; Fan, J.–T.; Zeng, G.–Z.; Kong, L.–D.; Tan, N.–H., Cyclopeptide alkaloids from *Ziziphus apetala. J. Nat. Prod*. **2011**, *74*, 2571–2575.

He, F.; Pan, Q.; Min, Z. A novel lupane triterpene from the seeds of *Ziziphus jujuba* var. *spinosa*. *Zhongcaoyao* **2006**, *37*, 168–171.

Higuchi, R.; Kubota, S.; Komori, T.; Kawasaki, T.; Pandey, V. B.; Singh, J. P.; Shah, A. H., Triterpenoid saponins from the bark of *Zizyphus joazeiro*. *Phytochemistry* **1984**, *23*, 2597–2600.

Hostettmann, K.; Marston, A. In: *Chemistry and pharmacology of natural products–Saponins*. Cambridge: Cambridge University Press, **1995**, p. 3.

Hout, S.; Chea, A.; Bun, S. S.; Elias, R.; Gasquet, M.; Timon–David, P.; Balansard, G.; Azas, N., Screening of selected indigenous plants of Cambodia for antiplasmodial activity. *J. Ethnopharm*. **2006**, *107*, 12–18.

Huang, R. L.; Wang, W. Y.; Kuo, Y. H.; Lin, Y. L., Cytotoxic triterpenes from the fruit of *Ziziphus jujuba*. *Chin. Pharm. J.* (Taipei) **2001**, *53*, 179–184.

Huh, J., In: *Dong Eut Bo Gum,* Namsandang, Seoul, Korea. **1981**, p. 216.

Hyz, K.; Kawecki, R.; Misior, A.; Bocian, W.; Bednarek, E.; Sitkowski, J.; Kozerski, L., Genistein binding mode to doubly nicked dumbbell DNA. Dynamic and diffusion ordered NMR study. *J. Med. Chem*. **2011**, *54*, 8386–8393.

Inayat–ur–Rahman; Khan, M. A.; Arfan, M.; Akhtar, G.; Khan, L.; Ahmad, V. U., A new 14–membered cyclopeptide alkaloid from *Zizyphus oxyphylla*. *Nat. Prod. Res.* **2007,** *21*, 243–253.

Ji, C. J.; Zeng, G. Z.; Han, J.; He, W. J.; Zhang, Y. M.; Tan, N. H., Zizimauritic acids A–C, three novel nortriterpenes from *Ziziphus mauritiana*. *Bioorg. Med. Chem. Lett.* **2012,** *22*, 6377–6380.

Jou, S. J.; Chen, C. H.; Guh, J. H.; Lee, C. N.; Lee, S. S., Flavonol glycosides and cytotoxic triterpenoids from *Alphitonia philippinesis*. *J. Chin. Chem. Soc.* (Taipei) **2004**, *51*, 827–834.

Joullie, M. M.; Nutt, R. F., In: *Alkaloids, Chemical and Biological Perspectives*; Pelletier, S. W., Ed.; John Wiley & Sons: New York, **1983**, Vol. 3, pp. 113–168.

Jung, H. A.; Su, B. N.; Keller, W.J.; Mehta, R. G.; Kinghorn, A. D., Antioxidant xanthones from the pericarp of *Garcinia mangostana* (Mangosteen). *J. Agric. Food Chem.* **2006**, *54*, 2077–2082.

Kaleem, W. A.; Muhammad, N.; Qayum, M.; Khan, H.; Khan, A.; Aliberti, L.; De Feo, V., Antinociceptive activity of cyclopeptide alkaloids isolated from *Ziziphus oxyphylla* Edgew (Rhamnaceae). *Fitoterapia* **2013**a**,** *91*, 154–158.

Kaleem, W. A.; Nisar, M.; Qayum, M.; Zia–Ul–Haq, M.; Adhikari, A.; De Feo, V., New 14–membered cyclopeptide alkaloids from *Zizyphus oxyphylla* Edgew. *Int. J. Mol. Sci.* **2012,** *13*, 11520–11529.

Kaleem, W. A.; Nisar, M.; Qayum, M.; Zia–Ul–Haq, M.; Choudhary, M. I.; Ercisli, S., Urease inhibitory potential of *Zizyphus oxyphylla* Edgew. extracts and isolated compounds. *Turk. J. Med. Sci.* **2013**b**,** *43*, 497–500.

Kaomongkolgit, R.; Jamdee, K.; Chaisomboon, N. Antifungal activity of alpha–mangostin against *Candida albicans*. *J. Oral Sci.* **2009**, *51*, 401–406.

Kashiwada, Y.; Nagao, T.; Hashimoto, A.; Ikeshiro, Y.; Okabe, H.; Cosentino, L. M.; Lee, K.–H., Anti–AIDS agents 38. Anti–HIV activity of 3–*O*–Acyl ursolic acid derivatives1. *J. Nat. Prod.* **2000,** *63*, 1619–1622.

Kirtikar, K. R., Basu, B. D., In: *Indian Medicinal Plants*. Springer, Berlin, **1984**, p. 593.

Kirtikar, K. R.; Basu, B. D. Blatter, E.; Cains, J. F.; Mhaskar K. S., In: *Indian Medicinal Plants*, Delhi: Periodical Experts., India. **1975**; Vol. 1 (1 eds), pp. 592–596.

Koh, J.–J.; Qiu, S.; Zou, H.; Lakshminarayanan, R.; Li, J.; Zhou, X.; Tang, C.; Saraswathi, P.; Verma, C.; Tan, D. T. H.; Tan, A. L.; Liu, S.; Beuerman, R. W., Rapid bactericidal action of alpha–mangostin against MRSA as an outcome of membrane targeting. *Biochim. Biophys. Acta* **2013**, *1828*, 834–844.

Kulshreshtha, M. J.; Rastogi, R. P., Chemical constituents of *Zizyphus rugosa*. *Indian J. Chem.* **1972**, *10*, 152–154.

Lagarias, J. C.; Goff, D.; Klein, F. K.; Rapoport, H., Cyclopeptide Alkaloids. Phencyclopeptines from the polymorphic species *Ceanothus integerrimus*. *J. Nat. Prod.* **1979,** *42*, 220–227.

Laib, T.; Bois–Choussy, M. I.; Zhu, J., The first total synthesis of mauritine A. *Tetrahedron Lett.* **2000,** *41*, 7645–7649.

Le, T.; Pandey, R.; Gurung, R.; Dhakal, D.; Sohng, J., Efficient enzymatic systems for synthesis of novel α–mangostin glycosides exhibiting antibacterial activity against Gram–positive bacteria. *Appl. Microbiol. Biotechnol.* **2014,** *98*, 8527–8538.

Lee, S. M.; Min, B. S.; Lee, C. G.; Kim, K. S.; Kho, Y. H., Cytotoxic Triterpenoids from the Fruits of *Zizyphus jujuba*. *Planta Med.* **2003**, *69*, 1051–1054.

Lee, S. M.; Park, J. G.; Lee, Y. H.; Lee, C. G.; Min, B. S.; Kim, J. H.; Lee, H. K., Anti–complementary activity of triterpenoides from fruits of *Zizyphus jujuba*. *Biol. Pharm. Bull.* **2004**, *27*, 1883–1886.

Lee, S. S.; Lin, B. F.; Chen, K. C. S., Chemical constituents from the roots of *Ziziphus jujuba* Mill. var. *spinosa* (Bunge) Hu.(II). *Chin. Pharm. J.* (Taipei) **1995**, *47*, 511–519.

Lee, S. S.; Lin, B. F.; Liu, K. C., Three triterpenes esters from *Zizyphus jujuba*. *Phytochemistry* **1996**, *43*, 847–851.

Lee, S. S.; Su, W. C.; Liu, K. C. S. C. Cyclopeptide alkaloids from stems of *Paliurus ramossisimus. Phytochemistry* **2001**, *58*, 1271–1276.

Lee, S. Y.; Ju, S. K.; Lee, J.–H.; Kim, Y. S.; Kang, S. S., A New Saponin from the Seeds of *Zizyphus jujuba* var. spinosa. *Bull. Korean Chem. Soc*. **2013**, *34*, 657–660.

Li, J. W.; Fan, L. P.; Ding, S. D.; Ding, X. L., Nutritional composition of five cultivars of chinese jujube. *Food Chem.* **2007**, *103*, 454–460.

Li, X.; Ohtsuki, T.; Shindo, S.; Sato, M.; Koyano, T.; Preeprame, S.; Kowithayakorn, T.; Ishibashi, M., Mangiferin identified in a screening study guided by neuraminidase inhibitory activity. *Planta Med.* **2007,** *73*, 1195–1196.

Liao, L.; Won, T.; Kang, S.; Shin, J., Simultaneous analysis of bioactive metabolites from *Ziziphus jujuba* by HPLC–DAD–ELSD–MS/MS. *J. Pharm. Invest.* **2012,** *42*, 21–31.

Lin, H.–Y.; Chen, C.–H.; Chen, L. K. C. S.; Lee, S.–S. 14–Membered cyclopeptides from *Paliurus ramosissimus* and *P. hemsleyanus*. *Helv. Chim. Acta* **2003**, *86*, 127–138.

Lin, H.–Y.; Chen, C.–H.; You, B.–J.; Liu, K. C. S. C.; Lee, S.–S., Cyclopeptide alkaloids from *Paliurus ramossisimus*. *J. Nat. Prod*. **2000**, *63*, 1338–1343.

Liu, Z.; Zhao, X.; Liu, B.; Liu, A.–j.; Li, H.; Mao, X.; Wu, B.; Bi, K.–S.; Jia, Y., Jujuboside A. A neuroprotective agent from semen *Ziziphi spinosae* ameliorates behavioral disorders of the dementia mouse model induced by Aβ1–42. *Eur. J. Pharmacol.* **2014,** *738*, 206–213.

Lomchoey, N. Cyclopeptide alkaloids from some *ziziphus* plants [Dissertation M.Sc. Chemistry]. Bangkok: Srinakharinwirot University; **2011**. pp. 1–85.

Lontsi, D.; Sondengam, B. L.; Ayafor, J. F.; Connolly, J. D., Cecropiacic acid, a new pentacyclic A–ring seco triterpenoid from *Musanga cecropioides*. *Tetrahedron Lett.* **1987,** *28*, 6683–6686.

Maciuk, A.; Ghedira, K.; Thepenier, P.; Lavaud, C.; Zeches–Hanrot, M., A new flavonol glycoside from leaves of *Zizyphus lotus*. *Pharmazie* **2003**, *58*, 158–159.

Maciuk, A.; Lavaud, C.; Thepenier, P.; Jacquier, M. J.; Ghedira, K.; Zeches–Hanrot, M., Four new dammarane saponins from *Zizyphus Lotus*. *J. Nat. Prod.* **2004**, *67*, 1639–1643.

Maharaj, S.; Dwivedi, R. N., Farmers preferences on tree/crop species and livestock feeding – a study through PRA approach. *Progress. Agri.* **2002**, *2*, 135–137.

Mahran, G. E.–D. H.; Glombitza, K.–W.; Mirhom, Y. W.; Hartmann, R.; Michel, C. G., Novel saponins from *Zizyphus spina–christi* growing in Egypt. *Planta Med.* **1996,** *62*, 163–165.

Maldaner, G.; Marangon, P.; Ilha, V.; Balparda Caro, M. S.; Burrow, R. A.; Dalcol, I. I.; Morel, A. F., Cyclopeptide alkaloids from *Scutia buxifolia* Reiss. *Phytochemistry* **2011,** *72*, 804–809.

Maneekaew, N., Major constituents of the twig of *Ziziphus attopoensis* Pierre [Dissertation M.Sc. Chemistry]. Bangkok: Srinakharinwirot University; **2007**. pp. 81–110.

Marfey, P.; Ottesen, M., Determination of *D*–amino acids. II. Use of a bifunctional reagent, 1,5–difluoro–2,4–dinitrobenzene. *Carl. Res. Commun.* 1984, *49*, 585–590

Mondal, D. N.; Kundu, A. B., A–nor–triterpenoid from *Zizyphus jujuba*. *J. Indian Chem. Soc.* **1998**, 75, 384–385.

Morel, A. F.; Araujo, C. A.; da Silva, U. F.; Hoelzel, S. C. S. M.; Záchia, R.; Bastos, N. R., Antibacterial cyclopeptide alkaloids from the bark of *Condalia buxifolia*. *Phytochemistry* **2002,** *61*, 561–566.

Morel, A. F.; Flach, A.; Zanatta, N.; Ethur, E. M.; Mostardeiro, M. A.; Gehrke, I. T. S. A new cyclopeptide alkaloid from the bark of *Waltheria douradinha*. *Tetrahedron Lett.* **1999**, *40*, 9205–9209.

Morel, A. F.; Gehrke, I. T. S.; Mostardeiro, M. A.; Ethur, E. M.; Zanatta, N.; Machado, E. C. S., Cyclopeptide alkaloids from the bark of *Waltheria douradinha*. *Phytochemistry* **1999,** *51*, 473–477.

Morel, A. F.; Maldaner, G.; Ilha, V.; Missau, F.; Silva, U. F.; Dalcol, I. I., Cyclopeptide alkaloids from *Scutia buxifolia* Reiss and their antimicrobial activity. *Phytochemistry* **2005,** *66*, 2571–2576.

Mostardeiro, M. A.; Ilha, V.; Dahmer, J.; Caro, M. S. B.; Dalcol, I. I.; da Silva, U. F.; Morel, A. F., Cyclopeptide Alkaloids: Stereochemistry and synthesis of the precursors of discarines C and D and myrianthine A. *J. Nat. Prod.* **2013,** *76*, 1343–1350.

Mydock, L. K.; Demchenko, A. V., Mechanism of chemical *O*-glycosylation: from early studies to recent discoveries. *Org. Biomol. Chem.* **2010,** *8*, 497-510.

Nagarajan, G. P. and Parmar, V. S., *Indian J. Chem.* **1977**, *158*, 955.

Nahar, N.; Das, R. N.; Shoeb, M.; Marma, M. S.; Aziz, M. A.; Mosihuzzaman, M., Four triterpenoids from bark of *Zizyphus rugosa* and *Zizyphus oenoplia*. *J. Bangladesh Acad. Sci*. **1997**, *21*, 151–158.

Naili, M. B.; Alghazeer, R. O.; Saleh, N. A.; Al–Najjar, A. Y., Evaluation of antibacterial and antioxidant activities of *Artemisia campestris* (Astraceae) and *Ziziphus lotus* (Rhamnacea). *Arabian J. Chem.* **2010,** *3*, 79–84.

Nakatani, K.; Nakahata, N.; Arakawa, T.; Yasuda, H.; Ohizumi, Y., Inhibition of cyclooxgenase and prostaglandia E2 synthesis by cmangostin, a xanthone derivative in mangosteen, in C6 rat glioma cells. *Biochem. Pharmacol*. **2002**, *63*, 73–79.

Netsawangwicha. J., A study on chemical constituents from the root barks of *Ziziphus rugosa* Lam. [Dissertation M.Sc. Chemistry]. Bangkok: Srinakharinwirot University; 2005. pp. 46–77.

Nigudkar, S. S.; Stine, K. J.; Demchenko, A. V., Regenerative glycosylation under nucleophilic catalysis. *J. Am. Chem. Soc.* **2014,** *136*, 921–923.

Nunes, P. H.; Marinho, L. C.; Nunes, M. L.; Soares, E. O. Antipyretic activity of an aqueous extract of *Zizyphus joazeiro* Mart. (Rhamnaceae). *Braz. J. Med. Biol. Res*. **1987**, *20*, 599–601.

Okamura, N.; Nohara, T.; Yagi, A.; Nishioka, I., Studies on the constituents of *Zizyphi fructus*. III. Structures of dammarane–type saponins. *Chem. Pharm. Bull.* **1981,** *29*, 676–683.

Osterberg, T.; Norinder, U., Prediction of drug transport processes using simple parameters and PLS statistics the use of ACD/logP and ACD/ChemSketch descriptors. *Eur. J. Pharm. Sci.* **2001,** *12*, 327–337.

Otsuka, H.; Akiyama, T.; Kawai, K.–I.; Shibata, S.; Inoue, O.; Ogihara, Y., The structure of jujubosides A and B, the saponins isolated from the seeds of *Zizyphus jujuba*. *Phytochemistry* **1978,** *17*, 1349–1352.

Pai, B. R.; Natarajan, S.; Suguna, H.; Kameswaran, L.; Shankaranarayan, D.; Gopalakrishnan, C., Synthesis and pharmacology of mangostin–3,6–di–*O*–glucoside. *J. Nat. Prod.* **1979,** *42*, 361–365.

Pandey, M. B.; Singh, A. K.; Singh, J. P.; Singh, V. P.; Pandey, V. B., Three new cyclopeptide alkaloids from *Zizyphus* species. *J. Asian Nat. Prod. Res.* **2008**a**,** *10*, 709–713.

Pandey, M. B.; Singh, A. K.; Singh, V. P.; Pandey, V. B., Cyclopeptide alkaloids from *Zizyphus sativa* bark. *Nat. Prod. Res.* **2008**b**,** *22*, 219–221.

Pandey, M. B.; Singh, J. P.; Singh, A. K.; Singh, V. P., Xylopyrine–F, a new cyclopeptide alkaloid from *Zizyphus xylopyra*. *J. Asian Nat. Prod. Res.* **2008**c**,** *10*, 725–728.

Pandey, M. B.; Singh, S.; Malhotra, M.; Pandey, V. B.; Singh, T. D., Two new 14–membered cyclopeptide alkaloids from *Zizyphus xylopyra*. *Nat. Prod. Res.* **2012,** *26*, 836–841.

Pandey, V. B.; Devi, S., Biologically active cyclopeptide alkaloids from Rhamnaceae plants. *Planta Med.* **1990,** *56*, 649–650.

Pandey, V. B.; Tripathi, Y. C., A new triterpenoid saponin from *Zizyphus rugosa*. *Fitoterapia* **1993**, *64*, 341–343.

Panseeta, P. Chemical constituents from the root barks of *Ziziphus cambodiana* Pierre. [Dissertation Ph.D. Applied Chemistry]. Bangkok: Srinakharinwirot University; **2009**. pp. 51–110.

Panseeta, P., Chemical constituents from the root barks of *Ziziphus cambodiana* Pierre [Dissertation M.Ed. Chemistry]. Bangkok: Srinakharinwirot University; **2004**. pp. 1–57.

Panseeta, P.; Lomchoey, K.; Prabpai, S.; Kongsaeree, P.; Suksamrarn, A.; Ruchirawat, S.; Suksamrarn, S., Antiplasmodial and antimycobacterial cyclopeptide alkaloids from the root of *Ziziphus mauritiana*. *Phytochemistry* **2011,** *72*, 909–915.

Pistorio, S. G.; Yasomanee, J. P.; Demchenko, A. V., Hydrogen–bond–mediated aglycone delivery: focus on β–mannosylation. *Org. Lett*. **2014,** *16*, 716–719.

Pundir, R.; Singh, G.; Pandey, A. A.; Saraf, S. A., Demand of herbal hepatoprotective formulations in Lucknow–A Survey. *The Pharm. Res*. **2009**, 1, 23–33.

Rambabu, P.; Ramana, K. V.; Ganapaty, S., Dammarane and ceanothane triterpenes from *Zizyphus xylopyra*. *Int. J. Chem. Sci.* **2010**, *8*, 1231–1239.

Rambabu, P.; Ramana, K. Venkata; Ganapaty, S., Isolation and characterization of triterpenes from *Zizyphus glabrata*. *Int. J. Chem. Sci.* **2011**, *9*, 1014–1024.

Renault, J. H.; Ghedira, K.; Thepenier, P.; Lavaud, C.; Zeches–Hanrot, M.; Le Men–Olivier, L., Dammarane saponins from *Zizyphus lotus*. *Phytochemistry* **1997,** *44*, 1321–1327.

Sahu, P. K.; Tripathi, D. K.; Mir, S. R.; Singh, O.; Ali, M., A new triterpenoid from leaves of *Zizyphus jujube*. *Indian J. Nat. Prod.* **2008**, *24*, 26–28.

Sakagami, Y.; Iinuma, M.; Piyasena, K.; Dharmaratne, H., Antibacterial activity of *α*–mangostin against vancomycin resistant Enterococci (VRE) and synergism with antibiotics. *Phytomedicine* **2005**, *12*, 203–208.

Schmidt, U.; Lieberknecht, A.; Bokens, H.; Griesser, H., Total synthesis of zizyphine A. Synthesis of peptide alkaloids. 8. Amino acids and peptides. 40. *J. Org. Chem.* **1983**, *48*, 2680–2685.

Schuhly, W.; Heilmann, J.; Çalis, I.; Sticher, O., Novel Triterpene Saponins from *Zizyphus joazeiro. Hel. Chim. Acta* **2000,** *83*, 1509–1516.

Shah, A. H.; Tariq, M.; Al–Yahya, M. A. Studies on the alkaloidal fraction from the stem bark of *Zizyphus nummularia*. *Fitoterapia* **1990**, *61*, 469.

Sharma, S. C.; Kumar, R., Constituents from leaves of *Zizyphus mauritiana* Lamk. *Pharmazie* **1982**, *37*, 809–810.

Silva, M.; Bhakuni, D. S.; Sammes, P. G.; Pais, M.; Jarreau, F. X., A new peptide alkaloid from *Discaria crenata*. *Phytochemistry* **1974,** *13*, 861–863.

Singh, A. K.; Pandey, M. B.; Singh, V. P.; Pandey, V. B. Mauritine K., A new antifungal cyclopeptide alkaloid from *Zizyphus mauritiana*. *J. Indian Chem. Soc.* **2007**a, *84*, 781–784.

Singh, A. K.; Pandey, M. B.; Singh, V. P.; Pandey, V. B., Xylopyrine C, a new cyclopeptide alkaloid from *Zizyphus xylopyra*. *J. Asian Nat. Prod. Res.* **2008,** *10*, 715–718.

Singh, A. K.; Pandey, M. B.; Singh, V. P.; Pandey, V. B., Xylopyrine A and xylopyrine–B, two new peptide alkaloids from *Zizyphus xylopyra*. *Nat. Prod. Res.* **2007**b**,** *21*, 1114–1120.

Singh, J. P.; Raghubanshi, S.; Yadava, A., Cyclopeptide alkaloids of *Zizyphus rugosa*. *JCBPSC*. **2013**, *3*, 994–997.

Singh, S.; Pandey, M. B.; Singh, J. P.; Pandey, V. B., Peptide alkaloids from *Zizyphus sativa* bark. *J. Asian Nat. Prod. Res.* **2006,** *8*, 733–737.

Smitinand, T. In: *Thai plant names*. Rev. ed. Bangkok: The forest herbarium, Royal Forest Department. **2001**, pp. 564–565.

Srivastava, S. K.; Srivastava, S. D., Structure of zizogenin, a new sapogenin from *Zizyphus mauritiana*. *Phytochemistry* **1979**, *18*, 1758–1759.

Sudta, P., Structural modifications of mangostin with enhanced antimycobacterial and antiviral activities and new synthetic strategy for angiogenesis inhibitor, Semaxanib [Dissertation Ph.D. Applied Chemistry]. Bangkok: Srinakharinwirot University; **2011**. pp. 37–38.

Sudta, P.; Jiarawapi, P.; Suksamrarn, A.; Hongmanee, P.; Suksamrarn, S., Potent activity against multidrug–resistant *Mycobacterium tuberculosis* of α–Mangostin Analogs. *Chem. Pharm. Bull.* **2013**, *61*, 194–203.

Suksamrarn, S.; Komutiban, O.; Ratananukul, P.; Chimnoi, N.; Lartpornmatulee, N.; Suksamrarn, A. Cytotoxic prenylated xanthones from the young fruit of *Garcinia mangostana*. *Chem. Pharm. Bull.* **2006**, *54*, 301–305.

Suksamrarn, S.; Panseeta, P.; Kunchanawatta, S.; Distaporn, T.; Ruktasing, S.; Suksamrarn, A., Ceanothane– and lupane–type triterpenes with antiplasmodial and antimycobacterial activities from *Ziziphus cambodiana*. *Chem. Pharm. Bull.* **2006,** *37*, 535–537.

Suksamrarn, S.; Suwannapoch, N.; Aunchai, N.; Kuno, M.; Ratananukul, P.; Haritakun, R.; Jansakul, C.; Ruchirawat, S. Ziziphine N, O, P and Q, new antiplasmodial cyclopeptide alkaloids from *Ziziphus oenoplia* var. *brunoniana*. *Tetrahedron* **2005,** *61*, 1175–1180.

Suksamrarn, S.; Suwannapoch, N.; Phakhodee, W.; Thanuhiranlert, J.; Ratananukul, P.; Chimnoi, N.; Suksamrarn, A. Antimycobacterial activity of prenylated xanthones from the fruits of *Garcinia mangostana*. *Chem. Pharm. Bull.* **2003**, *51*, 857–859.

Tan, N.–H., Zhou, J., Plant cyclopeptides. *Chem. Rev.* **2006**, *106*, 840–895.

Thibeault, D.; Gauthier, C.; Legault, J.; Bouchard, J.; Dufour, P.; Pichette, A., Synthesis–structure activity relationship study of cytotoxic germanicane– and lupane–type 3β–O–monodesmosidic saponins starting from betulin. *Bioorg. Med. Chem.* **2007,** *15*, 6144–6157.

Toumi, M.; Rincheval, V.; Young, A.; Gergeres, D.; Turos, E.; Couty, F.; Mignotte, B.; Evano, G., A general route to cyclopeptide alkaloids: Total syntheses and biological evaluation of paliurines E and F, ziziphines N and Q, abyssenine A, mucronine E, and analogues. *Eur. J. Org. Chem.* **2009,** *20*, 3368–3386.

Trager, W., Jensen, J. B., Human malaria parasites in continuous culture. *Science* **1976**, *193*, 673–675.

Trevisan, G.; Maldaner, G.; Velloso, N. d. A.; Sant'Anna, G. d. S.; Ilha, V.; Velho Gewehr, C. d. C.; Rubin, M. A.; Morel, A. F.; Ferreira, J., Antinociceptive effects of 14–membered cyclopeptide alkaloids., *J. Nat. Prod.* **2009,** *72*, 608–612.

Tripathy, Y. C.; Devi, S.; Pandey, V. B.; Shah, A. H., Phytochemical study of *Zizyphus rugosa*. *Fitoterapia* **1988**, *59*, 158.

Tschesche, R.; Ammermann, E., Alkaloide aus Rhamnaceen, XXIII. Scutianin–C, –D und –E, drei weitere Cyclopeptidalkaloide aus *Scutia buxifolia* Reiss. *Chem. Ber.* **1974a,** *107*, 2274–2283.

Tschesche, R.; David, S. T.; Zerbes, R.; Radloff, M. V.; Kaubmann, E. U.; Eckhardt, G., Alkaloide aus Rhamnaceen, XIX1) mucronin–E, –F, –G und –H sowie abyssenin–A, –B und –C, weitere 15 gliedrige cyclopeptidalkaloide. *Liebigs Ann. Chem.* **1974b,** *11*, 1915–1928.

Tschesche, R.; Elgamal, M.; Eckhardt, G., Alkaloide aus Rhamnaceen, XXVIII. Nummularin–G, –H und –K, weitere Peptidalkaloide aus *Ziziphus nummularia*. *Chem. Ber.* **1977**, *110*, 2649–2455.

Tschesche, R.; Kaubmann, E. U.; Manske, R. H. F., In: Chapter 4 *The Cyclopeptide Alkaloids. In Chemistry and Physiology*, Academic Press: **1975**, Vol. 15, pp. 165–205.

Udeani, G. O.; Zhao, G. M.; Geun Shin, Y.; Cooke, B. P.; Graham, J.; Beecher, C. W.; Kinghorn, A. D.; Pezzuto, J. M., Pharmacokinetics and tissue distribution of betulinic acid in CD–1 mice1. *Biopharm. Drug. Dispos.* **1999**, *20*, 379–383.

Wall, M. E.; Wani, M. C.; Brown, D. M.; Fullas, F.; Olwald, J. B.; Josephson, F. F.; Thornton, N. M.; Pezzuto, J. M.; Beecher, C. W. W.; Farnsworth, N. R.; Cordell, G. A.; Kinghorn, A. D., Effect of tannins on screening of plant extracts for enzyme inhibitory activity and techniques for their removal. *Phytomedicine* **1996**, *3*, 281–285.

Wang, B.; Zhu, H.–T.; Wang, D.; Yang, C.–R.; Xu, M.; Zhang, Y.–J., New spinosin derivatives from the seeds of *Ziziphus mauritiana*. *Nat. Prod. Bioprospect.* **2013,** *3*, 93–98.

Wang, J. Z.; Yang, J. S., Structural elucidation of triterpene saponins from the seeds of *Zizyphus jujuba* Mill. *Youji Huaxue* **2008**, *28*, 69–72.

Wang, Y.; Ding, B.; Luo, D.; Chen, L.–Y.; Hou, Y.–L.; Dai, Y.; Yao, X.–S., New triterpene glycosides from *Ziziphi Spinosae* Semen., *Fitoterapia* **2013,** *90*, 185–191.

Wu, Y.; Zhang, J.; Wang, D.; Liu, J.–G.; Hu, Y., Triterpenoid saponins from *Ziziphus jujuba* var. *spinosa*. *Chem. Nat. Compd.* **2013,** *49*, 677–681.

Xu, M.–Y.; Lee, S. Y.; Kang, S. S.; Kim, Y. S., Antitumor Activity of Jujuboside B and the underlying mechanism via induction of apoptosis and autophagy. *J. Nat. Prod.* **2014,** *77*, 370–376.

Xu, R.; Fazio, G. C.; Matsuda, S. P. T., On the origins of triterpenoid skeletal diversity. *Phytochemistry* **2004,** *65*, 261–291.

Yagi, A.; Okamura, N.; Haraguchi, Y.; Noda, K.; Nishioka, I. Studies on the constituents of *Zizyphi Fructus*. II. Structure new *p*–coumaroylates of maslinic acid. *Chem. Pharm. Bull*. **1978**a, *26*, 3075–3079.

Yagi, A.; Okamura, N.; Haraguchi, Y.; Noda, K.; Nishioka, I., Studies on the constituents of *Zizyphi fructus*. I. Structure of three new *p*–coumaroylates of alphitolic acid. *Chem. Pharm. Bull.* **1978**b, *26*, 1798–1802.

Yasomanee, J. P.; Demchenko, A. V., The effect of remote picolinyl and picoloyl substituents on the stereoselectivity of chemical glycosylation. *J. Am. Chem. Soc.* **2012**, *134*, 20097–20102.

Yoshikawa, K.; Shimono, N.; Arihara, S. Antisweet substances, jujubasaponins I–III from *Zizyphus jujuba* revised structure of ziziphin. *Tetrahedron Lett.* **1991,** *32*, 7059–7062.

Yoshikawa, K.; Shimono, N.; Arihara, S., Antisweet Natural Products. VI. Jujubasaponins IV, V and VI from *Zizyphus jujuba* MILL. *Chem. Pharm. Bull.* **1992,** *40*, 2275–2278.

Yoshikawa, M.; Murakami, T.; Ikebata, A.; Wakao, S.; Murakami, N.; Matsuda, H.; Yamahara, J., Bioactive Saponins and Glycosides. X. On the constituents of *Zizyphi spinosi* semen, the seeds of *Zizyphus jujuba* MILL. var. *spinosa* HU (1): Structures and histamine release–inhibitory effects of jujubosides A1 and C and acetyljujuboside B. *Chem. Pharm. Bull.* **1997,** *45*, 1186–1192.

You, Y. J.; Kim, Y.; Nam, N. H.; Ahn, B. Z., Synthesis and cytotoxic activity of a–ring modified betulinic acid derivatives. *Bioorg. Med. Chem. Lett.* **2003**, *13*, 3137–3140.

Yu, Z.; Wang, X. S.; Hu, Z. H., Dammarane–type saponins from *Ziziphus jujube*. *J. Asian Nat. Prod. Res.* **2014,** *16*, 200–205.

Zhu, J.; Zhang, W.; Hu, J. Copper-mediated fluoroalkylation reactions with iododifluoroacetamides: controlling the selectivity among cross-coupling, intramolecular cyclization, and homocoupling reactions. *J. Org. Chem.* **2010**, *75*, 5505-5512.

Ziegler, H. L.; Franzyk, H.; Sairafianpour, M.; Tabatabai, M.; Tehrani, M. D. Bagherzadeh, K.; Hagerstrand, H., Staerk, D.; Jaroszewski, J. W., Erythrocyte membrane modifying agents and the inhibition of *Plasmodium falciparum* growth: structure–activity relationships for betulinic acid analogues. *Bioorg. Med. Chem.* **2004**, *12*, 119–127.

Zuco, V.; Supino, R.; Righetti, S. C.; Cleris, L.; Marchesi, E.; Gambacorti–Passerini, C.; Formelli, F., Selective cytotoxicity of betulinic acid on tumor cell lines, but not on normal cells. *Cancer Lett*. **2002**, *175*, 17–25.

APPENDIX

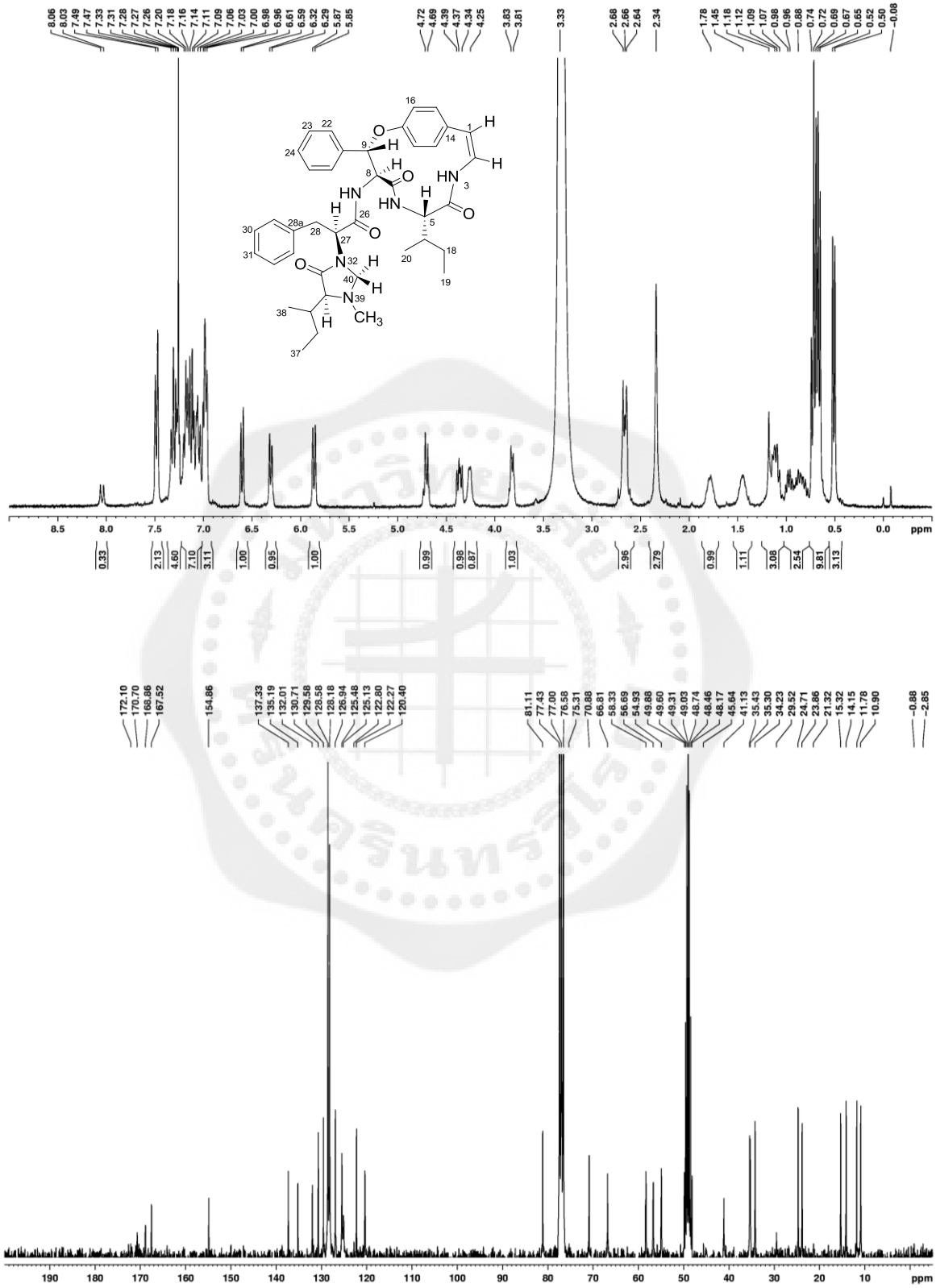

Figure 60 ^{1}H– and ^{13}C NMR of compound **A** in $CDCl_3$ + few drops of CD_3OD (sss3096, cambodine A)

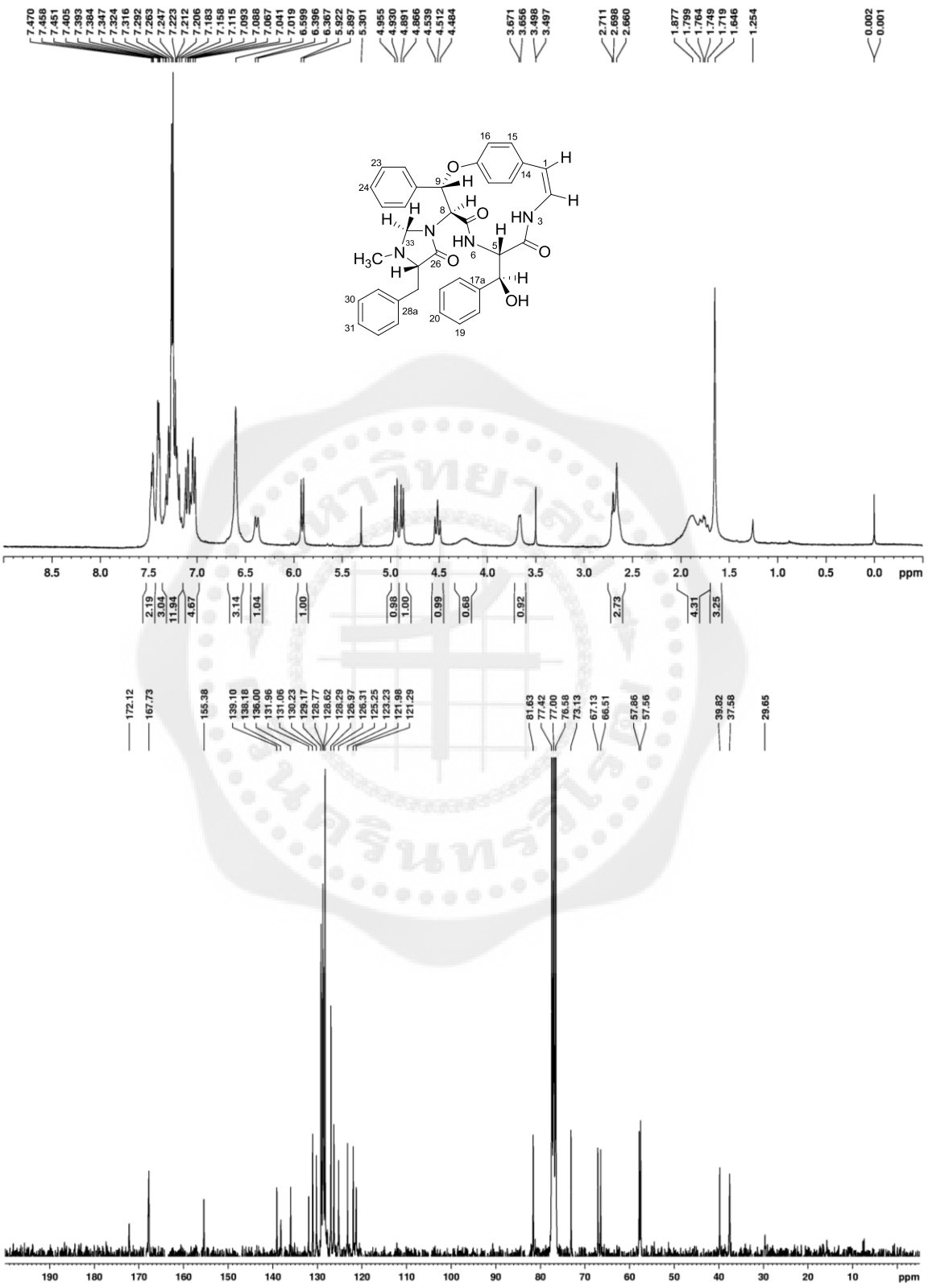

Figure 61 ^{1}H– and ^{13}C NMR of compound **B** in $CDCl_3$ (sss3155, cambodine B)

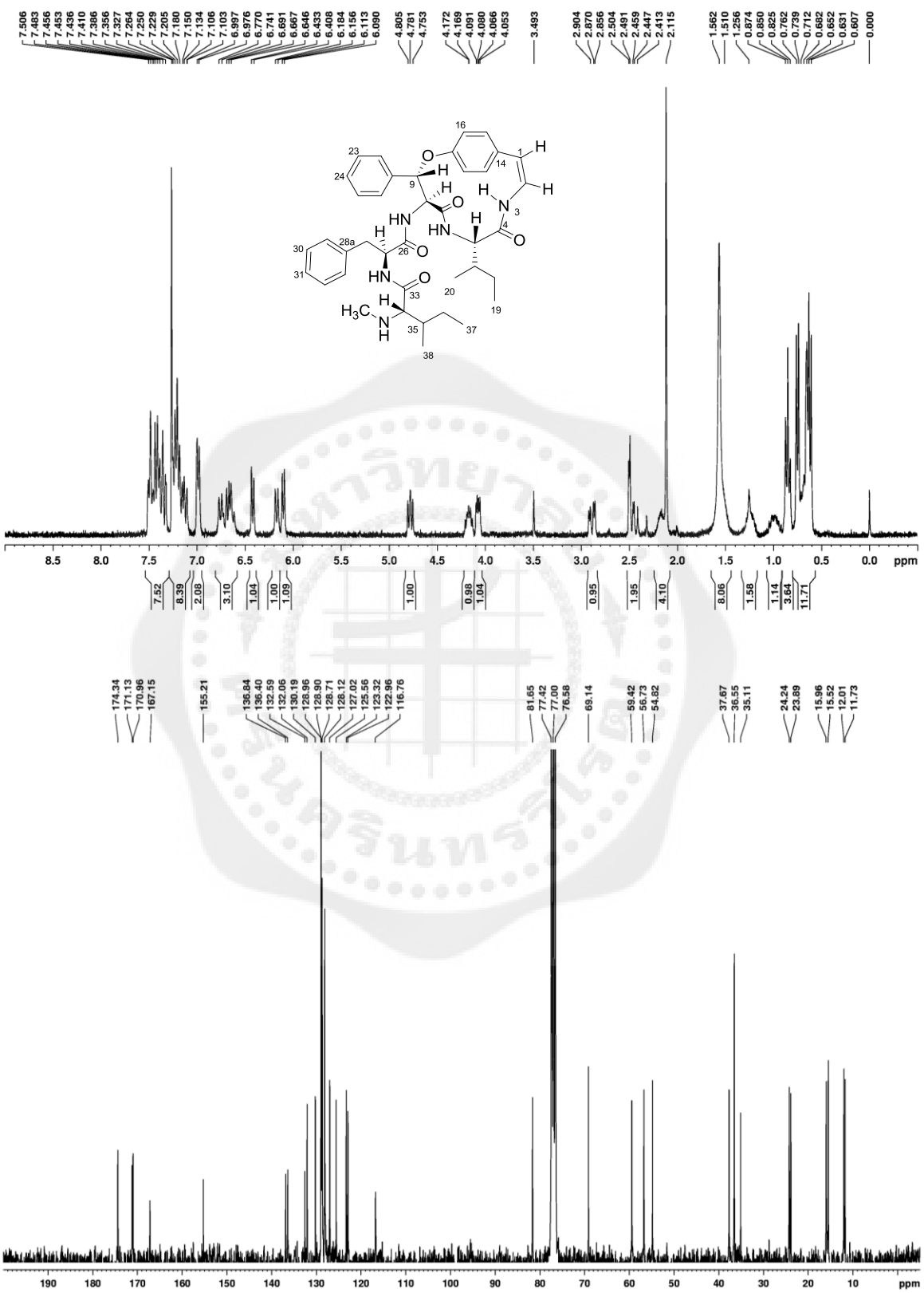

Figure 62 ^{1}H– and ^{13}C NMR of compound **C** in $CDCl_3$ (sss4402, cambodine C)

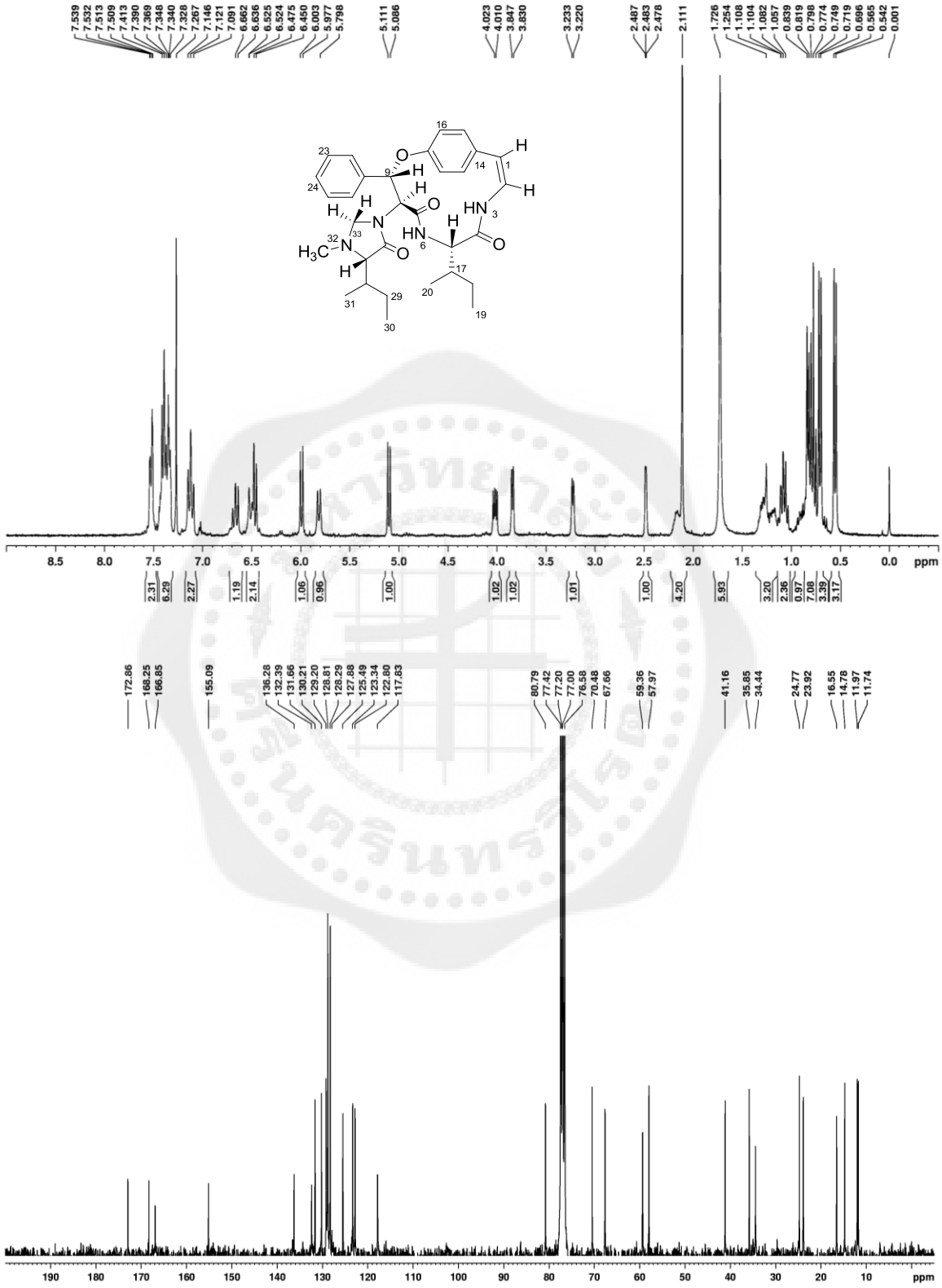

Figure 63 ^{1}H– and ^{13}C NMR of compound **D** in $CDCl_3$ (sss4732, cambodine D)

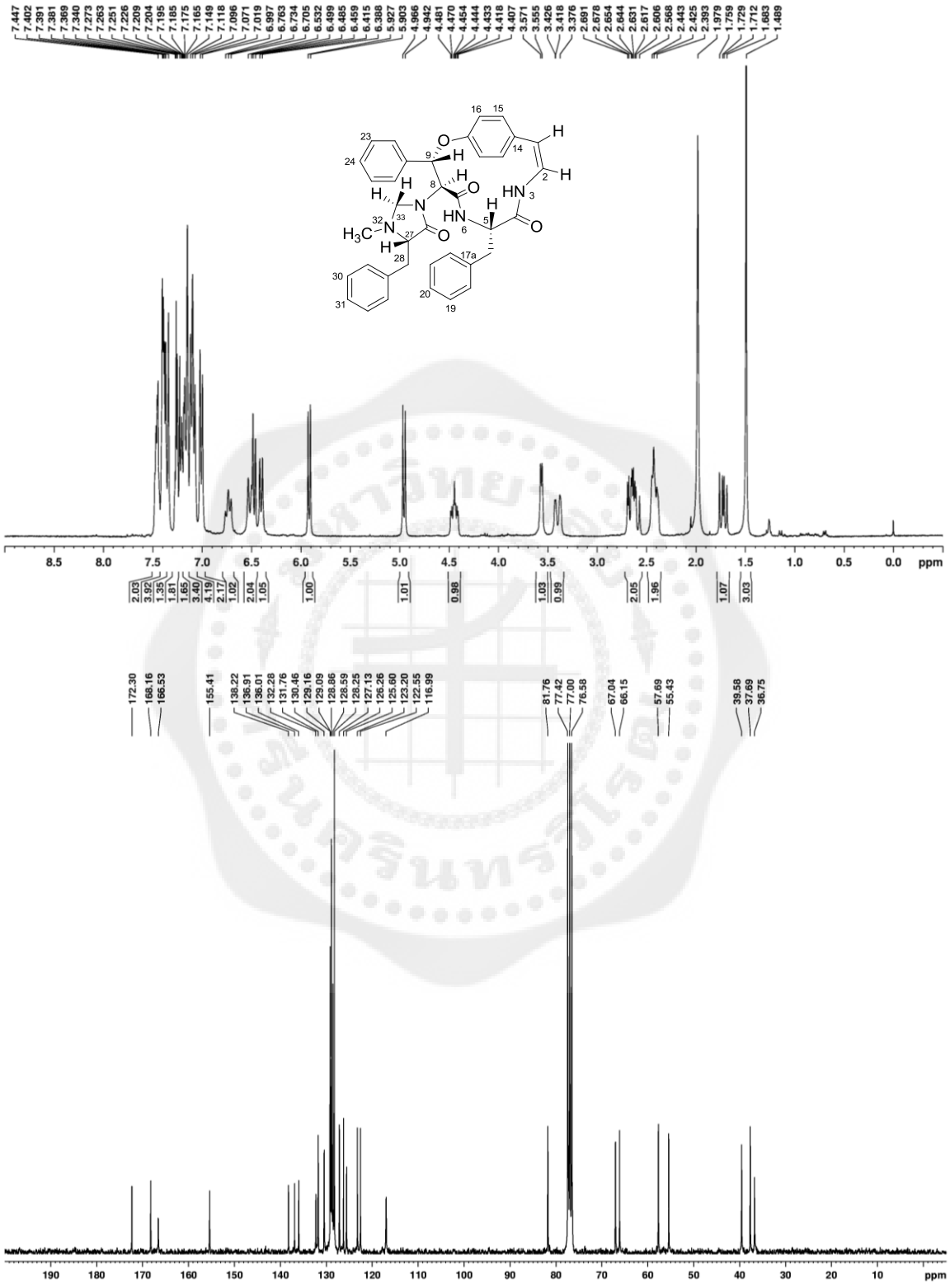

Figure 64 ^{1}H– and ^{13}C NMR of compound **E** in $CDCl_3$ (sss4759, cambodine E)

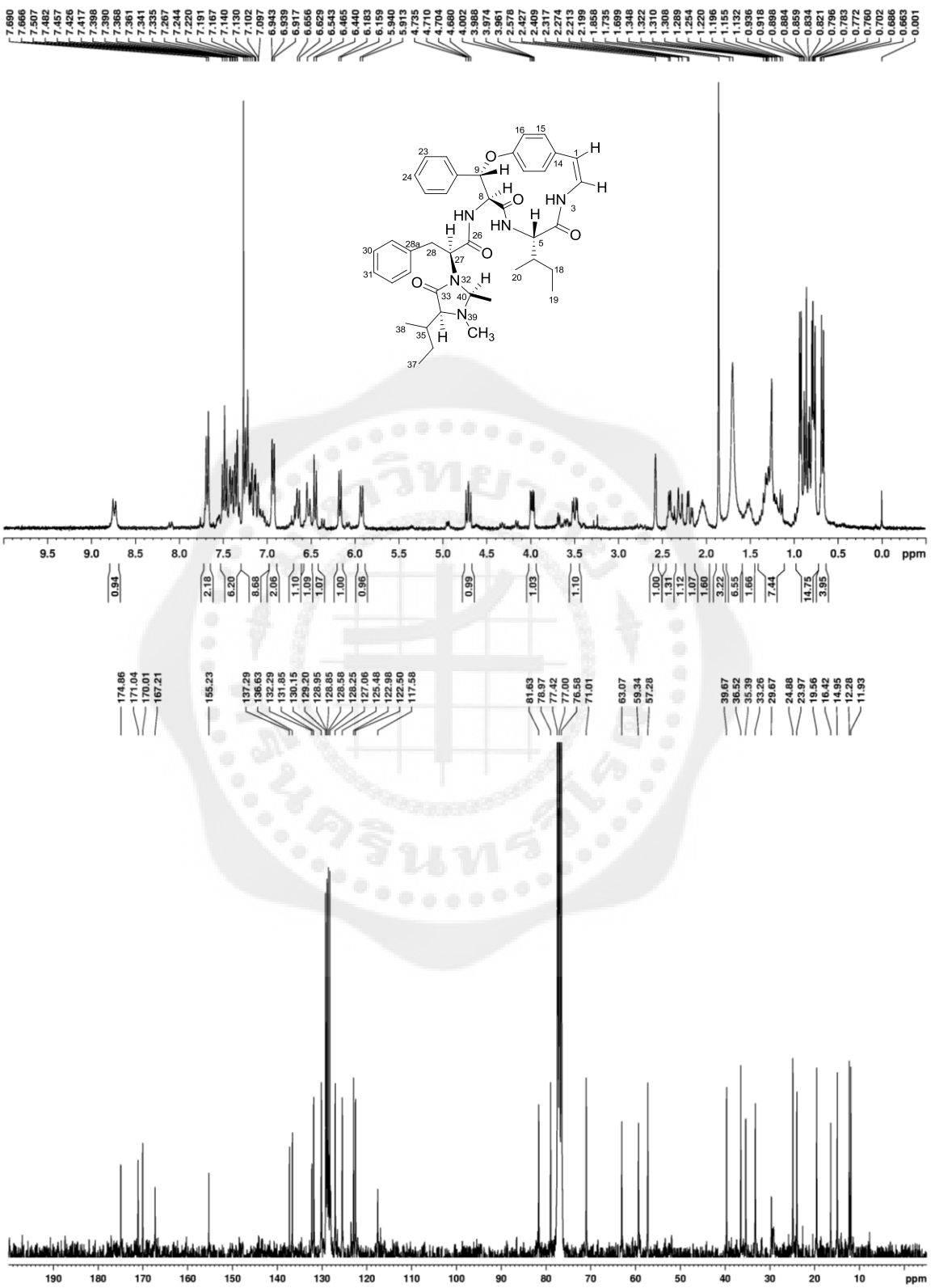

Figure 65 ^{1}H– and ^{13}C NMR of compound **F** in $CDCl_3$ (sss4759, cambodine F)

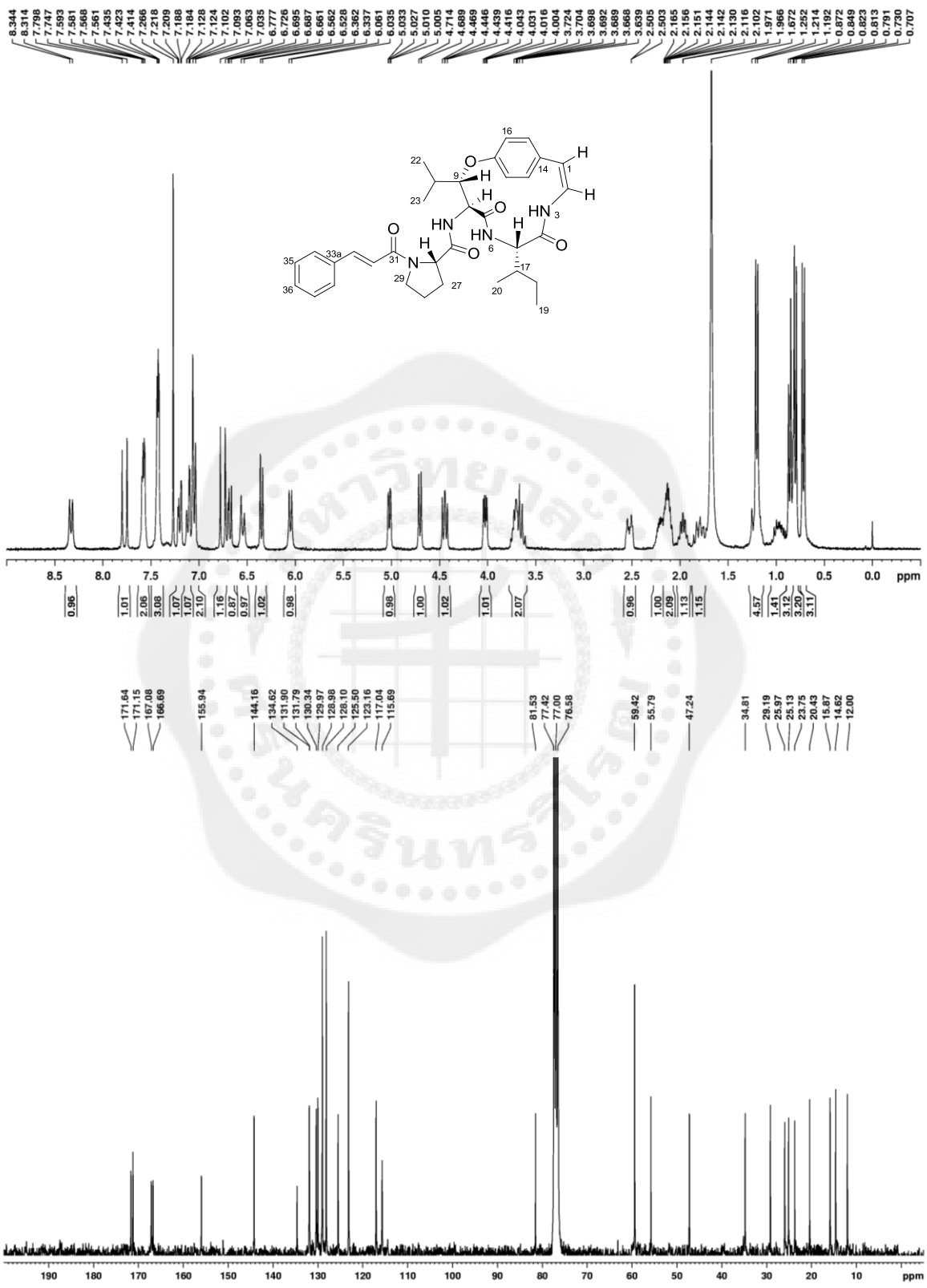

Figure 66 ^{1}H– and ^{13}C NMR of compound **G** in $CDCl_3$ (sss4767, cambodine G)

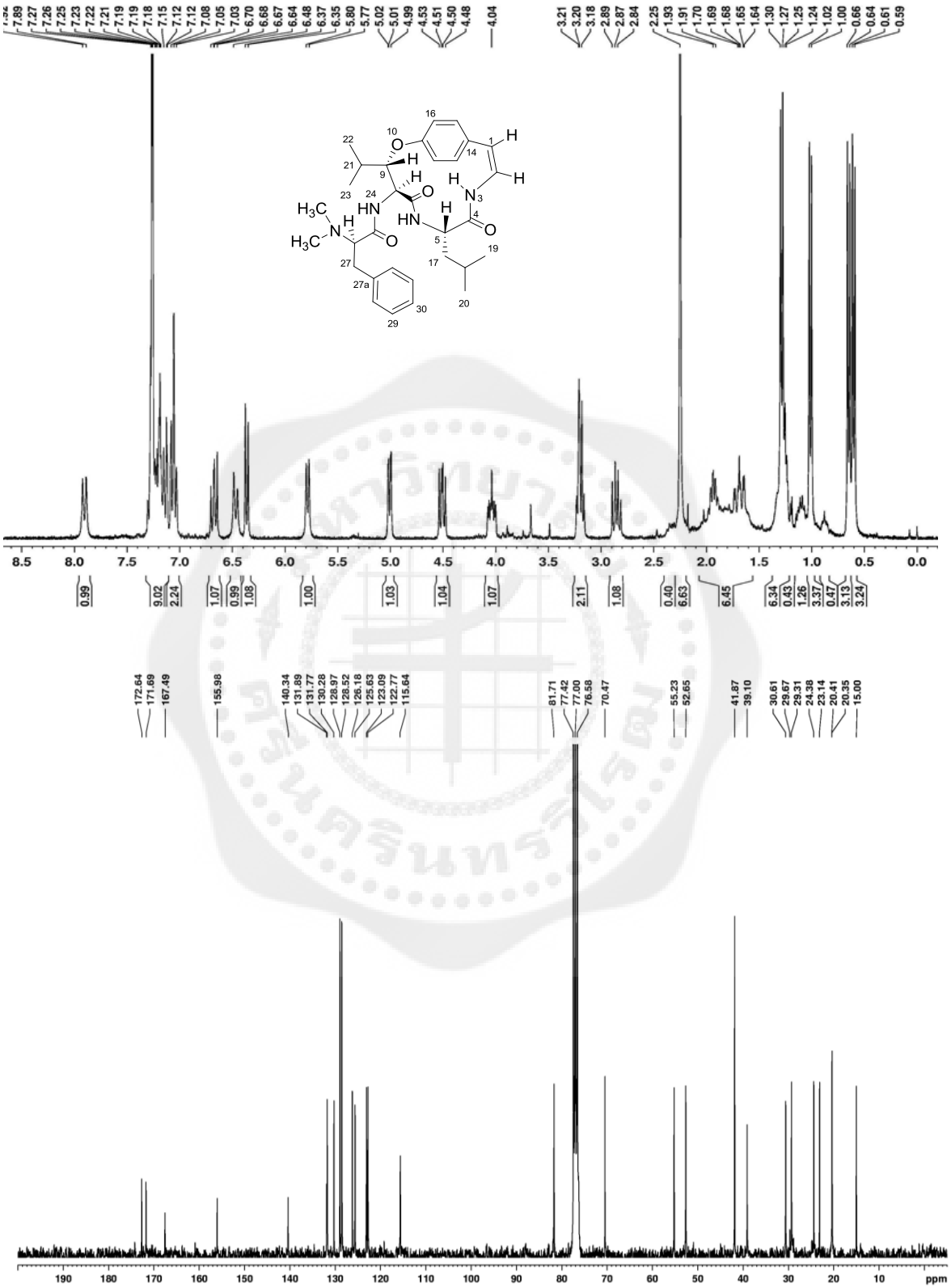

Figure 67 ^{1}H– and ^{13}C NMR of compound **H** in $CDCl_3$ (sss4449, frangufoline)

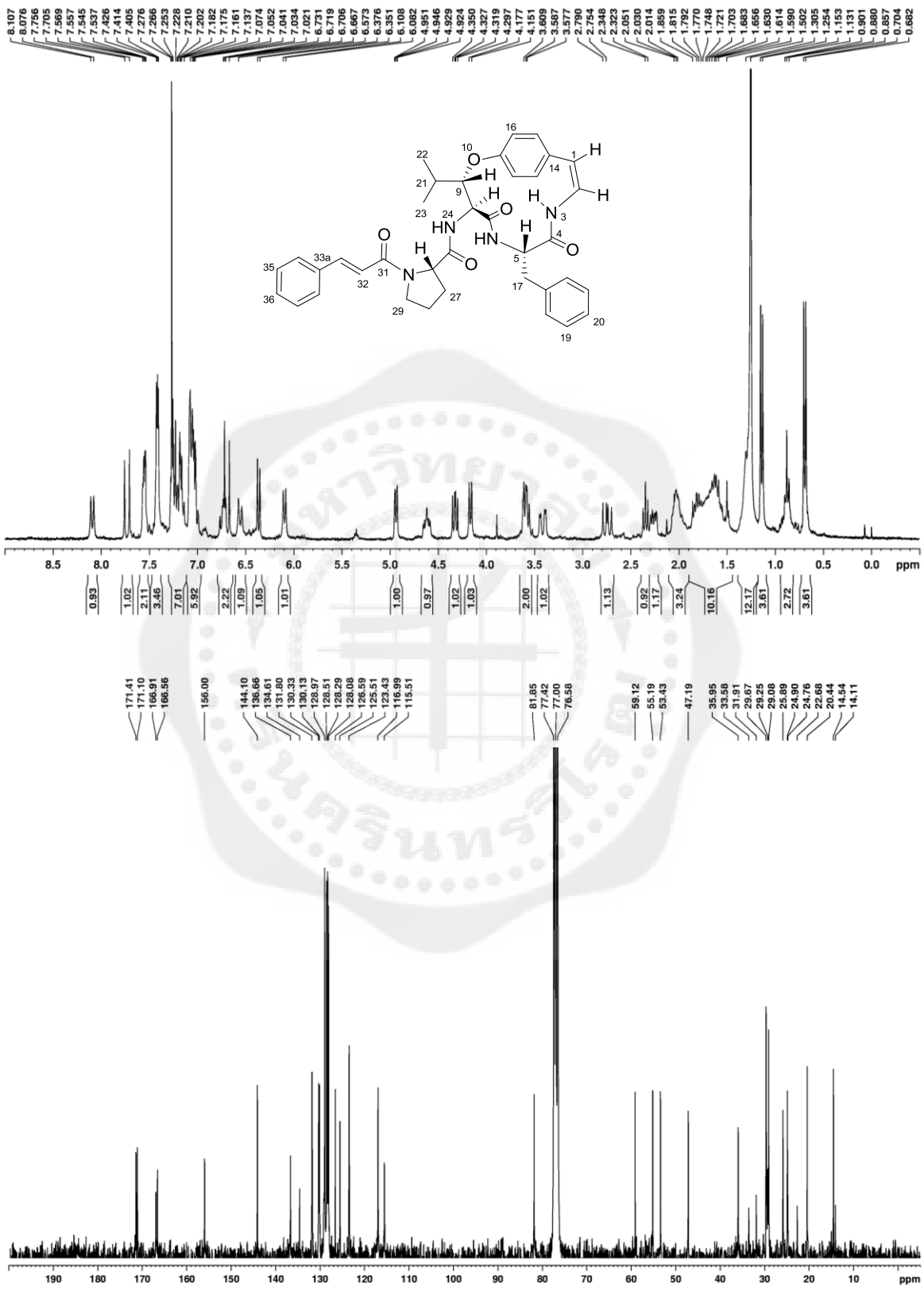

Figure 68 ^{1}H– and ^{13}C NMR of compound **I** in $CDCl_3$ (sss4635, lotusanine B)

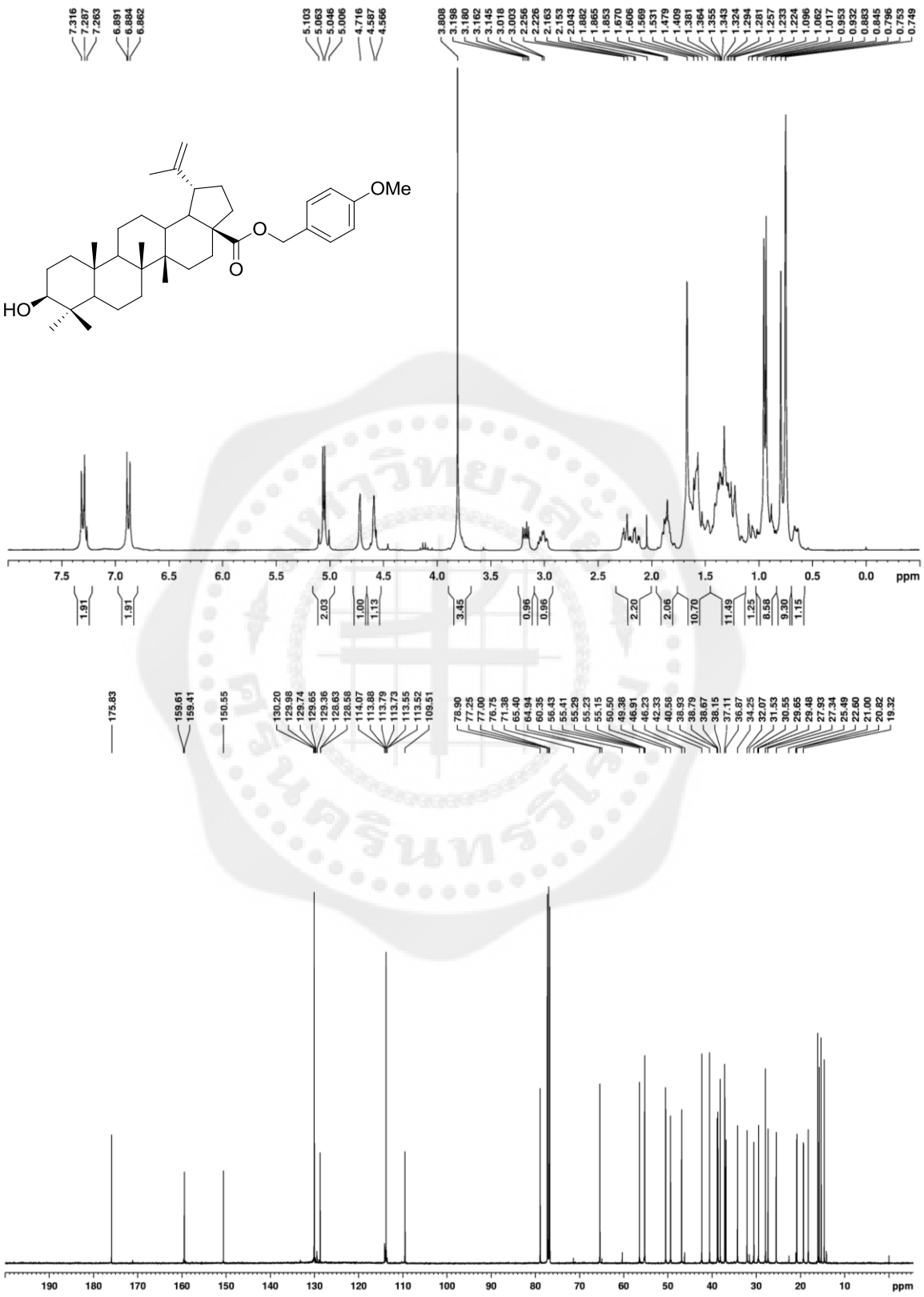

Figure 69 ^{1}H– and ^{13}C NMR of 28–*p*–methoxy–benzyl betulinic acid (**1′**) in $CDCl_3$ (sss6468)

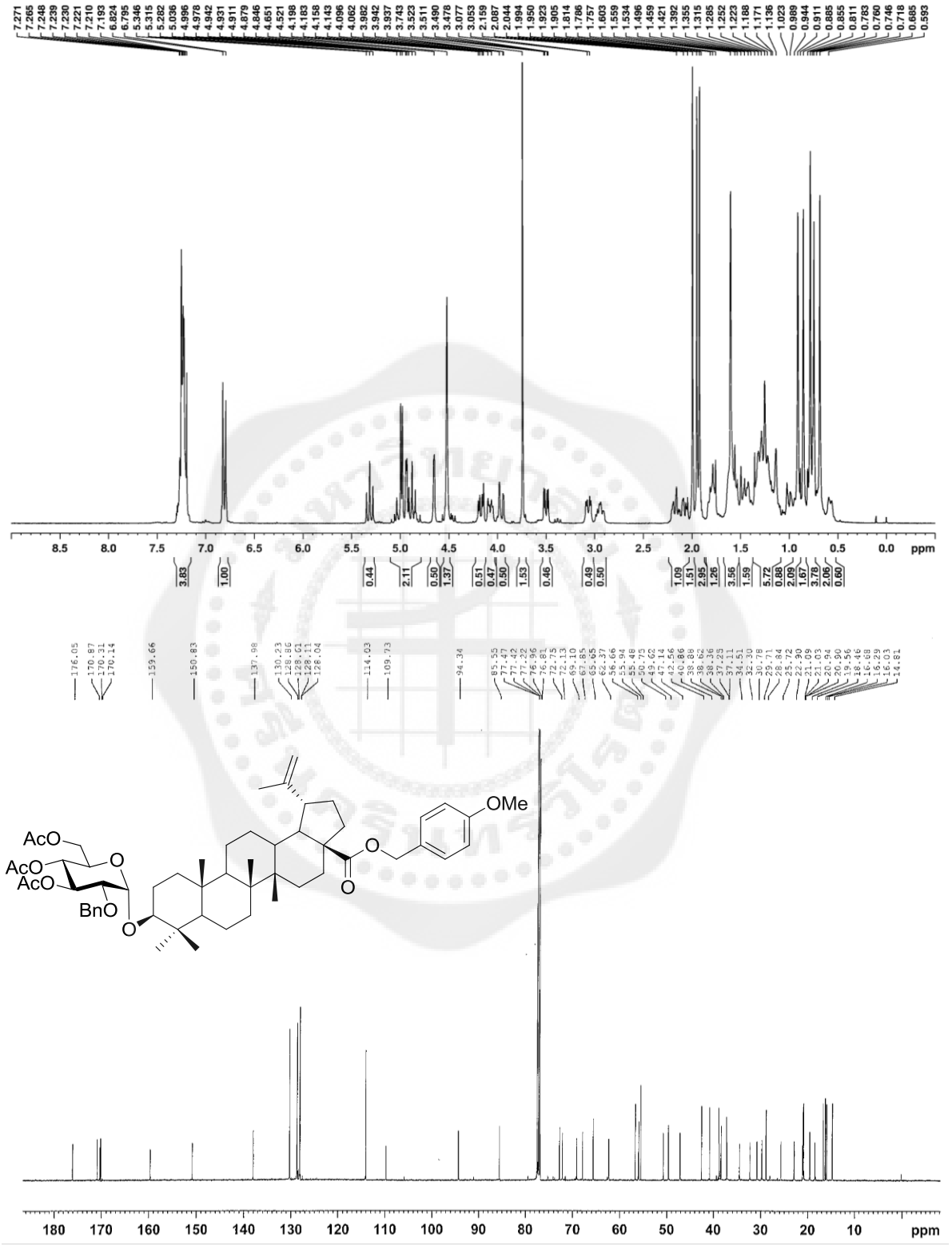

Figure 70 ^{1}H– and ^{13}C NMR of 3–*O*–(3,4,6–tri–*O*–acetyl–*α*–*D*–glucopyranosyl)–28–*p*–methoxy–benzyl betulinic acid (**290**) in $CDCl_3$

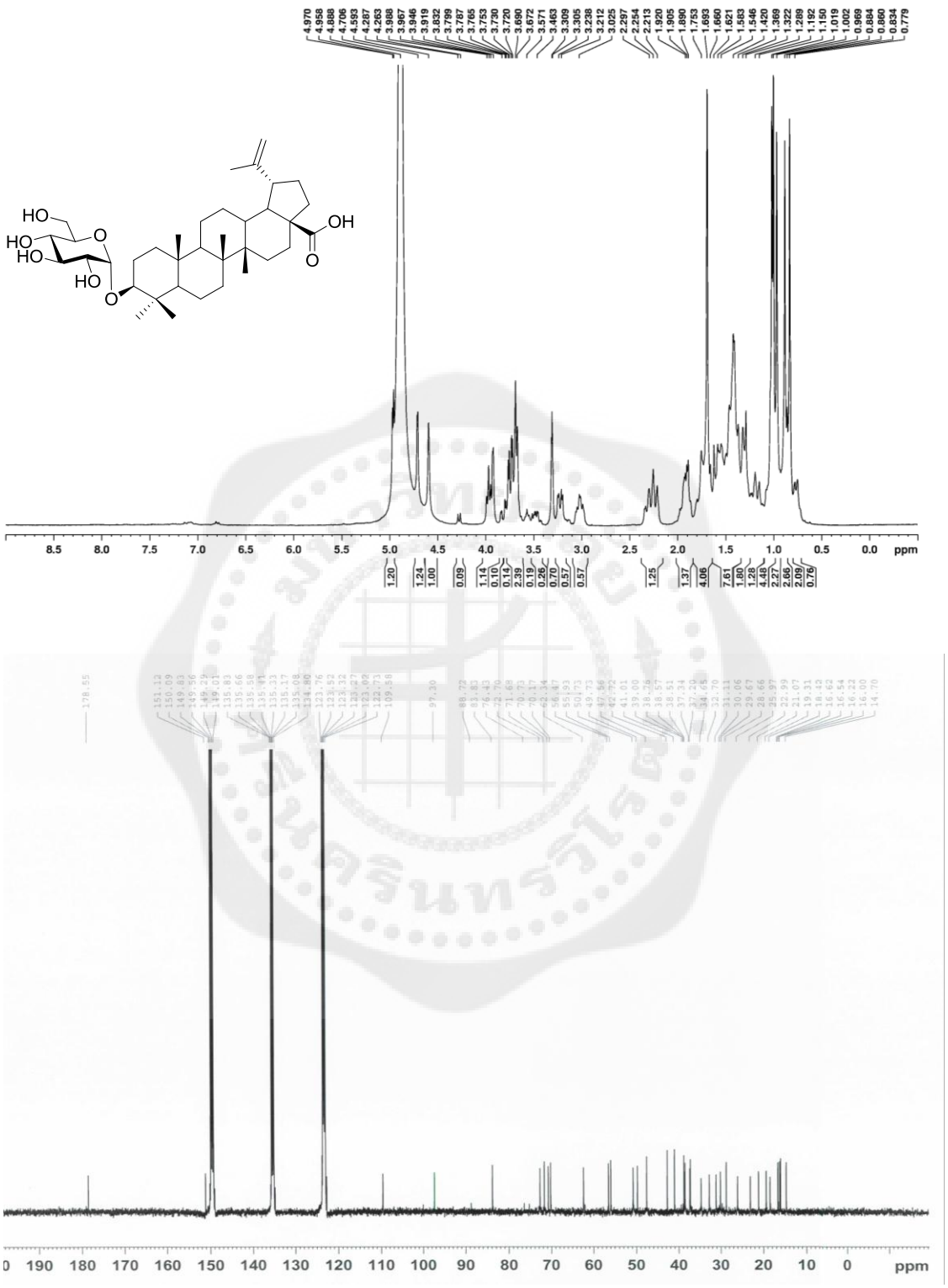

Figure 71 ^{1}H– and ^{13}C NMR of 3–*O*–α–*D*–glucopyranosyl betulinic acid (**291**) in methanol–d_4 (NL309, sss6463)

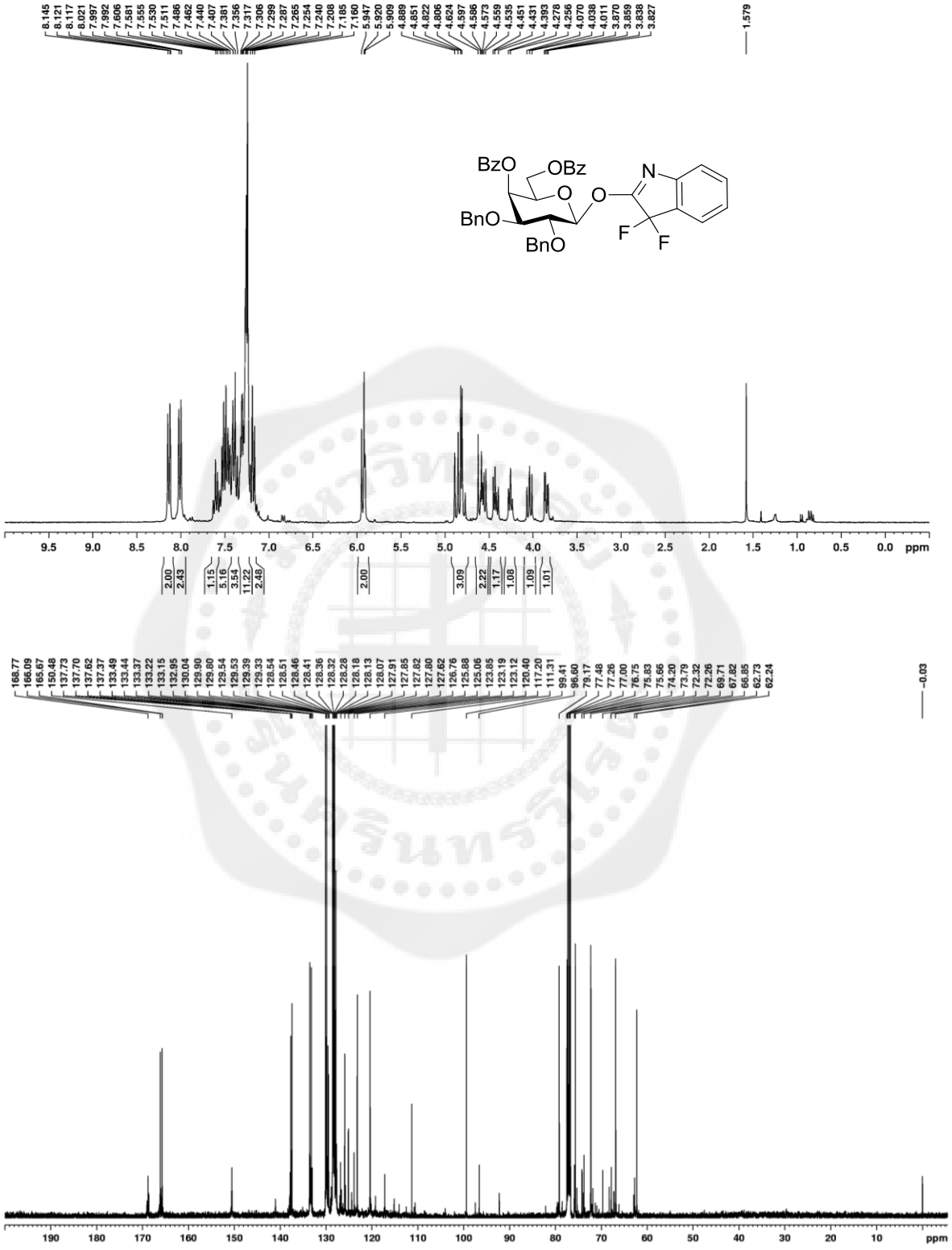

Figure 72 ^{1}H– and ^{13}C NMR of 3,3–Difluoro–3*H*–indol–2–yl 2,3–di–*O*–benzyl–4,6–*O*–benzoyl–α–*D*–galactopyranoside (**292**) in $CDCl_3$ (NL291, sss6459)

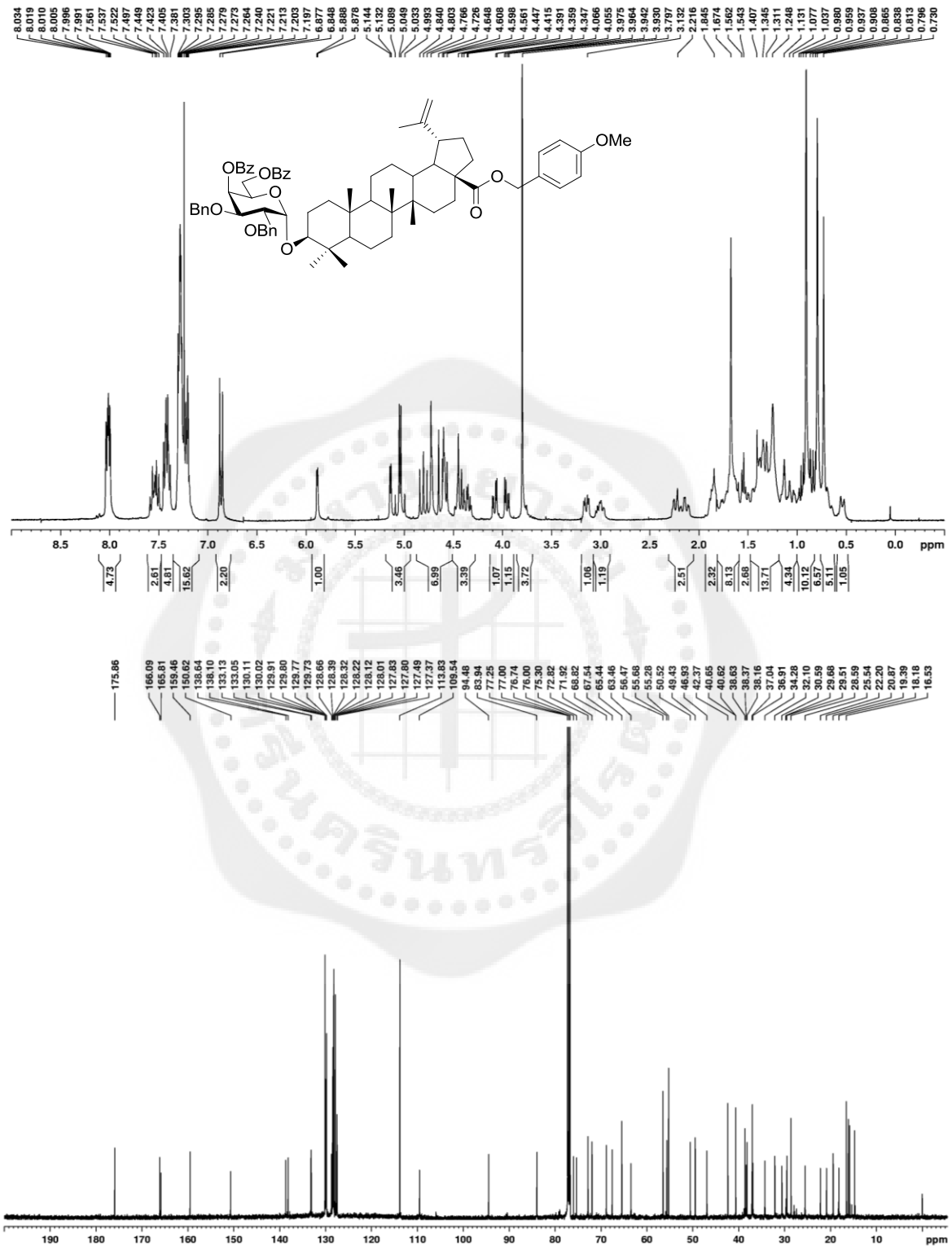

Figure 73 ^{1}H– and ^{13}C NMR of 3–*O*–(2,3–di–*O*–benzyl–4,6–di–*O*–benzoyl–*α*–*D*–galactopyranosyl)–28–*p*–methoxy–benzyl betulinic acid (**295**) in $CDCl_3$ (NL288, sss6455)

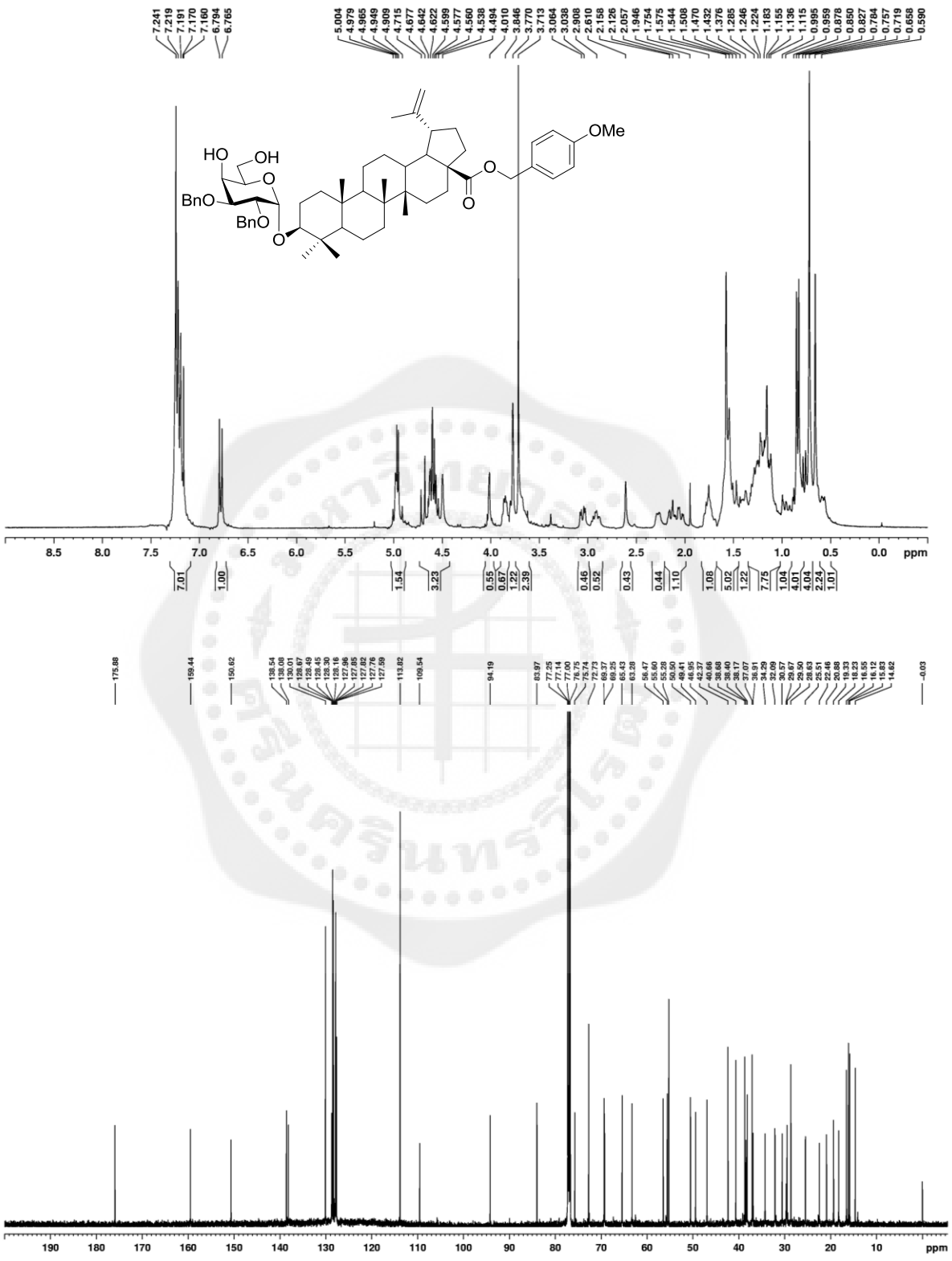

Figure 74 ^{1}H– and ^{13}C NMR of 3–*O*–(2,3–di–*O*–benzyl–*α*–*D*–galactopyranosyl)–28–*p*–methoxy–benzyl betulinic acid (**296**) in $CDCl_3$ (NL298(1), sss6456)

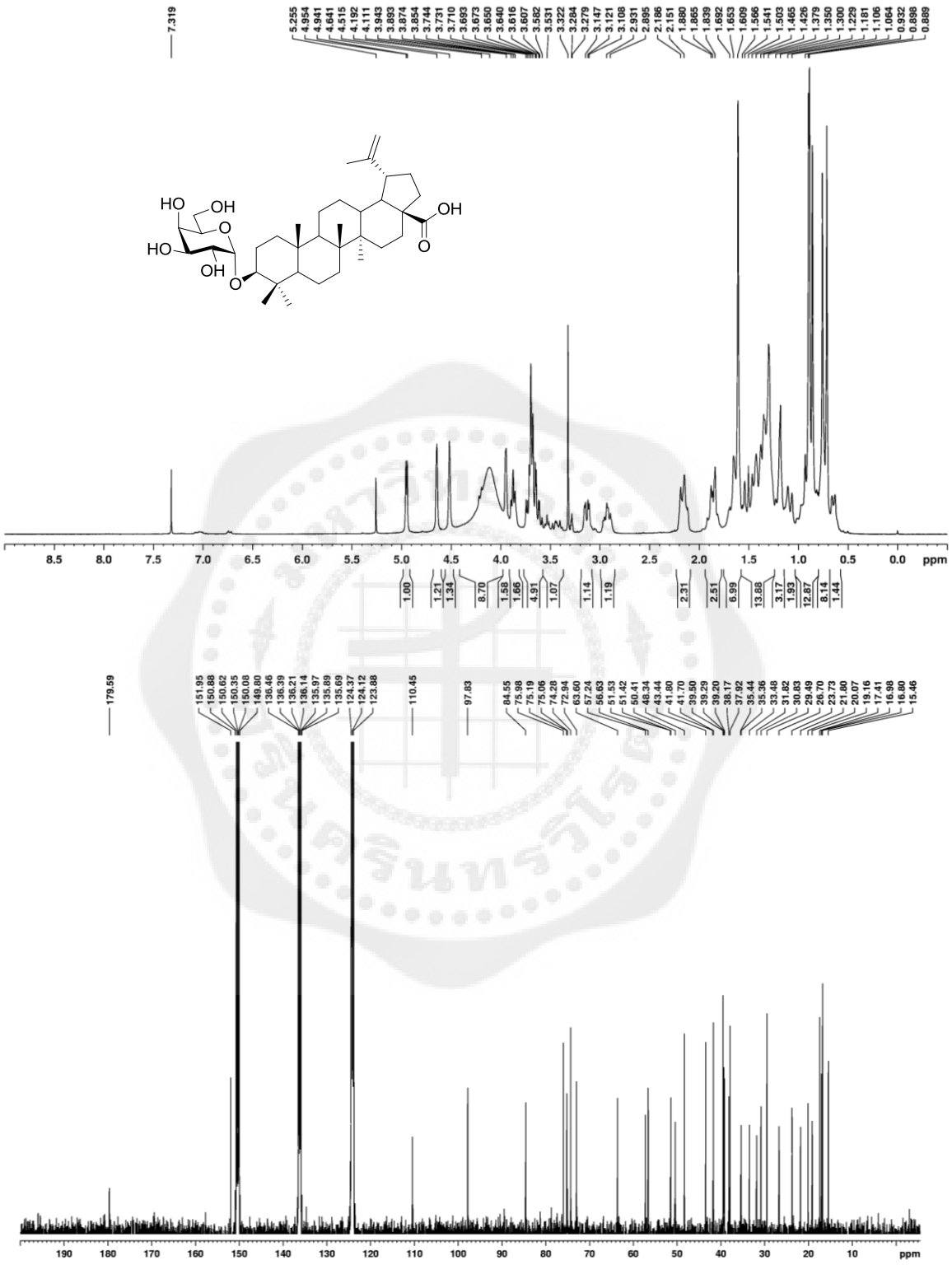

Figure 75 ^{1}H– and ^{13}C NMR of 3–*O*–α–*D*–galactopyranosyl betulinic acid (**297**) in $CDCl_3$ + pyridine–d_5 (NL307, sss6464)

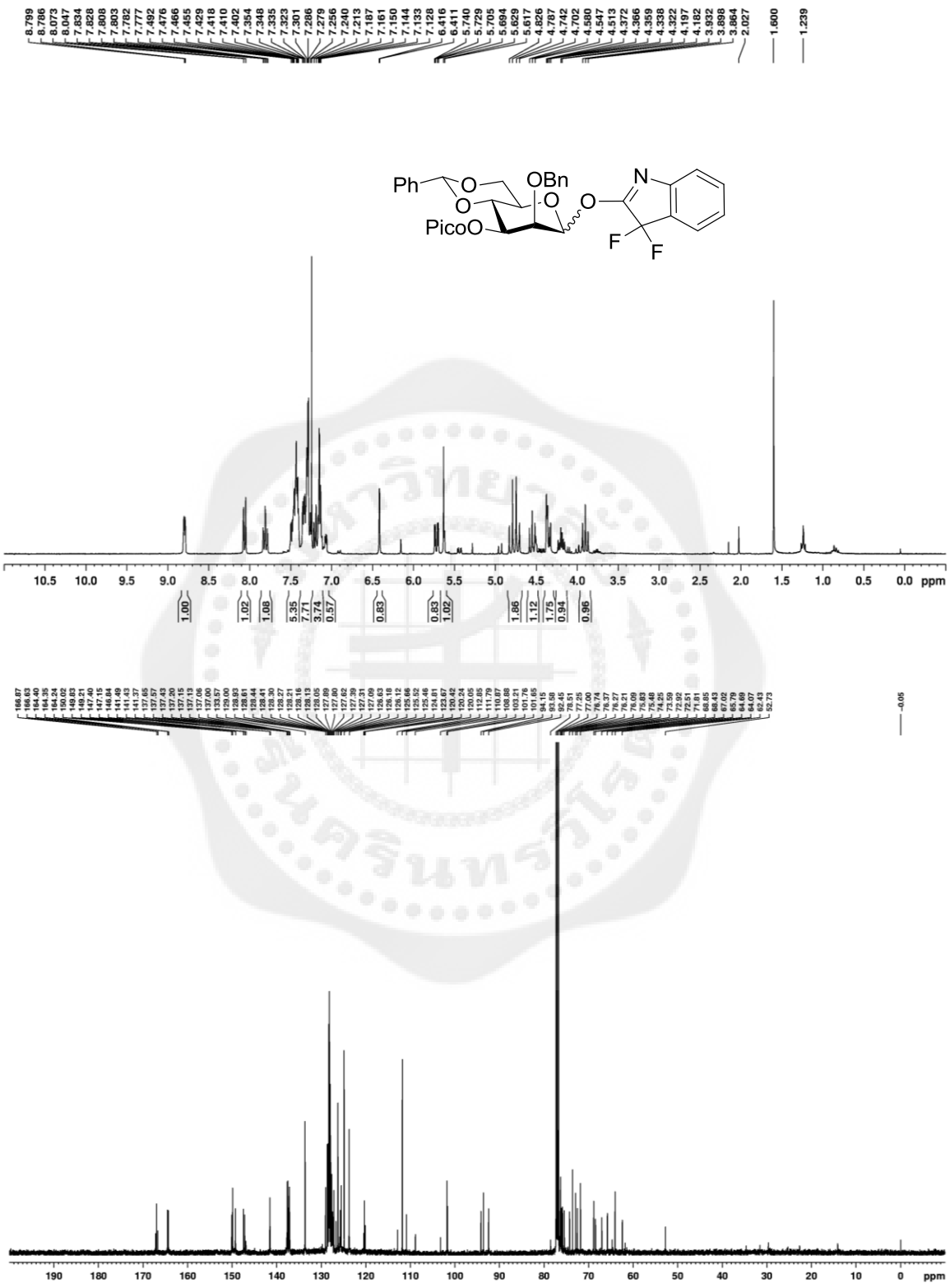

Figure 76 ^{1}H– and ^{13}C NMR of 3,3–Difluoro–3*H*–indol–2–yl 2–*O*–benzyl–4,6–*O*–benzylidene–3–*O*–picoloyl–α–*D*–mannopyranoside (**298**) in $CDCl_3$ (NL266, sss6460)

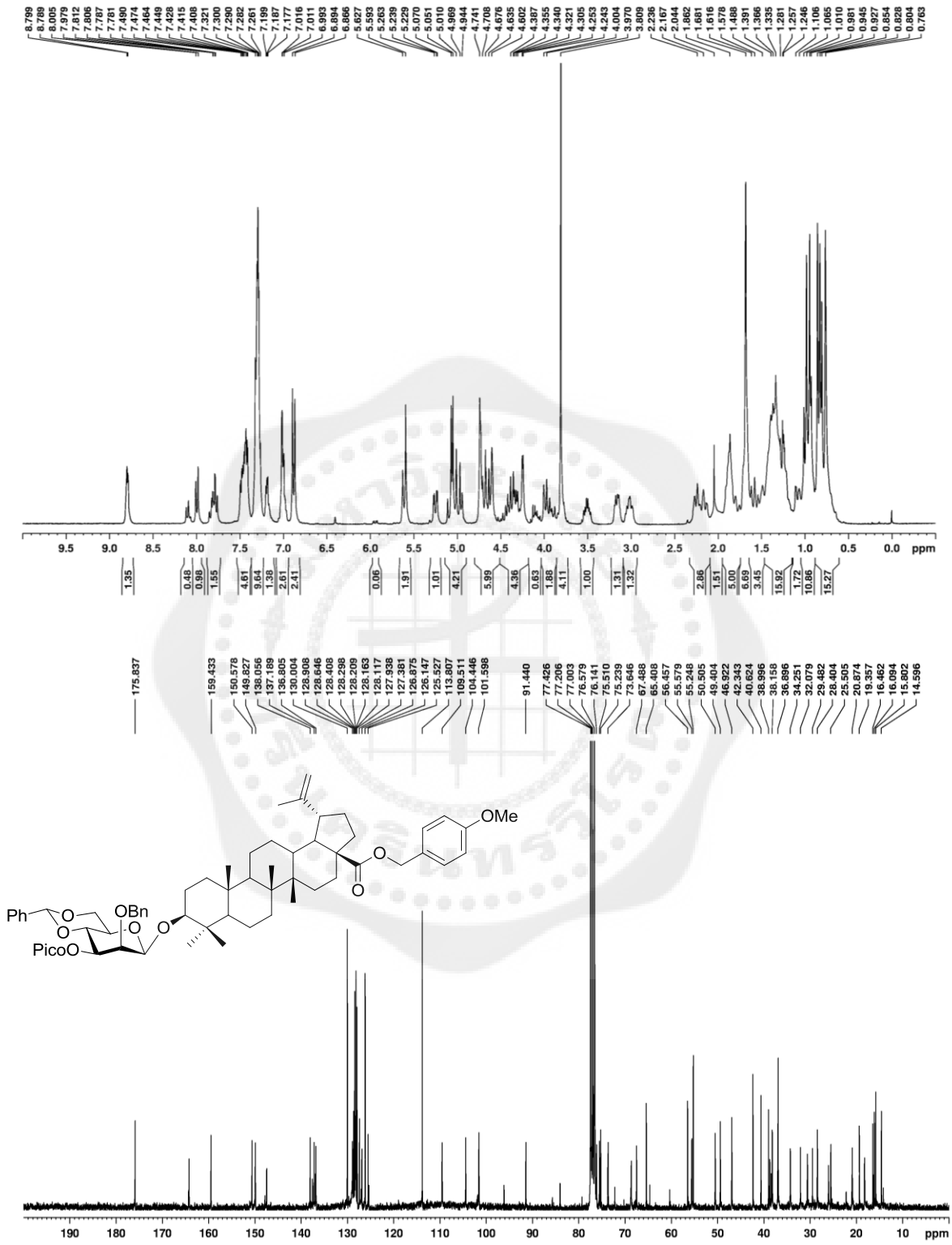

Figure 77 ^{1}H– and ^{13}C NMR of 3–*O*–(2–*O*–benzyl–4,6–*O*–benzylidene–3–*O*–picoloyl–*β*–*D*–mannopyranosyl)–28–*p*–methoxy–benzyl betulinic acid (**301**) in $CDCl_3$ (NL277, sss6458)

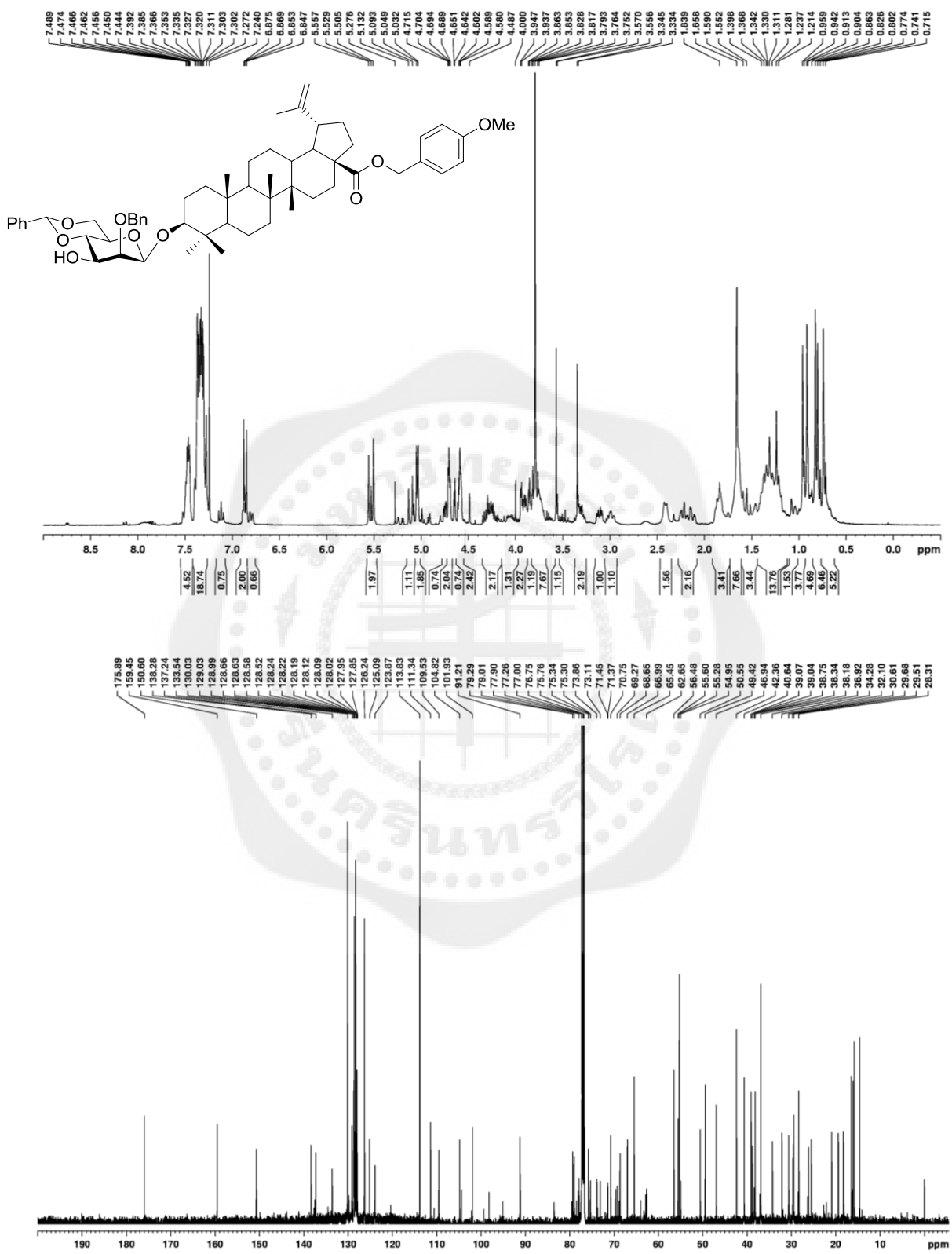

Figure 78 3–*O*–(2–*O*–benzyl–4,6–*O*–benzylidene–*β*–*D*–mannopyranosyl)–28–*p*–methoxy–benzyl betulinic acid (**302**) in $CDCl_3$ (NL299)

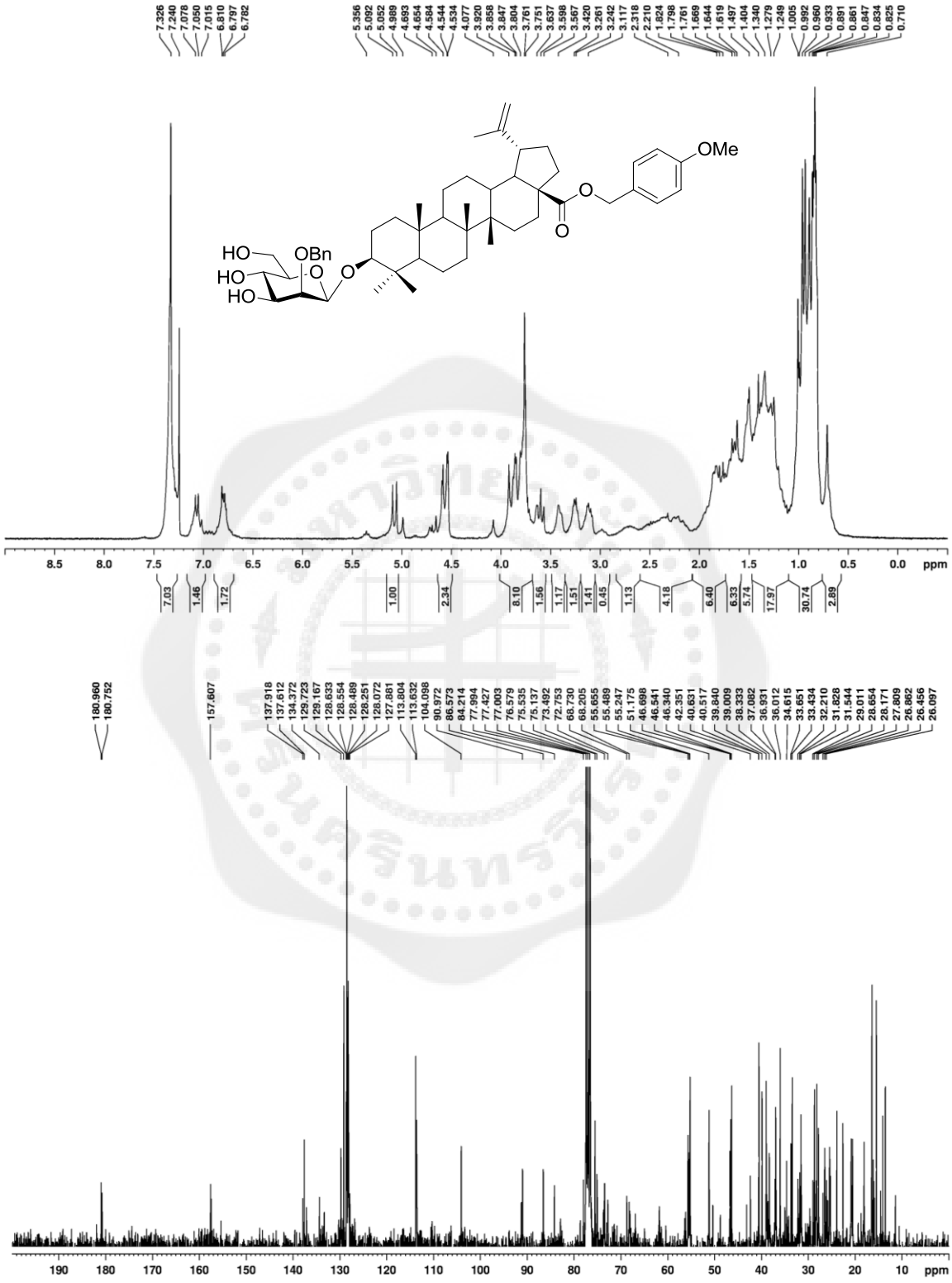

Figure 79 ^{1}H– and ^{13}C NMR of 3–*O*–(2–*O*–benzyl–*β*–*D*–mannopyranosyl)–28–*p*–methoxy–benzyl betulinic acid (**303**) in $CDCl_3$ (NL290)

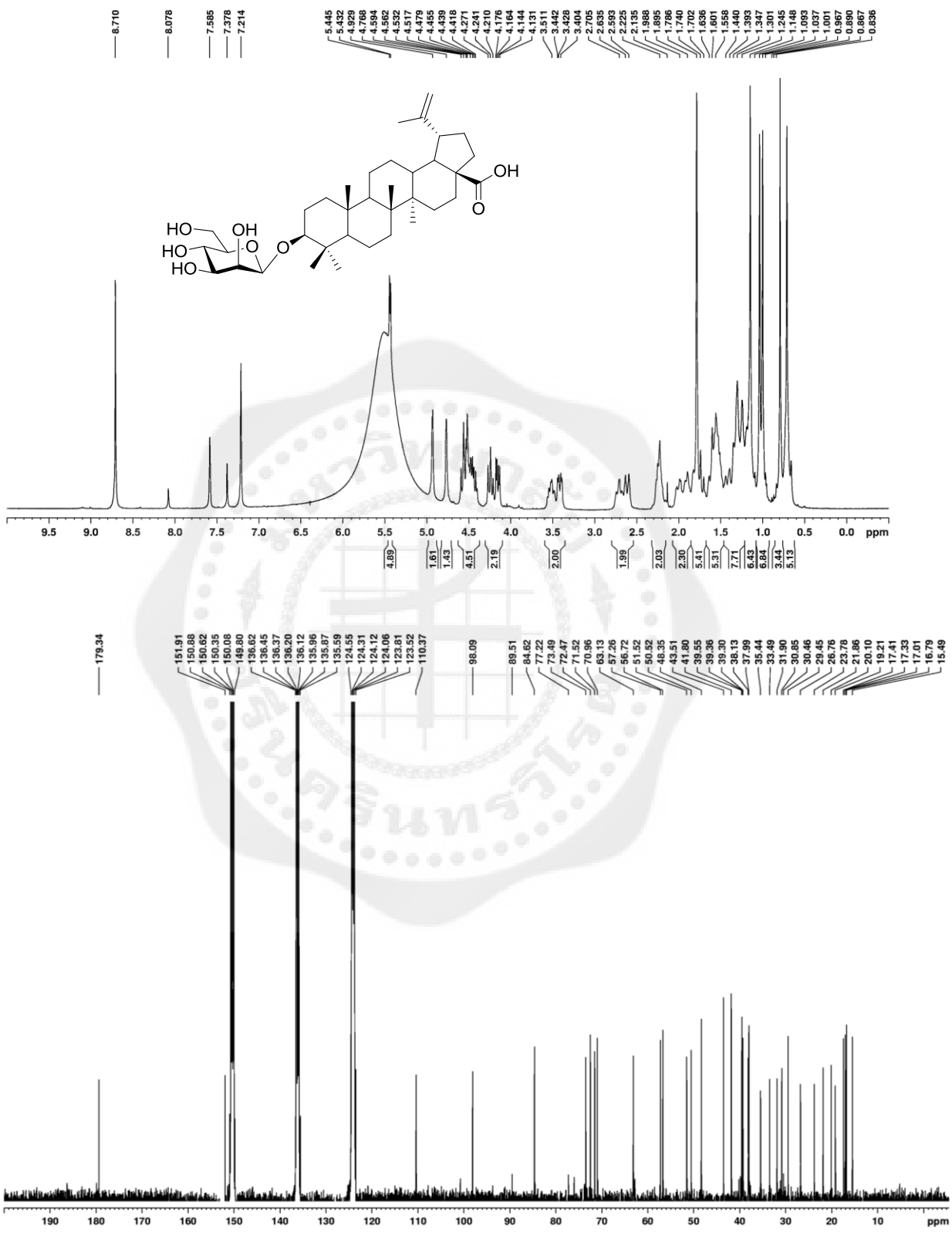

Figure 80 ^{1}H– and ^{13}C NMR of 3–*O*–*β*–*D*–mannopyranosyl betulinic acid (**304**) in methanol–d_4 pyridine–d_5 (NL309, sss6465)

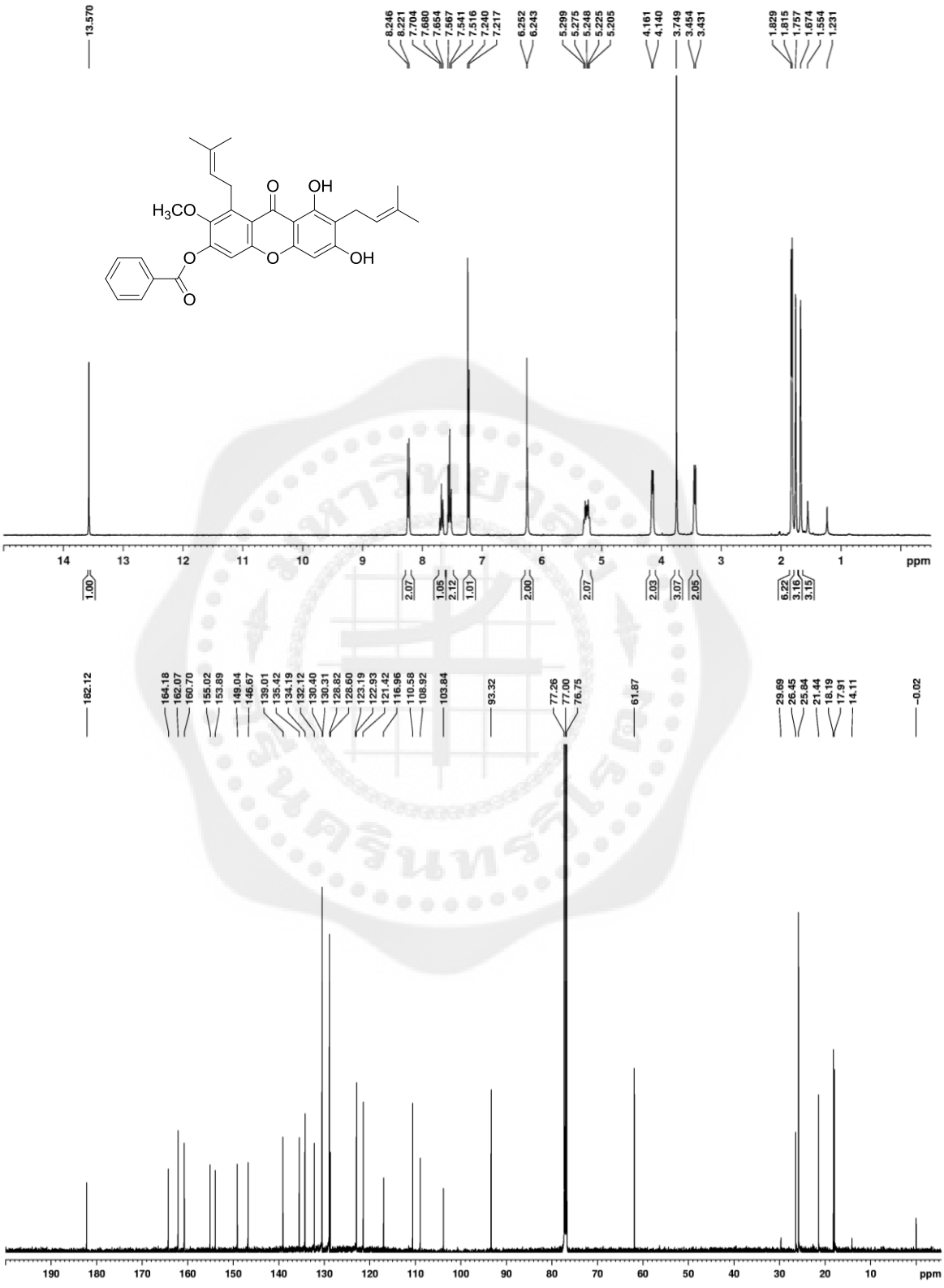

Figure 81 ^{1}H– and ^{13}C NMR of 6–*O*–benzoyl mangostin (**234′**) in $CDCl_3$ (NL110)

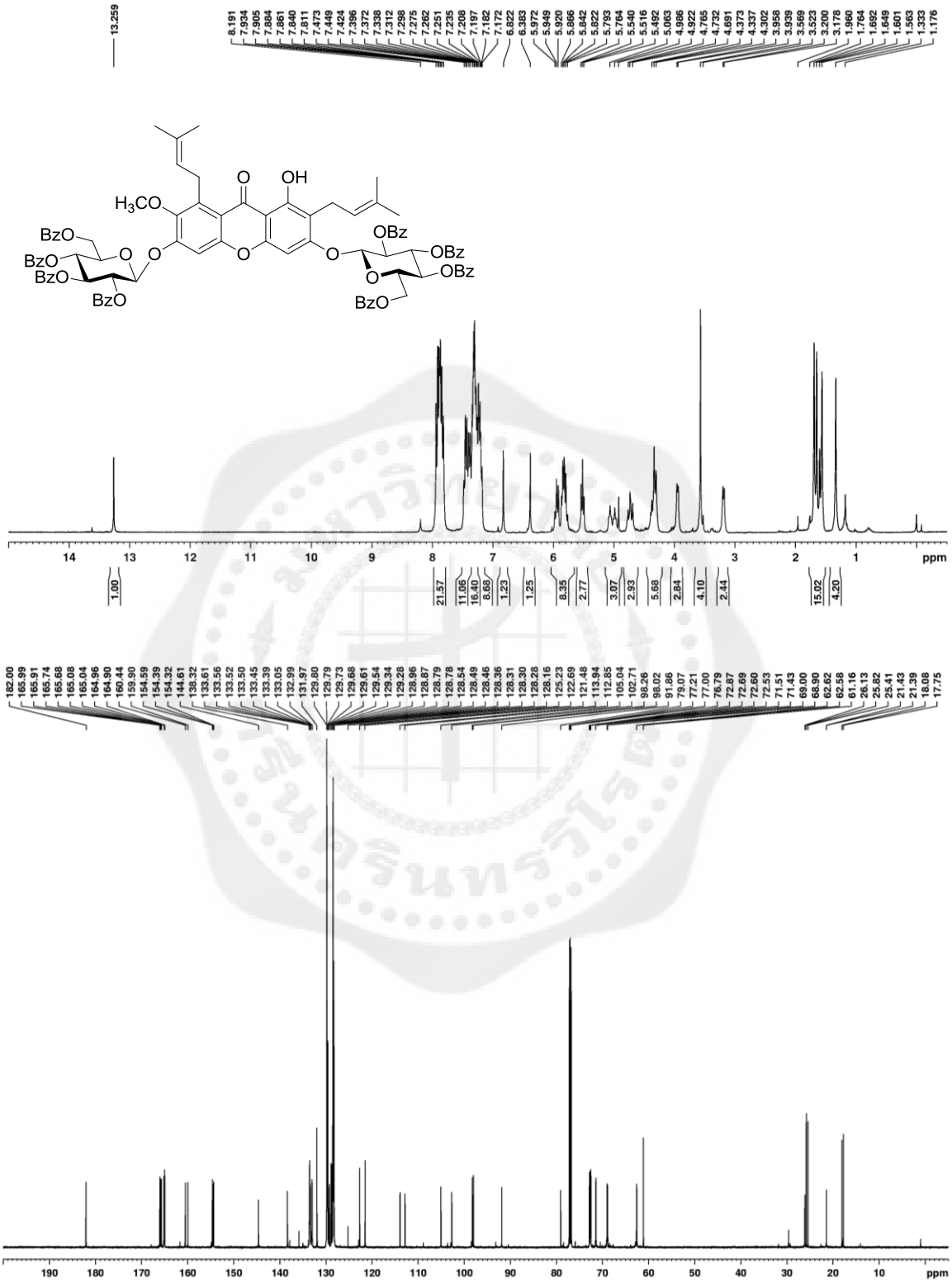

Figure 82 ^{1}H– and ^{13}C NMR of 3,6–di–*O*–(2,3,4,6–tetra–*O*–benzoyl–*β*–*D*–glucopyranosyl)–6–*O*–benzoyl mangostin (**311**) in $CDCl_3$ (NL93, sss6433)

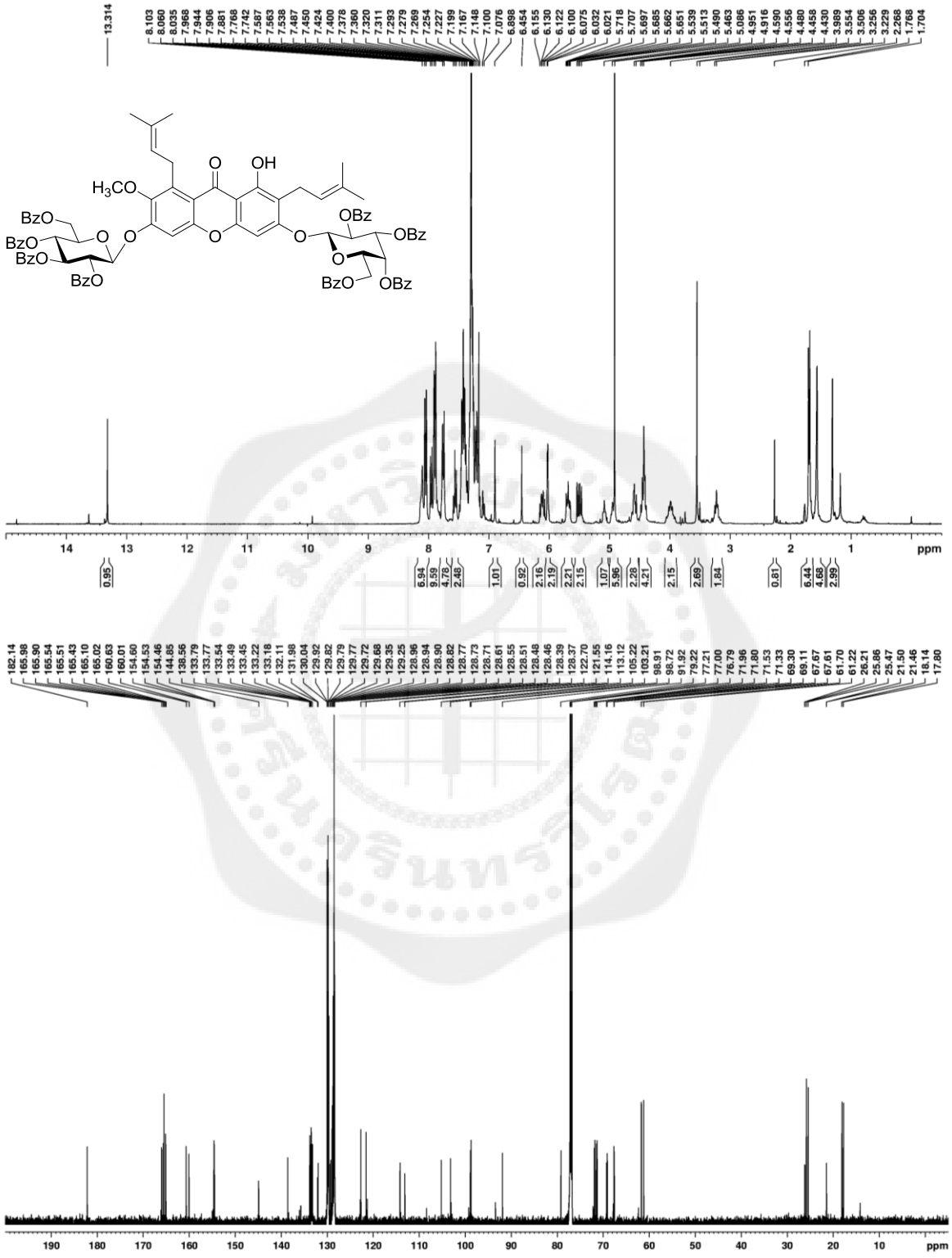

Figure 83 ^{1}H– and ^{13}C NMR of 3,6–di–*O*–(2,3,4,6–tetra–*O*–benzoyl–*β*–*D*–galactopyranosyl)–6–*O*–benzoyl mangostin (**312**) in $CDCl_3$ (NL59, NL96)

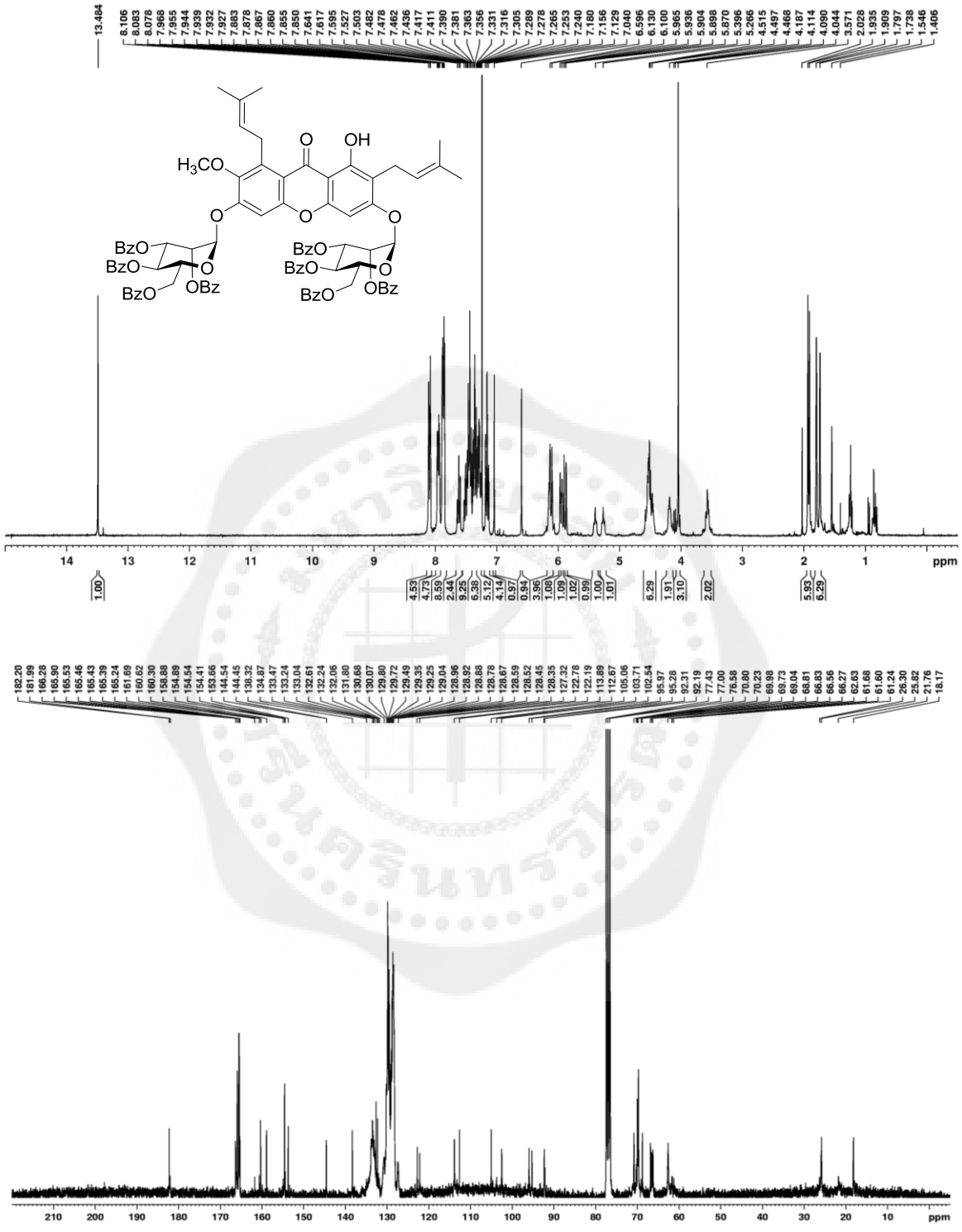

Figure 84 ^{1}H– and ^{13}C NMR of 3,6–di–*O*–(2,3,4,6–tetra–*O*–benzoyl–*α*–*D*–mannopyranosyl)–6–*O*–benzoyl mangostin (**313**) in $CDCl_3$ (NL122(1), sss6431)

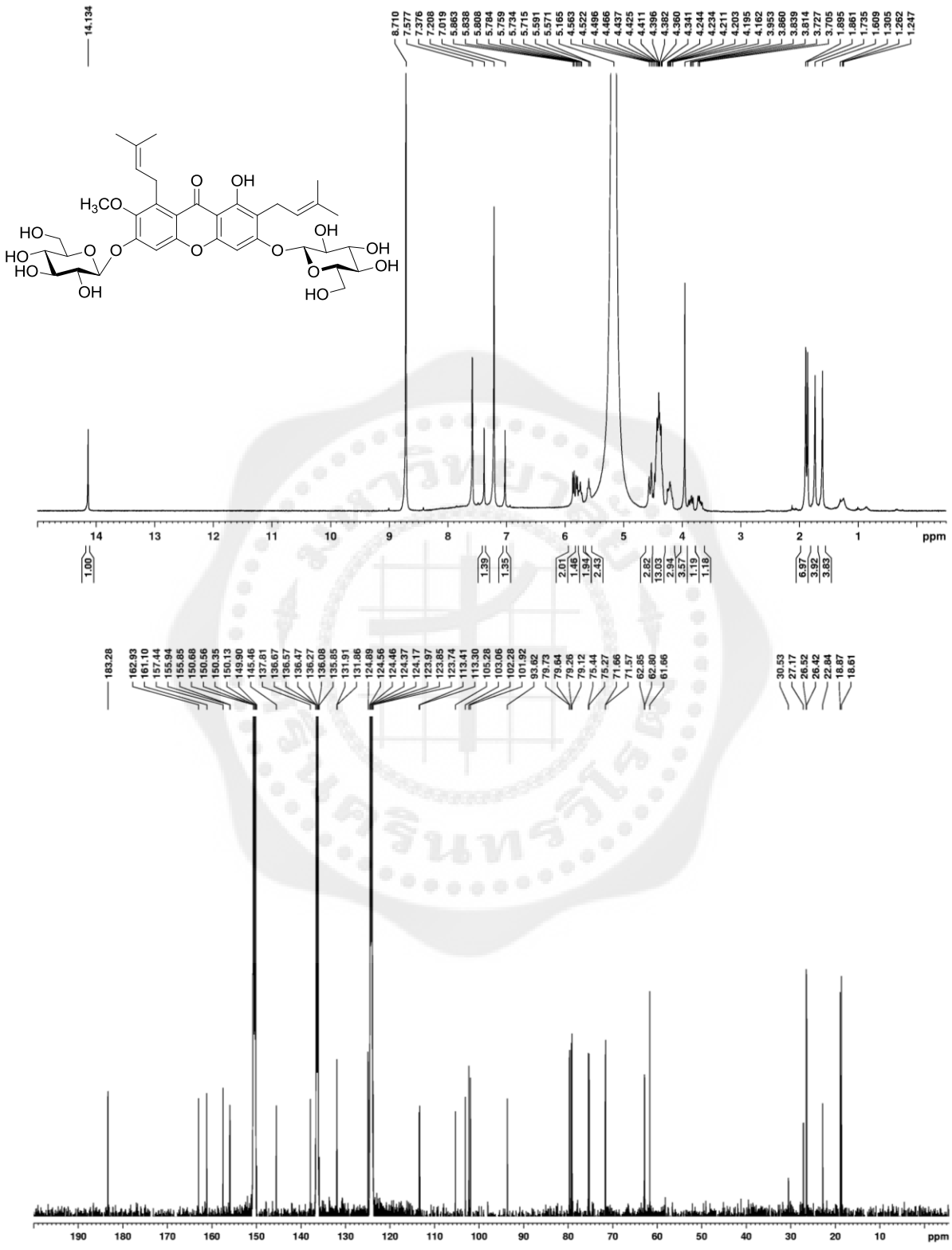

Figure 85 ^{1}H– and ^{13}C NMR of 3,6–di–*O*–*β*–*D*–glucopyranosyl mangostin (**272**) in pyridine–d_5 (NL259, sss6450)

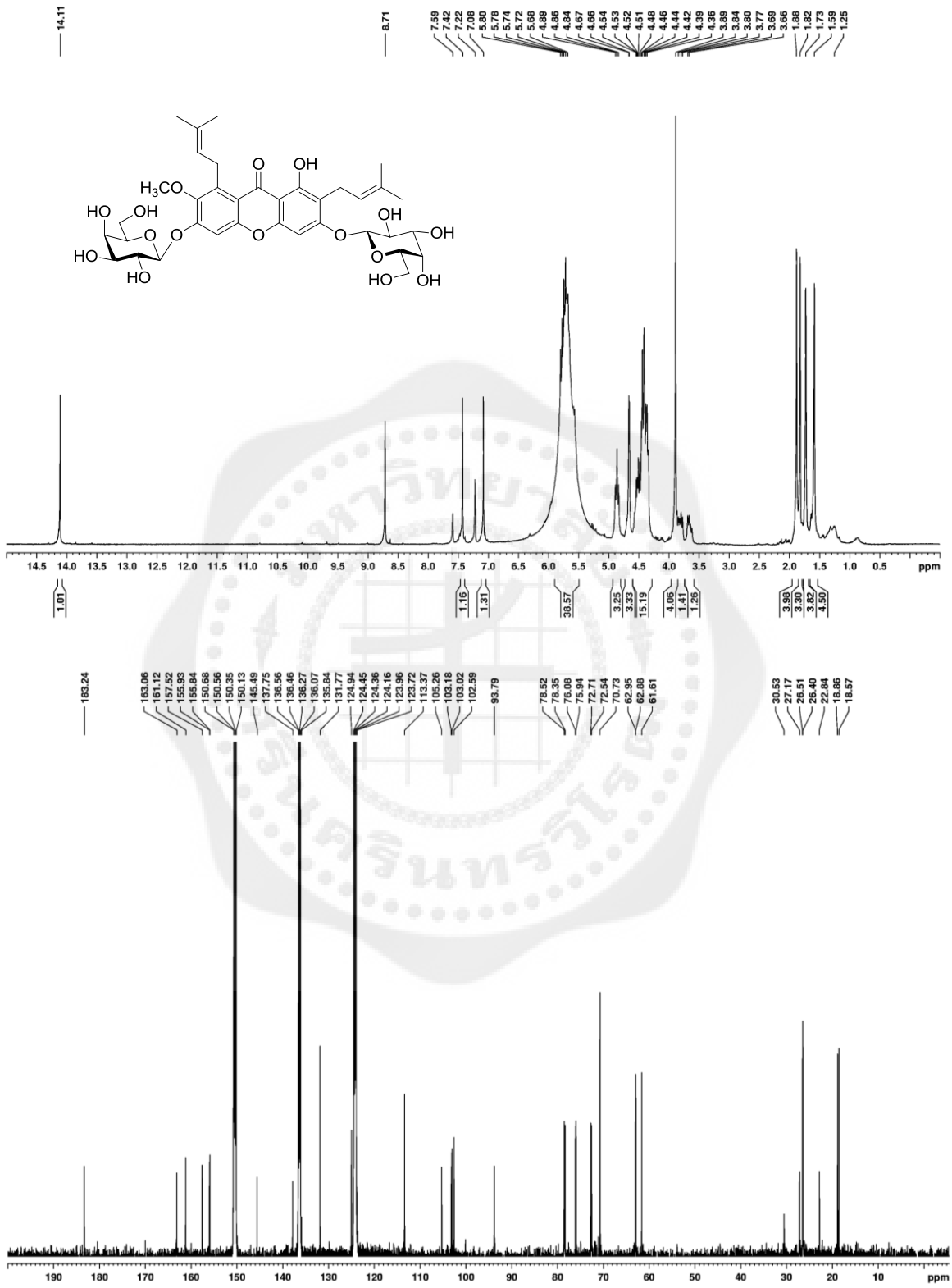

Figure 86 ^{1}H– and ^{13}C NMR of 3,6–di–*O*–*β*–*D*–galactopyranosyl mangostin (**314**) in pyridine–d_5 (NL247, sss6451)

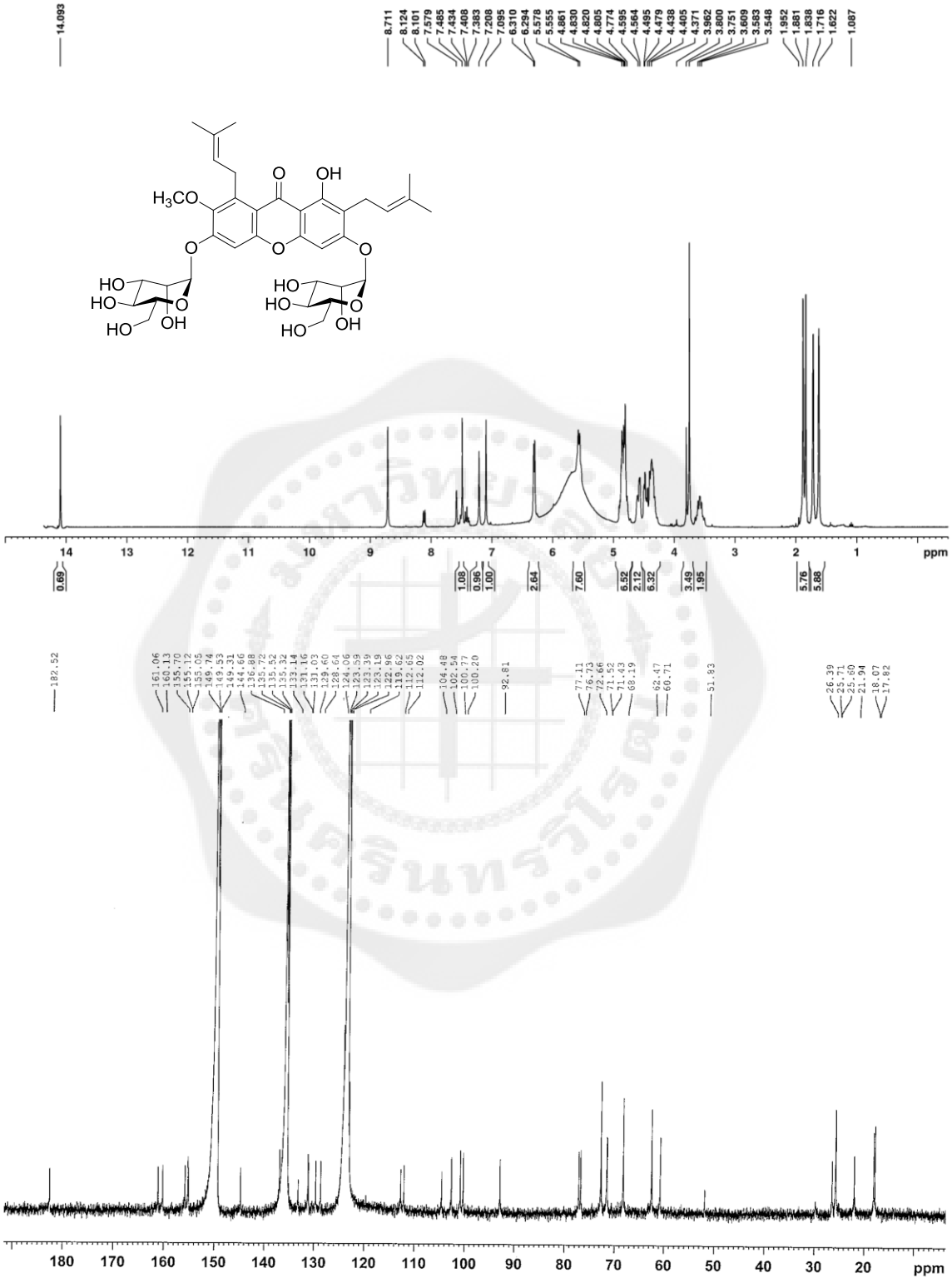

Figure 87 ^{1}H– and ^{13}C NMR of 3,6–di–*O*–α–*D*–mannopyranosyl mangostin (**315**) in pyridine–d_5 (NL267, sss6452)

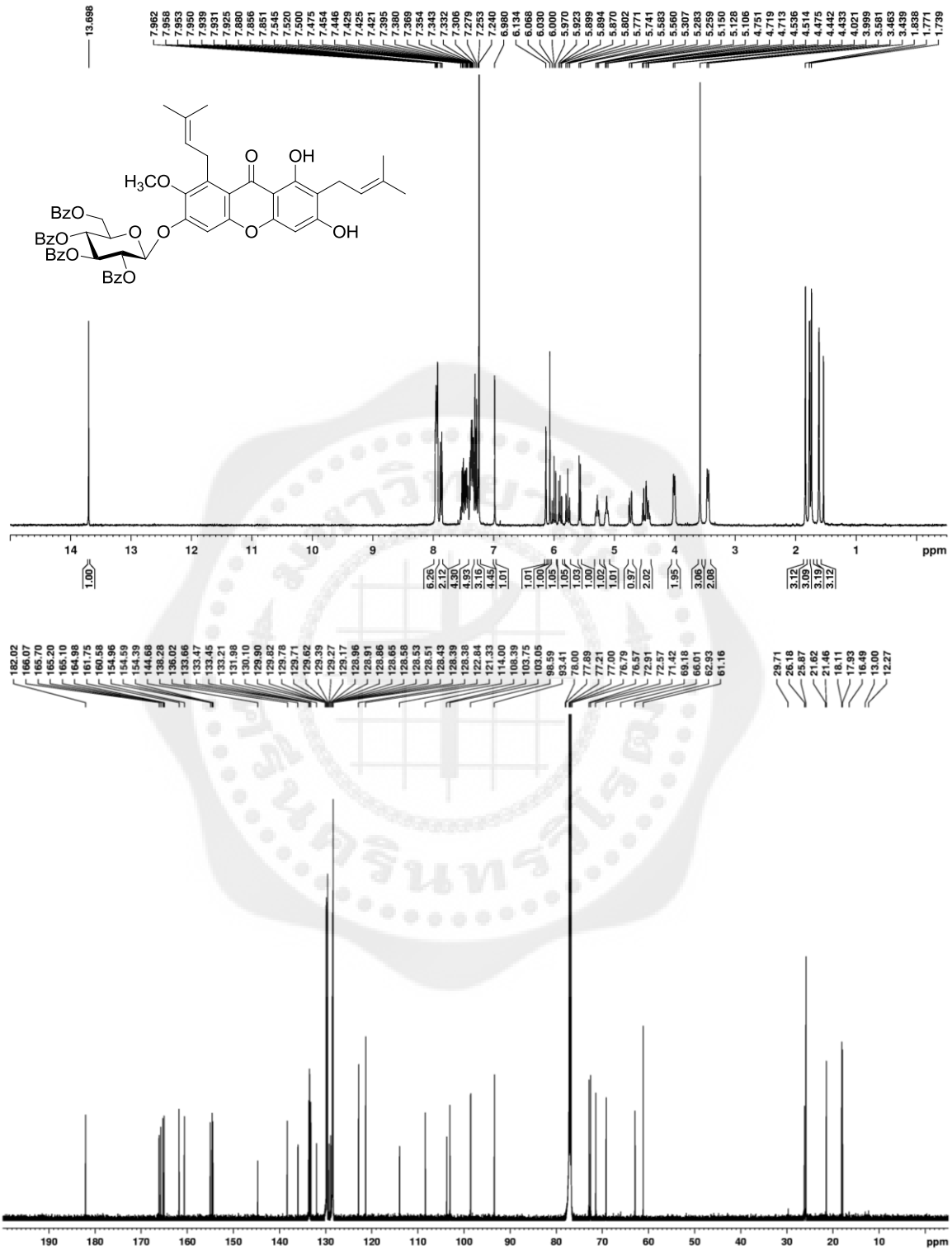

Figure 88 ^{1}H– and ^{13}C NMR of 6–*O*–(2,3,4,6–tetra–*O*–benzoyl–*β*–*D*–glucopyranosyl)–mangostin (**316**) in $CDCl_3$ (NL92)

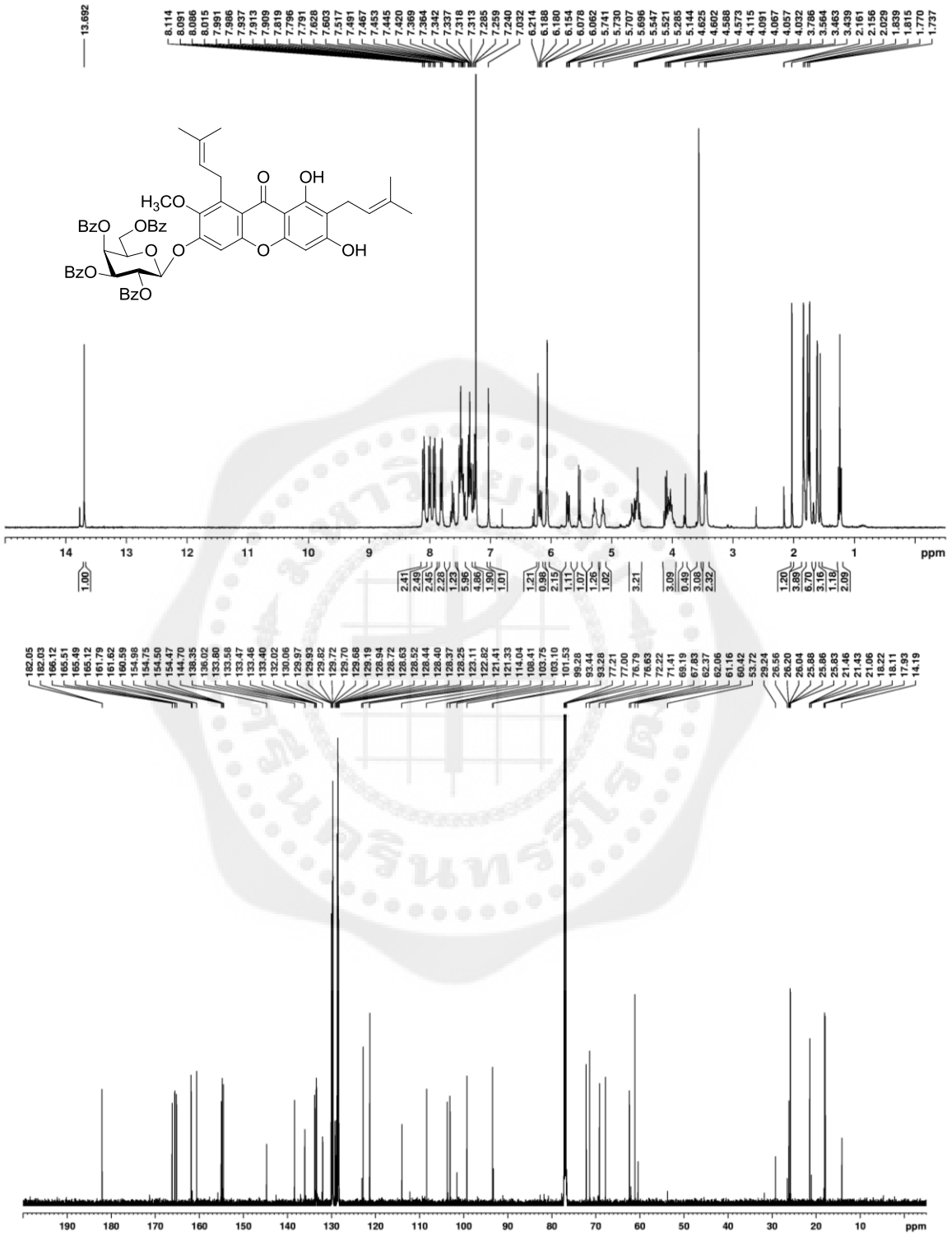

Figure 89 ^{1}H– and ^{13}C NMR of 6–*O*–(2,3,4,6–tetra–*O*–benzoyl–*β*–*D*–galactopyranosyl)–mangostin (**317**) in $CDCl_3$ (NL117, sss6436)

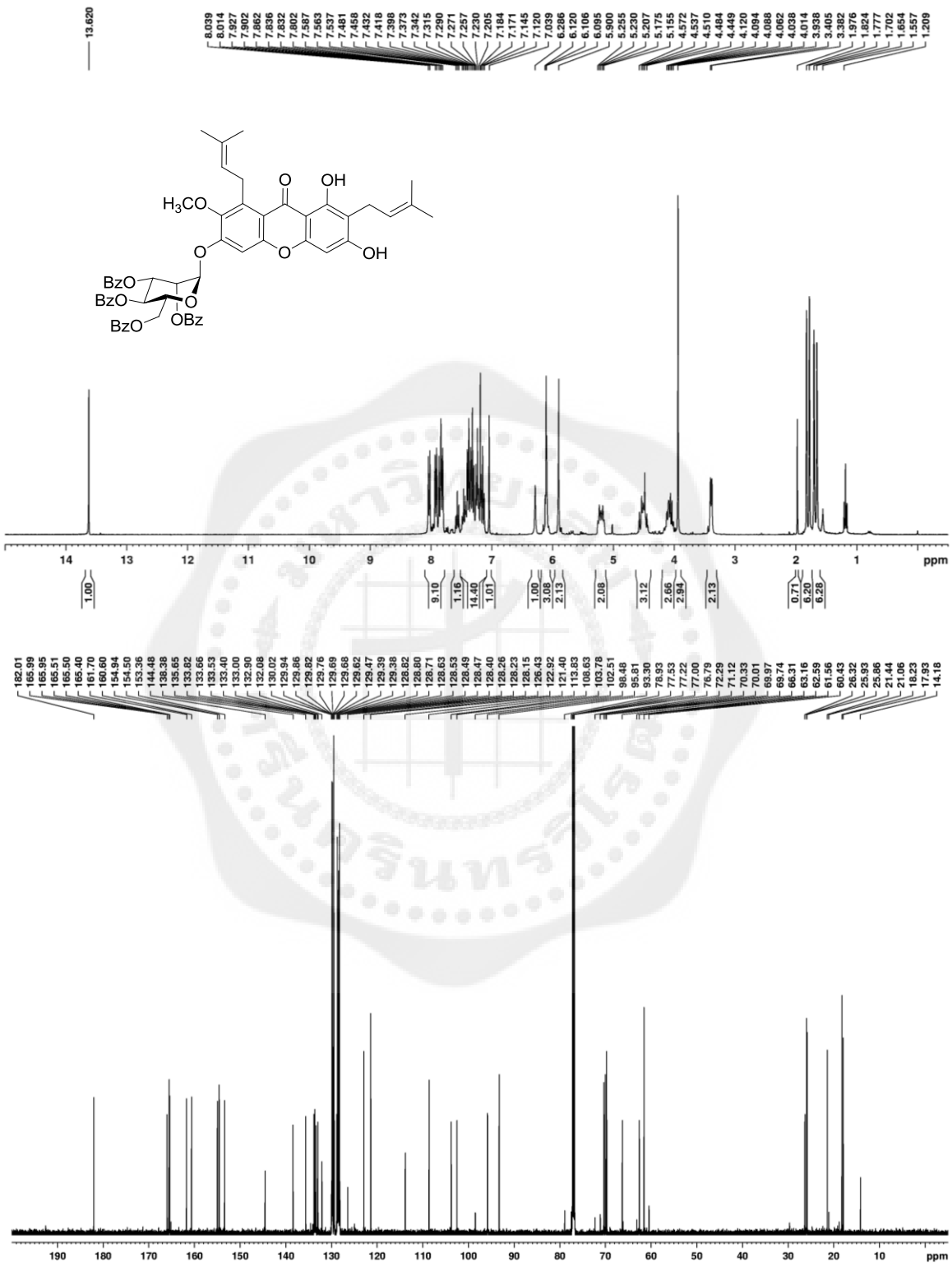

Figure 90 ^{1}H– and ^{13}C NMR of 6–*O*–(2,3,4,6–tetra–*O*–benzoyl–*α*–*D*–mannopyranosyl)–mangostin (**318**) in $CDCl_3$ (NL98(1))

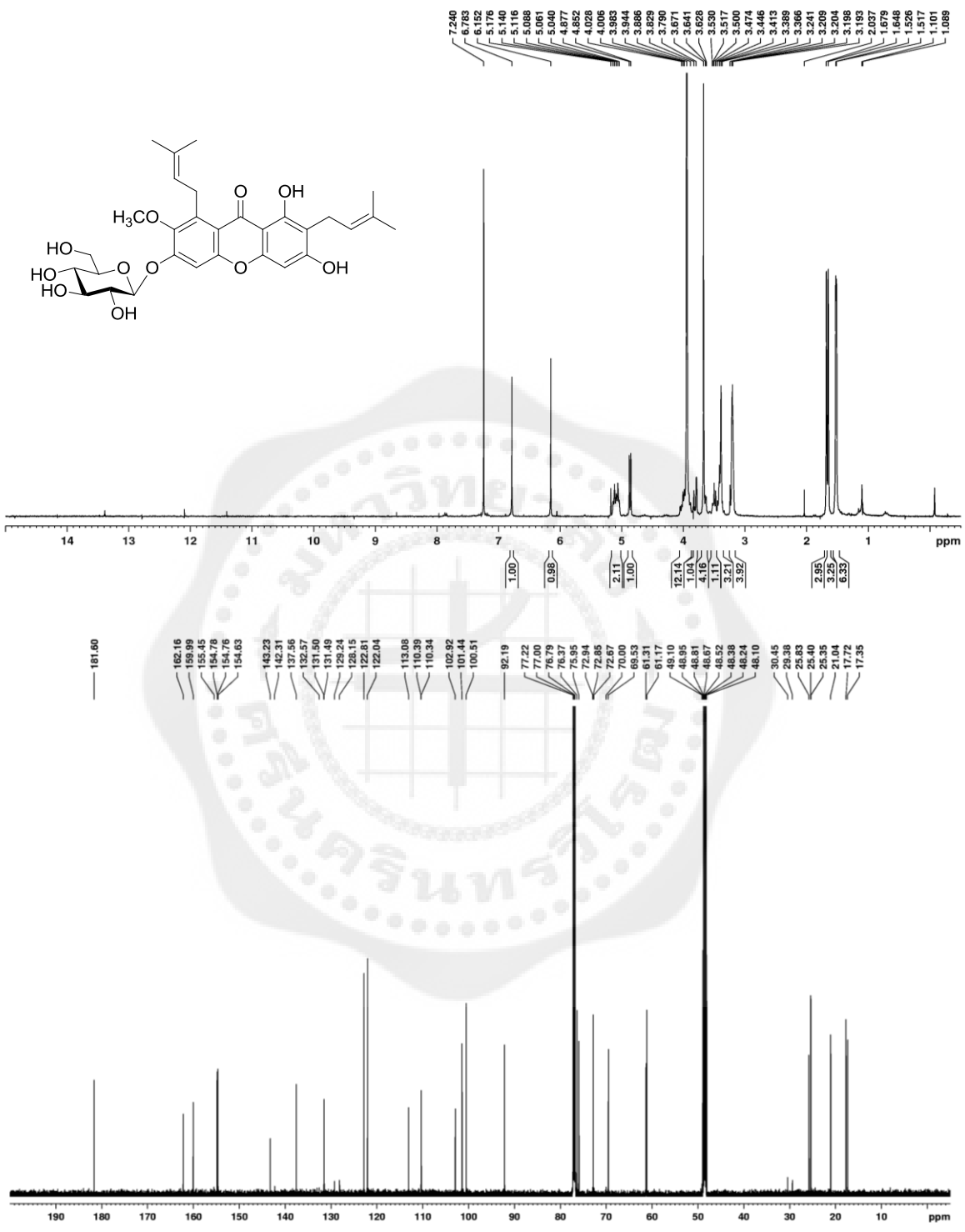

Figure 91 ^{1}H– and ^{13}C NMR of 6–*O*–*β*–*D*–glucopyranosyl mangostin (**273**) in $CDCl_3$ + 15 drops of methanol–d_4 (NL103)

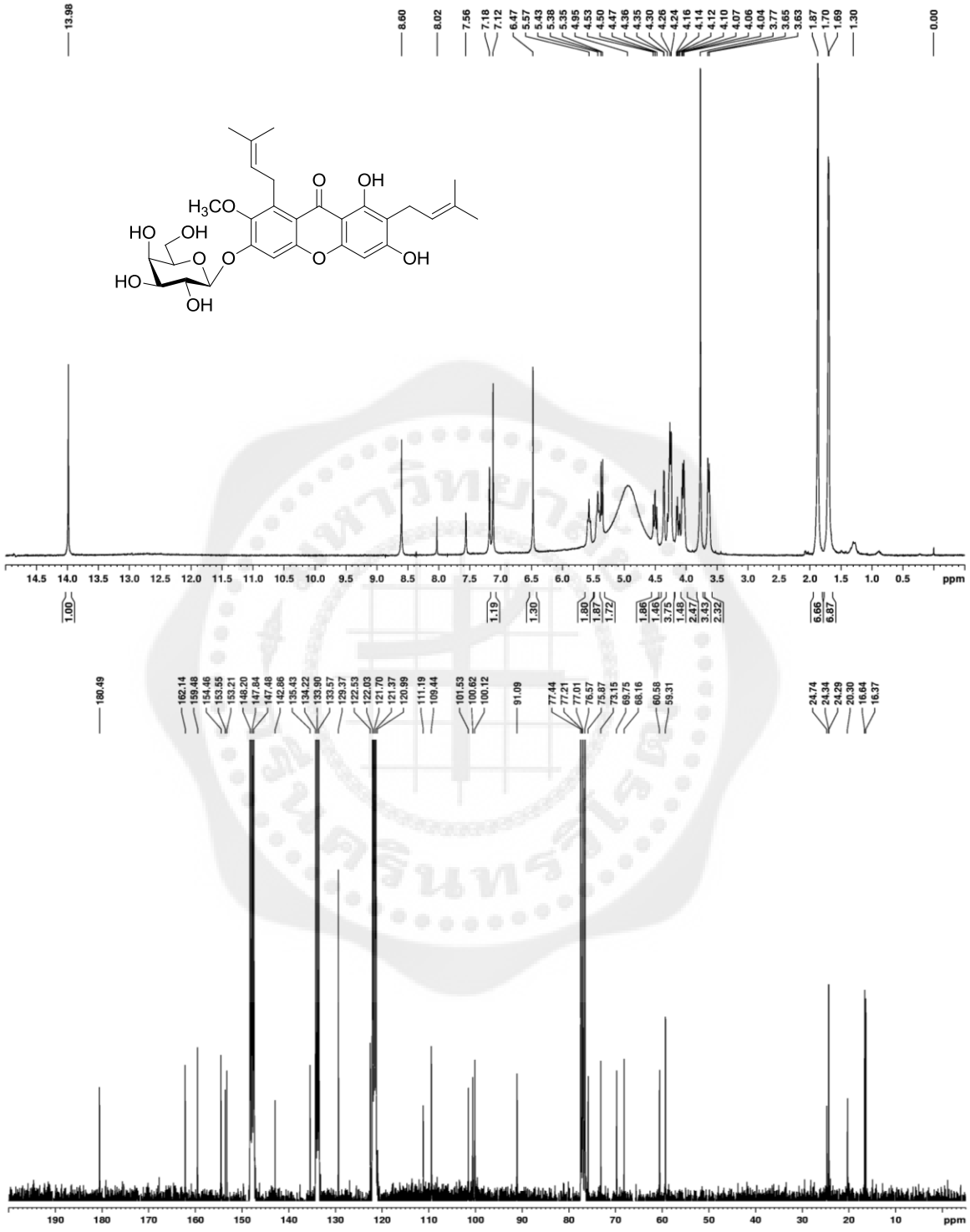

Figure 92 ^{1}H– and ^{13}C NMR of 6–*O*–*β*–*D*–galactopyranosyl mangostin (**319**) in $CDCl_3$ + 15 drops of pyridine–d_5 (NL114, sss6447)

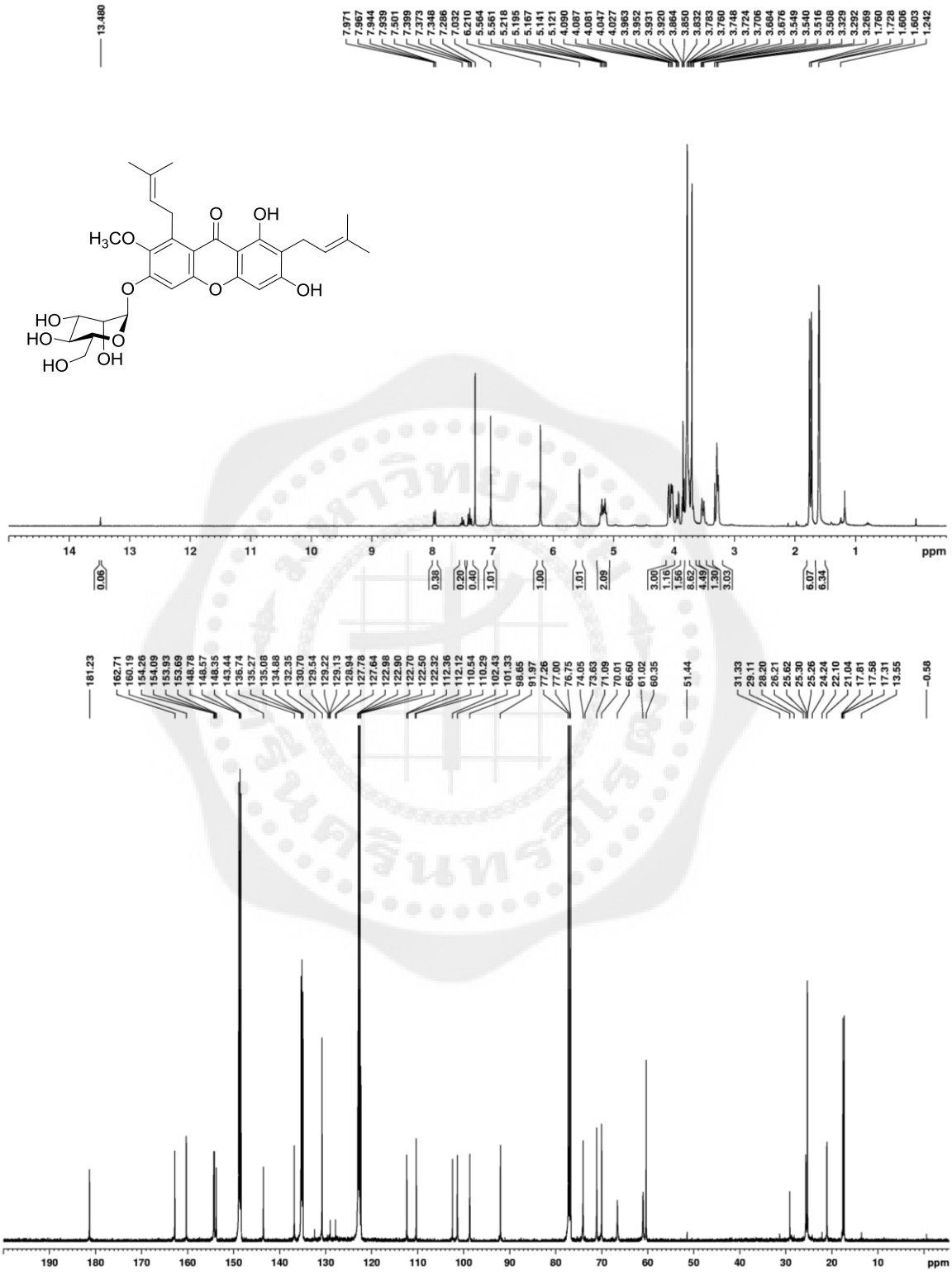

Figure 93 ^{1}H– and ^{13}C NMR of 6–*O*–α–*D*–mannopyranosyl mangostin (**320**) in $CDCl_3$ + 15 drops of pyridine–d_5 (NL246, sss6441)

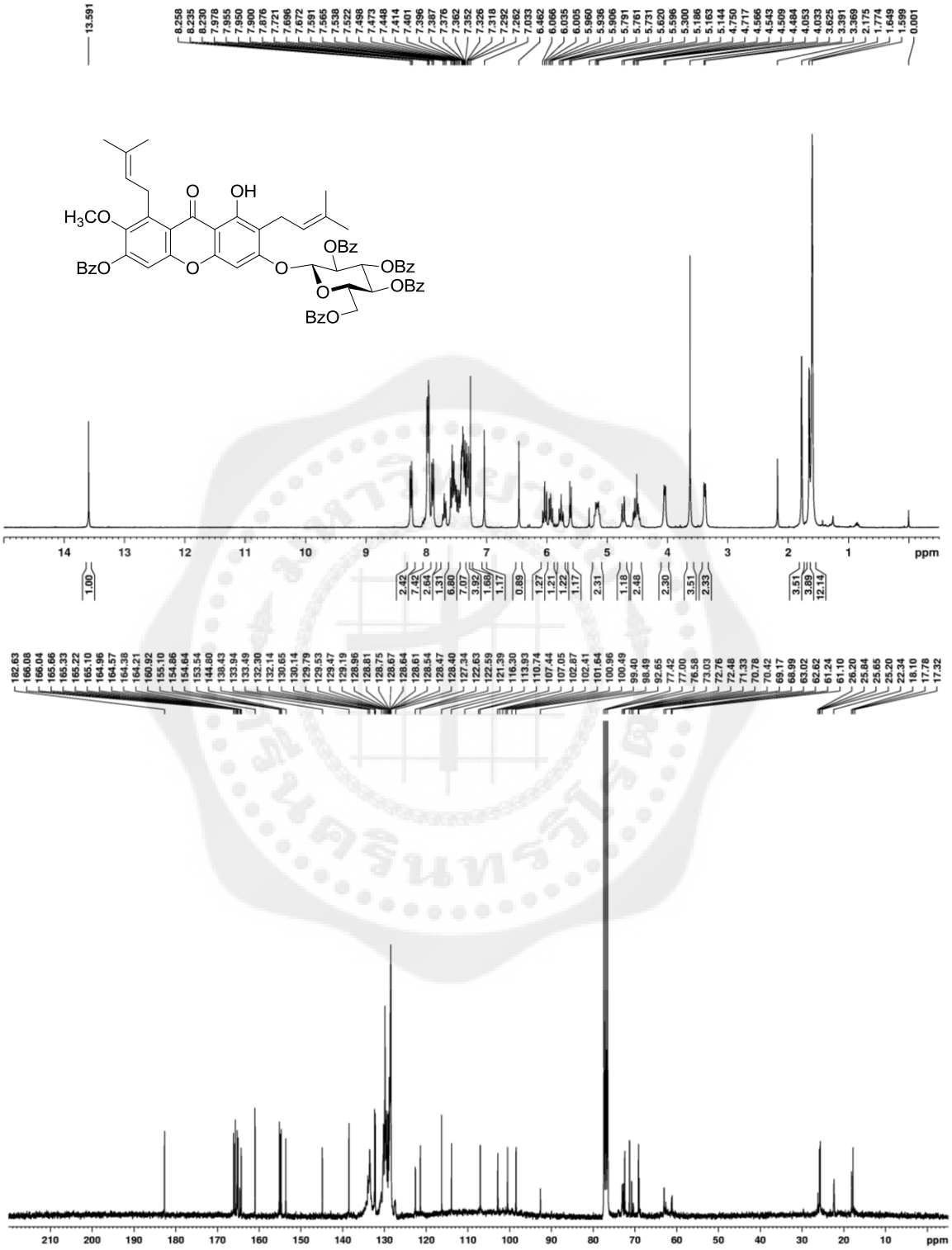

Figure 94 ^{1}H– and ^{13}C NMR of 3–*O*–(2,3,4,6–tetra–*O*–benzoyl–*β*–*D*–glucopyranosyl)–6–*O*–benzoyl mangostin (**321**) in $CDCl_3$ (NL128(1), sss6428)

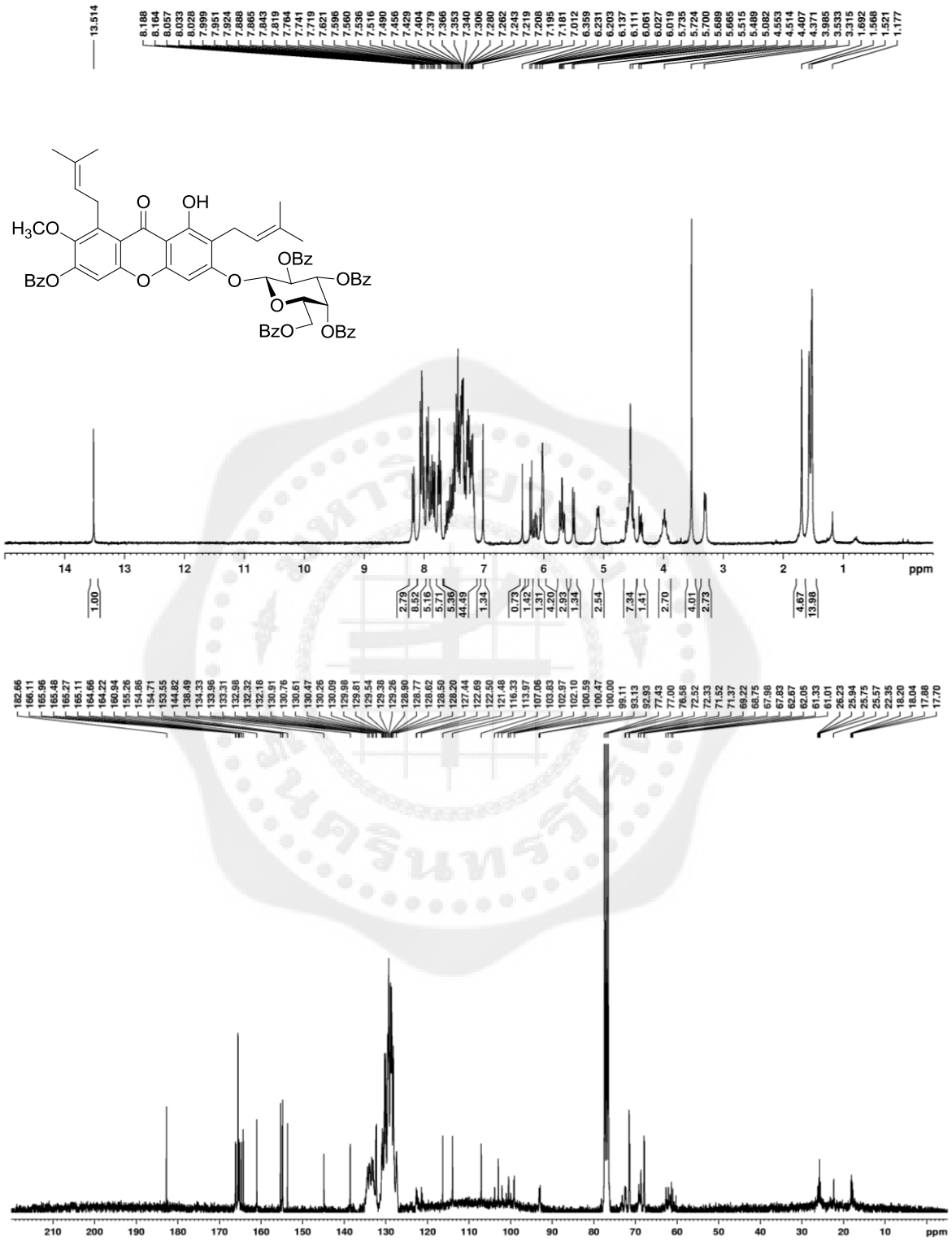

Figure 95 ^{1}H– and ^{13}C NMR of 3–*O*–(2,3,4,6–tetra–*O*–benzoyl–*β*–*D*–galactopyranosyl)–6–*O*–benzoyl mangostin (**322**) in $CDCl_3$ (NL238(1), sss6437)

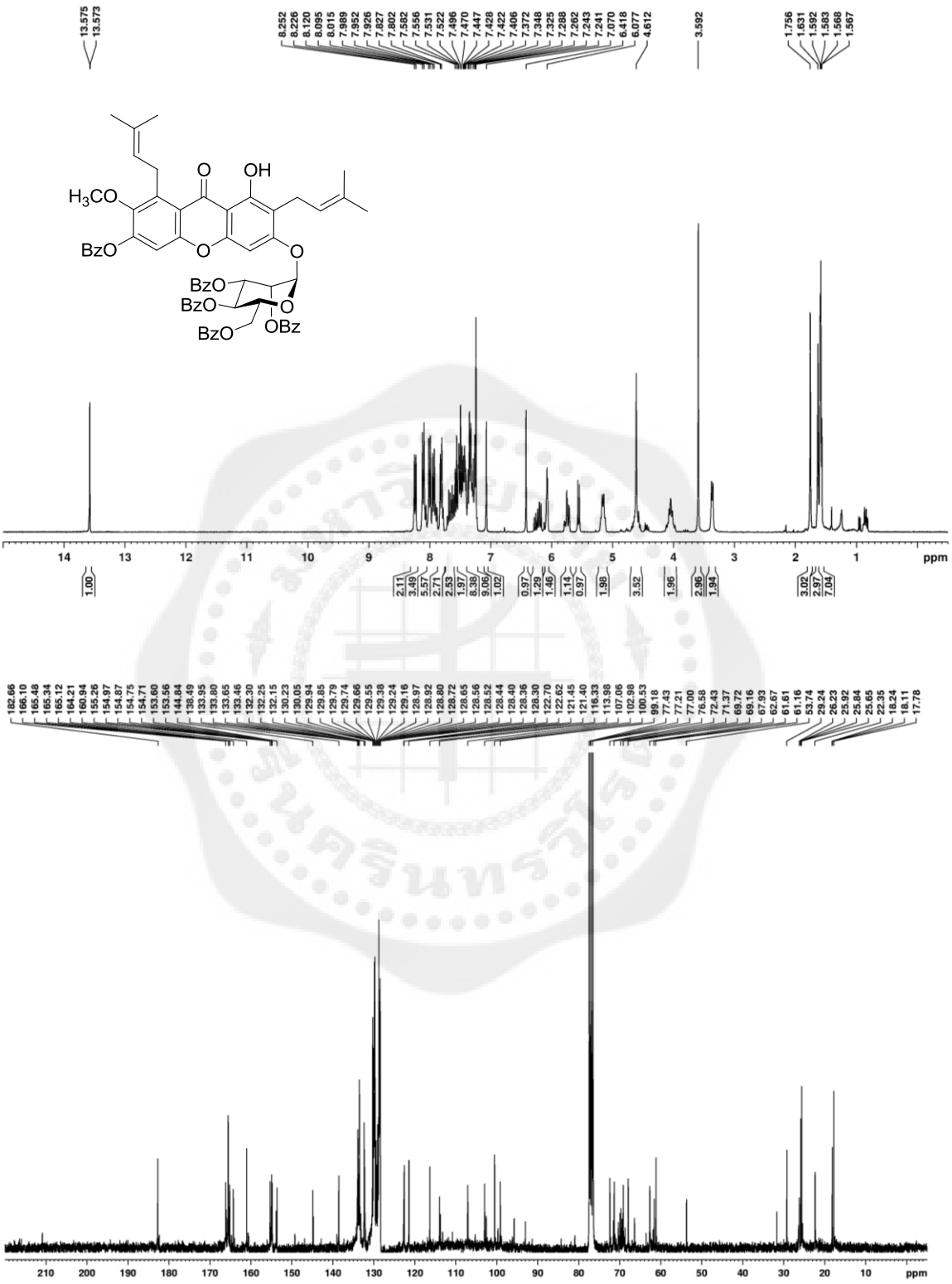

Figure 96 ^{1}H– and ^{13}C NMR of 3–*O*–(2,3,4,6–tetra–*O*–benzoyl–α–*D*–mannopyranosyl)–6–*O*–benzoyl mangostin (**323**) in $CDCl_3$ (NL254, sss6426)

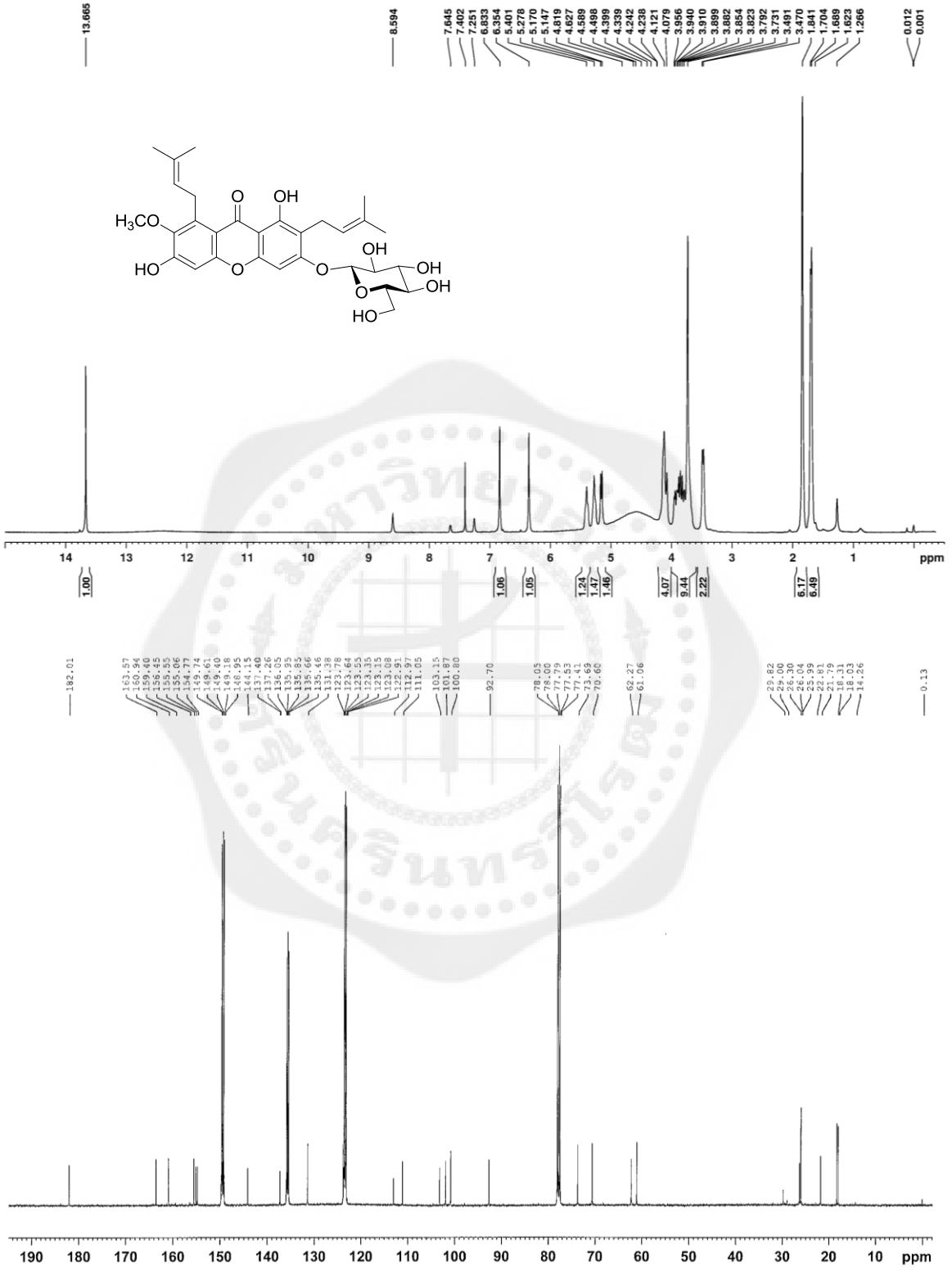

Figure 97 ^{1}H– and ^{13}C NMR of 3–*O*–*β*–*D*–glucopyranosyl mangostin (**324**) in $CDCl_3$ + 10 drops of pyridine–d_5 (NL260, sss6444)

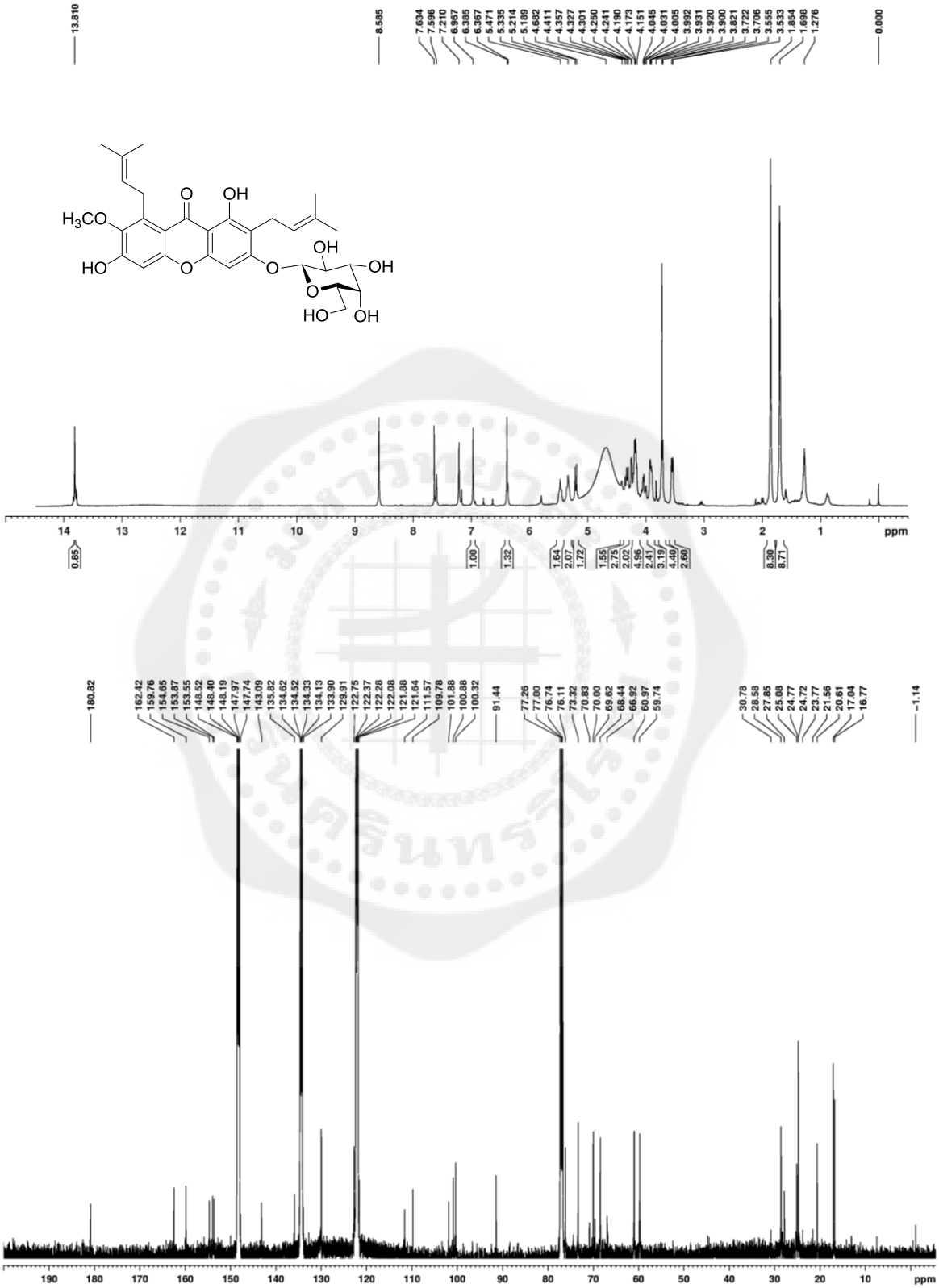

Figure 98 ^{1}H– and ^{13}C NMR of 3–*O*–*β*–*D*–galactopyranosyl mangostin (**325**) in $CDCl_3$ + 15 drops of pyridine–d_5 (NL261, sss6443)

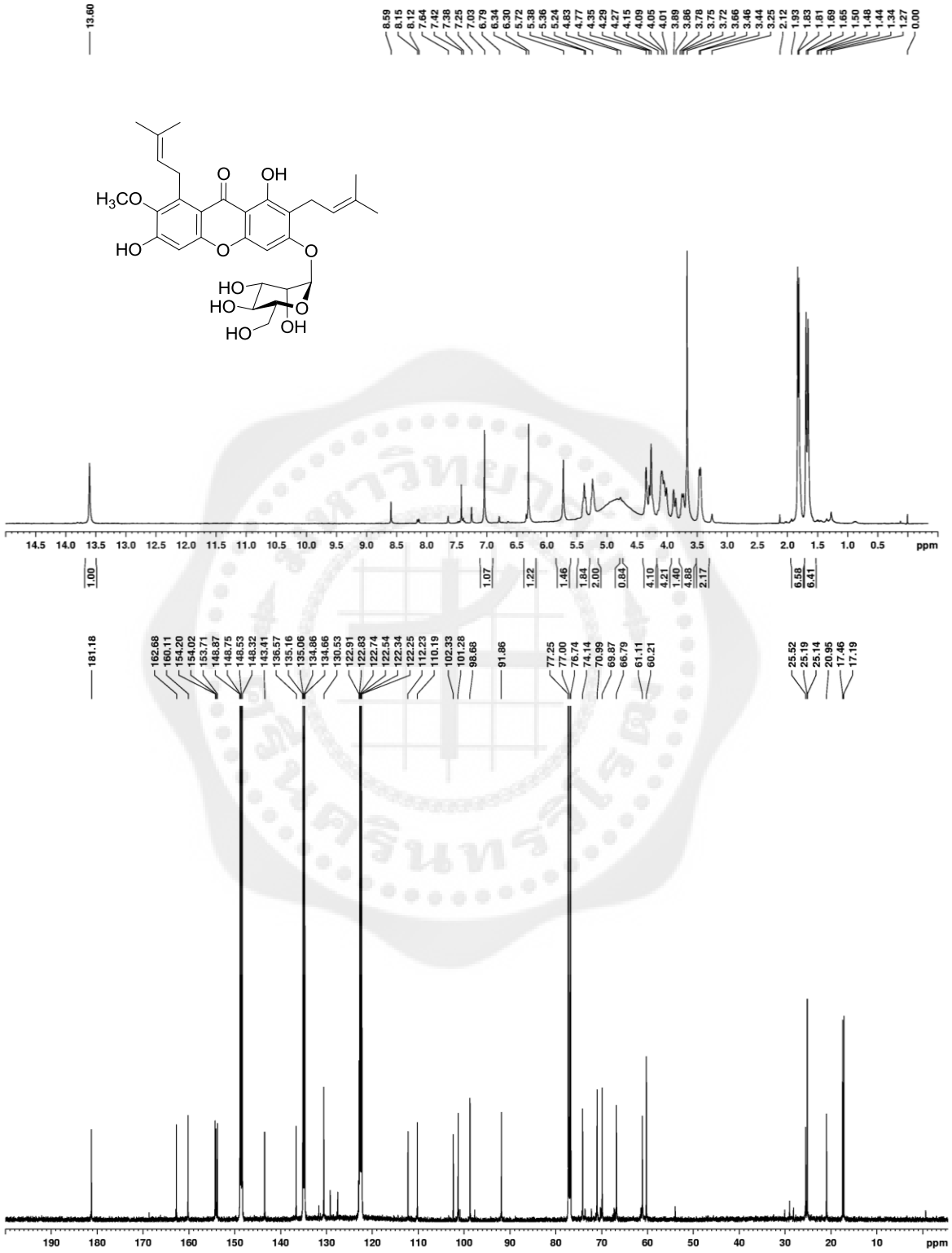

Figure 99 ^{1}H– and ^{13}C NMR of 3–*O*–α–*D*–mannopyranosyl mangostin (**325**) in $CDCl_3$ + 15 drops of pyridine–d_5 (NL262, sss6445)

GLOSSARY

LIST OF ABBREVIATIONS AND SYMBOLS

$[\alpha]_D^{23}$

Specific rotation at 23 °C and sodium D line

$[\alpha]_D^{24}$

Specific rotation at 24 °C and sodium D line

$[\alpha]_D^{25}$

Specific rotation at 25 °C and sodium D line

$[\alpha]_D^{26}$

Specific rotation at 26 °C and sodium D line

$[\alpha]_D^{27}$

Specific rotation at 27 °C and sodium D line

$[\alpha]_D^{28}$

Specific rotation at 28 °C and sodium D line

α

Alpha

β

Beta

δ

Chemical shift (for NMR data)

ε

Molar absorptivity

µL

Microliter

μL

Microliter

μM

Micromolar

λ_{max}

Wavelength at maximal absorption

ν_{max}

Wave number at maximal absorption

LIST OF ABBREVIATIONS AND SYMBOLS (continued)

$[M+H]^+$

Protonated molecular ion

^{13}C NMR

13–Carbon Nuclear Magnetic Resonance Spectroscopy

^{1}H NMR

Proton Nuclear Magnetic Resonance Spectroscopy

^{1}H–^{1}H COSY

Homonuclear (Proton–Proton) Correlation Spectroscopy

anh.

Anhydrous

Ar

Argon gass

ara–(1–2)–rha

Arabinosyl–(1→2)–α–*L*–rhamnoside

br d

Broad doublet (for NMR data)

br s

Broad singlet (for NMR data)

br t

Broad triplet (for NMR data)

C_6H_6

Benzene

calcd

Calculated

CC

Column chromatography

$CDCl_3$

Deuterated chloroform

LIST OF ABBREVIATIONS AND SYMBOLS (continued)

CH_2Cl_2

Dichloromethane

$CHCl_3$

Chloroform

cm

Centimeter

cm^{-1}

Reciprocal centimeter (unit of wave number)

d

Doublet (for NMR data)

dd

Doublet of doublets (for NMR data)

ddd

Double doublet of doublets (for NMR data)

dddd

Double doublet doublet of doublets (for NMR data)

DEPT

Distortionless Enhancement by Polarization Transfer

dq

Doublet of quartets (for NMR data)

dt

Doublet of triplets (for NMR data)

EIMS

Electron Impact Ionization Mass Spectrometry

ESIMS

Electrospray Ionization Mass Spectrometry

EtOAc

Ethyl acetate

LIST OF ABBREVIATIONS AND SYMBOLS (continued)

g

Gram

Glc

Glucosyl

h

Hour

H_2O

Water

HMBC

^{1}H–Detected Heteronuclear Multiple Bond Coherence

HMQC

^{1}H–Detected Heteronuclear Multiple Quantum Coherence

HRTOFMS

High Resolution Time of Flight Mass Spectrometry

Hz

Hertz

IC_{50}

50% Inhibitory Concentration

IC_{50}

50% Inhibitory Concentration

IR

Infrared spectroscopy

J

Coupling constant

KBr

Potassium bromide

kg

Kilogram

LIST OF ABBREVIATIONS AND SYMBOLS (continued)

L

Liter

log*P*

Octanol–water partitioning coefficients

m

Multiplet (for NMR data)

MeOH

Methanol

Methanol–d_4

Deuterated methanol

mg

Milligram

MIC

Minimum Inhibitory Concentration

mL

Milliliter

mm

Millimeter

***N*Me**

N–methyl

***N*Me$_2$**

N,N–dimethyl

NMR

Nuclear Magnetic Resonance Spectroscopy

NOESY

Nuclear Overhauser Effect Spectroscopy

°C

Degree Celsius

LIST OF ABBREVIATIONS AND SYMBOLS (continued)

Pyridine–*d5*

Deuterated pyridine

QCC

Quick column chromatography

quin

Quintet (for NMR data)

Rha

Rhamnosyl

s

Singlet (for NMR data)

sh

shoulder

t

Triplet (for NMR data)

TLC

Thin Layer Chromatography

UV

Ultraviolet

VITAE

VITAE

Name: Natthakaln Lomchoey

Date of Birth: September 01, 1985

Place of Birth: Surin

Address: 141, Moo 6 Ban Nongjonglong, Tawang, Buachet, Surin, Thailand 32230

Education:

2008 Bachelor's of Science Degree in Chemistry
Srinakharinwirot University, Bangkok, Thailand

2011 Master's of Science Degree in Chemistry
Srinakharinwirot University, Bangkok, Thailand

Publications:

1. Panseeta, P.; **Lomchoey, K.**; Prabpai, S.; Kongsaeree, P.; Suksamrarn, A.; Ruchirawat, S.; Kongsaeree, P.; Suksamrarn, A.; Ruchirawat, S.; Suksamrarn, S. Antiplasmodial and antimycobacterial cyclopeptide alkaloids from the root of *Ziziphus mauritiana*. *Phytochemistry* **2011**, 72, 909–915.
2. Prachayasittikul, S.; Worachartcheewan, A.; Yainoy, S.; **Lomchoey, N.**; Kittiphatcharin, P.; Ruchirawat, S.; Prachayasittikul, V., Antioxidant and antimicrobial activities of *Saraca thaipingensis* Cantley ex Prain. *Asian Pac. J. Trop. Biomed.* **2012**, *2*, S796–S799.
3. Saenkham, A.; **Lomchoey, N.**; Nontakham, J.; Taweechotipatr, M.; Suksamrarn, S. Lupane– and ceanothane–type triterpenes of *Ziziphus cambodiana* Pierre stem barks with anti–*Helicobacter pylori* activity. *KKU Science Journal.* **2015**, *3*, 43.

Scholarships:

2009–2010 The Center of Excellence for Innovation in Chemistry (PERCH–CIC)

2011 Research assistantship

2012–2015 The Royal Golden Jubilee Ph.D. (RGJ) Program, The Thailand Research Fund (TRF).

Work experience:

2014-2015 Research Fellow Department of Chemistry and Biochemistry University of Missouri–St. Louis, USA

Oral presentation:

Lomchoey, N.; Panseeta, P.; Prabpai, S.; Kongsaeree, P.; Suksamrarn, A.; Ruchirawat, S.; Suksamrarn, S. New Cyclopeptide Alkaloids with Antiplasmodial and Antimycobacterial Activities from the Root of *Ziziphus mauritiana* Lam. International Congress for Innovation in Chemistry (PERCH–CIC Congress VII), Jomtien Palm Beach Hotel & Resort, Thailand, May 4–7, 2011. Presentation number S2A–08.

Poster presentations:

1. **Lomchoey, K.**; Panseeta, P.; Thitivorn, Y.; Kongsomboon, P.; Suksamrarn, A.; Suksamrarn, S. Cyclopeptide alkaloids from *Ziziphus cambodiana* Pierre. Pure and Applied Chemistry International Conference 2011. Miracle Grand Hotel, Thailand, January 5–7, 2011. Poster number OM_O0062.
2. Panseeta, P.; **Lomchoey, K.**; Prabpai, S.; Kongsaeree, P.; Suksamrarn, A.; Ruchirawat, S.; Suksamrarn, S. Antiplasmodial and antimycobacterial cyclopeptide alkaloids from the root of *Ziziphus mauritiana* Lam. Pure and Applied Chemistry International Conference 2011. Miracle Grand Hotel, Thailand, January 5–7, 2011. Poster number OM_O0055.
3. Namdaung, U; **Lomchoey, N.** and Suksamrarn, S. Bioactive compounds from some Thai *Ziziphus* plants. Taiwan–Thailand. 2013.
4. **Lomchoey, N.**; Yasomanee, J. P.; Suksamrarn, S.; Demchenko, A. V. Glycosylation of α–mangostin and betulinic acid to enhance their hydrophilic property. 28th Annual Organic Chemistry Day April 11, 2015 at University of Missouri–Columbia 2015. Poster number 39.